JUSTUS-LIEBIG-
UNIVERSITÄT
GIESSEN

Physiology and Hydrodynamics Influence the Susceptibility of Reef-Building Corals to Ocean Acidification

Catarina Padilha Pires Martins

Doctoral Thesis | 2026

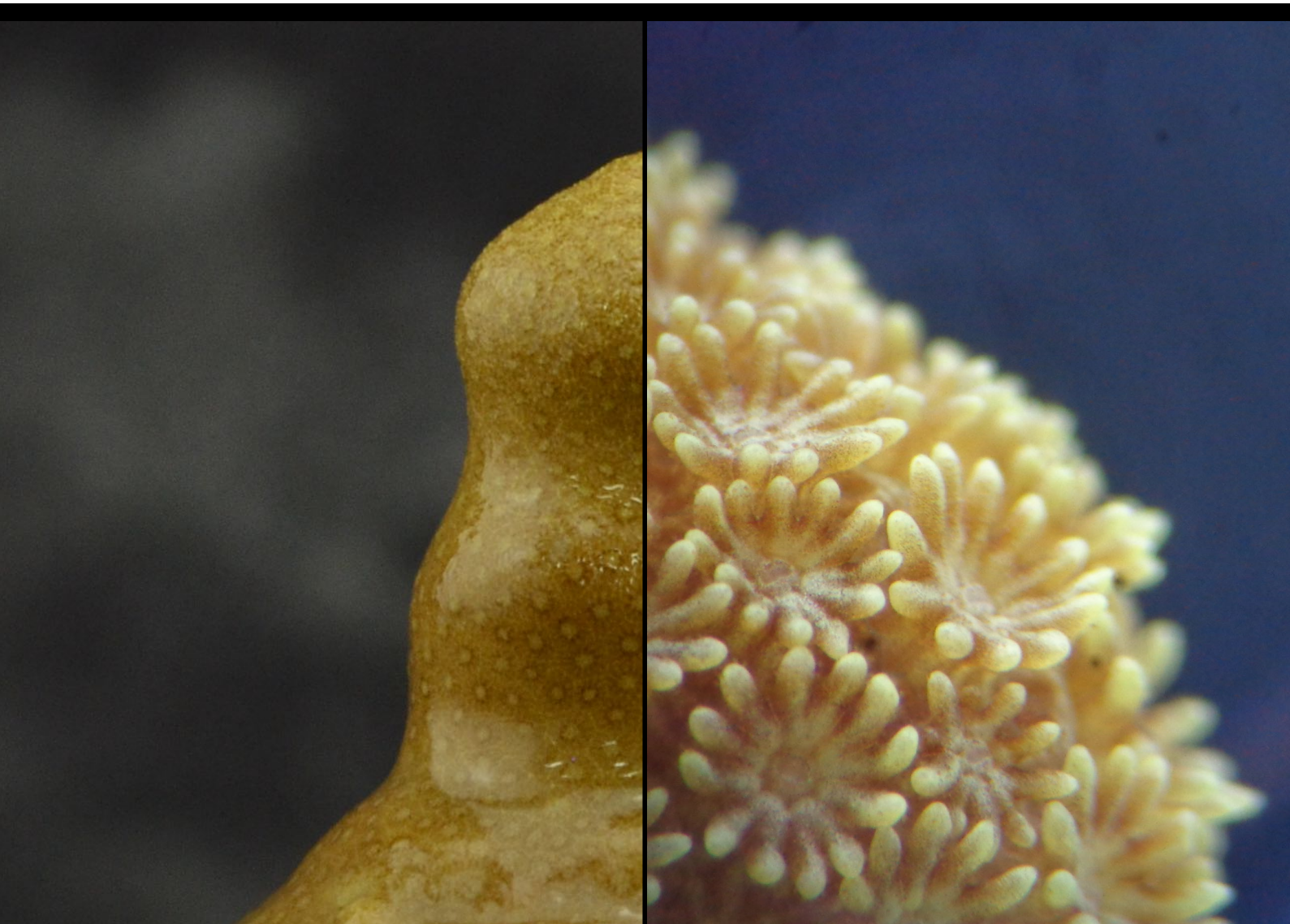

JUSTUS-LIEBIG-
UNIVERSITÄT
GIESSEN

Physiology and Hydrodynamics Influence the Susceptibility of Reef-Building Corals to Ocean Acidification

Physiologie und Hydrodynamik prägen die Anfälligkeit riffbildender Korallen als Antwort auf Ozeanversauerung

Catarina Padilha Pires Martins

Dissertation presented for the degree of
Doctor rerum naturalium
at Justus Liebig University Giessen

Faculty of Biology and Chemistry, Justus Liebig University Giessen
Giessen, 2026

Supervisor

Prof. Dr. Thomas Wilke

Systematics & Biodiversity, Department of Animal Ecology & Systematics, Faculty of Biology and Chemistry, Justus Liebig University Giessen, Germany

Dean

Prof. Dr. Holger Zorn

Department of Food Chemistry and Food Biotechnology, Faculty of Biology and Chemistry, Justus Liebig University Giessen, Germany

Cover: Colony-scale (left) and polyp-scale (right) photographs of *Porites cylindrica*. Credits: Catarina P. P. Martins

“Nowhere on the shore is the relation of a creature to its surroundings
a matter of a single cause and effect;
each living thing is bound to its world by many threads,
weaving the intricate design of the fabric of life.”

— Rachel Carson, *The Edge of the Sea*

Table of Contents

Table of Figures

Declaration

“I declare that I have completed this dissertation single-handedly without the unauthorized help of a second party and only with the assistance acknowledged therein. I have appropriately acknowledged and cited all text passages that are derived verbatim from or are based on the content of published work of others, and all information relating to verbal communications. I consent to the use of an anti-plagiarism software to check my thesis. I have abided by the principles of good scientific conduct laid down in the charter of the Justus Liebig University Giessen „Satzung der Justus-Liebig-Universität Gießen zur Sicherung guter wissenschaftlicher Praxis“ in carrying out the investigations described in the dissertation.”

Statement about the use of Artificial Intelligence (AI) based aids like ChatGPT or SchulKI by OpenAI, or Gemini by Google in the creation of my thesis (marked as applicable):

□ I have not used any Al tool in preparing this text

□ I used an Al tool in the following areas (multiple answers possible):

- □ Finding ideas, stimulating my creativity
- □ Understanding concepts, researching facts and definitions
- □ Optimising a text that I drafted myself
- □ Creating entire text passages following my prompts

I used the following AI tools to improve the given passages of the text in the manner stated:

Date: _____ Signature: _____

Abstract

Ocean acidification (OA) poses a major future threat to tropical coral reefs. This is primarily due to its effects on reef-building coral species, which vary in their susceptibility to this climate change stressor. However, the potential factors underlying the range of susceptibilities observed among reef-building corals remain poorly understood. Therefore, this doctoral thesis investigates the influence of species-specific physiology and water flow conditions on coral susceptibility to OA. Using an experimental, multi-scale approach, the present thesis addresses this knowledge gap in a total of four studies and focuses on the physiological response of three major reef-building coral genera (*Acropora*, *Pocillopora*, and *Porites*) to prolonged exposure of OA conditions (> three months).

The results showed that (1) variable decreases in coral growth under OA were mediated by differential changes in maintenance and cellular stress parameters. This physiological interplay was genus-specific for *Acropora* and *Pocillopora*, and was species-specific for *Porites* spp. Moreover, assessments of the combined effects of OA and changes in water flow conditions indicated that (2) temporarily reduced water flow may mitigate OA effects on *Acropora* and *Porites* spp. Still, simultaneous changes in seawater chemistry and flow led to changes in coral physiology with complex and species-specific patterns. Finally, at the microscale, characterisation of the effects of OA and water flow on the concentration boundary layer (CBL) at the coral surface revealed that (3) OA was an overall weak modulator of this layer, regardless of flow conditions and CBL variability among species. Despite minor OA effects, however, the results also suggested that the CBL had a limited OA-buffering capacity due to thin pH gradients across the CBL. Nonetheless, low flow potentially enhanced CBL sheltering from acidified seawater by elevating pH at the coral surface.

In summary, this thesis provides evidence that both species physiology and water flow conditions shape coral susceptibility to OA in species-specific patterns and contributes novel insights into the potential links, between colony and CBL levels, involved in shaping it. Furthermore, the findings of this thesis showcase the potential of low-flow environments as refugia for coral species under OA and highlight the importance of including reef hydrodynamics in future OA scenarios, which will require consideration of different spatial and temporal scales. Altogether, the knowledge provided here may help improve projections of coral community dynamics under future OA and inform conservation efforts.

Zusammenfassung

Die Ozeanversauerung stellt eine erhebliche Bedrohung für tropische Korallenriffe dar. Dies ist vor allem auf ihre Auswirkungen auf riffbildende Korallenarten zurückzuführen, die unterschiedlich auf diesen Stressfaktor des Klimawandels reagieren. Die zugrunde liegenden Ursachen dieser Variabilität sind jedoch bislang unzureichend erforscht. Daher untersucht diese Dissertation, wie die artspezifische Physiologie und die Wasserströmungsbedingungen die Anfälligkeit von Korallen gegenüber der Ozeanversauerung beeinflussen. Die vorliegende Dissertation schließt diese Wissenslücke mit einem experimentellen, multiskaligen Ansatz und umfasst insgesamt vier Studien, die sich auf die physiologischen Reaktionen dreier wichtiger riffbildender Korallengattungen (*Acropora*, *Pocillopora* und *Porites*) auf eine langfristige Exposition gegenüber den Bedingungen der Ozeanversauerung (> drei Monate) konzentrieren. Die Ergebnisse zeigten, dass (1) die Varianz im Rückgang des Korallenwachstums während der Ozeanversauerung durch unterschiedliche Veränderungen der Haltungsbedingungen und der zellulären Stressparameter entstanden ist. Dieses physiologische Zusammenspiel war gattungsspezifisch für *Acropora* und *Pocillopora* und artspezifisch für *Porites* spp. Darüber hinaus ergab die Auswertung des kombinierten Effektes von Ozeanversauerung und Wasserströmungen, dass (2) temporär verringerte Wasserströmungen die Effekte der Ozeanversauerung auf *Acropora* und *Porites* spp. abmildern können. Dennoch, führten gleichzeitige Veränderungen der Meerwasserchemie und der Wasserströmungen zu Veränderungen der Korallenphysiologie mit komplexen und artspezifischen Mustern. Schließlich ergab die mikroskopische Charakterisierung der Auswirkungen der Ozeanversauerung und der Wasserströmungen auf die Konzentrationsgrenzschicht an der Korallenoberfläche, dass (3) die Ozeanversauerung insgesamt ein schwacher Modulator dieser Schicht ist, unabhängig von den Strömungsbedingungen und der Variabilität der Konzentrationsgrenzschicht bei den untersuchten Korallenarten. Die Ergebnisse legen jedoch nahe, dass die Konzentrationsgrenzschicht aufgrund des geringen pH-Gradienten in dieser Schicht nur eine begrenzte Pufferkapazität gegen Ozeanversauerung hat. Eine geringe Wasserströmung könnte dennoch den Schutz durch die Konzentrationsgrenzschicht erhöhen, indem sie den pH-Wert an der Korallenoberfläche anhebt.

Zusammenfassend liefert diese Dissertation Beweise dafür, dass sowohl die artspezifische Physiologie als auch die Wasserströmungsbedingungen die Anfälligkeit von Korallen gegenüber der Ozeanversauerung prägen. Zudem liefert sie neue Einblicke in die Beziehungen zwischen der Korallenkolonie und ihrer Konzentrationsgrenzschicht. Darüber hinaus unterstreichen die Ergebnisse dieser Dissertation das Potenzial von Umgebungen mit geringer Strömung als Refugien für Korallenarten unter den Bedingungen der Ozeanversauerung. Sie heben des Weiteren die Bedeutung der Einbeziehung der Riffhydrodynamik in zukünftige Szenarien der Ozeanversauerung hervor, die die Berücksichtigung verschiedener räumlicher und zeitlicher

Skalen erfordern. Insgesamt tragen die hier gewonnenen Erkenntnisse dazu bei, die Vorhersagen über die Dynamik von Korallengemeinschaften unter dem Einfluss der zukünftigen Ozeanversauerung zu verbessern und Informationen für Schutzbemühungen zu liefern.

SYNTHESIS

1 Introduction

1.1 Ocean Acidification (OA)

The ocean is a key component of global biogeochemical cycles and is undergoing fundamental chemical changes, due to the exponential influx of anthropogenic CO_2 into the atmosphere since the beginning of the industrial period (Friedlingstein et al. 2025). Atmospheric CO_2 concentrations are currently 1.5 times the pre-industrial levels, with 72 % of this increase occurring over the last 60 years (Lan and Keeling 2026). As a major carbon sink for the atmosphere, the ocean has more than doubled its uptake of atmospheric CO_2 since the 1960s, driven by the increased atmospheric CO_2 concentration (Friedlingstein et al. 2025). This ocean CO_2 uptake, however, causes a process known as ocean acidification (OA), whereby seawater pH decreases and carbonate chemistry shifts (Doney et al. 2009). Specifically, higher levels of dissolved CO_2 in seawater result in increased concentrations of H^+ and HCO_3^- ions and increased dissolved inorganic carbon, alongside reduced pH, CO_3^{2-} ion concentration, and calcium carbonate mineral saturation states (Gattuso and Hansson 2011). Over the past two decades, surface ocean pH has been consistently decreasing (Canadell et al. 2021) with variable rates across regions (Sutton et al. 2019) driven by regional trends and global scale changes (Bindoff et al. 2019). Surface ocean aragonite saturation state has also been declining and has recently exceeded risk thresholds identified in the Planetary Boundary Framework (Findlay et al. 2025). During the current century, atmospheric CO_2 and OA are projected to continue to increase further with varying magnitude depending on a range of plausible future scenarios combining climatic and socio-economic factors assessed by the Intergovernmental Panel on Climate Change (IPCC; Lee et al. 2021).

1.2 Coral Reefs and OA

Tropical coral reefs are the most biodiverse marine ecosystems per unit area on the planet (Sala and Knowlton 2006; Knowlton et al. 2010), harbouring over one third of the global marine biodiversity (Fisher et al. 2015) (Fig. 1A). They typically occur in areas of warm, shallow water within the tropics (UNEP-WCMC et al. 2021) and provide crucial ecosystem services such as fisheries, coastal protection, and tourism (Woodhead et al. 2019) to almost one billion people worldwide (Sing Wong et al. 2022). These ecosystems, however, are among the most sensitive to climate change (Hoegh-Guldberg and Bruno 2010; Hoegh-Guldberg et al. 2017), leading to their ongoing decline (Souter et al. 2021). In particular, OA constitutes an important future threat to coral reefs (Doney et al. 2009) with potentially large effects on reef diversity and

functioning (Sunday et al. 2017; Noonan et al. 2018; Cornwall et al. 2021). This is primarily due to the effects of OA on reef-building corals, which are highly sensitive to this stressor (Leung et al. 2022) and constitute the main engineers of the framework that sustains coral reef ecosystems (Hofmann et al. 2010).

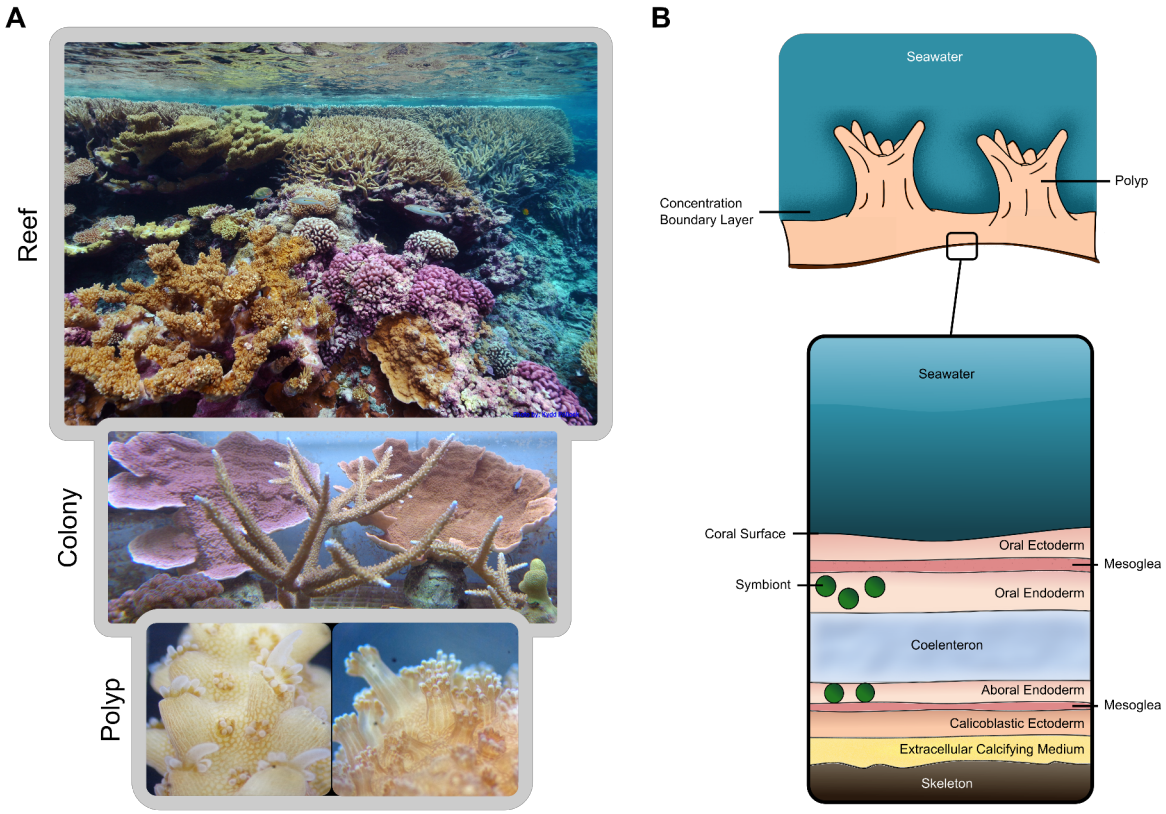

Figure 1. Reef-building corals. (A) Photographs of reef-building corals at different spatial scales, from large scale (reef) to small scale (polyp). At the colony scale, the centre image depicts colonies of *Montipora* (back), *Acropora* (centre), *Pocillopora* (front left), and *Porites* (front right). At the polyp scale, the bottom images depict polyps of *Acropora cytherea* (left) and *Pocillopora verrucosa* (right). Photo credits: (top) Kydd Pollock, cropped from original and used under CC BY 2.0 <https://creativecommons.org/licenses/by/2.0>, via Wikimedia Commons <https://commons.wikimedia.org/wiki/File:Coral_reef_98.jpg>; (centre and bottom) Catarina P. P. Martins. (B) Schematic representation of coral polyps surrounded by the concentration boundary layer, with a simplified diagram of the coral tissue structure. Different terms exist for oral ectoderm (epidermis), oral and aboral endoderm (gastrodermis), coelenteron (gastrovascular cavity or gastric cavity), calicoblastic ectoderm (calicoblastic epithelium or calicodermis), and extracellular calcifying medium (calcifying fluid) (compiled in Tambutté et al. 2011; Hughes et al. 2022). Illustration by Catarina P. P. Martins, redrawn with modifications after Tambutté et al. (2011).

1.3 Effects of OA on Reef-Building Corals

Reef-building corals (Phylum Cnidaria, Class Hexacorallia, Order Scleractinia) (WoRMS 2026) are colonial animals composed of interconnected clonal polyps (Sheppard et al. 2018) (Fig. 1A), which live in symbiosis with unicellular microalgae belonging to the family Symbiodiniaceae

(LaJeunesse et al. 2018) and a diverse consortium of other microorganisms (Bonacolta et al. 2023; Mohamed et al. 2023). Together, the coral host and its associated microorganisms are termed coral holobiont (Rohwer et al. 2002). Reef-building corals are characterised by their skeletons of aragonite (a metastable form of $CaCO_3$), which are produced through calcification at the base of the microenvironmentally complex coral tissue (Venn et al. 2025). Specifically, coral calcification occurs in a specialised compartment with a biologically-controlled medium known as 'calcifying fluid' or 'extracellular calcifying medium' (Tambutté et al. 2011) (Fig. 1B). Crucially, calcification is fundamental to both coral individual function and reef ecosystems, as it generates the complex, three-dimensional, wave-resistant reef structures that support the high reef biodiversity (Veron 2011).

In reef-building corals, OA generally decreases calcification rates (Chan and Connolly 2013; Kroeker et al. 2013) and skeletal density (Tambutté et al. 2015; Mollica et al. 2018), thereby impairing the ability of corals to build their skeleton. However, these organisms display a range of sensitivities to OA in their calcification responses. OA-induced decreases differ in magnitude among taxa (Kornder et al. 2018) and some species may even maintain calcification rates stable (e.g., Comeau et al. 2013). While this heterogeneity of responses is partially linked to differential abilities to mediate OA-induced shifts in the pH and carbonate chemistry of the calcifying fluid (Schoepf et al. 2017; Comeau et al. 2019b), OA effects on physiological parameters other than calcification could potentially contribute to it. However, such effects are also heterogenous among species (Sweet and Brown 2016; Godefroid et al. 2022). For instance, photosynthesis—the major source of energy for reef-building corals (Muscatine et al. 1981; Davies 1991)—has been reported to remain stable (e.g., Comeau et al. 2017), decrease (e.g., Bedwell-Ivers et al. 2017), and increase under OA (e.g., Noonan and Fabricius 2016). Other factors may also underlie the variability of coral responses to OA. Coral OA susceptibility is proposed to be influenced by life stage (Kleypas and Yates 2009), species-specific traits and physiology (e.g., tissue thickness and growth rates; Edmunds 2011; Comeau et al. 2014a), energetic status (Cohen and Holcomb 2009), and environmental conditions (Comeau and Cornwall 2017). Their respective role, however, remains largely unresolved (Kornder et al. 2018). Among these potential drivers, variability of environmental factors such as water flow is especially interesting due to its known influence on coral physiology (Hoogenboom et al. 2011) and could be key in the ability of species to mediate OA effects (Boyd et al. 2016; Putnam et al. 2017).

1.4 Reef Hydrodynamics and Coral Physiology

Coral reefs are environmentally heterogeneous and dynamic ecosystems where water flow is an important environmental gradient. Water flow shapes gradients of water temperature and chemistry, and it modulates reef metabolism and coral physiology (Shashar et al. 1996; Lowe

and Falter 2015). It is generated by surface waves, tides, and wind (as well as thermohaline processes and regional-scale ocean circulation in some cases) (Monismith 2007; Lowe and Falter 2015), and is modulated by reef topographic complexity. Reef morphology therefore alters the relative importance of these hydrodynamic factors within reefs, creating high spatial variation in water flow conditions (Madin et al. 2006; Davis et al. 2021). Thus, although coral reefs occur in high-energy environments, low flow velocities (< 5 cm s^{-1}) may be common in zones such as reef flats (e.g., Reid et al. 2020) and lagoons (e.g., Grimaldi et al. 2022). For example, a coral reef terrace with high coral cover may present flow velocities of 0–3 cm s^{-1} during a one-month period (Rogers et al. 2016). Reef water flow conditions also vary on long (seasonally and annually) and short timescales (hours and days). For instance, within individual reef locations, flow velocities may range from 0–30 cm s^{-1} over one year (Roik et al. 2016) and from 0–10 cm s^{-1} during a diel cycle, with changes associated with tidal stages (Green et al. 2018).

In reef-building corals, water flow can affect coral respiration (e.g., Patterson et al. 1991), photosynthesis (e.g., Lesser et al. 1994), calcification (e.g., Edmunds and Burgess 2018), morphology (e.g., Chindapol et al. 2013), prey capture (e.g., Sebens et al. 1998), nutrient uptake (e.g., Thomas and Atkinson 1997), metabolic waste removal (Armoza-Zvuloni and Shaked 2014), transcriptomics (Fifer et al. 2021), reproduction (Jokiel 1978; Mass et al. 2011), larvae swimming and settlement (e.g., Iwasaki et al. 2018; Levenstein et al. 2022), coral–algal and coral–coral interactions (Brown and Carpenter 2015; Jorissen et al. 2016; McWilliam et al. 2018), heat exchange (Jimenez et al. 2011; Stocking et al. 2018), and bleaching sensitivity (e.g., Nakamura and Van Woesik 2001). Water flow generally influences coral physiology by modulating the coral concentration boundary layer (CBL; Noisette et al. 2022) (Fig. 1B). This is a thin layer of seawater that surrounds the coral surface and controls mass transfer between the coral colony and surrounding seawater (Jørgensen and Revsbech 1985). From the coral surface down to the calicodermis (Fig. 1B), reef-building corals possess cilia across all tissue layers (Tambutté et al. 2021). These cilia exhibit variable structure and likely have distinct functions (Mariscal 1974; Shapiro et al. 2014; Tambutté et al. 2021). At the coral surface, specifically, mobile cilia can modulate the CBL, particularly under low bulk flow conditions (Shapiro et al. 2014; Pacherres et al. 2020).

1.5 Effects of Water Flow on Coral Responses to OA

Water flow may also modulate coral physiological responses to OA. However, the combined effects of OA and flow appear complex, potentially interactive and species-specific, and differ with scale and exposure time. At the community scale, increased water flow generally alleviates OA-induced decreases in community calcification (Anthony et al. 2013; Comeau et al. 2014b, 2016), although the spacing of individuals within a community may alter this effect (Evensen

and Edmunds 2017). In contrast, OA-induced decreases in net photosynthesis and increases in respiration of a coral community of *Acropora aspera* were marginally larger with increased flow (Anthony et al. 2013). At the colony scale, increased water flow may alleviate OA effects on calcification in some species and have the opposite effect on others (Comeau et al. 2019a). Moreover, increased water flow has also been reported to both alleviate and exacerbate the effects of two-month OA exposure on net photosynthesis, depending on coral species (Comeau et al. 2019a), with no effect observed during 1-h short-term OA exposure (Osinga et al. 2017). Finally, at the microscale, flow and OA effects on the CBL appear to be interactive and species-specific after over four months under OA (Comeau et al. 2019a), with some species reportedly already displaying effects during 30-min exposure to OA (Chan et al. 2016).

2 Rationale

2.1 Lack of Knowledge

The effects of OA on reef-building corals are characterised by being species-specific (reviewed in Krämer et al. 2022). This range of coral susceptibilities to OA is proposed to be influenced by a diverse set of factors (Kornder et al. 2018), including species physiology (Comeau et al. 2014a) and water flow conditions (Comeau et al. 2014b). However, the role of these two factors remains overall poorly understood. Understanding the differential ability of reef-building corals to cope with OA and identifying factors capable of alleviating OA challenges is crucial due to the potential of species-specific OA susceptibility to lead to altered future reefs (Evensen et al. 2021), with potential downstream losses in coral reef ecosystem functioning and services (Doney et al. 2020).

2.2 General and Specific Objectives

The overarching objective of this doctoral thesis is to elucidate the factors underlying the differential susceptibility of the major reef-building coral genera *Acropora*, *Pocillopora*, and *Porites* to OA. Using an experimental, multi-scale approach, this thesis specifically aims to:

1) Test whether the ability to compensate OA effects on coral growth involves physiological processes other than calcification and whether physiological patterns differ among genera and species. This objective investigates the role of species physiology in determining coral susceptibility to OA.

2) Test whether water flow conditions modulate the effects of OA on colony physiology and influence coral susceptibility to OA.

3) Test whether water flow conditions modulate the effects of OA on the coral CBL. This objective investigates the coral CBL and changes at this scale as a potential underlying mechanism of the effects of water flow on colony responses to OA.

3 Publication Outlines

This cumulative doctoral thesis consists of three peer-reviewed, published manuscripts and one manuscript submitted to a peer-reviewed journal. The first and second manuscripts address the first and second specific aims of the thesis, respectively, and the last two manuscripts focus on the third specific aim of the thesis. To address this last aim, I first characterise in detail the variability of the coral CBL among species (Manuscript III). Then, using the knowledge developed in the third manuscript to accurately characterise coral CBL traits, I investigate the effects of OA and water flow on the coral CBL (Manuscript IV).

3.1 Coral Physiological Interplay During Stress (Manuscript I)

Martins CPP, Arnold AL, Kömpf K, Schubert P, Ziegler M, Wilke T, Reichert J (2022) Growth response of reef-building corals to ocean acidification is mediated by interplay of taxon-specific physiological parameters. *Frontiers in Marine Science* 9:872631. DOI: 10.3389/fmars.2022.872631

Outline

This study focuses on species physiology as a potential mediating factor of coral susceptibility to OA. Here, we assessed multiple physiological parameters of six reef-building coral species belonging to the genera *Acropora*, *Pocillopora*, and *Porites* exposed to control and OA conditions for three months. The results showed differential decreases in coral growth among species under OA, which occurred alongside changes in maintenance and cellular stress parameters. In addition, physiological changes were genus-specific for *Acropora* and *Pocillopora*, and species-specific for *Porites*. Overall, in this study we establish that coral susceptibility to OA differs among three major reef-building coral genera, mediated by a differential interplay of physiological parameters.

Author contributions

PS, TW, and JR designed the study. AA and KK performed the experiment, with assistance from PS and JR. **CM** curated and analysed the data and prepared the figures and tables. TW secured funding. **CM** drafted the manuscript with assistance from MZ and JR. **CM**, PS, MZ, TW, and JR contributed to writing, reviewing, and editing of the final manuscript.

3.2 Flow Effects on Corals Under OA (Manuscript II)

Martins CPP, Simancas-Giraldo SM, Schubert P, Wall M, Wild C, Wilke T, Ziegler M (2024) Short periods of decreased water flow may modulate long-term ocean acidification in reef-building corals. Preprint (Version 1) at *bioRxiv*. DOI: 10.1101/2024.02.23.581783 *Submitted to the peer-reviewed journal Marine Biology*.

Outline

This study investigates the role of hydrodynamics in coral susceptibility to OA. Specifically, the three species *Acropora cytherea*, *Pocillopora verrucosa*, and *Porites cylindrica*, belonging to the three coral genera studied in Manuscript I, were exposed to control and OA conditions for three months and their physiological responses to changes in water flow were assessed. All species showed decreased calcification and growth rates, which constitutes a typical coral response to long-term exposure to OA. Temporarily reduced water flow modulated coral physiological responses to OA in complex and species-specific patterns, mitigating OA effects on *A. cytherea* and *P. cylindrica*. These findings highlight that the combination of long-term OA exposure in the variable hydrodynamic conditions of coral reefs may lead to complex biological outcomes.

Author contributions

CM and MZ designed the study. **CM** and SS performed the experiment, with assistance from PS. **CM** analysed the data and prepared the figures and tables. TW secured funding. **CM** drafted the manuscript with assistance from MZ. All authors contributed to writing, reviewing, and editing of the final manuscript.

3.3 Variability of Coral Concentration Boundary Layers (Manuscript III)

Martins CPP, Wall M, Schubert P, Wilke T, Ziegler M (2024) Variability of the surface boundary layer of reef-building coral species. *Coral Reefs* 43:1223–1233. DOI: 10.1007/s00338-024-02531-7

Outline

This study provides baseline insights into the variability of the coral CBL. Using microsensors, over 100 profiles of dissolved O_2 concentration at the coral surface were recorded in the three reef-building coral species *A. cytherea*, *P. verrucosa*, and *P. cylindrica*, investigated in Manuscript II. We characterised the O_2 CBL under light and darkness and different water flow conditions. The results revealed that CBL traits differed between species. In addition, O_2 gradients in the CBL occurred in different profile shapes. The formation of these profiles differed in prevalence among species and was generally dependent on flow conditions. Overall, in this study we demonstrate that CBL traits may differ among small-polyped reef-building corals and establish that the three species investigated in this thesis have different CBLs.

Author contributions

CM, MW, and MZ designed the study. **CM** collected and analysed the data and prepared the figures and tables. **CM** performed coral care and maintenance with assistance from PS. MW provided the microsensor measuring system. TW secured funding. **CM** drafted the manuscript

with assistance from MZ. All authors contributed to writing, reviewing, and editing of the final manuscript.

3.4 Coral Boundary Layers Under OA (Manuscript IV)

Martins CPP, Ziegler M, Schubert P, Wilke T, Wall M (2024) Effects of water flow and ocean acidification on oxygen and pH gradients in coral boundary layer. *Scientific Reports* 14:12757. DOI: 10.1038/s41598-024-63210-9

Outline

This study investigates CBL changes as a potential mechanism underlying the effects of water flow on coral responses to OA. Here, the species *A. cytherea*, *P. verrucosa*, and *P. cylindrica*, investigated in Manuscript II and III, were preconditioned to control and OA conditions for four months and the effects of temporarily reduced water flow on O_2 and H^+ CBL traits were assessed. Our results show that the coral CBL is strongly influenced by changes in water flow but reveal OA as a weak to null modulator of the CBL, even after prolonged exposure. Still, we observed species-specific interactive effects of flow and OA on O_2 CBL thickness, which might underlie differences in colony-level responses. Furthermore, we characterised coral H^+ CBL thickness under OA for the first time and documented the absence of a significantly differentiated pH microenvironment separating the coral from bulk seawater under OA. Overall, in this study we establish that small-polyped reef-building corals may not rely on their pH boundary layer to alleviate OA challenges, though temporarily reduced flow may enhance CBL sheltering.

Author contributions

CM, MZ, and MW designed the study. **CM** performed the experiment with assistance from PS. **CM** collected and analysed the data and prepared the figures and tables. MW provided the microsensor measuring system. TW secured funding. **CM** drafted the manuscript with assistance from MW. All authors contributed to writing, reviewing, and editing of the final manuscript.

4 Discussion

The studies presented in this thesis explore the role of species physiology and hydrodynamics as potential mediating factors of coral responses to OA. Overall, these studies provide evidence of the differential mediating effects of these two factors, shaping different susceptibility among coral species with potential complex downstream consequences in reef composition and functioning.

4.1 Differential Interplay of Physiological Parameters Under OA

The physiological patterns underlying the variability of coral growth responses to OA is a challenging but meaningful aspect of understanding OA effects on reef-building corals. The first study of this thesis aimed to unravel these patterns using six reef-building coral species and revealed a mediation of coral growth under OA by differential changes in physiological parameters. Specifically, the results indicate that the decrease in growth under OA was mediated differently in *Acropora* and *Pocillopora* but was unmediated in *Porites* spp. Both *Acropora* spp. maintained coral growth under OA at the expense of elevated cellular stress, which is in line with previous reports of up-regulated gene expression patterns of caspase and caspase-like enzymes in *Acropora* spp. (Kaniewska et al. 2012, 2015). These findings point to an unsuccessful acclimatisation to OA of *Acropora*, which might underlie the reported low coral cover of *Acropora* spp. at CO_2 seeps (Fabricius et al. 2011; Strahl et al. 2015). In contrast, the physiological changes observed in *Pocillopora* spp. and *Porites lutea* indicate a successful acclimatisation via marginally decreased energy reserves and increased tissue thickness. Tissue thickening, in particular, may serve as a mediating strategy against OA effects by creating a larger pH-regulated separation between the calicodermis and ambient seawater (Krief et al. 2010; Edmunds 2011), which could indicate a focus on pH regulation. Given the absence of a cellular stress response in these taxa here and their presence in some CO_2 seeps (Comeau et al. 2022), this may be a costly yet sustainable strategy, enabling endurance without compromising survival. Finally, *P. cylindrica* presented a different pattern, which consisted of decreased volume growth without major changes of the underlying physiological parameters. This pattern could be common to branching *Porites* spp. during prolonged stress (McLachlan et al. 2022) and constitute a strategy that increases colony survival at the expense of growth and by suppressing cellular stress alarms. Interestingly, while branching *Porites* spp. are rarely reported at CO_2 seeps (e.g., Fabricius et al. 2011), they may occur at other naturally acidified sites (Crook et al. 2012), where *P. cylindrica* may be a dominant coral species (Kurihara et al. 2021). Overall, the findings of Manuscript I indicate that reef-building coral species employ different physiological strategies to cope with OA, which can lead to ecological shifts and altered ecosystems in future oceans (Cornwall et al. 2024).

4.2 Decreased Water Flow as a Potential Mitigating Factor of OA

In the second study of this thesis, the physiological coral response to changes in water flow under conditions of ambient pH and OA was assessed. This study revealed complex results, which indicated that water flow may modulate OA effects on coral physiology with species-specific patterns. In particular, three-month monitoring of coral P:R ratio responses revealed a decrease in *A. cytherea* and *P. cylindrica* at moderate flow, while in *P. verrucosa*, the P:R ratio remained stable regardless of flow conditions. Interestingly, taken together with the findings of Manuscript I, the results of *P. verrucosa* could indicate that the mobilisation of energy reserves in this species can meet its energy demands under OA, while maintaining a stable balance between energy production and consumption. A key aspect to achieve this might be the ability of pocilloporids to enhance the efficiency of basal metabolic processes under OA (Vidal-Dupiol et al. 2013; Liew et al. 2018). Conversely, OA-induced decreases in P:R ratios observed here in *A. cytherea* and *P. cylindrica*, but also in other species (Bahr et al. 2018), suggest an increasing reliance on heterotrophically fixed energy under OA. The species patterns observed here could thus be associated with variable trophic dependence. In line with this hypothesis, *Acropora* and *Porites* spp. possess a lower contribution from heterotrophic feeding and physiological plasticity than *Pocillopora* spp. (Hoogenboom et al. 2015; Radice et al. 2019), which are characterised by a trophic mode associated with lower susceptibility to other environmental stress, such as high temperature (Conti-Jerpe et al. 2020).

The interactive effects of OA and flow in *A. cytherea* and *P. cylindrica* observed in the current study support existing frameworks of stronger effects under moderate flow than low flow (Hurd 2015). This could be related to the thickening of the coral CBL under low flow (Kühl et al. 1995), which is proposed to mitigate OA effects by providing a larger buffer between the coral and acidified surrounding seawater, as well as create localised environmental fluctuation that could potentially enhance OA resilience (Hurd 2015; Chan et al. 2016; Noisette et al. 2022). However, the role of flow in reef-building corals under OA may be species-specific. While the results presented here for *A. cytherea* are in agreement with previously observed low-flow mitigation of OA effects on calcification of *Acropora yongei* (Comeau et al. 2019a), other coral species have displayed alleviated effects under moderate flow (Osinga et al. 2017; Comeau et al. 2019a). Overall, the findings of the present study underline the importance of water flow conditions in the coral response to OA and support the inclusion of certain coral species among the calcifying organisms for which low-flow environments may constitute refugia from OA (Hurd 2015).

4.3 The Role of Boundary Layers Under OA and the Influence of Water Flow

The third and fourth studies of this thesis aimed to investigate the CBL of *A. cytherea*, *P. verrucosa*, and *P. cylindrica*, and its role in the coral response to OA and water flow. The detailed

characterisation of the CBL of these three small-polyped species performed in Manuscript III showed that CBL traits differed between species and revealed that O_2 gradients in the coral CBL had different profile shapes—diffusive, S-shaped, and complex (Fig. 2A). These profile types differed in CBL thickness and flux, and occurred with varying frequency between species. S-shaped and complex profiles largely corresponded to the profile shapes created by the activity of cilia on the coral surface (Shapiro et al. 2014; Pacherres et al. 2020). Therefore, the different frequency of profile types between species and the resulting variability in CBL traits could be due to differences in cilia characteristics and activity (Lewis and Price 1976), as well as small-scale morphological complexity (Reichert et al. 2017; Hossain and Staples 2020). Crucially, CBL variability may have potential downstream consequences on colony physiology due to its role in mass transfer limitation (Falter et al. 2004) and has been proposed to underlie the range of coral susceptibilities to climate change (Putnam et al. 2017). However, the findings of the fourth study of this thesis, which investigated the effects of OA and water flow on the coral CBL, suggest a potentially complex relationship between CBL dynamics and OA susceptibility.

Manuscript IV constitutes the first study to investigate the effects of prolonged OA on coral O_2 CBL thickness and flux, and only the second study overall, following a prior study assessing the effects of 30-min exposure in the large-polyped coral *Favites* sp. (Chan et al. 2016). The results of Manuscript IV revealed that while water flow strongly modulated the coral CBL, consistent with previous studies (e.g., Kühl et al. 1995), OA had a comparatively weaker to null effect (Fig. 2B). Under OA, CBL traits remained stable, except O_2 CBL thickness and flux, which showed species-specific effects, and surface pH, which was lower across species. In *A. cytherea*, OA effects on O_2 CBL thickness were also interactive with flow, showing a CBL thickening under OA combined with low flow. This effect at the CBL scale could explain the OA-decreased P:R ratio documented in *A. cytherea* in Manuscript II and could be associated with changes in cilia activity, observed previously in bivalves (Ertl et al. 2016; Meseck et al. 2020). However, OA effects on O_2 CBL thickness may be species-specific and differentially modulated by water flow, as evidenced by contrasting patterns observed previously in *Favites* sp. (Chan et al. 2016). Furthermore, the fourth study presented here demonstrates that some species may maintain O_2 flux stable even after prolonged exposure to OA (as observed in *P. verrucosa* and *P. cylindrica*), while others experience a reduction (as seen in *A. cytherea*). Again, these OA effects on the CBL of *A. cytherea* might help explain its OA-decreased net photosynthesis documented in Manuscript II and for other acroporids (e.g., Anthony et al. 2008; Kaniewska et al. 2012), highlighting a potential link in the response of *Acropora* spp. to OA from the microscale to the colony level.

Manuscript IV is also the first report of the thickness dynamics of the coral H^+ CBL under OA. In this study, the H^+ CBL was markedly thin across species and led to lower surface pH, indicating

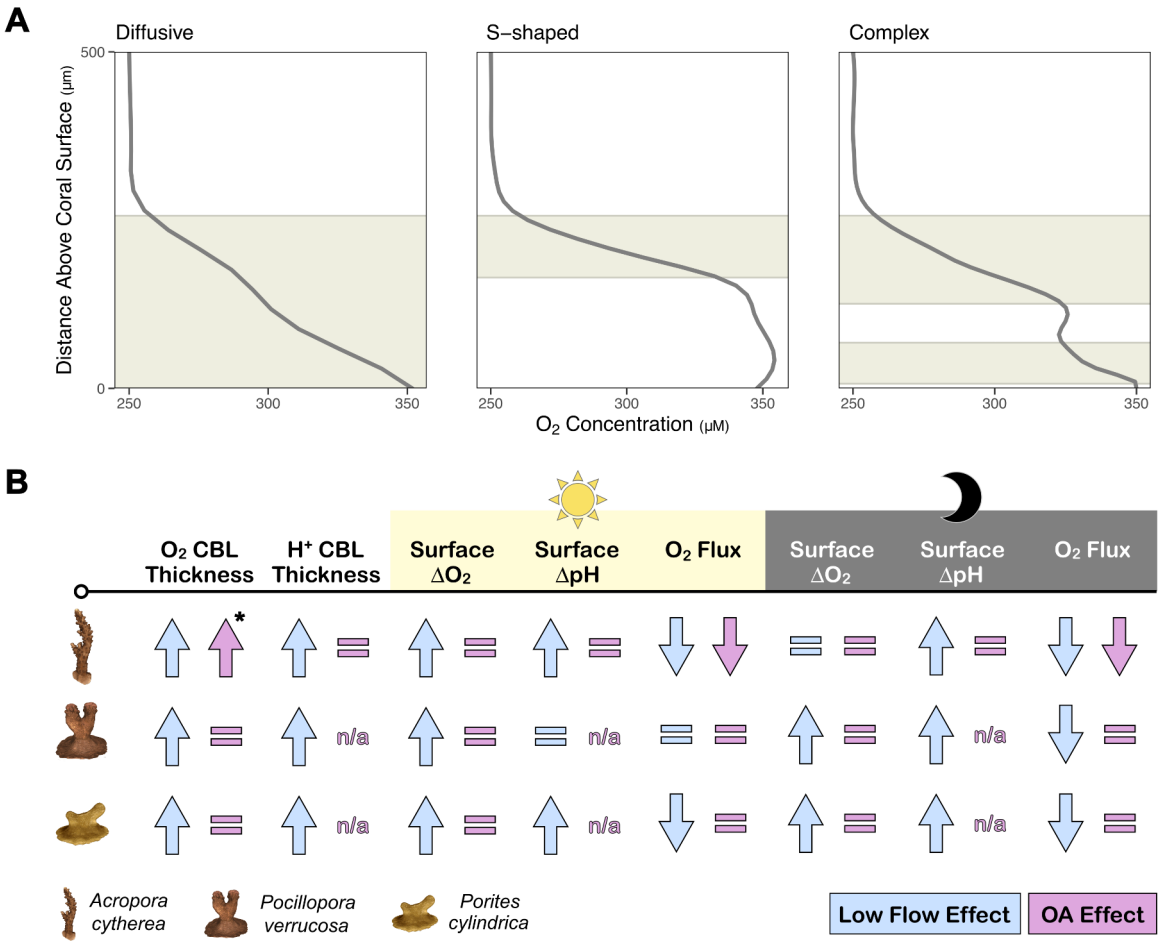

Figure 2. The concentration boundary layer of reef-building corals and the effects of ocean acidification and hydrodynamics. (A) Schematic profile representing O_2 concentration gradients across the concentration boundary layer (CBL) with three types of profile structure (diffusive, S-shaped, and complex). Diagrams represent profiles under light conditions and shaded areas mark regions where mass transport is dominantly diffusive. Figure reproduced with minor modifications from Martins et al. (2024b). (B) Summary diagram of the effects of ocean acidification (OA) and water flow on traits of the CBL of *Acropora cytherea*, *Pocillopora verrucosa*, and *Porites cylindrica*. Effects on CBL thickness are presented pooled over light conditions, while the difference between the coral surface and bulk seawater in O_2 concentration (surface ΔO_2) and pH (surface ΔpH), and O_2 flux are presented in light and darkness. Asterisk indicates OA effects present exclusively under low flow conditions. n/a, not available. Figure reproduced with minor modifications from Martins et al. (2024a).

that it did not mitigate OA challenges. Even so, low flow may enhance CBL sheltering from acidified seawater by thickening H^+ CBLs and mildly elevating surface pH in light. Overall, these findings nonetheless suggest that H^+ CBL variability may not underlie differential coral susceptibility to OA, which differed between the three investigated species, as shown in Manuscript I and II and supported by meta-analyses (Kornder et al. 2018). This was particularly discernible when OA effects on *P. verrucosa* at the different investigated scales were integrated. Although *P. verrucosa* under OA presented the smallest elevation of surface pH and the largest pH reduction in darkness, this did not coincide with greater colony susceptibility to OA. As

documented in Manuscript I and II, OA-induced reductions in calcification and growth in *Pocillopora* spp. were overall similar to those of *Porites* spp. and smaller than in *Acropora* spp. Instead, *P. verrucosa* showed reduced energy reserves trends, which were not present in *Acropora* and *Porites* spp. (Manuscript I) and could indicate an energetically costly increased regulation of internal pH. This regulation, which involves ion channels (Zoccola et al. 2015; Capasso et al. 2021; Rangel-Yescas et al. 2021) and paracellular transport (Venn et al. 2020), is upregulated in pocilloporids under OA (Vidal-Dupiol et al. 2013). Yet, its full extent remains unclear. While strong pH regulation is observed at the calcification site of the pocilloporid *Stylophora pistillata* (Venn et al. 2022), pH gradients in its other compartments remain uncharacterised under OA, likely varying also with light and colony area (Crovetto et al. 2024). However, knowledge of these gradients is essential for accurately estimating the energetic costs of pH regulation (Yuan et al. 2018). Specifically, costs may be underestimated by models based on the pH difference between bulk seawater and the calcifying fluid (McCulloch et al. 2012), which can be smaller than the gradients between tissue compartments under OA (Yuan et al. 2018; Venn et al. 2022). Altogether, the findings documented here reveal the absence of a buffer against acidified seawater at the surface of major reef-building corals and further support species-specific internal pH regulation (Venn et al. 2019) as an important aspect of coral susceptibility to OA (Cornwall et al. 2024).

4.4 Implications and Future Work

Overall, this thesis furthers a holistic understanding of taxon-specific coral susceptibility to OA, which may enable more realistic projections of coral community dynamics under climate change (Kim et al. 2023). This is particularly relevant for projections that include OA scenarios due to the large genus- and species-specific component of OA effects, evidenced in this thesis in Manuscripts I and II. Including taxonomically variable responses to OA and multiple physiological parameters can thus improve the modelling of future coral performance and community dynamics across large spatio-temporal scales (Evensen et al. 2021; Klein et al. 2022). However, OA effects on coral physiology also vary at colony level (e.g., Kavousi et al. 2016; Manullang et al. 2024). Therefore, future studies that assess the variability of colony responses, which is proving to be key in the coral response to heat stress (e.g., Drury et al. 2022), will be important to better understand the intraspecific component of coral OA responses and further refine projections.

The findings of this thesis may also inform management and conservation efforts. Refuge areas can be an effective technique from the portfolio of actions needed to manage coral reefs for future OA (Albright and Cooley 2019). Reef hydrodynamics, specifically, are heavily involved in the formation of environments that may provide refuge from climate change (Noisette et al. 2022). However, while the findings of Manuscript II and IV indicate that low flow could

alleviate OA effects on coral species, low flow conditions could become less frequent in future reefs due to surface ocean acceleration (Peng et al. 2022) and sea level rise (Storlazzi et al. 2018). Yet, low-flow areas and periods are unlikely to disappear in future reefs (East et al. 2020). Therefore, future changes to reef hydrodynamics make the inclusion of low-flow refuge areas all the more important in coral reef conservation strategies that address OA challenges on coral species. Beyond conservation, the findings of this thesis may also support restoration efforts by informing reef site selection (Schill et al. 2021) that address specific intervention objectives (Pascoe et al. 2024), particularly in areas affected by coastal acidification (Meléndez et al. 2020). Nonetheless, as presented in this thesis, understanding the combined effects of OA and flow remains a challenging undertaking given their complex, species-specific nature. Thus, further research is yet needed to better establish which coral species can benefit from low-flow refugia.

Since OA is not an isolated phenomenon, the management of coral reefs for future climate change will undoubtedly need to address challenges brought on by multiple stressors and in particular, ocean warming. Reef hydrodynamics can also mediate coral responses to heat stress (Page et al. 2019), potentially leading to opposite bleaching outcomes such as mortality versus recovery (Lentz et al. 2024). However, in contrast to OA, the effects of thermal stress on coral species may be stronger under low flow than moderate flow (Nakamura and Van Woesik 2001; Page et al. 2021), with recovery from bleaching responses also occurring faster under high flow (Nakamura et al. 2003; Fifer et al. 2021). Nonetheless, field studies have also found lower bleaching intensity at lagoon sites than high-flow environments (McClanahan et al. 2007; Hoogenboom et al. 2017), which may not be the case across all reefs (e.g., Ainsworth et al. 2021). Therefore, coral reef conservation strategies to address climate change will likely benefit from a diverse portfolio of refuge areas to balance trade-offs, using multi-step decision frameworks based on cost-benefit approaches (e.g., Viehman et al. 2023) to design reef-specific strategies.

5 Conclusions

Overall, the results of this thesis indicate that both species physiology and water flow conditions shape coral susceptibility to OA in species-specific patterns. Species with lower susceptibility presented physiological strategies that involved increased metabolic maintenance, while low flow conditions potentially mitigated OA effects on species with higher susceptibility. Exploring OA and flow effects at both the colony level and microscale, this thesis advances our understanding of taxon-specific susceptibility to OA, while also providing novel baseline knowledge about the coral CBL. Specifically:

1) Assessment of the OA effects on multiple physiological parameters in six reef-building corals showed that variable OA-induced decreases in coral growth were mediated by differential changes in maintenance and cellular stress parameters. These results indicated that the decrease in growth under OA was mediated differently in *Acropora* and *Pocillopora* spp. but was unmediated in *Porites* spp. with species-specific physiological changes. These findings improve our ability to better predict coral susceptibility to OA and coral community dynamics under climate change.

2) Examination of the effects of OA and changes in water flow on colony physiology revealed complex results, which suggested that temporarily reduced water flow may modulate OA effects with species-specific patterns. In particular, *A. cytherea* and *P. cylindrica* displayed decreased P:R ratio responses under OA when combined with moderate flow, indicating that OA effects were potentially mitigated under temporarily reduced water flow and that low-flow environments may serve as potential OA refugia for these species.

3) Characterisation of the CBL and its response to OA and water flow showed that *A. cytherea*, *P. verrucosa*, and *P. cylindrica* differed in CBL traits and revealed an overall minor effect of OA on the coral CBL, with species-specific interactive flow and OA effects on certain traits. Yet, the CBL was strongly modulated by flow and in particular, low flow conditions potentially enhanced CBL sheltering from acidified seawater. Moreover, leading investigation of H^+ CBL traits revealed the absence of a significantly differentiated pH microenvironment separating the coral from bulk seawater under OA. These findings shine light on the limited OA-buffering capacity of the CBL of reef-building coral species and underline the value of multi-scale approaches to further a mechanistic understanding of coral susceptibility to OA.

6 References

Ainsworth TD, Leggat W, Silliman BR, Lantz CA, Bergman JL, Fordyce AJ, Page CE, Renzi JJ, Morton J, Eakin CM, Heron SF (2021) Rebuilding relationships on coral reefs: Coral bleaching knowledge-sharing to aid adaptation planning for reef users. BioEssays 43:2100048. DOI: 10.1002/bies.202100048

Albright R, Cooley S (2019) A review of interventions proposed to abate impacts of ocean acidification on coral reefs. Reg Stud Mar Sci 29:100612. DOI: 10.1016/j.rsma.2019.100612

Anthony KRN, Kline DI, Diaz-Pulido G, Dove S, Hoegh-Guldberg O (2008) Ocean acidification causes bleaching and productivity loss in coral reef builders. Proc Natl Acad Sci 105:17442–17446. DOI: 10.1073/pnas.0804478105

Anthony KRN, Diaz-Pulido G, Verlinden N, Tilbrook B, Andersson AJ (2013) Benthic buffers and boosters of ocean acidification on coral reefs. Biogeosciences 10:4897–4909. DOI: 10.5194/bg-10-4897-2013

Armoza-Zvuloni R, Shaked Y (2014) Release of hydrogen peroxide and antioxidants by the coral *Stylophora pistillata* to its external milieu. Biogeosciences 11:4587–4598. DOI: 10.5194/bg-11-4587-2014

Bahr KD, Rodgers KS, Jokiel PL (2018) Ocean warming drives decline in coral metabolism while acidification highlights species-specific responses. Mar Biol Res 14:924–935. DOI: 10.1080/17451000.2018.1551616

Bedwell-Ivers HE, Koch MS, Peach KE, Joles L, Dutra E, Manfrino C (2017) The role of *in hospite* zooxanthellae photophysiology and reef chemistry on elevated pCO_2 effects in two branching Caribbean corals: *Acropora cervicornis* and *Porites divaricata*. ICES J Mar Sci 74:1103–1112. DOI: 10.1093/icesjms/fsw026

Bindoff NL, Cheung WWL, Kairo JG, Arístegui J, Guinder VA, Hallberg R, Hilmi N, Jiao N, Karim MS, Levin L, O'Donoghue S, Purca Cuicapusa SR, Rinkevich B, Suga T, Tagliabue A, Williamson P (2019) Changing ocean, marine ecosystems, and dependent communities. In: Pörtner H-O, Roberts DC, Masson-Delmotte V, Zhai P, Tignor M, Poloczanska E, Mintenbeck K, Alegría A, Nicolai M, Okem A, Petzold J, Rama B, Weyer NM (eds) IPCC special report on the ocean and cryosphere in a changing climate. Cambridge University Press, Cambridge, UK and New York, NY, USA, pp 447–588

Bonacolta AM, Weiler BA, Porta-Fitó T, Sweet M, Keeling P, del Campo J (2023) Beyond the Symbiodiniaceae: Diversity and role of microeukaryotic coral symbionts. Coral Reefs 42:567–577. DOI: 10.1007/s00338-023-02352-0

Boyd PW, Cornwall CE, Davison A, Doney SC, Fourquez M, Hurd CL, Lima ID, McMinn A (2016) Biological responses to environmental heterogeneity under future ocean conditions. Glob Chang Biol 22:2633–2650. DOI: 10.1111/gcb.13287

Brown AL, Carpenter RC (2015) Water flow influences the mechanisms and outcomes of interactions between massive *Porites* and coral reef algae. Mar Biol 162:459–468. DOI: 10.1007/s00227-014-2593-5

Canadell JG, Monteiro PMS, Costa MH, Cotrim da Cunha L, Cox PM, Eliseev AV, Ishii M, Jaccard S, Koven C, Lohila A, Patra PK, Piao S, Rogelj J, Syampungani S, Zaehle S, Zickfeld K (2021) Global carbon and other biogeochemical cycles and feedbacks. In: Masson-Delmotte V, Zhai P, Pirani A, Connors SL, Péan C, Berger S, Caud N, Chen Y, Goldfarb L, Gomis MI, Huang M, Leitzell K, Lonnoy E, Matthews JBR, Maycock TK, Waterfield T, Yelekçi O, Yu R, Zhou B (eds) Climate change 2021: The physical science basis. Contribution of Working Group I to the sixth assessment report of the Intergovernmental Panel on Climate Change. Cambridge University Press, Cambridge, UK and New York, NY, USA, pp 673–816

Capasso L, Ganot P, Planas-Bielsa V, Tambutté S, Zoccola D (2021) Intracellular pH regulation: Characterization and functional investigation of H^+ transporters in *Stylophora pistillata*. BMC Mol Cell Biol 22:18. DOI: 10.1186/s12860-021-00353-x

Chan NCS, Connolly SR (2013) Sensitivity of coral calcification to ocean acidification: A meta-analysis. Glob Chang Biol 19:282–290. DOI: 10.1111/gcb.12011

Chan NCS, Wangpraseurt D, Kühl M, Connolly SR (2016) Flow and coral morphology control coral surface pH: Implications for the effects of ocean acidification. Front Mar Sci 3:1–11. DOI: 10.3389/fmars.2016.00010

Chindapol N, Kaandorp JA, Cronemberger C, Mass T, Genin A (2013) Modelling growth and form of the scleractinian coral *Pocillopora verrucosa* and the influence of hydrodynamics. PLoS Comput Biol 9:e1002849. DOI: 10.1371/journal.pcbi.1002849

Cohen A, Holcomb M (2009) Why corals care about ocean acidification: Uncovering the mechanism. Oceanography 22:118–127. DOI: 10.5670/oceanog.2009.102

Comeau S, Cornwall CE (2017) Contrasting effects of ocean acidification on coral reef "animal forests" versus seaweed "kelp forests." In: Rossi S, Bramanti L, Gori A, Orejas C (eds) Marine animal forests. Springer International Publishing, Cham, pp 1083–1107

Comeau S, Edmunds PJ, Spindel NB, Carpenter RC (2013) The responses of eight coral reef calcifiers to increasing partial pressure of CO_2 do not exhibit a tipping point. Limnol Oceanogr 58:388–398. DOI: 10.4319/lo.2013.58.1.0388

Comeau S, Edmunds PJ, Spindel NB, Carpenter RC (2014a) Fast coral reef calcifiers are more sensitive to ocean acidification in short-term laboratory incubations. Limnol Oceanogr 59:1081–1091. DOI: 10.4319/lo.2014.59.3.1081

Comeau S, Edmunds PJ, Lantz CA, Carpenter RC (2014b) Water flow modulates the response of coral reef communities to ocean acidification. Sci Rep 4:1–6. DOI: 10.1038/srep06681

Comeau S, Lantz CA, Edmunds PJ, Carpenter RC (2016) Framework of barrier reefs threatened by ocean acidification. Glob Chang Biol 22:1225–1234. DOI: 10.1111/gcb.13023

Comeau S, Carpenter RC, Edmunds PJ (2017) Effects of pCO_2 on photosynthesis and respiration of tropical scleractinian corals and calcified algae. ICES J Mar Sci 74:1092–1102. DOI: 10.1093/icesjms/fsv267

Comeau S, Cornwall CE, Pupier CA, DeCarlo TM, Alessi C, Trehern R, McCulloch MT (2019a) Flow-driven micro-scale pH variability affects the physiology of corals and coralline algae

under ocean acidification. Sci Rep 9:12829. DOI: 10.1038/s41598-019-49044-w

Comeau S, Cornwall CE, DeCarlo TM, Doo SS, Carpenter RC, McCulloch MT (2019b) Resistance to ocean acidification in coral reef taxa is not gained by acclimatization. Nat Clim Chang 9:477–483. DOI: 10.1038/s41558-019-0486-9

Comeau S, Cornwall CE, Shlesinger T, Hoogenboom M, Mana R, McCulloch MT, Rodolfo-Metalpa R (2022) pH variability at volcanic CO_2 seeps regulates coral calcifying fluid chemistry. Glob Chang Biol 28:2751–2763. DOI: 10.1111/gcb.16093

Conti-Jerpe IE, Thompson PD, Wong CWM, Oliveira NL, Duprey NN, Moynihan MA, Baker DM (2020) Trophic strategy and bleaching resistance in reef-building corals. Sci Adv 6:eaaz5443. DOI: 10.1126/sciadv.aaz5443

Cornwall CE, Comeau S, Kornder NA, Perry CT, van Hooidonk R, DeCarlo TM, Pratchett MS, Anderson KD, Browne N, Carpenter R, Diaz-Pulido G, D'Olivo JP, Doo SS, Figueiredo J, Fortunato SA V., Kennedy E, Lantz CA, McCulloch MT, González-Rivero M, Schoepf V, Smithers SG, Lowe RJ (2021) Global declines in coral reef calcium carbonate production under ocean acidification and warming. Proc Natl Acad Sci 118:e2015265118. DOI: 10.1073/pnas.2015265118

Cornwall CE, Comeau S, Harvey BP (2024) Are physiological and ecosystem-level tipping points caused by ocean acidification? A critical evaluation. Earth Syst Dyn 15:671–687. DOI: 10.5194/esd-15-671-2024

Crook ED, Potts D, Rebolledo-Vieyra M, Hernandez L, Paytan A (2012) Calcifying coral abundance near low-pH springs: Implications for future ocean acidification. Coral Reefs 31:239–245. DOI: 10.1007/s00338-011-0839-y

Crovetto L, Venn AA, Sevilgen D, Tambutté S, Tambutté E (2024) Spatial variability of and effect of light on the cœlenteron pH of a reef coral. Commun Biol 7:246. DOI: 10.1038/s42003-024-05938-8

Davies PS (1991) Effect of daylight variations on the energy budgets of shallow-water corals. Mar Biol 108:137–144. DOI: 10.1007/BF01313481

Davis KA, Pawlak G, Monismith SG (2021) Turbulence and coral reefs. Ann Rev Mar Sci 13:343–373. DOI: 10.1146/annurev-marine-042120-071823

Doney SC, Fabry VJ, Feely RA, Kleypas JA (2009) Ocean acidification: The other CO_2 problem. Ann Rev Mar Sci 1:169–192. DOI: 10.1146/annurev.marine.010908.163834

Doney SC, Busch DS, Cooley SR, Kroeker KJ (2020) The impacts of ocean acidification on marine ecosystems and reliant human communities. Annu Rev Environ Resour 45:83–112. DOI: 10.1146/annurev-environ-012320-083019

Drury C, Bean NK, Harris CI, Hancock JR, Huckeba J, H CM, Roach TNF, Quinn RA, Gates RD (2022) Intrapopulation adaptive variance supports thermal tolerance in a reef-building coral. Commun Biol 5:486. DOI: 10.1038/s42003-022-03428-3

East HK, Perry CT, Beetham EP, Kench PS, Liang Y (2020) Modelling reef hydrodynamics and sediment mobility under sea level rise in atoll reef island systems. Glob Planet Change

192:103196. DOI: 10.1016/j.gloplacha.2020.103196

Edmunds PJ (2011) Zooplanktivory ameliorates the effects of ocean acidification on the reef coral *Porites* spp. Limnol Oceanogr 56:2402–2410. DOI: 10.4319/lo.2011.56.6.2402

Edmunds PJ, Burgess SC (2018) Colony size and turbulent flow speed modulate the calcification response of the coral *Pocillopora verrucosa* to temperature. Mar Biol 165:13. DOI: 10.1007/s00227-017-3257-z

Ertl NG, O'Connor WA, Wiegand AN, Elizur A (2016) Molecular analysis of the Sydney rock oyster (*Saccostrea glomerata*) CO_2 stress response. Clim Chan Responses 3:1–19. DOI: 10.1186/s40665-016-0019-y

Evensen NR, Edmunds PJ (2017) Conspecific aggregations mitigate the effects of ocean acidification on calcification of the coral *Pocillopora verrucosa*. J Exp Biol 220:1097–1105. DOI: 10.1242/jeb.152488

Evensen NR, Bozec Y-M, Edmunds PJ, Mumby PJ (2021) Scaling the effects of ocean acidification on coral growth and coral-coral competition on coral community recovery. PeerJ 9:e11608. DOI: 10.7717/peerj.11608

Fabricius KE, Langdon C, Uthicke S, Humphrey C, Noonan S, De'ath G, Okazaki R, Muehllehner N, Glas MS, Lough JM (2011) Losers and winners in coral reefs acclimatized to elevated carbon dioxide concentrations. Nat Clim Chang 1:165–169. DOI: 10.1038/nclimate1122

Falter JL, Atkinson MJ, Merrifield MA (2004) Mass-transfer limitation of nutrient uptake by a wave-dominated reef flat community. Limnol Oceanogr 49:1820–1831. DOI: 10.4319/lo.2004.49.5.1820

Fifer J, Bentlage B, Lemer S, Fujimura AG, Sweet M, Raymundo LJ (2021) Going with the flow: How corals in high-flow environments can beat the heat. Mol Ecol 30:2009–2024. DOI: 10.1111/mec.15869

Findlay HS, Feely RA, Jiang L, Pelletier G, Bednaršek N (2025) Ocean acidification: Another planetary boundary crossed. Glob Chang Biol 31:e70238. DOI: 10.1111/gcb.70238

Fisher R, O'Leary RA, Low-Choy S, Mengersen K, Knowlton N, Brainard RE, Caley MJ (2015) Species richness on coral reefs and the pursuit of convergent global estimates. Curr Biol 25:500–505. DOI: 10.1016/j.cub.2014.12.022

Friedlingstein P, O'Sullivan M, Jones MW, Andrew RM, Hauck J, Landschützer P, Le Quéré C, Li H, Luijkx IT, Olsen A, Peters GP, Peters W, Pongratz J, Schwingshackl C, Sitch S, Canadell JG, Ciais P, Jackson RB, Alin SR, Arneth A, Arora V, Bates NR, Becker M, Bellouin N, Berghoff CF, Bittig HC, Bopp L, Cadule P, Campbell K, Chamberlain MA, Chandra N, Chevallier F, Chini LP, Colligan T, Decayeux J, Djeutchouang LM, Dou X, Duran Rojas C, Enyo K, Evans W, Fay AR, Feely RA, Ford DJ, Foster A, Gasser T, Gehlen M, Gkritzalis T, Grassi G, Gregor L, Gruber N, Gürses Ö, Harris I, Hefner M, Heinke J, Hurtt GC, Iida Y, Ilyina T, Jacobson AR, Jain AK, Jarníková T, Jersild A, Jiang F, Jin Z, Kato E, Keeling RF, Klein Goldewijk K, Knauer J, Korsbakken JI, Lan X, Lauvset SK, Lefèvre N, Liu Z, Liu J, Ma L, Maksyutov S, Marland G, Mayot N, McGuire PC, Metzl N, Monacci NM, Morgan EJ, Nakaoka S-I, Neill C, Niwa Y, Nützel T, Olivier L, Ono T, Palmer PI, Pierrot D, Qin Z, Resplandy L, Roobaert A, Rosan TM,

Rödenbeck C, Schwinger J, Smallman TL, Smith SM, Sospedra-Alfonso R, Steinhoff T, Sun Q, Sutton AJ, Séférian R, Takao S, Tatebe H, Tian H, Tilbrook B, Torres O, Tourigny E, Tsujino H, Tubiello F, van der Werf G, Wanninkhof R, Wang X, Yang D, Yang X, Yu Z, Yuan W, Yue X, Zaehle S, Zeng N, Zeng J (2025) Global carbon budget 2024. Earth Syst Sci Data 17:965–1039. DOI: 10.5194/essd-17-965-2025

Gattuso J-P, Hansson L (2011) Acidification: Background and history. In: Gattuso J-P, Hansson L (eds) Ocean acidification. Oxford University Press, Oxford, UK, pp 1–20

Godefroid M, Dupont S, Metian M, Hédouin L (2022) Two decades of seawater acidification experiments on tropical scleractinian corals: Overview, meta-analysis and perspectives. Mar Pollut Bull 178:113552. DOI: 10.1016/j.marpolbul.2022.113552

Green RH, Lowe RJ, Buckley ML (2018) Hydrodynamics of a tidally forced coral reef atoll. J Geophys Res Oceans 123:7084–7101. DOI: 10.1029/2018JC013946

Grimaldi CM, Lowe RJ, Benthuysen JA, Green RH, Reyns J, Kernkamp H, Gilmour J (2022) Wave and tidally driven flow dynamics within a coral reef atoll off northwestern Australia. J Geophys Res Oceans 127:e2021JC017583. DOI: 10.1029/2021JC017583

Hoegh-Guldberg O, Bruno JF (2010) The impact of climate change on the world's marine ecosystems. Science 328:1523–1528. DOI: 10.1126/science.1189930

Hoegh-Guldberg O, Poloczanska ES, Skirving W, Dove S (2017) Coral reef ecosystems under climate change and ocean acidification. Front Mar Sci 4:1–20. DOI: 10.3389/fmars.2017.00158

Hofmann GE, Barry JP, Edmunds PJ, Gates RD, Hutchins DA, Klinger T, Sewell MA (2010) The effect of ocean acidification on calcifying organisms in marine ecosystems: An organism-to-ecosystem perspective. Annu Rev Ecol Evol Syst 41:127–147. DOI: 10.1146/annurev.ecolsys.110308.120227

Hoogenboom M, Rottier C, Sikorski S, Ferrier-Pagès C (2015) Among-species variation in the energy budgets of reef-building corals: Scaling from coral polyps to communities. J Exp Biol 218:3866–3877. DOI: 10.1242/jeb.124396

Hoogenboom MO, Connolly SR, Anthony KRN (2011) Biotic and abiotic correlates of tissue quality for common scleractinian corals. Mar Ecol Prog Ser 438:119–128. DOI: 10.3354/meps09271

Hoogenboom MO, Frank GE, Chase TJ, Jurriaans S, Álvarez-Noriega M, Peterson K, Critchell K, Berry KLE, Nicolet KJ, Ramsby B, Paley AS (2017) Environmental drivers of variation in bleaching severity of *Acropora* species during an extreme thermal anomaly. Front Mar Sci 4:376. DOI: 10.3389/fmars.2017.00376

Hossain MM, Staples AE (2020) Effects of coral colony morphology on turbulent flow dynamics. PLoS One 15:1–25. DOI: 10.1371/journal.pone.0225676

Hughes DJ, Raina J-B, Nielsen DA, Suggett DJ, Kühl M (2022) Disentangling compartment functions in sessile marine invertebrates. Trends Ecol Evol 37:740–748. DOI: 10.1016/j.tree.2022.04.008

Hurd CL (2015) Slow-flow habitats as refugia for coastal calcifiers from ocean acidification. J

Phycol 51:599–605. DOI: 10.1111/jpy.12307

Iwasaki S, Suzuki A, Iguchi A, Sasaki O, Kano H, Ohno Y, Enomoto K (2018) Effect of seawater turbulence on formation of coral primary polyp skeletons. Coral Reefs 37:939–944. DOI: 10.1007/s00338-018-1719-5

Jimenez IM, Kühl M, Larkum AWD, Ralph PJ (2011) Effects of flow and colony morphology on the thermal boundary layer of corals. J R Soc Interface 8:1785–95. DOI: 10.1098/rsif.2011.0144

Jokiel PL (1978) Effects of water motion on reef corals. J Exp Mar Biol Ecol 35:87–97. DOI: 10.1016/0022-0981(78)90092-8

Jørgensen BB, Revsbech NP (1985) Diffusive boundary layers and the oxygen uptake of sediments and detritus. Limnol Oceanogr 30:111–122. DOI: 10.4319/lo.1985.30.1.0111

Jorissen H, Skinner C, Osinga R, de Beer D, Nugues MM (2016) Evidence for water-mediated mechanisms in coral-algal interactions. Proc R Soc B Biol Sci 283:20161137. DOI: 10.1098/rspb.2016.1137

Kaniewska P, Campbell PR, Kline DI, Rodriguez-Lanetty M, Miller DJ, Dove S, Hoegh-Guldberg O (2012) Major cellular and physiological impacts of ocean acidification on a reef building coral. PLoS One 7:e34659. DOI: 10.1371/journal.pone.0034659

Kaniewska P, Chan CKK, Kline D, Ling EYS, Rosic N, Edwards D, Hoegh-Guldberg O, Dove S (2015) Transcriptomic changes in coral holobionts provide insights into physiological challenges of future climate and ocean change. PLoS One 10:e0139223. DOI: 10.1371/journal.pone.0139223

Kavousi J, Tanaka Y, Nishida K, Suzuki A, Nojiri Y, Nakamura T (2016) Colony-specific calcification and mortality under ocean acidification in the branching coral *Montipora digitata*. Mar Environ Res 119:161–165. DOI: 10.1016/j.marenvres.2016.05.025

Kim SW, Sommer B, Beger M, Pandolfi JM (2023) Regional and global climate risks for reef corals: Incorporating species-specific vulnerability and exposure to climate hazards. Glob Chang Biol 29:4140–4151. DOI: 10.1111/gcb.16739

Klein SG, Geraldi NR, Anton A, Schmidt-Roach S, Ziegler M, Cziesielski MJ, Martin C, Rädecker N, Frölicher TL, Mumby PJ, Pandolfi JM, Suggett DJ, Voolstra CR, Aranda M, Duarte CM (2022) Projecting coral responses to intensifying marine heatwaves under ocean acidification. Glob Chang Biol 28:1753–1765. DOI: 10.1111/gcb.15818

Kleypas J, Yates K (2009) Coral reefs and ocean acidification. Oceanography 22:108–117. DOI: 10.5670/oceanog.2009.101

Knowlton N, Brainard RE, Fisher R, Moews M, Plaisance L, Caley MJ (2010) Coral reef biodiversity. In: McIntyre AD (ed) Life in the world's oceans: Diversity, distribution, and abundance. John Wiley & Sons, Ltd, Oxford, UK, pp 65–78

Kornder NA, Riegl BM, Figueiredo J (2018) Thresholds and drivers of coral calcification responses to climate change. Glob Chang Biol 24:5084–5095. DOI: 10.1111/gcb.14431

Krämer WE, Iglesias-Prieto R, Enríquez S (2022) Evaluation of the current understanding of the impact of climate change on coral physiology after three decades of experimental research. Commun Biol 5:1418. DOI: 10.1038/s42003-022-04353-1

Krief S, Hendy EJ, Fine M, Yam R, Meibom A, Foster GL, Shemesh A (2010) Physiological and isotopic responses of scleractinian corals to ocean acidification. Geochim Cosmochim Acta 74:4988–5001. DOI: 10.1016/j.gca.2010.05.023

Kroeker KJ, Kordas RL, Crim R, Hendriks IE, Ramajo L, Singh GS, Duarte CM, Gattuso J (2013) Impacts of ocean acidification on marine organisms: Quantifying sensitivities and interaction with warming. Glob Chang Biol 19:1884–1896. DOI: 10.1111/gcb.12179

Kühl M, Cohen Y, Dalsgaard T, Jørgensen B, Revsbech N (1995) Microenvironment and photosynthesis of zooxanthellae in scleractinian corals studied with microsensors for O_2, pH and light. Mar Ecol Prog Ser 117:159–172. DOI: 10.3354/meps117159

Kurihara H, Watanabe A, Tsugi A, Mimura I, Hongo C, Kawai T, Reimer JD, Kimoto K, Gouezo M, Golbuu Y (2021) Potential local adaptation of corals at acidified and warmed Nikko Bay, Palau. Sci Rep 11:11192. DOI: 10.1038/s41598-021-90614-8

LaJeunesse TC, Parkinson JE, Gabrielson PW, Jeong HJ, Reimer JD, Voolstra CR, Santos SR (2018) Systematic revision of Symbiodiniaceae highlights the antiquity and diversity of coral endosymbionts. Curr Biol 28:2570–2580. DOI: 10.1016/j.cub.2018.07.008

Lan X, Keeling R (2026) Trends in atmospheric carbon dioxide: Mauna Loa CO_2 annual mean data. In: National Oceanic and Atmospheric Administration Global Monitoring Laboratory (NOAA/GML). https://gml.noaa.gov/ccgg/trends/data.html. Accessed 24 Jan 2026

Lee J-Y, Marotzke J, Bala G, Cao L, Corti S, Dunne JP, Engelbrecht F, Fischer E, Fyfe JC, Jones C, Maycock A, Mutemi J, Ndiaye O, Panickal S, Zhou T (2021) Future global climate: Scenario-based projections and near-term information. In: Masson-Delmotte V, Zhai P, Pirani A, Connors SL, Péan C, Berger S, Caud N, Chen Y, Goldfarb L, Gomis MI, Huang M, Leitzell K, Lonnoy E, Matthews JBR, Maycock TK, Waterfield T, Yelekçi O, Yu R, Zhou B (eds) Climate change 2021: The physical science basis. Contribution of Working Group I to the sixth assessment report of the Intergovernmental Panel on Climate Change. Cambridge University Press, Cambridge, UK and New York, NY, USA, pp 553–672

Lentz ME, Freel EB, Forsman ZH, Schar DWH, Toonen RJ (2024) Flow rates alter the outcome of coral bleaching and growth experiments. Discov Oceans 1:31. DOI: 10.1007/s44289-024-00034-5

Lesser MP, Weis VM, Patterson MR, Jokiel PL (1994) Effects of morphology and water motion on carbon delivery and productivity in the reef coral, *Pocillopora damicornis* (Linnaeus): Diffusion barriers, inorganic carbon limitation, and biochemical plasticity. J Exp Mar Biol Ecol 178:153–179. DOI: 10.1016/0022-0981(94)90034-5

Leung JYS, Zhang S, Connell SD (2022) Is ocean acidification really a threat to marine calcifiers? A systematic review and meta-analysis of 980+ studies spanning two decades. Small 18:2107407. DOI: 10.1002/smll.202107407

Levenstein MA, Gysbers DJ, Marhaver KL, Kattom S, Tichy L, Quinlan Z, Tholen HM, Wegley

Kelly L, Vermeij MJA, Wagoner Johnson AJ, Juarez G (2022) Millimeter-scale topography facilitates coral larval settlement in wave-driven oscillatory flow. PLoS One 17:e0274088.

Lewis JB, Price WS (1976) Patterns of ciliary currents in Atlantic reef corals and their functional significance. J Zool 178:77–89. DOI: 10.1111/j.1469-7998.1976.tb02264.x

Liew YJ, Zoccola D, Li Y, Tambutté E, Venn AA, Michell CT, Cui G, Deutekom ES, Kaandorp JA, Voolstra CR, Forêt S, Allemand D, Tambutté S, Aranda M (2018) Epigenome-associated phenotypic acclimatization to ocean acidification in a reef-building coral. Sci Adv 4:1–10. DOI: 10.1126/sciadv.aar8028

Lowe RJ, Falter JL (2015) Oceanic forcing of coral reefs. Ann Rev Mar Sci 7:43–66. DOI: 10.1146/annurev-marine-010814-015834

Madin JS, Black KP, Connolly SR (2006) Scaling water motion on coral reefs: From regional to organismal scales. Coral Reefs 25:635–644. DOI: 10.1007/s00338-006-0137-2

Manullang C, Tarigan AI, Iguchi A, Nakamura T (2024) Intraspecific variation in response to elevated pCO_2 and temperature in the branching reef coral *Acropora digitifera* from different habitats. Coral Reefs 43:1071–1081. DOI: 10.1007/s00338-024-02523-7

Mariscal RN (1974) Scanning electron microscopy of the sensory surface of the tentacles of sea anemones and corals. Zeitschrift für Zellforschung und Mikroskopische Anatomie 147:149–156. DOI: 10.1007/BF00582789

Martins CPP, Ziegler M, Schubert P, Wilke T, Wall M (2024a) Effects of water flow and ocean acidification on oxygen and pH gradients in coral boundary layer. Sci Rep 14:12757. DOI: 10.1038/s41598-024-63210-9

Martins CPP, Wall M, Schubert P, Wilke T, Ziegler M (2024b) Variability of the surface boundary layer of reef-building coral species. Coral Reefs 43:1223–1233. DOI: 10.1007/s00338-024-02531-7

Mass T, Brickner I, Hendy E, Genin A (2011) Enduring physiological and reproductive benefits of enhanced flow for a stony coral. Limnol Oceanogr 56:2176–2188. DOI: 10.4319/lo.2011.56.6.2176

McClanahan TR, Ateweberhan M, Muhando CA, Maina J, Mohammed MS (2007) Effects of climate and seawater temperature variation on coral bleaching and mortality. Ecol Monogr 77:503–525. DOI: 10.1890/06-1182.1

McCulloch M, Falter J, Trotter J, Montagna P (2012) Coral resilience to ocean acidification and global warming through pH up-regulation. Nat Clim Chang 2:623–627. DOI: 10.1038/nclimate1473

McLachlan RH, Price JT, Muñoz-Garcia A, Weisleder NL, Levas SJ, Jury CP, Toonen RJ, Grottoli AG (2022) Physiological acclimatization in Hawaiian corals following a 22-month shift in baseline seawater temperature and pH. Sci Rep 12:3712. DOI: 10.1038/s41598-022-06896-z

McWilliam M, Chase TJ, Hoogenboom MO (2018) Neighbor diversity regulates the productivity of coral assemblages. Curr Biol 28:3634-3639.e3. DOI: 10.1016/j.cub.2018.09.025

Meléndez M, Salisbury J, Gledhill D, Langdon C, Morell JM, Manzello D, Rodriguez-Abudo S, Musielewicz S, Sutton A (2020) Seasonal variations of carbonate chemistry at two western Atlantic coral reefs. J Geophys Res Oceans. DOI: 10.1029/2020JC016108

Meseck SL, Sennefelder G, Krisak M, Wikfors GH (2020) Physiological feeding rates and cilia suppression in blue mussels (*Mytilus edulis*) with increased levels of dissolved carbon dioxide. Ecol Indic 117:106675. DOI: 10.1016/j.ecolind.2020.106675

Mohamed AR, Ochsenkühn MA, Kazlak AM, Moustafa A, Amin SA (2023) The coral microbiome: Towards an understanding of the molecular mechanisms of coral-microbiota interactions. FEMS Microbiol Rev 47:fuad005. DOI: 10.1093/femsre/fuad005

Mollica NR, Guo W, Cohen AL, Huang K, Foster GL, Donald HK, Solow AR (2018) Ocean acidification affects coral growth by reducing skeletal density. Proc Natl Acad Sci 115:1754–1759. DOI: 10.1073/pnas.1712806115

Monismith SG (2007) Hydrodynamics of coral reefs. Annu Rev Fluid Mech 39:37–55. DOI: 10.1146/annurev.fluid.38.050304.092125

Muscatine L, R. McCloskey L, E. Marian R (1981) Estimating the daily contribution of carbon from zooxanthellae to coral animal respiration. Limnol Oceanogr 26:601–611. DOI: 10.4319/lo.1981.26.4.0601

Nakamura T, Van Woesik R (2001) Water-flow rates and passive diffusion partially explain differential survival of corals during the 1998 bleaching event. Mar Ecol Prog Ser 212:301–304. DOI: 10.3354/meps212301

Nakamura T, Yamasaki H, van Woesik R (2003) Water flow facilitates recovery from bleaching in the coral *Stylophora pistillata*. Mar Ecol Prog Ser 256:287–291. DOI: 10.3354/meps256287

Noisette F, Pansch C, Wall M, Wahl M, Hurd CL (2022) Role of hydrodynamics in shaping chemical habitats and modulating the responses of coastal benthic systems to ocean global change. Glob Chang Biol 28:3812–3829. DOI: 10.1111/gcb.16165

Noonan SHC, Fabricius KE (2016) Ocean acidification affects productivity but not the severity of thermal bleaching in some tropical corals. ICES J Mar Sci 73:715–726. DOI: 10.1093/icesjms/fsv127

Noonan SHC, Kluibenschedl A, Fabricius KE (2018) Ocean acidification alters early successional coral reef communities and their rates of community metabolism. PLoS One 13:e0197130. DOI: 10.1371/journal.pone.0197130

Osinga R, Derksen-Hooijberg M, Wijgerde T, Verreth JAJ (2017) Interactive effects of oxygen, carbon dioxide and flow on photosynthesis and respiration in the scleractinian coral *Galaxea fascicularis*. J Exp Biol 220:2236–2242. DOI: 10.1242/jeb.140509

Pacherres CO, Ahmerkamp S, Schmidt-Grieb GM, Holtappels M, Richter C (2020) Ciliary vortex flows and oxygen dynamics in the coral boundary layer. Sci Rep 10:7541. DOI: 10.1038/s41598-020-64420-7

Page CE, Leggat W, Heron SF, Choukroun SM, Lloyd J, Ainsworth TD (2019) Seeking resistance

in coral reef ecosystems: The interplay of biophysical factors and bleaching resistance under a changing climate. BioEssays 41:1800226. DOI: 10.1002/bies.201800226

Page CE, Leggat W, Heron SF, Fordyce AJ, Ainsworth TD (2021) High flow conditions mediate damaging impacts of sub-lethal thermal stress on corals' endosymbiotic algae. Conserv Physiol 9:1–19. DOI: 10.1093/conphys/coab046

Pascoe S, Anthony K, Scheufele G, Pears RJ (2024) Identifying coral reef restoration objectives: A framework. Ocean Coast Manag 251:107081. DOI: 10.1016/j.ocecoaman.2024.107081

Patterson MR, Sebens KP, Olson RR (1991) In situ measurements of flow effects on primary production and dark respiration in reef corals. Limnol Oceanogr 36:936–948. DOI: 10.4319/lo.1991.36.5.0936

Peng Q, Xie S-P, Wang D, Huang RX, Chen G, Shu Y, Shi J-R, Liu W (2022) Surface warming-induced global acceleration of upper ocean currents. Sci Adv 8:eabj8394. DOI: 10.1126/sciadv.abj8394

Putnam HM, Barott KL, Ainsworth TD, Gates RD (2017) The vulnerability and resilience of reef-building corals. Curr Biol 27:R528–R540. DOI: 10.1016/j.cub.2017.04.047

Radice VZ, Brett MT, Fry B, Fox MD, Hoegh-Guldberg O, Dove SG (2019) Evaluating coral trophic strategies using fatty acid composition and indices. PLoS One 14:e0222327. DOI: 10.1371/journal.pone.0222327

Rangel-Yescas G, Cervantes C, Cervantes-Rocha MA, Suárez-Delgado E, Banaszak AT, Maldonado E, Ramsey IS, Rosenbaum T, Islas LD (2021) Discovery and characterization of Hv1-type proton channels in reef-building corals. Elife 10:e69248. DOI: 10.7554/eLife.69248

Reichert J, Backes AR, Schubert P, Wilke T (2017) The power of 3D fractal dimensions for comparative shape and structural complexity analyses of irregularly shaped organisms. Methods Ecol Evol 8:1650–1658. DOI: 10.1111/2041-210X.12829

Reid EC, Lentz SJ, DeCarlo TM, Cohen AL, Davis KA (2020) Physical processes determine spatial structure in water temperature and residence time on a wide reef flat. J Geophys Res Oceans 125:e2020JC016543. DOI: 10.1029/2020JC016543

Rogers JS, Monismith SG, Koweek DA, Torres WI, Dunbar RB (2016) Thermodynamics and hydrodynamics in an atoll reef system and their influence on coral cover. Limnol Oceanogr 61:2191–2206. DOI: 10.1002/lno.10365

Rohwer F, Seguritan V, Azam F, Knowlton N (2002) Diversity and distribution of coral-associated bacteria. Mar Ecol Prog Ser 243:1–10. DOI: 10.3354/meps243001

Roik A, Röthig T, Roder C, Ziegler M, Kremb SG, Voolstra CR (2016) Year-long monitoring of physico-chemical and biological variables provide a comparative baseline of coral reef functioning in the central Red Sea. PLoS One 11:e0163939. DOI: 10.1371/journal.pone.0163939

Sala E, Knowlton N (2006) Global marine biodiversity trends. Annu Rev Environ Resour 31:93–122. DOI: 10.1146/annurev.energy.31.020105.100235

Schill SR, Asner GP, McNulty VP, Pollock FJ, Croquer A, Vaughn NR, Escovar-Fadul X, Raber G, Shaver E (2021) Site selection for coral reef restoration using airborne imaging spectroscopy. Front Mar Sci 8:698004. DOI: 10.3389/fmars.2021.698004

Schoepf V, Jury CP, Toonen RJ, McCulloch MT (2017) Coral calcification mechanisms facilitate adaptive responses to ocean acidification. Proc R Soc B Biol Sci 284:20172117. DOI: 10.1098/rspb.2017.2117

Sebens KP, Grace SP, Helmuth B, Maney EJ, Miles JS (1998) Water flow and prey capture by three scleractinian corals, *Madracis mirabilis*, *Montastrea cavernosa* and *Porites porites* in a field enclosure. Mar Biol 131:347–360. DOI: 10.1007/s002270050328

Shapiro OH, Fernandez VI, Garren M, Guasto JS, Debaillon-Vesque FP, Kramarsky-Winter E, Vardi A, Stocker R (2014) Vortical ciliary flows actively enhance mass transport in reef corals. Proc Natl Acad Sci 111:13391–13396. DOI: 10.1073/pnas.1323094111

Shashar N, Kinane S, Jokiel PL, Patterson MR (1996) Hydromechanical boundary layers over a coral reef. J Exp Mar Biol Ecol 199:17–28. DOI: 10.1016/0022-0981(95)00156-5

Sheppard C, Davy S, Pilling G, Graham N (2018) The main reef builders and space occupiers. In: The biology of coral reefs, 2nd ed. Oxford University Press, Oxford, UK,

Sing Wong A, Vrontos S, Taylor ML (2022) An assessment of people living by coral reefs over space and time. Glob Chang Biol 28:7139–7153. DOI: 10.1111/gcb.16391

Souter D, Planes S, Wicquart J, Logan M, Obura D, Staub F (eds) (2021) Status of coral reefs of the world: 2020 report. Global Coral Reef Monitoring Network (GCRMN) and International Coral Reef Initiative (ICRI). DOI: 10.59387/WOTJ9184.

Stocking JB, Laforsch C, Sigl R, Reidenbach MA (2018) The role of turbulent hydrodynamics and surface morphology on heat and mass transfer in corals. J R Soc Interface 15:20180448. DOI: 10.1098/rsif.2018.0448

Storlazzi CD, Gingerich SB, van Dongeren A, Cheriton OM, Swarzenski PW, Quataert E, Voss CI, Field DW, Annamalai H, Piniak GA, McCall R (2018) Most atolls will be uninhabitable by the mid-21st century because of sea-level rise exacerbating wave-driven flooding. Sci Adv 4:eaap9741. DOI: 10.1126/sciadv.aap9741

Strahl J, Stolz I, Uthicke S, Vogel N, Noonan SHC, Fabricius KE (2015) Physiological and ecological performance differs in four coral taxa at a volcanic carbon dioxide seep. Comp Biochem Physiol Part A Mol Integr Physiol 184:179–186. DOI: 10.1016/j.cbpa.2015.02.018

Sunday JM, Fabricius KE, Kroeker KJ, Anderson KM, Brown NE, Barry JP, Connell SD, Dupont S, Gaylord B, Hall-Spencer JM, Klinger T, Milazzo M, Munday PL, Russell BD, Sanford E, Thiyagarajan V, Vaughan MLH, Widdicombe S, Harley CDG (2017) Ocean acidification can mediate biodiversity shifts by changing biogenic habitat. Nat Clim Chang 7:81–86. DOI: 10.1038/NCLIMATE3161

Sutton AJ, Feely RA, Maenner-Jones S, Musielwicz S, Osborne J, Dietrich C, Monacci N, Cross J, Bott R, Kozyr A, Andersson AJ, Bates NR, Cai W-J, Cronin MF, De Carlo EH, Hales B, Howden SD, Lee CM, Manzello DP, McPhaden MJ, Meléndez M, Mickett JB, Newton JA, Noakes SE,

Noh JH, Olafsdottir SR, Salisbury JE, Send U, Trull TW, Vandemark DC, Weller RA (2019) Autonomous seawater pCO_2 and pH time series from 40 surface buoys and the emergence of anthropogenic trends. Earth Syst Sci Data 11:421–439. DOI: 10.5194/essd-11-421-2019

Sweet MJ, Brown BE (2016) Coral responses to anthropogenic stress in the twenty-first century: An ecophysiological perspective. Oceanography and Marine Biology: An Annual Review 54:271–314.

Tambutté E, Venn AA, Holcomb M, Segonds N, Techer N, Zoccola D, Allemand D, Tambutté S (2015) Morphological plasticity of the coral skeleton under CO_2-driven seawater acidification. Nat Commun 6:7368. DOI: 10.1038/ncomms8368

Tambutté E, Ganot P, Venn AA, Tambutté S (2021) A role for primary cilia in coral calcification? Cell Tissue Res 383:1093–1102. DOI: 10.1007/s00441-020-03343-1

Tambutté S, Holcomb M, Ferrier-Pagès C, Reynaud S, Tambutté É, Zoccola D, Allemand D (2011) Coral biomineralization: From the gene to the environment. J Exp Mar Biol Ecol 408:58–78. DOI: 10.1016/j.jembe.2011.07.026

Thomas FIM, Atkinson MJ (1997) Ammonium uptake by coral reefs: Effects of water velocity and surface roughness on mass transfer. Limnol Oceanogr 42:81–88. DOI: 10.4319/lo.1997.42.1.0081

UNEP-WCMC, WorldFish Centre, WRI, TNC (2021) Global distribution of warm-water coral reefs, compiled from multiple sources including the Millennium Coral Reef Mapping Project. Version 4.1. Includes contributions from IMaRS-USF and IRD (2005), IMaRS-USF (2005) and Spalding et al. (2001). In: UN Environment World Conservation Monitoring Centre. Cambridge, UK. https://doi.org/10.34892/t2wk-5t34. Accessed 24 Jan 2026

Venn AA, Tambutté E, Caminiti-Segonds N, Techer N, Allemand D, Tambutté S (2019) Effects of light and darkness on pH regulation in three coral species exposed to seawater acidification. Sci Rep 9:2201. DOI: 10.1038/s41598-018-38168-0

Venn AA, Bernardet C, Chabenat A, Tambutté E, Tambutté S (2020) Paracellular transport to the coral calcifying medium: Effects of environmental parameters. J Exp Biol 223: jeb227074. DOI: 10.1242/jeb.227074

Venn AA, Tambutté E, Comeau S, Tambutté S (2022) Proton gradients across the coral calcifying cell layer: Effects of light, ocean acidification and carbonate chemistry. Front Mar Sci 9:1–15. DOI: 10.3389/fmars.2022.973908

Venn AA, Tambutté E, Crovetto L, Tambutté S (2025) pH regulation in coral photosymbiosis and calcification: A compartmental perspective. New Phytol 247:487–503. DOI: 10.1111/nph.70200

Veron JEN (2011) Corals: Biology, skeletal deposition, and reef-building. In: Hopley D (ed) Encyclopedia of Modern Coral Reefs. Encyclopedia of Earth Sciences Series. Springer Netherlands, Dordrecht, Netherlands, pp 275–281

Vidal-Dupiol J, Zoccola D, Tambutté E, Grunau C, Cosseau C, Smith KM, Freitag M, Dheilly NM, Allemand D, Tambutté S (2013) Genes related to ion-transport and energy production are

upregulated in response to CO_2-driven pH decrease in corals: New insights from transcriptome analysis. PLoS One 8:e58652. DOI: 10.1371/journal.pone.0058652

Viehman TS, Reguero BG, Lenihan HS, Rosman JH, Storlazzi CD, Goergen EA, Canals Silander MF, Groves SH, Holstein DM, Bruckner AW, Carrick J V., Haus BK, Royster JB, Duvall MS, Torres WI, Hench JL (2023) Coral restoration for coastal resilience: Integrating ecology, hydrodynamics, and engineering at multiple scales. Ecosphere 14:e4517. DOI: 10.1002/ecs2.4517

Woodhead AJ, Hicks CC, Norström A V, Williams GJ, Graham NAJ (2019) Coral reef ecosystem services in the Anthropocene. Funct Ecol 33:1023–1034. DOI: 10.1111/1365-2435.13331

WoRMS (2026) Scleractinia. https://www.marinespecies.org/aphia.php?p=taxdetails&id=1363. Accessed 24 Jan 2026

Yuan X, Cai W-J, Meile C, Hopkinson BM, Ding Q, Schoepf V, Warner ME, Hoadley KD, Chen B, Liu S, Huang H, Ye Y, Grottoli AG (2018) Quantitative interpretation of vertical profiles of calcium and pH in the coral coelenteron. Mar Chem 204:62–69. DOI: 10.1016/j.marchem.2018.06.001

Zoccola D, Ganot P, Bertucci A, Caminiti-Segonds N, Techer N, Voolstra CR, Aranda M, Tambutté E, Allemand D, Casey JR, Tambutté S (2015) Bicarbonate transporters in corals point towards a key step in the evolution of cnidarian calcification. Sci Rep 5:9983. DOI: 10.1038/srep09983

PUBLICATIONS

1 Coral Physiological Interplay During Stress (Manuscript I)

Martins CPP, Arnold AL, Kömpf K, Schubert P, Ziegler M, Wilke T, Reichert J (2022) Growth response of reef-building corals to ocean acidification is mediated by interplay of taxon-specific physiological parameters. *Frontiers in Marine Science* 9:872631. DOI: 10.3389/fmars.2022.872631

frontiers | Frontiers in Marine Science

ORIGINAL RESEARCH
published: 09 June 2022
doi: 10.3389/fmars.2022.872631

Growth Response of Reef-Building Corals to Ocean Acidification Is Mediated by Interplay of Taxon-Specific Physiological Parameters

Catarina P. P. Martins, Angelina L. Arnold, Katharina Kömpf, Patrick Schubert, Maren Ziegler, Thomas Wilke and Jessica Reichert*

Department of Animal Ecology and Systematics, Justus Liebig University Giessen, Giessen, Germany

OPEN ACCESS

Edited by:
Aldo Cróquer, The Nature Conservancy (Dominican Republic), Dominican Republic

Reviewed by:
Ian C. Enochs, Atlantic Oceanographic and Meteorological Laboratory (NOAA), United States
Sam Dupont, University of Gothenburg, Sweden

***Correspondence:**
Catarina P. P. Martins
catarina.padilha-pires-martins@bio.uni-giessen.de

Specialty section:
This article was submitted to Coral Reef Research, a section of the journal Frontiers in Marine Science

Received: *09 February 2022*
Accepted: *06 May 2022*
Published: *09 June 2022*

Citation:
Martins CPP, Arnold AL, Kömpf K, Schubert P, Ziegler M, Wilke T and Reichert J (2022) Growth Response of Reef-Building Corals to Ocean Acidification Is Mediated by Interplay of Taxon-Specific Physiological Parameters. Front. Mar. Sci. 9:872631. doi: 10.3389/fmars.2022.872631

Ocean acidification (OA) poses a major threat to calcifying organisms such as reef-building corals, typically leading to reduced calcification rates. Mechanisms to compensate the effects of OA on coral growth may, however, involve processes other than calcification. Yet, the physiological patterns mediating coral growth under OA are not fully understood, despite an extensive body of literature characterizing physiological changes in corals under OA. Therefore, we conducted a three-month laboratory experiment with six scleractinian coral species (*Acropora humilis*, *Acropora millepora*, *Pocillopora damicornis*, *Pocillopora verrucosa*, *Porites cylindrica*, and *Porites lutea*) to assess physiological parameters that potentially characterize growth (calcification, volume, and surface area), maintenance (tissue biomass, and lipid and protein content), and cellular stress (apoptotic activity) response under ambient (pH 7.9) and low pH (pH 7.7). We identified genus- and species-specific physiological parameters potentially mediating the observed growth responses to low pH. We found no significant changes in calcification but species showed decreasing growth in volume and surface area, which occurred alongside changes in maintenance and cellular stress parameters that differed between genera and species. *Acropora* spp. showed elevated cellular stress and *Pocillopora* spp. showed changes in maintenance-associated parameters, while both genera largely maintained growth under low pH. Conversely, *Porites* spp. experienced the largest decreases in volume growth but showed no major changes in parameters related to maintenance or cellular stress. Our findings indicate that growth- and calcification-related responses alone may not fully reflect coral susceptibility to OA. They may also contribute to a better understanding of the complex physiological processes leading to differential growth changes of reef-building corals in response to low pH conditions.

Keywords: ocean acidification, scleractinian corals, eco-physiology, susceptibility, coral metabolism

1 INTRODUCTION

Ocean acidification (OA)—a process characterized by decreased pH and altered carbonate chemistry—is considered one of the main future threats to coral reefs (Anthony, 2016), with potentially large impacts on reef diversity and functioning (Gaylord et al., 2015; Sunday et al., 2017). In scleractinian corals, the main framework builders of tropical coral reef ecosystems, OA generally reduces calcification rates (Chan and Connolly, 2013; Kroeker et al., 2013). Calcification is the process of calcium carbonate deposition (Al-Horani, 2015), which underlies skeletal growth and occurs through the combination of extension and densification phases of skeletal elements (Cuif and Dauphin, 2005). These two phases can be affected differently by OA, leading to coral skeletons with lower density (Mollica et al., 2018) and higher porosity through changes in the internal architecture of the skeleton (Tambutté et al., 2015). The magnitude of OA-induced decreases in calcification differs among (Kornder et al., 2018) and within coral species (e.g., Kavousi et al., 2016; Enochs et al., 2018). Maintaining calcification during OA is generally seen as indication of low susceptibility (Comeau et al., 2013). This is partially linked to the ability of species to mediate OA-induced shifts in the carbonate chemistry of the calcifying fluid (Schoepf et al., 2017; Comeau et al., 2019). Some coral species, however, maintain calcification rates under OA despite low control over homeostasis of the calcifying fluid (Comeau et al., 2017).

In addition to calcification (reflecting skeletal growth), coral growth is also characterized by increases in different colony dimensions (e.g., volume growth, surface area growth, linear extension; Buddemeier and Kinzie, 1976). Linear extension, measured as the rate of branch extension, is a common length-based method (Pratchett et al., 2015) but it differs from surface area growth, which considers the entire growth surface and growth in any direction (Buddemeier and Kinzie, 1976). This distinction is also reflected under OA, where effects on linear extension are generally null (e.g., Tambutté et al., 2015) while surface area growth generally decreases (Horwitz et al., 2017). This is currently associated to a higher calcifying fluid pH in branch tips than in lateral growth regions (Holcomb et al., 2014). Similarly, calcification may not always relate directly to changes in coral volume due to variation in skeletal density and porosity (Buddemeier et al., 1974). However, mechanisms to compensate the effects of OA on growth in volume and surface area may differ among species and involve processes other than calcification. The respective physiological changes, however, are not always consistent. For example, coral energy reserves may remain unchanged or increase during OA (Strahl et al., 2016; Wall et al., 2017). Therefore, the physiological patterns mediating coral growth under OA and leading to different growth responses are not fully understood, despite an extensive body of literature characterizing physiological changes in corals under OA. Additionally, OA studies characterizing coral growth in colony surface area and volume are few, despite the advantage of providing ecologically relevant information of realized growth and occupied space (Edmunds, 2007; Pratchett et al., 2015) that could inform coral demography projections (Edmunds et al., 2014; Kayal et al., 2019) and modeling of OA impacts across large spatio-temporal scales (Evensen et al., 2021).

Therefore, the goal of this study was to unravel the physiological patterns in coral metabolism that underlie changes in coral growth response to OA. For this, we conducted a three-month experiment in which corals were exposed to a low and ambient pH scenario and assessed growth parameters (calcification, volume, and surface area) alongside maintenance (tissue biomass, and lipid and protein content) and cellular stress (apoptotic activity) parameters of six scleractinian coral species. We studied *Acropora humilis* (Dana, 1846), *Acropora millepora* (Ehrenberg, 1834), *Pocillopora damicornis* (Linnaeus, 1758), *Pocillopora verrucosa* (Ellis and Solander, 1786), *Porites cylindrica* Dana, 1846, and *Porites lutea* Milne Edwards and Haime, 1851, which are common reef-builders and represent major coral families. Specifically, we tested (i) which physiological changes underlie the growth response of corals to OA and (ii) whether the observed patterns in physiological responses are consistent across the tested genera and species. This comprehensive approach will help to disentangle physiological trade-offs of coral species under low pH conditions and better understand coral susceptibility to OA.

2 MATERIALS AND METHODS

2.1 Experimental Design and Study Species

The physiological responses of Indo-Pacific corals to low pH were studied in a controlled three-month laboratory experiment. The experiment was conducted from 31 October 2014 to 12 January 2015. Six coral species, *A. humilis*, *A. millepora, P. damicornis*, *P. verrucosa*, *P. cylindrica*, and *P. lutea*, were exposed to ambient and low pH. Coral colonies were imported from Indonesia in 2014 (**Supplementary Table S1**) and were acclimated to laboratory conditions for 5–6 months prior to the experiment. Corals were maintained at the 'Ocean2100' long-term coral experimental facility at Justus Liebig University Giessen, Germany, under laboratory conditions (in accordance with the institutional animals' care guidelines, long-term rearing: 10:14 light:dark photoperiod, light intensity (PAR) 200 μmol photons m^{-2} s^{-1}, and temperature 26 ± 0.5°C). Three colonies per species were cut into six fragments of 3–5 cm height each using a small angle grinder (Dremel Multitool 3000-15, The Netherlands). Fragments were attached to self-made concrete bases with two-component glue (CoraFix SuperFast, Grotech, Germany). Coral fragments were arranged randomly in six tanks (3 fragments per species per tank, 9 fragments per species per treatment) and acclimated to experimental tank conditions one week prior to the start of the experiment. One coral fragment of *A. humilis* from the ambient pH treatment and one from the low pH treatment, three coral fragments of *A. millepora* from the ambient pH treatment, and one entire colony of *P. lutea* from both treatments died during the course of the experiment and were excluded from the analyses.

2.2 Tank Setup and Treatment Conditions

The experiment was conducted in six 45 L tanks (**Supplementary Figure S1**). The experimental tanks were part of a 4000 L closed recirculating system and were maintained with a water exchange rate of 60 L h^{-1} (corresponding to a 100% tank volume turnover every 45 min). Tanks were cleaned twice per week to minimize biofilm growth. Temperature was maintained at 26°C through a feedback-controlled heater (Titanium heater, Schego, Germany; 300 W), and water flow was generated with a propeller pump (Resun S-700, Resun, China) at a flow rate of 700 L h^{-1}. Light was set to 10:14 h light:dark photoperiod at 135–142 µmol m^{-2} s^{-1} with a simulated midday high-light period at 270–395 µmol m^{-2} s^{-1} of four hours (80 W Aquablue Special and Blue Plus, ATI, Germany). The corals were fed indirectly *via* the connected water system, which was provided with frozen food daily (i.e., copepods, *Mysis* sp.). Water parameters (salinity: 33, nitrate: < 10–50 mg L^{-1}, phosphate: < 0.05–0.5 mg L^{-1}, calcium: 400–420 mg L^{-1}, magnesium: 1250–1350 mg L^{-1}) were monitored twice a week in the system and maintained constant through dosing of $MgCl_2$, $CaCl_2$, and NaCl-free salt. Alkalinity was maintained by an in-house constructed calcium reactor (pH 6.2–6.4, coral rubble) and dosing of $NaHCO_3$. For this, alkalinity was measured in the recirculating system once a week in the morning with a titration-based alkalinity test (precision 0.5 dKH, Tropic Marin, Germany). pH was constantly monitored (Profilux 3, GHL, Germany) with pH electrodes in each tank (GHL, Germany), which were calibrated using NBS buffers. Values of pH_{NBS} were converted to total scale (pH_T) using equations from Millero (2013) and Takahashi (1982). pH values are expressed in total scale throughout the text.

Coral fragments were exposed to ambient and low pH (**Table 1**; **Supplementary Figure S2**; **Supplementary Table S2**). Low pH conditions were generated *via* pH-controlled bubbling of CO_2 to three tanks (low pH), while three other tanks were not bubbled with CO_2 (ambient pH). The pH in the low pH treatment tanks was reduced by ~0.2 pH units (~350 µatm pCO_2 higher) to simulate 'near-future' conditions under moderately high CO_2 emissions predicted by the IPCC (RCP6.0; IPCCCore Writing Team, 2014). This resulted in a diel pH range of 0.2 pH units. The seawater of the ambient pH treatment tanks was not manipulated with CO_2 to mimic baseline conditions in the main system and represent conditions already experienced by some reefs (~500 µatm pCO_2; Ziegler et al., 2021), resulting in a diel pH range of 0.6 pH units (similar to that of some reefs; Ohde and Van Woesik, 1999; Shaw et al., 2012). Statistical analyses of seawater chemistry showed that target pH levels were successfully maintained during the three-month experiment (**Supplementary Text** and **Supplementary Table S3**).

The CO_2 was pumped individually into the tanks of the low pH treatment, which was activated when pH increased 0.1 pH units above the target pH level of 7.7. Solenoid valves controlled the release of CO_2 into a diffuser, which was connected to a driving pump (Resun 700, China). The CO_2 diffuser broke down the gas into smaller bubbles before it was delivered into the seawater to facilitate CO_2 diffusion. To maintain equal water flow in all tanks, diffusers were also included within ambient pH tanks, without adding CO_2 to the water. Alkalinity values were converted to values in meq L^{-1} with two significant digits and then to µmol H^+ kg $seawater^{-1}$ to calculate carbonate chemistry using CO2SYS (v25; Pelletier et al., 2007). Values of pCO_2 and Ω_{Ar} were calculated from days with alkalinity measurements using measured pH_{NBS} and temperature values of a whole day, with carbonic acid dissociation constants from Mehrbach et al. (1973) refit by Dickson and Millero (1987). This approach is suitable for biological OA experiments with treatments that have differences larger than 100 µatm pCO_2 (Watson et al., 2017) and allowed us to account for the diel oscillation of pH in the tanks. Alkalinity values were assumed to be representative of the alkalinity of the whole day it was measured on. No temperature or pH values were recorded during one of the alkalinity measurement days therefore carbonate chemistry was calculated for a total of 15 days throughout the experiment. A summary of the complete recording of temperature and pH values in each tank is provided in **Supplementary Table S4**.

2.3 Determination of Calcification Rates

Calcification rates were calculated as the difference in buoyant weight (Spencer Davies, 1989) of all coral fragments, measured at the beginning (t_0) and at the end (t_1) of the experiment. For this, corals were weighed in a separate 12 L tank placed under a balance (Kern KB 360-3N, Kern & Sohn, Germany; precision: 0.001 g). The change in buoyant weight was converted to dry weight using an aragonite density of 2.93 g cm^{-3} (Spencer Davies, 1989). Calcification rates were standardized to surface area of the coral fragments at t_0 and to time (month).

2.4 Determination of Growth Rates in Volume and Surface Area

Growth rates in volume and surface area were determined using 3D scanning (Artec Spider 3D with Artec Studio 9, Artec 3D,

TABLE 1 | Seawater chemistry in the two experimental treatments.

Treatment Name	Temperature (°C)	Salinity	pH_T	TA (µmol kg^{-1})	pCO_2 (µatm)	Ω_{Ar}	Daily Minimum pH_T	Daily Maximum pH_T
Ambient pH	25.4 ± 0.4 (543)	33.5 ± 0.6 (4)	7.92 ± 0.18 (458)	2172 ± 240 (16)	577 ± 246 (458)	2.61 ± 1.00 (458)	7.66 ± 0.04 (69)	8.28 ± 0.09 (69)
Low pH	25.2 ± 0.6 (543)		7.74 ± 0.07 (543)		871 ± 160 (543)	1.79 ± 0.40 (543)	7.62 ± 0.06 (69)	7.81 ± 0.09 (69)

Values are expressed as mean ± sd, together with measurement replication (n). Average daily minimum and maximum pH was calculated from the complete recording of pH values. Ω_{Ar}, aragonite saturation; pCO_2, partial pressure of CO_2; pH_T, pH on total scale; TA, total alkalinity.

Luxembourg). The size of coral fragments was documented at t_0 and at t_1, according to previous studies (Reichert et al., 2016). Briefly, corals were placed on a rotating plate and scans were captured in air within 60–90 seconds. 3D models were calculated performing fine serial registration, global registration (minimal distance: 10, iterations: 100, based on geometry), and sharp fusion (resolution 0.2, fill holes by radius, max. hole radius: 5). Artefact objects were removed (small objects filter). To determine volume increases, meshes of the same individuals from all time points were aligned and trimmed horizontally. All meshes were exported as Wavefront ".obj" files to MeshLab Visual Computing Lab-ISTI-CNR (v1.3.4, BETA, 2014; Cignoni et al., 2008) and volume and surface area were calculated using the "compute geometric measures" tool. Since coral growth is size-dependent (Dornelas et al., 2017), growth rates were normalized by initial surface area of coral fragments. Additionally, growth rates were standardized to time (month).

2.5 Sample Preparation

At the end of the experiment, all fragments were snap-frozen in liquid nitrogen and stored at -80°C. Biochemical parameters were measured for each coral fragment. For this, the concrete base and glue were carefully removed and the coral fragment was crushed with mortar and pestle while constantly being cooled down with liquid nitrogen. The coral powder was split for analysis of ash-free dry weight, total lipid content, protein content, and apoptotic activity.

2.6 Biochemical Analyses

2.6.1 Dry Weight and Ash-Free Dry Weight

Dry weight (DW) was determined by drying 60 mg pre-weighed coral samples for 24 h at 60°C. Subsequently, ash-free dry weight (AFDW) was determined by burning the remaining sample for 24 h at 550°C in a muffle furnace (Heraeus Typ M 110, Heraeus Instruments, Germany; 1100°C nominal temperature). Samples were weighed on a Kern ABS 220-4N Precision Balance (KERN & SOHN, Germany; precision: 0.0001 g) and AFDW was standardized to DW following Conlan et al. (2017) to characterize tissue biomass.

2.6.2 Total Lipid Content

Total lipid content was determined using a dichloromethane: methanol (MeOH) extraction, according to Folch et al. (1957) following modifications of Conlan et al. (2014). 2.5 mL of MeOH (2:1) were added to 0.5 g of coral sample in a scintillation vial. Then, samples were sonicated for 5 min (Sonorex Super 10P, Bandelin, Germany; amplitude 6.0) to disrupt cell membranes. The solvent was filtered three times through a cotton-stuffed filter glass Pasteur pipette to remove all solid residues. The sample was washed with 3.5 mL potassium chloride (0.44% in water:MeOH [3:1]) and incubated for 12 h in the dark. Then, the water phase on top was discarded and the liquid methanol phase containing the lipids transferred to pre-weighed clean 15 mL Falcon tubes. The solvent was dried at 30°C in a Dri-block (Techne, UK) under a flow of nitrogen. The dried lipid content was weighed (Kern ABS 220-4N Precision Balance) and standardized to AFDW.

2.6.3 Protein Content

Protein content was analyzed using the 2-D Quant kit (GE Healthcare Life Sciences, USA) according to kit descriptions. Briefly, 10–20 mg of coral sample were transferred into 100 µl standard 2D lysis buffer and stored at -20°C. Absorbance at 480 nm was measured and used to determine protein concentrations against a bovine serum albumin (BSA) standard. Energy content (kJ g^{-1} AFDW) was additionally calculated from the enthalpy of combustion for the sum of lipid (39.5 kJ g^{-1}) and protein (23.9 kJ g^{-1}) content using values by Gnaiger and Bitterlich (1984) and can be inspected in **Supplementary Material (Supplementary Figure S4)**.

2.6.4 Apoptotic Activity

Apoptotic activity was determined by measuring Caspase-3 and -7 activities modified after Liu et al. (2004), using the Caspase-Glo® 3/7 Assay kit (Promega, USA). 60 and 70 mg of the frozen coral sample, respectively, were mixed with a lysis buffer in a ratio of 1:19 (w/v). Lysis buffer (0.5 mL mL^{-1} 50 mM HEPES, 0.468 mg mL^{-1} EGTA, 1.017 mg mL^{-1} $MgCl_2$*$6H_2O$, 1.867 µL mL^{-1} Protease Inhibitor Cocktail (Sigma Aldrich, 8340), and 7.5 mL mL^{-1} MilliQ) was prepared daily to ensure full activity of all components. Samples were homogenized with glass beads (1.0 mm, Cat. No. 11079110, BioSpec Products, USA) for 2 min in a swing mill (MM 200, Retsch, Germany). Then, samples were centrifuged (15 000 x g, 4°C, 15 minutes) and the supernatant was recovered and stored on ice. Three replicate samples were each mixed with Caspase-Glo reagent (1:1) in white-walled 96-well microplates and stored in the dark at RT for 90 min. Luminescence in relative light units (RLU) of all samples was determined on a microplate-reader (ClarioStar, BMG LABTECH, Germany). The obtained RLU corrected against blanks is proportional to the caspase activity of the sample and was normalized to protein content, resulting in apoptotic activity expressed as RLU µg $protein^{-1}$.

2.7 Statistical Analyses

Physiological responses of six coral species to OA were investigated using a Bayesian generalized linear latent variable model (GLLVM; Hui, 2016). This method extends the generalized linear model (GLM) by including latent variables, which include any residual correlations between responses not accounted for by model predictors (Hui, 2016). The model was fit using the physiological parameters as model response, and species and treatment as model predictors with an interaction between them. Tank and coral colony were used as random effects and two latent variables were used to account for unknown interactions between the physiological parameters and shared responses to unknown predictors (Hui, 2016). Physiological parameters were log-transformed to meet model assumptions and scaled (i.e., subtracting the mean and dividing by the standard deviation). Potential outliers were detected by inspecting boxplots and Cleveland dotplots of parameters (Zuur et al., 2010) and were excluded from the GLLVM and subsequent statistical analyses. The GLLVM was performed with 60 000 iterations, with the first 10 000 discarded as burn-in, a thinning rate of 30, a set seed of 123, and using a normal distribution to

model the response data. Model convergence was checked *via* model diagnostic tools using Dunn–Smyth residuals and normal quantile plot of residuals (Hui, 2016; **Supplementary Figure S5**).

Differences between treatments were tested by performing multiple comparisons using the GLLVM and assessed for each physiological parameter and for all parameters combined. Statistically significant differences were estimated from multiple comparisons of the posterior distributions of regression coefficients of each model simulation and assessed through 95% credible intervals (CIs), which capture the 95% most probable values of the parameter (Kruschke, 2018). 75% CIs were used to assess trends. In contrast to traditional null hypothesis testing, no test statistic is required in a Bayesian framework because the uncertainty in model parameter values is indicated by the width of the parameter distribution, which is given by the 95% CI. When the probability distribution over the parameter space is narrower, certainty in the model estimate is higher (Kruschke, 2018). In addition, since hypotheses are tested by directly contrasting the posterior distributions of regression coefficients of each model simulation (Neath and Cavanaugh, 2006), no statistical corrections are needed and are directly assessed through 95% CIs. If the CI of a particular comparison does not include zero, it indicates a credible difference between groups (Kruschke, 2010).

Principal component analyses (PCA) were performed to visualize treatment effects on the combined physiological parameters (hereafter referred to as overall response) and to investigate patterns among coral species. PCAs were conducted using seven variables: calcification, volume growth ($growth_V$), surface area growth ($growth_{SA}$), tissue biomass (biomass), lipid content (lipids), protein content (proteins), and apoptotic activity (apoptosis). Data were centered and scaled and only individuals with values for all variables were used. PCAs were performed for all species together and for each genus separately.

All statistical analyses were performed in R (v.4.1.0; R Core Team, 2021) using RStudio (v1.4.1103; R Studio Team, 2021). The GLLVM was fit using the R package *boral* (v.1.9; 2020; Hui, 2016) and PCAs were performed and visualized using the R packages *FactoMineR* (v.2.4; Lê et al., 2008) and *factoextra* (v.1.0.7; Kassambara and Mundt, 2020). Plots were created using R package *ggplot2* (v.3.3.5; Wickham, 2016).

3 RESULTS

3.1 Ocean Acidification Reduces Coral Growth and Affects Metabolic Maintenance and Cellular Stress

After three months' exposure to ambient or low pH, the seven physiological parameters relating to growth (calcification, volume, and surface area), maintenance (tissue biomass, and lipid and protein content), and cellular stress (apoptotic activity) varied between coral species (**Table 2**; **Supplementary Figures S3, 4**). The low pH treatment induced differential changes in the physiological parameters with few significant effects (GLLVM, **Figure 1**; **Supplementary Table S5**). Coral species generally showed significant changes in different physiological parameters but calcification was largely maintained in all species (GLLVM, **Figure 1A**). Volume growth decreased significantly by 129% in *P. cylindrica* (GLLVM, **Figure 1B**; ambient pH: 0.07 ± 0.08 mm^3 mm^{-2} $month^{-1}$ *vs*. low pH: -0.02 ± 0.06 mm^3 mm^{-2} $month^{-1}$) and by 64% in *P. lutea* (GLLVM, **Figure 1B**; ambient pH: 0.25 ± 0.19 mm^3 mm^{-2} $month^{-1}$ *vs*. low pH: 0.09 ± 0.07 mm^3 mm^{-2} $month^{-1}$). Surface area growth decreased significantly by 53% in *P. verrucosa* (GLLVM, **Figure 1C**; ambient pH: 21.73 ± 9.11% $month^{-1}$ *vs*. low pH: 10.16 ± 6.23% $month^{-1}$). Significant changes in tissue biomass were only observed in *P. damicornis* (GLLVM, **Figure 1D**; ambient pH: 43.1 ± 14.2 mg g DW^{-1} *vs*. low pH: 74.1 ± 43.5 mg g DW^{-1}), which presented a 72% increase. Apoptotic activity increased significantly by 101% in *A. millepora* (GLLVM, **Figure 1G**; ambient pH: 206 ± 137 RLU µg $protein^{-1}$ *vs*. low pH: 415 ± 151 RLU µg $protein^{-1}$). Lipid and protein content were largely maintained in all species (GLLVM, **Figures 1E, F**).

3.2 Combined Changes in Physiological Parameters Reveal Genus- and Species-Specific Responses to Ocean Acidification

We found no unifying response to the low pH treatment across our six coral species (**Figure 2A**, no significant difference in the overall response of all species pooled, GLLVM, **Table 3**). Instead, PCA analyses revealed a taxonomic separation in the overall response to low pH at the genus level (**Figures 2B–D**). In the PCA projection of *Acropora* and *Pocillopora*, low pH treatment groups separated from their respective ambient pH groups in the same direction along the PC1 axis regardless of species (no significant difference between species within genera, GLLVM, **Table 3**), indicating a genus-specific response to low pH. In *Acropora*, the low pH treatment was associated with increased apoptotic activity and decreased growth in volume and surface area (**Figure 2B**). In *Pocillopora*, the low pH treatment was associated with increased biomass and decreased growth (calcification, volume, and surface area) as well as lipid and protein content (**Figure 2C**). *Porites* revealed a contrasting response to the low pH treatment. Although both *Porites* spp. showed a significant decrease in volume growth rates (**Figure 1B**), treatment groups of *P. cylindrica* and *P. lutea* separated differently from their respective ambient pH groups in the PCA (**Figure 2D**), indicating a species-specific response to low pH in this genus. However, this difference between *Porites* spp. was not statistically significant (GLLVM, **Table 3**), potentially due to lower sample size in *P. lutea*, introduced through mortality of one colony. In *P. cylindrica*, the separation of the low and ambient pH groups was associated with increased protein content and decreased volume and surface area growth and apoptotic activity. In *P. lutea*, it was associated with increased biomass and decreased volume and surface area growth as well as lipid and protein content (**Figure 2D**).

4 DISCUSSION

Our study suggests that the growth response in volume and surface area of the six investigated coral species under low pH

TABLE 2 | Physiological parameters (mean ± sd) of *Acropora humilis*, *Acropora millepora*, *Pocillopora damicornis*, *Pocillopora verrucosa*, *Porites cylindrica*, and *Porites lutea* maintained in ambient and low pH treatments, for three months.

Species	Treatment	Calcification (mg $CaCO_3$ cm^{-2} $month^{-1}$)	Volume Growth (mm^3 mm^{-2} $month^{-1}$)	Surface Area Growth (% $month^{-1}$)	Tissue Biomass (mg g DW^{-1})	Protein Content (mg g $AFDW^{-1}$)	Lipid Content (mg g $AFDW^{-1}$)	Apoptotic Activity (RLU µg $protein^{-1}$)
Acropora	Ambient pH	40 ± 35	0.12 ± 0.11	16.78 ± 11.31	59.8 ± 26.8	146.7 ± 102.5	169.5 ± 119.6	276 ± 182
humilis	Low pH	30 ± 25	0.05 ± 0.06	10.96 ± 9.72	46.3 ± 26.7	237.1 ± 226.3	135.3 ± 119.6	410 ± 218
Acropora	Ambient pH	36 ± 18	0.03 ± 0.12	5.50 ± 10.82	43.4 ± 15.4	304.2 ± 127.8	206.5 ± 97.8	206 ± 137
millepora	Low pH	34 ± 19	-0.03 ± 0.04	2.07 ± 4.97	40.6 ± 9.3	235.9 ± 111.0	148.8 ± 39.6	415 ± 151
Pocillopora	Ambient pH	31 ± 18	0.13 ± 0.14	16.48 ± 8.26	43.1 ± 14.2	190.1 ± 71.7	203.2 ± 56.0	260 ± 140
damicornis	Low pH	24 ± 7	0.05 ± 0.05	10.85 ± 4.49	74.1 ± 43.5	229.3 ± 153.6	126.1 ± 85.4	225 ± 112
Pocillopora	Ambient pH	37 ± 12	0.10 ± 0.11	21.73 ± 9.11	33.1 ± 7.2	236.3 ± 102.7	156.1 ± 73.1	243 ± 160
verrucosa	Low pH	24 ± 14	0.06 ± 0.08	10.16 ± 6.23	37.9 ± 10.2	153.3 ± 87.3	100.0 ± 52.0	235 ± 190
Porites	Ambient pH	33 ± 17	0.07 ± 0.08	14.71 ± 9.54	75.5 ± 39.9	155.9 ± 99.9	129.7 ± 82.8	102 ± 57
cylindrica	Low pH	23 ± 18	-0.02 ± 0.06	9.28 ± 4.09	54.8 ± 11.4	169.4 ± 54.1	138.1 ± 16.4	62 ± 27
Porites	Ambient pH	183 ± 98	0.25 ± 0.19	44.15 ± 19.48	41.0 ± 5.1	227.5 ± 93.9	156.3 ± 49.3	76 ± 29
lutea	Low pH	148 ± 94	0.09 ± 0.07	34.12 ± 12.13	65.2 ± 17.8	180.8 ± 54.1	141.7 ± 53.2	80 ± 44

AFDW, ash-free dry weight; DW, dry weight; RLU, rapid light units.

may be mediated by differential changes in maintenance and cellular stress parameters. Our results indicate that these patterns are genus-specific for *Acropora* and *Pocillopora*, and species-specific for *Porites*.

While calcification rates remained largely unaffected in our study, growth in volume and surface area generally declined under low pH. These declines differed in magnitude among species. Significant decreases in volume growth were observed in *P. cylindrica* and *P. lutea*. These two species are also known to respond with decreased calcification under low pH (e.g., Bahr et al., 2016; Kavousi et al., 2016), which highlights the negative effects of OA. However, *Porites compressa* from a naturally acidified reef (pH 7.9) have been shown to maintain calcification under pH 7.7 by upregulating pH of the calcifying fluid but maintaining its DIC relatively low (Schoepf et al., 2017). A similar strategy to regulate calcifying fluid conditions might have been employed by the *Porites* spp. tested here and explain the lack of calcification impacts. Low pH effects on calcification and volume growth may differ from each other in intensity (Enochs et al., 2014) due to changes in skeletal density and porosity (Tambutté et al., 2015; Mollica et al., 2018) and might explain the lack of differences observed here for calcification alongside decreased volume growth. Additionally, the high precision of the 3D scanning method used to study volume and surface area growth (Reichert et al., 2016) was able to document subtle changes in volume and surface area, which might have also contributed to this picture. Effects on volume and surface area growth were also not always consistent in this study, despite being related (Pratchett et al., 2015). For example, *P. verrucosa* showed no major changes in volume growth but experienced the largest reduction in surface area growth, as seen in previous studies (Horwitz et al., 2017). In sum, our findings suggest that the coral species tested exhibited different strategies to cope with the low pH treatment.

OA effects were strongest in *Acropora*. Although *Acropora* spp. showed a potential mediation of low pH effects on calcification and growth, the underlying changes included an increase in cellular stress. This increase can become detrimental to fitness when acute and prolonged (Sørensen et al., 2003), suggesting that the patterns observed in *Acropora* spp. constitute a 'dead-end strategy'. The elevated cellular stress observed in *Acropora* is the first report of increased apoptosis in scleractinian corals in response to low pH inferred from caspase activity—a response previously suspected based on up-regulated gene expression patterns of caspase and caspase-like enzymes (Kaniewska et al., 2012; Kaniewska et al., 2015). These findings, however, stand in contrast with observations from *A. millepora* living in CO_2 seeps, where gene expression of chaperones (proteins also involved in cellular stress response) is found to be down-regulated (Kenkel et al., 2018). Although factors of the experimental setup might also contribute to this picture, this finding potentially indicates that the activation of a cellular stress response depends on the duration of low pH conditions and represent a short- to medium-term response.

In contrast, *Pocillopora* spp. and *P. lutea* showed no increase in stress level but a tendency to decrease lipid and protein content. This might indicate an ability to better mobilize existing energy reserves in response to low pH. This pattern has not been observed in previous studies (e.g., Schoepf et al., 2013; Strahl et al., 2016), suggesting that this OA response may also depend on other factors, such as variable feeding capabilities (Palardy et al., 2005; Towle et al., 2015). In *Pocillopora* spp., the changes in maintenance-associated parameters occurred without major reductions of calcification and volume growth under low pH. This was more pronounced in *P. damicornis*, which showed increased biomass while surface area growth decreased. The latter pattern might constitute a 'buffering strategy' *via* tissue thickening, previously observed only in *Stylophora pistillata* (Krief et al., 2010), but not in *P. damicornis* (Comeau et al., 2013; Schoepf et al., 2013). Thicker tissues might alleviate low pH effects by creating a larger pH-regulated separation between the calicoblastic layer and ambient seawater (Krief et al., 2010; Edmunds, 2011). Tissue thickness is thus considered a mediating trait of coral susceptibility to environmental stress (Loya et al., 2001; Thornhill et al., 2011), including OA (Putnam et al., 2017). A 'buffering strategy' might also be available to *P.*

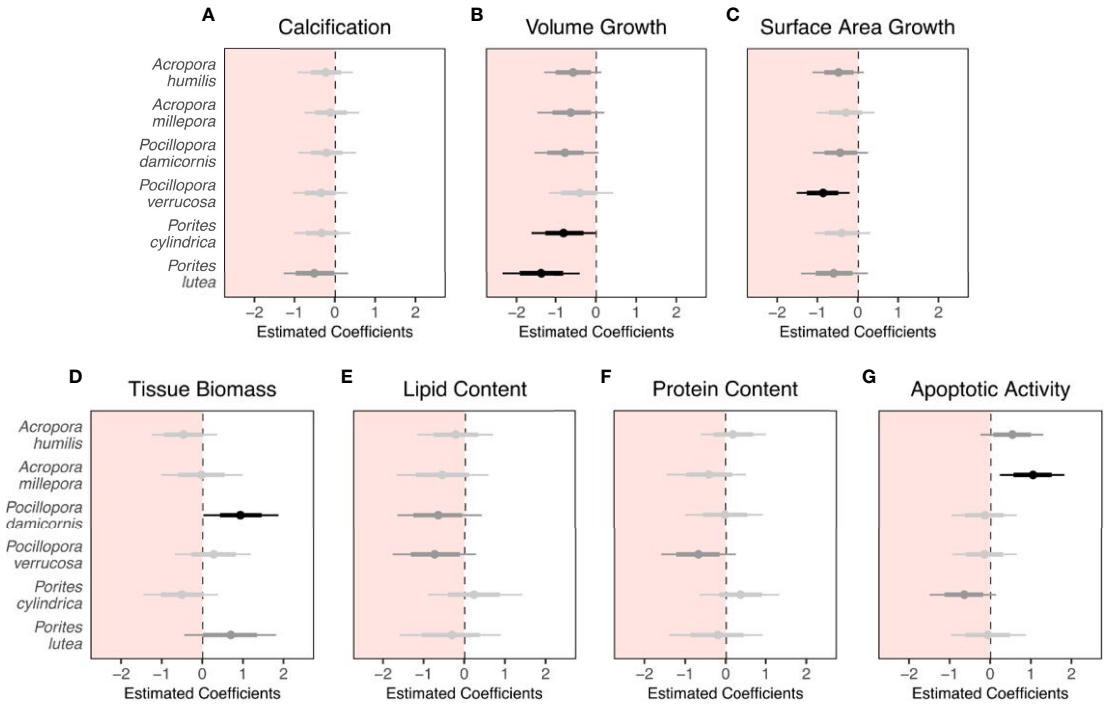

FIGURE 1 | Effect of three-month low pH treatment on **(A)** calcification, **(B)** volume growth, **(C)** surface area growth, **(D)** tissue biomass, **(E)** lipid content, **(F)** protein content, and **(G)** apoptotic activity of six scleractinian coral species (n = 9 fragments per species per treatment). Points indicate the median of modeled regression coefficients of comparisons between treatment groups within a Bayesian framework from a generalized linear latent variable model (GLLVM). Thin and thick lines are 95% and 75% credible intervals (CIs), respectively. Statistically significant effects (i.e., 95% CIs that do not overlap zero) are colored black, trends (i.e., 75% CIs that do not overlap zero) are colored dark grey, and non-significant effects are colored light grey. Summarized parameter coefficients and CIs extracted from the GLLVM are provided in **Supplementary Table S5**.

lutea due to the tendency observed here to increase tissue biomass while surface area growth decreased. However, this assumption needs to be further tested since both increases and no changes in area-normalized tissue biomass have been observed in massive *Porites* spp. (Edmunds, 2012; Brown and Edmunds, 2016).

The response of *P. cylindrica* presents another pattern, which has not previously been described. The marked reductions in volume growth were accompanied by a tendency to decrease cellular stress but without major changes of the underlying physiological parameters. This overall response to low pH was different to the one observed in *P. lutea* and could potentially be related to the morphological differences between these two species. However, similar calcification responses to OA have been found between mounding and branching morphologies (Comeau et al., 2014b) and both mounding and branching species have shown stronger impacts in multispecies comparisons (e.g., Brown and Edmunds, 2016; Godefroid et al., 2021). Instead, a potential explanation might be that *P. cylindrica* responds to low pH with a 'hibernation strategy'. Accordingly, this species may avoid buffering the growth decrease through other physiological processes and suppress cellular stress alarms to potentially survive prolonged periods of stress. For instance, under high temperature stress coral species are able to avoid colony death following bleaching events by down-regulating caspase activity (Tchernov et al., 2011). Thus, at the expense of growth, this strategy might cause the least harm to the overall survival of the colony despite its weedy life-history (Darling et al., 2012).

Other factors may have contributed to the species-specific growth rates under OA in our study. First, coral responses to OA may be determined by growth rates, with faster calcifying corals experiencing larger calcification decreases than slower calcifying corals (Comeau et al., 2014b). Accordingly, the stronger low pH impacts observed here on growth of *Porites* spp. than *Acropora* spp. could be due to species' growth rates during this study. Second, coral surface area growth is generally influenced by environmental parameters such as light or water flow (Schutter et al., 2011). However, additional external factors present in the system may also have played a role. In our study, volume and surface area growth were relatively low in general, especially in *Acropora* spp., which could potentially be attributed to indirect competition through allelopathy (Gross, 2003) and explain the null low pH effects on surface area growth of this genus (Horwitz et al., 2017). Furthermore, our massive *Porites* spp. showed higher volume and surface area growth rates than *Acropora* spp. despite being slow- and fast-growing corals, respectively (Darling et al., 2012 and references therein). This might be due to

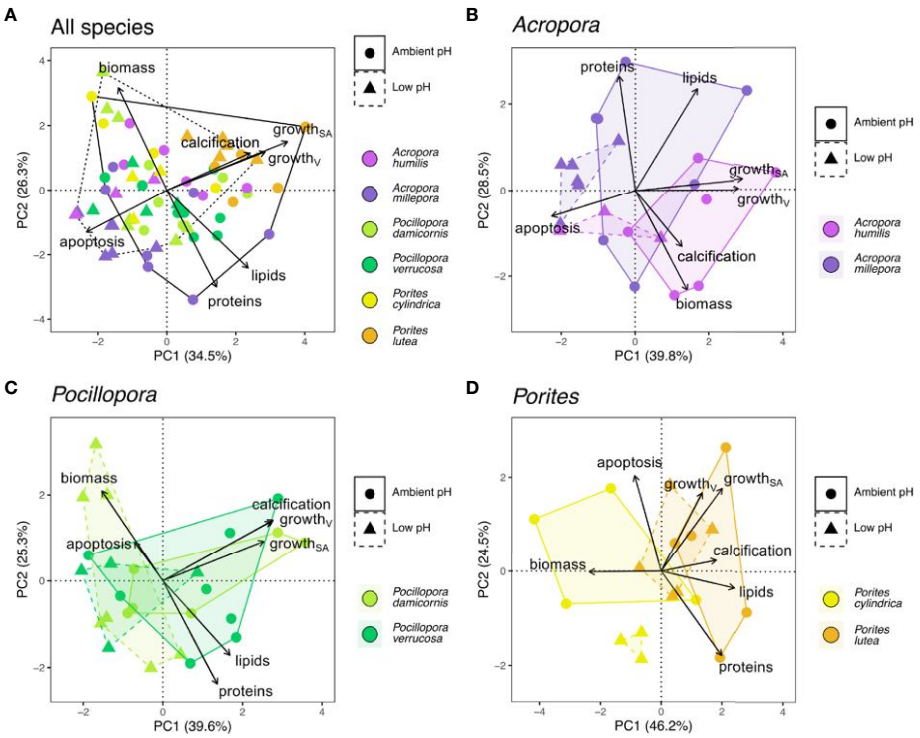

FIGURE 2 | Principal component analyses (PCA) using seven physiological parameters (calcification; growth$_V$, volume growth; growth$_{SA}$, surface area growth; biomass, tissue biomass; lipids, lipid content; proteins, protein content; apoptosis, apoptotic activity) of six scleractinian coral species maintained in ambient and low pH treatments. PCAs were performed for **(A)** all coral species and for two species each in the genera **(B)** *Acropora*, **(C)** *Pocillopora*, and **(D)** *Porites*. Convex polygons outline ambient pH (solid line) and low pH (dashed line) treatments.

TABLE 3 | Pairwise comparison of estimated coefficients from generalized linear latent variable model (GLLVM) of the overall response (i.e., of all physiological parameters combined) to the low pH treatment.

				All Parameters Combined		
Ambient pH	*vs.*	Low pH	Median		-0.26	
All Species		All Species	95% CI	]-0.59		0.10
Low pH	*vs.*	Low pH	Median		-0.04	
Acropora humilis		*Acropora millepora*	95% CI	-0.40		0.33
Low pH	*vs.*	Low pH	Median		0.23	
Pocillopora damicornis		*Pocillopora verrucosa*	95% CI	-0.13		0.59
Low pH	*vs.*	Low pH	Median		0.04	
Porites cylindrica		*Porites lutea*	95% CI	-0.37		0.46

Comparisons were performed between treatments with all species pooled and between each pair of congeners' response to the low pH treatment. Statistically significant effects are indicated by 95% credible intervals (CI) that do not overlap zero.

the colony fragmentation of our *Porites* spp., which provided more surface for the coral fragment to overgrow and led to an initial high growth response regardless of treatment. Third, coral growth responses to OA may also vary intraspecifically at colony level (e.g., Kavousi et al., 2016; Shaw et al., 2016). However, only three coral colonies per species were included in our study, which does not allow for investigation of colony sensitivity to low pH and was thus beyond the scope of our study. Fourth, OA effects on calcification are strongly determined by minimum pH values experienced (Vargas et al., 2022) and may be exacerbated by diel pH oscillation (Comeau et al., 2014a). In this study, acclimation and the ambient pH treatment had a larger pH range (ΔpH 0.6 units) than the low pH treatment (ΔpH 0.2 units). Therefore, our low pH effects might be underestimated. Similarly, variability experienced naturally by our colonies may have had further unknown effects. In summary, our findings indicate that growth responses alone may not fully reflect coral susceptibility to OA. Therefore, future studies incorporating non-calcification parameters and non-calcifying early coral life stages (e.g., Moya et al., 2015) will be important to better understand coral OA susceptibility. In addition, incorporating natural pH oscillation regimes may help understand the role of pH variability in coral acclimatization to

OA, which is key since diel pH ranges are predicted to increase under future OA conditions (Shaw et al., 2013).

5 CONCLUSIONS

Our study suggests that coral growth under low pH is (i) mediated by different physiological parameters, whose interplay is (ii) genus- or species-specific. Specifically, our results indicate that the decrease in growth under low pH is mediated differently in *Acropora* and *Pocillopora* but is unmediated in *Porites* spp. These different physiological changes may include successful acclimatization as seen in *Pocillopora* and *Porites* spp. *via* buffering or hibernation strategies, but also unsuccessful acclimatization as seen in *Acropora* spp., in which growth was maintained at the expense of cellular stress. These findings underline the value of a multi-parametric approach to assess coral susceptibility to OA. This might help to improve our ability to interpret growth changes that reef-building corals experience under OA conditions and better predict the susceptibility of coral species to OA.

DATA AVAILABILITY STATEMENT

Details of experimental tanks and coral species, seawater chemistry data and results of its statistical analysis, processed physiological data, model diagnostic plots, and model coefficients and CIs used in Figure 1 can be accessed in the Supplementary Material (Supplementary Figures S1–5, Supplementary Tables S1–5). Raw data and the physiological basis calculated from it were uploaded to figshare and are accessible at https://doi.org/10.6084/m9.figshare.19107380.

AUTHOR CONTRIBUTIONS

Conceptualization: JR, PS, and TW; Investigation: AA, KK, PS, and JR; Formal analysis, Visualization, Writing – original draft: CM; Writing – review and editing: CM, MZ, TW, and JR; Project administration: JR; Funding acquisition: TW. All authors contributed to the article and approved the submitted version.

FUNDING

This study was conducted as part of the 'Ocean2100' global change simulation project of the Colombian-German Center of Excellence in Marine Sciences (CEMarin), funded by the German Academic Exchange Service. (DAAD, project number 57480468).

ACKNOWLEDGMENTS

We thank Thomas Timm and Silvia Nachtigall for their support in the lab and Torsten Hauffe for his help with the statistical analyses.

SUPPLEMENTARY MATERIAL

The Supplementary Material for this article can be found online at: https://www.frontiersin.org/articles/10.3389/fmars.2022.872631/full#supplementary-material

REFERENCES

Al-Horani, F. A. (2015). "Physiology of Skeletogenesis in Scleractinian Coral," in *Diseases of Coral* (Hoboken, NJ: John Wiley & Sons, Inc), 192–205. doi: 10.1002/9781118828502.ch12

Anthony, K. R. N. (2016). Coral Reefs Under Climate Change and Ocean Acidification: Challenges and Opportunities for Management and Policy. *Annu. Rev. Environ. Resour.* 41, 59–81. doi: 10.1146/annurev-environ-110615-085610

Bahr, K. D., Jokiel, P. L., and Ku'ulei, R. (2016). Relative Sensitivity of Five Hawaiian Coral Species to High Temperature Under High-Pco_2 Conditions. *Coral Reefs* 35, 729–738. doi: 10.1007/s00338-016-1405-4

Brown, D., and Edmunds, P. J. (2016). Differences in the Responses of Three Scleractinians and the Hydrocoral *Millepora Platyphylla* to Ocean Acidification. *Mar. Biol.* 163, 1–10. doi: 10.1007/s00227-016-2837-7

Buddemeier, R. W., and Kinzie, R. A. (1976). Coral Growth. *Oceanogr. Mar. Biol. Annu. Rev.* 14, 183–225.

Buddemeier, R. W., Maragos, J. E., and Knutson, D. W. (1974). Radiographic Studies of Reef Coral Exoskeletons: Rates and Patterns of Coral Growth. *J. Exp. Mar. Bio. Ecol.* 14, 179–199. doi: 10.1016/0022-0981(74)90024-0

Chan, N. C. S., and Connolly, S. R. (2013). Sensitivity of Coral Calcification to Ocean Acidification: A Meta-Analysis. *Glob. Change Biol.* 19, 282–290. doi: 10.1111/gcb.12011

Cignoni, P., Callieri, M., Corsini, M., Dellepiane, M., Ganovelli, F., and Ranzuglia, G. (2008). MeshLab: An Open-Source Mesh Processing Tool. *Sixth Eurographics Ital. Chapter Conf.* 129–136. doi: 10.2312/LocalChapterEvents/ItalChap/ItalianChapConf2008/129-136

Comeau, S., Cornwall, C. E., DeCarlo, T. M., Doo, S. S., Carpenter, R. C., and McCulloch, M. T. (2019). Resistance to Ocean Acidification in Coral Reef Taxa is Not Gained by Acclimatization. *Nat. Clim. Change* 9, 477–483. doi: 10.1038/s41558-019-0486-9

Comeau, S., Cornwall, C. E., and McCulloch, M. T. (2017). Decoupling Between the Response of Coral Calcifying Fluid pH and Calcification to Ocean Acidification. *Sci. Rep.* 7, 7573. doi: 10.1038/s41598-017-08003-z

Comeau, S., Edmunds, P. J., Spindel, N. B., and Carpenter, R. C. (2013). The Responses of Eight Coral Reef Calcifiers to Increasing Partial Pressure of CO_2 Do Not Exhibit a Tipping Point. *Limnol. Oceanogr.* 58, 388–398. doi: 10.4319/lo.2013.58.1.0388

Comeau, S., Edmunds, P. J., Spindel, N. B., and Carpenter, R. C. (2014a). Diel Pco_2 Oscillations Modulate the Response of the Coral *Acropora Hyacinthus* to Ocean Acidification. *Mar. Ecol. Prog. Ser.* 501, 99–111. doi: 10.3354/meps10690

Comeau, S., Edmunds, P. J., Spindel, N. B., and Carpenter, R. C. (2014b). Fast Coral Reef Calcifiers Are More Sensitive to Ocean Acidification in Short-Term Laboratory Incubations. *Limnol. Oceanogr.* 59, 1081–1091. doi: 10.4319/lo.2014.59.3.1081

Conlan, J. A., Jones, P. L., Turchini, G. M., Hall, M. R., and Francis, D. S. (2014). Changes in the Nutritional Composition of Captive Early-Mid Stage *Panulirus Ornatus* Phyllosoma Over Ecdysis and Larval Development. *Aquaculture* 434, 159–170. doi: 10.1016/j.aquaculture.2014.07.030

Conlan, J. A., Rocker, M. M., and Francis, D. S. (2017). A Comparison of Two Common Sample Preparation Techniques for Lipid and Fatty Acid Analysis in Three Different Coral Morphotypes Reveals Quantitative and Qualitative Differences. *PeerJ* 5, e3645. doi: 10.7717/peerj.3645

Cuif, J.-P., and Dauphin, Y. (2005). The Two-Step Mode of Growth in the Scleractinian Coral Skeletons From the Micrometre to the Overall Scale. *J. Struct. Biol.* 150, 319–331. doi: 10.1016/j.jsb.2005.03.004

Darling, E. S., Alvarez-Filip, L., Oliver, T. A., McClanahan, T. R., and Côté, I. M. (2012). Evaluating Life-History Strategies of Reef Corals From Species Traits. *Ecol. Lett.* 15, 1378–1386. doi: 10.1111/j.1461-0248.2012.01861.x

Dickson, A. G., and Millero, F. J. (1987). A Comparison of the Equilibrium Constants for the Dissociation of Carbonic Acid in Seawater Media. *Deep Sea Res. Part A. Oceanogr. Res. Pap.* 34, 1733–1743. doi: 10.1016/0198-0149(87)90021-5

Dornelas, M., Madin, J. S., Baird, A. H., and Connolly, S. R. (2017). Allometric Growth in Reef-Building Corals. *Proc. R. Soc B Biol. Sci.* 284, 20170053. doi: 10.1098/rspb.2017.0053

Edmunds, P. (2007). Evidence for a Decadal-Scale Decline in the Growth Rates of Juvenile Scleractinian Corals. *Mar. Ecol. Prog. Ser.* 341, 1–13. doi: 10.3354/meps341001

Edmunds, P. J. (2011). Zooplanktivory Ameliorates the Effects of Ocean Acidification on the Reef Coral Porites spp. *Limnol. Oceanogr.* 56, 2402–2410. doi: 10.4319/lo.2011.56.6.2402

Edmunds, P. J. (2012). Effect of Pco_2 on the Growth, Respiration, and Photophysiology of Massive *Porites* spp. In Moorea, French Polynesia. *Mar. Biol.* 159, 2149–2160. doi: 10.1007/s00227-012-2001-y

Edmunds, P. J., Burgess, S. C., Putnam, H. M., Baskett, M. L., Bramanti, L., Fabina, N. S., et al. (2014). Evaluating the Causal Basis of Ecological Success Within the Scleractinia: An Integral Projection Model Approach. *Mar. Biol.* 161, 2719–2734. doi: 10.1007/s00227-014-2547-y

Enochs, I. C., Manzello, D. P., Carlton, R., Schopmeyer, S., van Hooidonk, R., and Lirman, D. (2014). Effects of Light and Elevated Pco_2 on the Growth and Photochemical Efficiency of *Acropora Cervicornis*. *Coral Reefs* 33, 477–485. doi: 10.1007/s00338-014-1132-7

Enochs, I. C., Manzello, D. P., Jones, P. J., Aguilar, C., Cohen, K., Valentino, L., et al. (2018). The Influence of Diel Carbonate Chemistry Fluctuations on the Calcification Rate of *Acropora Cervicornis* Under Present Day and Future Acidification Conditions. *J. Exp. Mar. Bio. Ecol.* 506, 135–143. doi: 10.1016/j.jembe.2018.06.007

Evensen, N. R., Bozec, Y.-M., Edmunds, P. J., and Mumby, P. J. (2021). Scaling the Effects of Ocean Acidification on Coral Growth and Coral–Coral Competition on Coral Community Recovery. *PeerJ* 9, e11608. doi: 10.7717/peerj.11608

Folch, J., Lees, M., and Stanley, G. H. S. (1957). A Simple Method for the Isolation and Purification of Total Lipides From Animal Tissues. *J. Biol. Chem.* 226, 497–509. doi: 10.1016/S0021-9258(18)64849-5

Gaylord, B., Kroeker, K. J., Sunday, J. M., Anderson, K. M., Barry, J. P., Brown, N. E., et al. (2015). Ocean Acidification Through the Lens of Ecological Theory. *Ecology* 96, 3–15. doi: 10.1890/14-0802.1

Gnaiger, E., and Bitterlich, G. (1984). Proximate Biochemical Composition and Caloric Content Calculated From Elemental CHN Analysis: A Stoichiometric Concept. *Oecologia* 62, 289–298. doi: 10.1007/BF00384259

Godefroid, M., Arçuby, R., Lacube, Y., Espiau, B., Dupont, S., Gazeau, F., et al. (2021). More Than Local Adaptation: High Diversity of Response to Seawater Acidification in Seven Coral Species From the Same Assemblage in French Polynesia. *J. Mar. Biol. Assoc. United Kingdom* 101, 675–683. doi: 10.1017/S0025315421000618

Gross, E. M. (2003). Allelopathy of Aquatic Autotrophs. *CRC. Crit. Rev. Plant* 22, 313–339. doi: 10.1080/713610859

Holcomb, M., Venn, A. A., Tambutté, E., Tambutté, S., Allemand, D., Trotter, J., et al. (2014). Coral Calcifying Fluid pH Dictates Response to Ocean Acidification. *Sci. Rep.* 4, 1–4. doi: 10.1038/srep05207

Horwitz, R., Hoogenboom, M. O., and Fine, M. (2017). Spatial Competition Dynamics Between Reef Corals Under Ocean Acidification. *Sci. Rep.* 7, 40288. doi: 10.1038/srep40288

Hui, F. K. C. (2016). BORAL – Bayesian Ordination and Regression Analysis of Multivariate Abundance Data in R. *Methods Ecol. Evol.* 7, 744–750. doi: 10.1111/2041-210X.12514

Hui, F. K. C. (2020) *Boral: Bayesian Ordination and Regression Analysis*. Available at: https://CRAN.R-project.org/package=boral.

IPCC and Core Writing Team (2014). *Climate Change 2014: Synthesis Report. Contribution of Working Groups I, II and III to the Fifth Assessment Report of the Intergovernmental Panel on Climate Change*. Eds. R. K. Pachauri and L. A. Meyer (Geneva, Switzerland: IPCC).

Kaniewska, P., Campbell, P. R., Kline, D. I., Rodriguez-Lanetty, M., Miller, D. J., Dove, S., et al. (2012). Major Cellular and Physiological Impacts of Ocean Acidification on a Reef Building Coral. *PloS One* 7, e34659. doi: 10.1371/journal.pone.0034659

Kaniewska, P., Chan, C. K., Kline, D., Yew, E., Ling, S., Rosic, N., et al. (2015). Transcriptomic Changes in Coral Holobionts Provide Insights Into Physiological Challenges of Future Climate and Ocean Change. *PloS One* 10, e0139223. doi: 10.1371/journal.pone.0139223

Kassambara, A., and Mundt, F. (2020) *Factoextra: Extract and Visualize the Results of Multivariate Data Analyses*. Available at: https://CRAN.R-project.org/package=factoextra.

Kavousi, J., Tanaka, Y., Nishida, K., Suzuki, A., Nojiri, Y., and Nakamura, T. (2016). Colony-Specific Calcification and Mortality Under Ocean Acidification in the Branching Coral *Montipora Digitata*. *Mar. Environ. Res.* 119, 161–165. doi: 10.1016/j.marenvres.2016.05.025

Kayal, M., Lenihan, H. S., Brooks, A. J., Holbrook, S. J., Schmitt, R. J., and Kendall, B. E. (2019). Predicting Coral Community Recovery Using Multi-Species Population Dynamics Models. *Ecol. Lett.* 22, 605–615. doi: 10.1111/ele.13203

Kenkel, C. D., Moya, A., Strahl, J., Humphrey, C., and Bay, L. K. (2018). Functional Genomic Analysis of Corals From Natural CO_2-Seeps Reveals Core Molecular Responses Involved in Acclimatization to Ocean Acidification. *Glob. Change Biol.* 24, 158–171. doi: 10.1111/gcb.13833

Kornder, N. A., Riegl, B. M., and Figueiredo, J. (2018). Thresholds and Drivers of Coral Calcification Responses to Climate Change. *Glob. Change Biol.* 24, 5084–5095. doi: 10.1111/gcb.14431

Krief, S., Hendy, E. J., Fine, M., Yam, R., Meibom, A., Foster, G. L., et al. (2010). Physiological and Isotopic Responses of Scleractinian Corals to Ocean Acidification. *Geochim. Cosmochim. Acta* 74, 4988–5001. doi: 10.1016/j.gca.2010.05.023

Kroeker, K. J., Kordas, R. L., Crim, R., Hendriks, I. E., Ramajo, L., Singh, G. S., et al. (2013). Impacts of Ocean Acidification on Marine Organisms: Quantifying Sensitivities and Interaction With Warming. *Glob. Change Biol.* 19, 1884–1896. doi: 10.1111/gcb.12179

Kruschke, J. K. (2010). *Doing Bayesian Data Analysis: A Tutorial With R and BUGS. 1st ed* (Cambridge, MA: Academic Press).

Kruschke, J. K. (2018). Rejecting or Accepting Parameter Values in Bayesian Estimation. *Adv. Methods Pract. Psychol. Sci.* 1, 270–280. doi: 10.1177/2515245918771304

Lê, S., Josse, J., and Husson, F. (2008). FactoMineR: An R Package for Multivariate Analysis. *J. Stat. Software* 25, 1–18. doi: 10.18637/jss.v025.i01

Liu, T., Brouha, B., and Grossman, D. (2004). Rapid Induction of Mitochondrial Events and Caspase-Independent Apoptosis in Survivin-Targeted Melanoma Cells. *Oncogene* 23, 39–48. doi: 10.1038/sj.onc.1206978

Loya, Y., Sakai, K., Yamazato, K., Nakano, Y., Sambali, H., and Van Woesik, R. (2001). Coral Bleaching: The Winners and the Losers. *Ecol. Lett.* 4, 122–131. doi: 10.1046/j.1461-0248.2001.00203.x

Mehrbach, C., Culberson, C. H., Hawley, J. E., and Pytkowicx, R. M. (1973). Measurement of the Apparent Dissociation Constants of Carbonic Acid in Seawater at Atmospheric Pressure. *Limnol. Oceanogr.* 18, 897–907. doi: 10.4319/lo.1973.18.6.0897

Millero, F. J. (2013). *Chemical Oceanography. 4th ed* (Boca Raton, FL: CRC Press).

Mollica, N. R., Guo, W., Cohen, A. L., Huang, K., Foster, G. L., Donald, H. K., et al. (2018). Ocean Acidification Affects Coral Growth by Reducing Skeletal Density. *Proc. Natl. Acad. Sci.* 115, 1754–1759. doi: 10.1073/pnas.1712806115

Moya, A., Huisman, L., Forêt, S., Gattuso, J.-P., Hayward, D. C., Ball, E. E., et al. (2015). Rapid Acclimation of Juvenile Corals to CO_2-Mediated Acidification by Upregulation of Heat Shock Protein and Bcl-2 Genes. *Mol. Ecol.* 24, 438–452. doi: 10.1111/mec.13021

Neath, A. A., and Cavanaugh, J. E. (2006). A Bayesian Approach to the Multiple Comparisons Problem. *J. Data Sci.* 4, 131–146. doi: 10.6339/JDS.2006.04(2).266

Ohde, S., and Van Woesik, R. (1999). Carbon Dioxide Flux and Metabolic Processes of a Coral Reef, Okinawa. *Bull. Mar. Sci.* 65, 559–576.

Palardy, J., Grottoli, A., and Matthews, K. (2005). Effects of Upwelling, Depth, Morphology and Polyp Size on Feeding in Three Species of Panamanian Corals. *Mar. Ecol. Prog. Ser.* 300, 79–89. doi: 10.3354/meps300079

Pelletier, G., Lewis, E., and Wallace, D. (2007). CO2Sys. Xls: A Calculator for the CO_2 System in Seawater for Microsoft Excel/VBA. *Washingt. State Dep. Ecol. Natl. Lab. Olympia WA/Upton NY U.S.A*.

Pratchett, M. S., Anderson, K. D., Hoogenboom, M. O., Widman, E., Baird, A. H., Pandolfi, J. M., et al. (2015). Spatial, Temporal and Taxonomic Variation in Coral Growth—Implications for the Structure and Function of Coral Reef Ecosystems. *Oceanogr. Mar. Biol. Annu. Rev.* 53, 215–295.

Putnam, H. M., Barott, K. L., Ainsworth, T. D., and Gates, R. D. (2017). The Vulnerability and Resilience of Reef-Building Corals. *Curr. Biol.* 27, R528–R540. doi: 10.1016/j.cub.2017.04.047

R Core Team (2021) *R: A Language and Environment for Statistical Computing*. Available at: https://www.r-project.org/.

Reichert, J., Schellenberg, J., Schubert, P., and Wilke, T. (2016). 3D Scanning as a Highly Precise, Reproducible, and Minimally Invasive Method for Surface Area and Volume Measurements of Scleractinian Corals. *Limnolgy Oceanogr. Methods* 14, 518–526. doi: 10.1002/lom3.10109

R Studio Team (2021) *RStudio: Integrated Development Environment for R*. Available at: http://www.rstudio.com/.

Sørensen, J. G., Kristensen, T. N., and Loeschcke, V. (2003). The Evolutionary and Ecological Role of Heat Shock Proteins. *Ecol. Lett.* 6, 1025–1037. doi: 10.1046/j.1461-0248.2003.00528.x

Schoepf, V., Grottoli, A. G., Warner, M. E., Cai, W. J., Melman, T. F., Hoadley, K. D., et al. (2013). Coral Energy Reserves and Calcification in a High-CO_2 World at Two Temperatures. *PloS One* 8, e75049. doi: 10.1371/journal.pone.0075049

Schoepf, V., Jury, C. P., Toonen, R. J., and McCulloch, M. T. (2017). Coral Calcification Mechanisms Facilitate Adaptive Responses to Ocean Acidification. *Proc. R. Soc B Biol. Sci.* 284, 20172117. doi: 10.1098/rspb.2017.2117

Schutter, M., Kranenbarg, S., Wijffels, R. H., Verreth, J., and Osinga, R. (2011). Modification of Light Utilization for Skeletal Growth by Water Flow in the Scleractinian Coral *Galaxea Fascicularis*. *Mar. Biol.* 158, 769–777. doi: 10.1007/s00227-010-1605-3

Shaw, E. C., Carpenter, R. C., Lantz, C. A., and Edmunds, P. J. (2016). Intraspecific Variability in the Response to Ocean Warming and Acidification in the Scleractinian Coral *Acropora Pulchra*. *Mar. Biol.* 163, 1–11. doi: 10.1007/s00227-016-2986-8

Shaw, E. C., McNeil, B. I., and Tilbrook, B. (2012). Impacts of Ocean Acidification in Naturally Variable Coral Reef Flat Ecosystems. *J. Geophys. Res. Ocean.* 117, 1–14. doi: 10.1029/2011JC007655

Shaw, E. C., McNeil, B. I., Tilbrook, B., Matear, R., and Bates, M. L. (2013). Anthropogenic Changes to Seawater Buffer Capacity Combined With Natural Reef Metabolism Induce Extreme Future Coral Reef CO_2 Conditions. *Glob. Change Biol.* 19, 1632–1641. doi: 10.1111/gcb.12154

Spencer Davies, P. (1989). Short-Term Growth Measurements of Corals Using an Accurate Buoyant Weighing Technique. *Mar. Biol.* 101, 389–395. doi: 10.1007/BF00428135

Strahl, J., Francis, D. S., Doyle, J., Humphrey, C., and Fabricius, K. E. (2016). Biochemical Responses to Ocean Acidification Contrast Between Tropical Corals With High and Low Abundances at Volcanic Carbon Dioxide Seeps. *ICES J. Mar. Sci.* 73, 897–909. doi: 10.1093/icesjms/fsv194

Sunday, J. M., Fabricius, K. E., Kroeker, K. J., Anderson, K. M., Brown, N. E., Barry, J. P., et al. (2017). Ocean Acidification can Mediate Biodiversity Shifts by Changing Biogenic Habitat. *Nat. Clim. Change* 7, 81–86. doi: 10.1038/NCLIMATE3161

Takahashi, T. (1982). "Carbonate Chemistry," in *GEOSECS Pacific Expedition, Volume 3, Hydrographic Data 1973-1974* (Washington, DC: National Science Foundation), 77–83.

Tambutté, E., Venn, A. A., Holcomb, M., Segonds, N., Techer, N., Zoccola, D., et al. (2015). Morphological Plasticity of the Coral Skeleton Under CO_2-Driven Seawater Acidification. *Nat. Commun.* 6, 7368. doi: 10.1038/ncomms8368

Tchernov, D., Kvitt, H., Haramaty, L., Bibbyd, T. S., Gorbunov, M. Y., Rosenfeld, H., et al. (2011). Apoptosis and the Selective Survival of Host Animals Following Thermal Bleaching in Zooxanthellate Corals. *Proc. Natl. Acad. Sci. U. S. A.* 108, 9905–9909. doi: 10.1073/pnas.1106924108

Thornhill, D. J., Rotjan, R. D., Todd, B. D., Chilcoat, G. C., Iglesias-prieto, R., Kemp, D. W., et al. (2011). A Connection Between Colony Biomass and Death in Caribbean Reef-Building Corals. *PloS One* 6, e29535. doi: 10.1371/journal.pone.0029535

Towle, E. K., Enochs, I. C., and Langdon, C. (2015). Threatened Caribbean Coral is Able to Mitigate the Adverse Effects of Ocean Acidification on Calcification by Increasing Feeding Rate. *PloS One* 10, 1–17. doi: 10.1371/journal.pone.0123394

Vargas, C. A., Cuevas, L. A., Broitman, B. R., San Martin, V. A., Lagos, N. A., Gaitán-Espitia, J. D., et al. (2022). Upper Environmental Pco_2 Drives Sensitivity to Ocean Acidification in Marine Invertebrates. *Nat. Clim. Change* 12, 200–207. doi: 10.1038/s41558-021-01269-2

Wall, C. B., Mason, R. A. B., Ellis, W. R., Cunning, R., and Gates, R. D. (2017). Elevated Pco_2 Affects Tissue Biomass Composition, But Not Calcification, in a Reef Coral Under Two Light Regimes. *R. Soc Open Sci.* 4, 170683. doi: 10.1098/rsos.170683

Watson, S. A., Fabricius, K. E., and Munday, P. L. (2017). Quantifying Pco_2 in Biological Ocean Acidification Experiments: A Comparison of Four Methods. *PloS One* 12, e0185469. doi: 10.1371/journal.pone.0185469

Wickham, H. (2016). *Ggplot2: Elegant Graphics for Data Analysis* (New York: Springer). Available at: https://ggplot2.tidyverse.org.

Ziegler, M., Anton, A., Klein, S. G., Rädecker, N., Geraldi, N. R., Schmidt-Roach, S., et al. (2021). Integrating Environmental Variability to Broaden the Research on Coral Responses to Future Ocean Conditions. *Glob. Change Biol.* 27, 5532–5546. doi: 10.1111/gcb.15840

Zuur, A. F., Ieno, E. N., and Elphick, C. S. (2010). A Protocol for Data Exploration to Avoid Common Statistical Problems. *Methods Ecol. Evol.* 1, 3–14. doi: 10.1111/j.2041-210X.2009.00001.x

Conflict of Interest: The authors declare that the research was conducted in the absence of any commercial or financial relationships that could be construed as a potential conflict of interest.

Publisher's Note: All claims expressed in this article are solely those of the authors and do not necessarily represent those of their affiliated organizations, or those of the publisher, the editors and the reviewers. Any product that may be evaluated in this article, or claim that may be made by its manufacturer, is not guaranteed or endorsed by the publisher.

Supplementary Material

Growth response of reef-building corals to ocean acidification is mediated by interplay of taxon-specific physiological parameters

Catarina P.P. Martins*, Angelina L. Arnold, Katharina Kömpf, Patrick Schubert, Maren Ziegler, Thomas Wilke, Jessica Reichert

Department of Animal Ecology & Systematics, Justus Liebig University Giessen, D-35392, Giessen, Germany

*corresponding author: catarina.padilha-pires-martins@bio.uni-giessen.de

Content:

Supplementary Text

1. Seawater chemistry

1.1. Description of statistical analyses

Differences in seawater carbonate chemistry between treatments and tanks were tested using daily mean values from days with alkalinity measurements. Differences between treatments were tested using a two-way ANOVA with treatment as fixed factor (2 levels) and tank as random factor nested in treatment (3 levels). Differences between tanks within treatments were tested using separate one-way ANOVAs with tank as fixed factor (3 levels). Statistical assumptions of normality and homoscedasticity for ANOVA were verified by graphical inspection of residuals. Statistical analyses were performed in R (v.4.1.0; R Core Team, 2021) using RStudio (v1.4.1103; RStudio Team, 2021) and packages *stats*, *car* (v.3.0-11; Fox and Weisberg, 2019), and *lme4* (v.1.1-27.1; Bates et al., 2015).

1.2. Results

The analyses revealed that pH was significantly different between replicate ambient pH tanks (Supplementary Table S3), with tank effects reflected in differences of 0.1 pH units. Temperature was significantly different between replicate tanks of both treatments (Supplementary Table S3), which reflected differences of 0.2 and 0.5 ºC in ambient and low pH treatments, respectively. These tank effects of pH and temperature might be attributed to the accuracy of the used sensors (pH: ± 0.1 pH units, temperature: ± 0.1°C). A summary of the complete recording of temperature and pH conditions in each tank is provided in Supplementary Table S4.

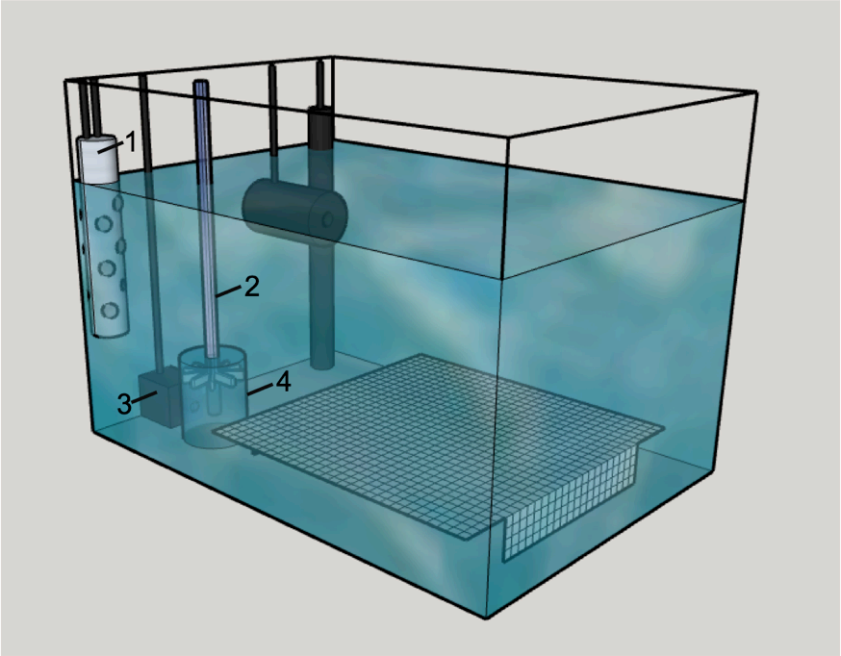

Supplementary Figure S1. Schematic drawing of an experimental tank with all the elements of CO_2 control and release marked: 1. pH probe housed inside a perforated PVC tube; 2. CO_2-gas tube; 3. diffuser pump; 4. CO_2 diffuser.

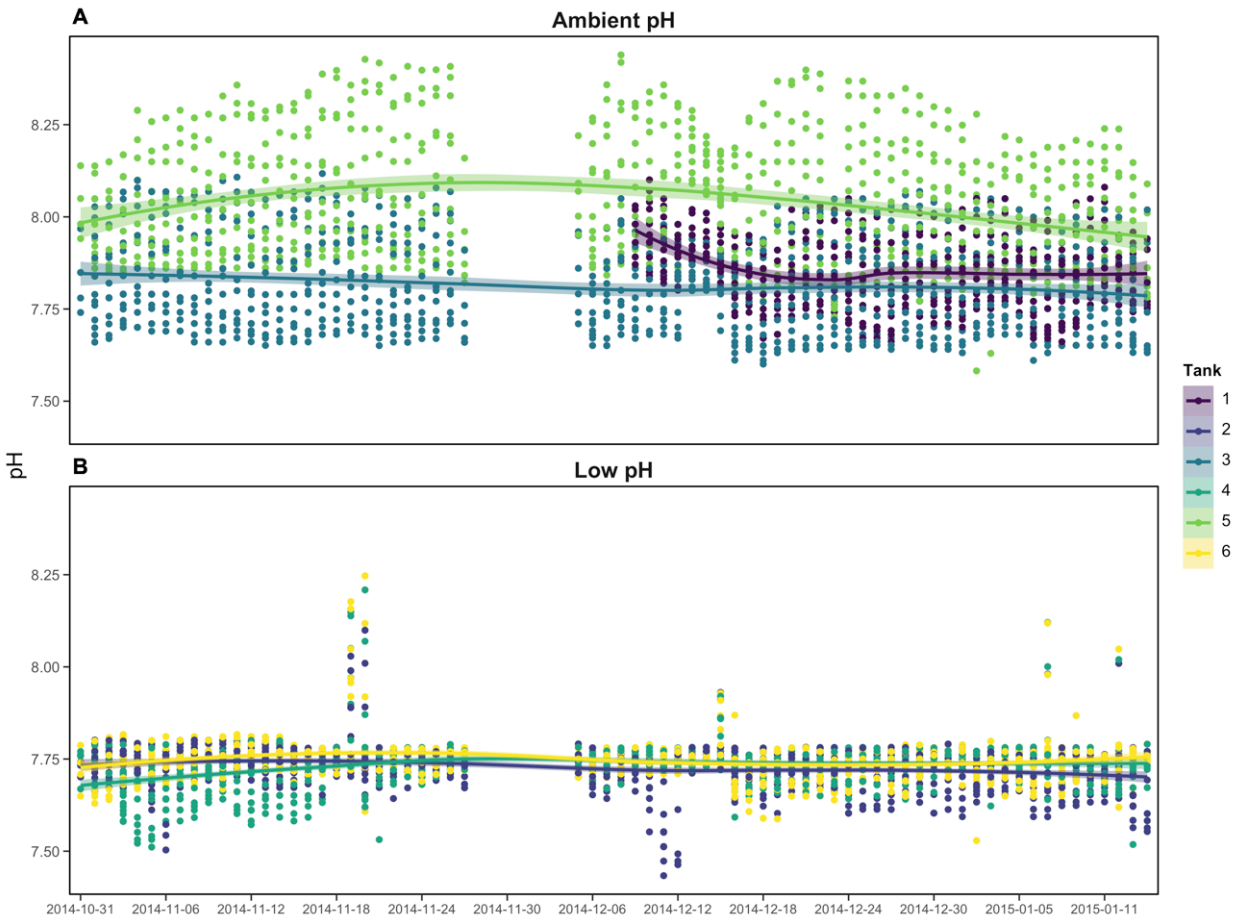

Supplementary Figure S2. Seawater pH values on total scale in the (A) ambient pH and (B) low pH treatment, of a three-month experiment. Lines are local polynomial regression fitting with 95% confidence intervals (shaded area).

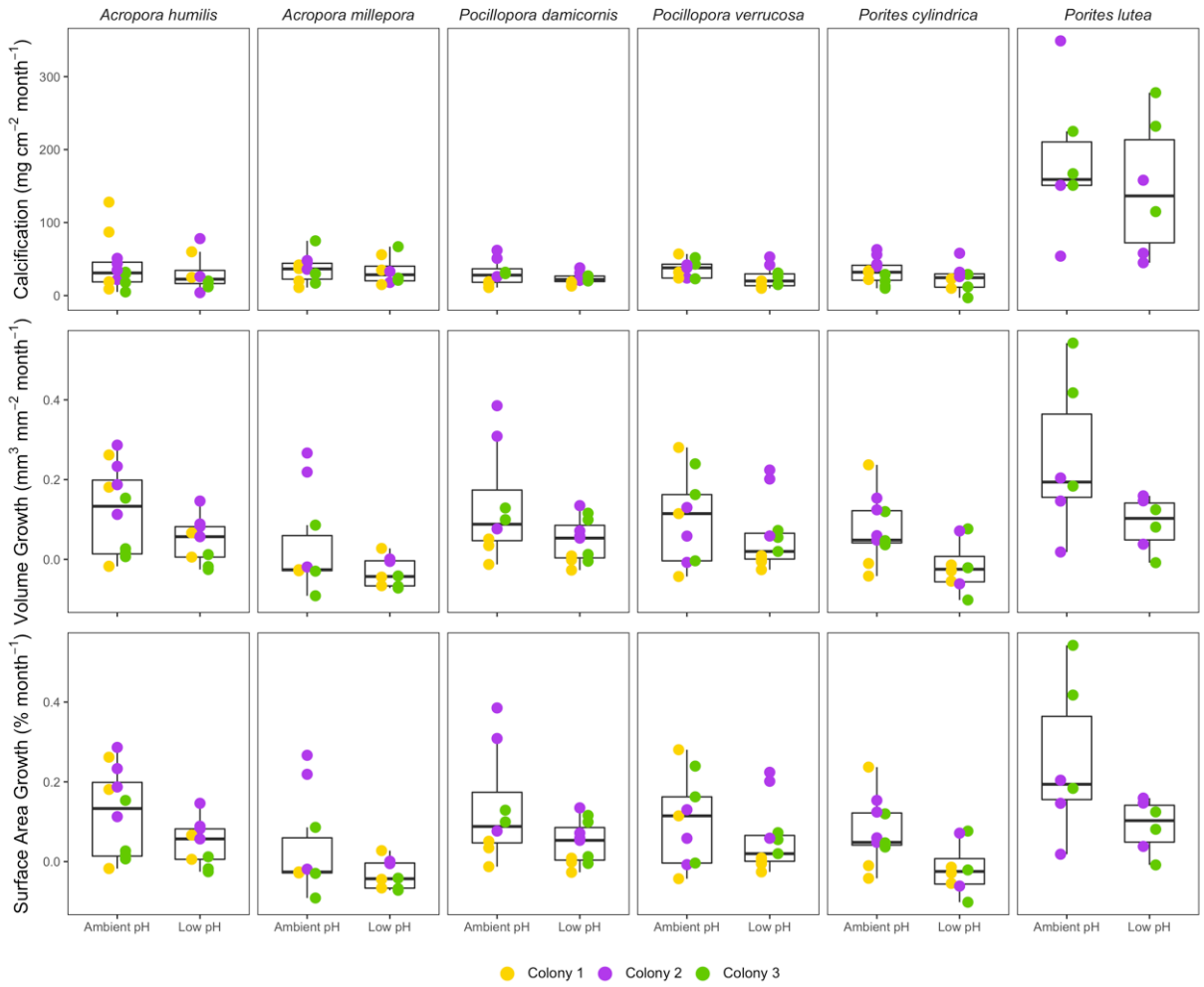

Supplementary Figure S3. Data values of calcification, volume growth and surface area growth from six scleractinian coral species maintained in ambient and low pH treatments for three months. Boxes of box plots represent the first and third quartiles with lines as medians and whiskers as the 1.5 * interquartile range (IQR).

Supplementary Figure S4. Data values of physiological parameters associated to maintenance (tissue biomass, lipid and protein content, and energy content) and cellular stress (apoptotic activity) from six scleractinian coral species maintained in ambient and low pH treatments for three months. Boxes of box plots represent the first and third quartiles with lines as medians and whiskers as the 1.5 * interquartile range (IQR). AFDW, ash-free dry weight; DW, dry weight; RLU, rapid light units

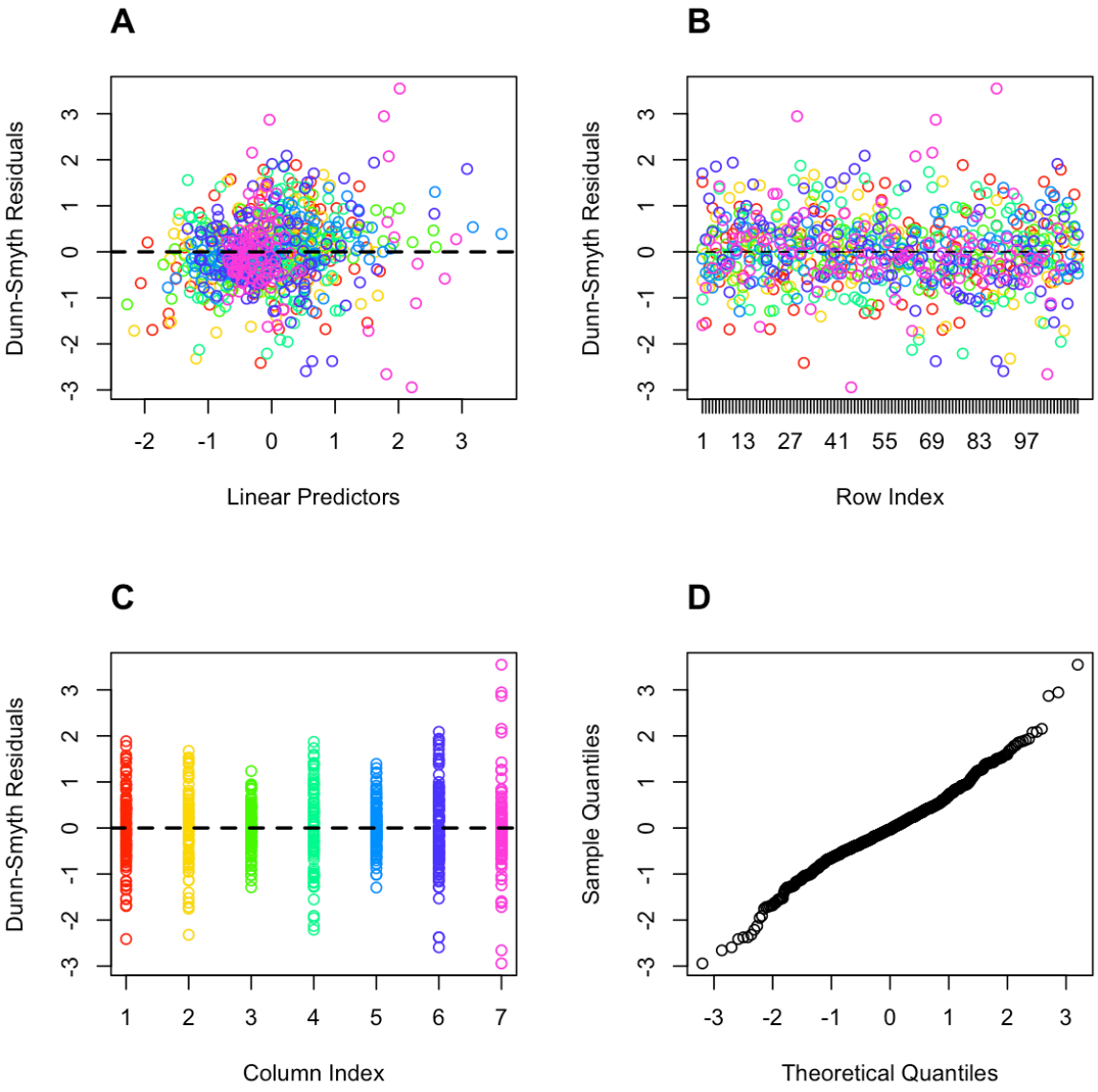

Supplementary Figure S5. Plots of residual analysis from the Bayesian generalized linear latent variable model. Plots are (A) Dunn-Smyth residuals vs. linear predictors, (B) Dunn-Smyth residuals vs. row index (i.e., individuals), (C) Dunn-Smyth residuals vs. column index (i.e., physiological variables), and (D) normal quantile plot of Dunn-Smyth residuals. Each color represents one of the seven physiological variables studied.

Supplementary Table S1. Details on coral species used in the experiment. Origin, date of collection, date of arrival at the aquarium facilities at Justus Liebig University, and CITES numbers of coral species are provided.

Species	Origin	Collection	Arrival	CITES number
Acropora humilis	Bali (Indonesia)	20/03/2014	11/04/2014	14NL2147/32/11
Acropora millepora	Bali (Indonesia)	20/03/2014	11/04/2014	14NL214731/11
Pocillopora damicornis	Bali (Indonesia)	03/04/2014, 10/04/2014	11/04/2014, 12/05/2014	14NL214371/11 14NL214367/11
Pocillopora verrucosa	Bali (Indonesia)	10/04/2014	12/05/2014	14NL214371/11
Porites cylindrica	Bali (Indonesia)	10/04/2014	12/05/2014	14NL214371/11
Porites lutea	Bali (Indonesia)	01/05/2014	12/05/2014	14NL216270/11

Supplementary Table S2. Mean seawater chemistry in the six experimental tanks. Values are expressed as mean ± s.d., together with measurement replication (*n*). Tank 1 has lower replication for measurements of pH, pCO_2, and Ω_{Ar} due to a malfunction during which the values measured by the pH sensor in this tank (ambient pH treatment) were not recorded, but still monitored, for a total of 32 days. Values of pCO_2 and Ω_{Ar} were calculated from days with alkalinity measurements. No temperature or pH values were recorded during one of the alkalinity measurement days therefore carbonate chemistry was calculated for a total of 15 days throughout the experiment. Average daily minimum and maximum pH was calculated from the complete recording of pH values. A summary of the complete recording of temperature and pH values in each tank is provided in Supplementary Table S4. Ω_{Ar}, aragonite saturation; pCO_2, partial pressure of CO_2; pH_T, pH on total scale; TA, total alkalinity

Tank	Treatment Name	Temperature (ºC)	Salinity	pH_T	TA (µmol kg^{-1})	pCO_2 (µatm)	Ω_{Ar}	Daily Minimum pH_T	Daily Maximum pH_T
1	Ambient pH	25.3 ± 0.3 (181)	33.5 ± 0.6 (4)	7.86 ± 0.10 (96)	2172 ± 240 (16)	620 ± 166 (96)	2.11 ± 0.47 (96)	7.74 ± 0.06 (37)	8.02 ± 0.04 (37)
2	Low pH	24.8 ± 0.5 (181)		7.74 ± 0.05 (181)		873 ± 136 (181)	1.75 ± 0.34 (181)	7.64 ± 0.06 (69)	7.80 ± 0.07 (69)
3	Ambient pH	25.4 ± 0.4 (181)		7.82 ± 0.12 (181)		727 ± 231 (181)	2.16 ± 0.63 (181)	7.67 ± 0.03 (69)	8.02 ± 0.06 (69)
4	Low pH	25.1 ± 0.5 (181)		7.73 ± 0.07 (181)		896 ± 195 (181)	1.75 ± 0.40 (181)	7.66 ± 0.06 (69)	7.80 ± 0.09 (69)
5	Ambient pH	25.3 ± 0.6 (181)		8.06 ± 0.17 (181)		404 ± 178 (181)	3.33 ± 1.08 (181)	7.84 ± 0.07 (69)	8.28 ± 0.10 (69)
6	Low pH	25.7 ± 0.5 (181)		7.76 ± 0.07 (181)		843 ± 139 (181)	1.87 ± 0.45 (181)	7.68 ± 0.04 (69)	7.81 ± 0.09 (69)

Supplementary Table S3. Results of two-way ANOVAs testing differences between treatments and one-way ANOVAs testing differences between replicate tanks, for seawater chemistry parameters. Significant effects at the level of $\alpha < 0.05$ are marked in bold. Ω_{Ar}, aragonite saturation; pCO_2, partial pressure of CO_2

Variable	Effect	Df	F	p-value
pH	Treatment	1	5.58	**0.018**
	Tank (ambient pH)	2	107.55	**< 0.001**
	Tank (low pH)	2	1.02	0.368
pCO_2	Treatment	1	7.75	**0.005**
	Tank (ambient pH)	2	64.51	**< 0.001**
	Tank (low pH)	2	0.73	0.489
Ω_{Ar}	Treatment	1	4.49	**0.034**
	Tank (ambient pH)	2	40.71	**< 0.001**
	Tank (low pH)	2	0.74	0.481
Temperature	Treatment	1	0.26	0.614
	Tank (ambient pH)	2	5.46	**0.009**
	Tank (low pH)	2	108.71	**< 0.001**

Supplementary Table S4. Mean temperature and pH in the six experimental tanks recorded during the three-month experiment. Tank 1 has lower replication for measurements of pH due to a malfunction during which the values measured by the pH sensor in this tank (ambient pH treatment) were not recorded, but still monitored, for a total of 32 days. pH_T, pH on total scale

Tank	Treatment Name	Temperature (ºC)	pH_T
1	Ambient pH	25.3 ± 0.3 (805)	7.85 ± 0.10 (434)
2	Low pH	24.8 ± 0.5 (805)	7.73 ± 0.06 (805)
3	Ambient pH	25.4 ± 0.4 (805)	7.82 ± 0.13 (805)
4	Low pH	25.0 ± 0.5 (805)	7.73 ± 0.06 (804)
5	Ambient pH	25.3 ± 0.6 (805)	8.04 ± 0.17 (805)
6	Low pH	25.7 ± 0.5 (805)	7.75 ± 0.06 (798)

Supplementary Table S5. Pairwise comparison of estimated coefficients, from a Bayesian generalized linear latent variable model, of ambient pH treatment groups against low pH treatment groups. Statistically significant effects (i.e., 95% credible intervals [CI] that do not overlap zero) are marked in bold and 75% credible intervals that do not overlap zero are indicative of trends.

		Calcification		Volume Growth		Surface Area Growth		Tissue Biomass		Lipid Content		Protein Content		Apoptotic Activity	
Acropora humilis	Median	-0.22		-0.57		-0.48		-0.47		-0.23		0.19		0.54	
	95% CI	-0.92	0.45	-1.30	0.13	-1.13	0.15	-1.25	0.37	-1.17	0.69	-0.59	1.00	-0.25	1.30
	75% CI	-0.59	0.15	-1.00	-0.12	-0.83	-0.11	-0.95	0.00	-0.77	0.32	-0.29	0.69	0.07	0.99
Acropora millepora	Median	-0.11		-0.62		-0.29		-0.02		-0.57		-0.40		1.05	
	95% CI	-0.75	0.60	-1.47	0.21	-1.02	0.41	-1.01	0.99	-1.68	0.58	-1.44	0.52	**0.23**	**1.81**
	75% CI	-0.49	0.30	-1.09	-0.12	-0.71	0.11	-0.60	0.55	-1.21	0.10	-0.96	0.17	0.57	1.51
Pocillopora damicornis	Median	-0.20		-0.77		-0.44		0.93		-0.66		-0.01		-0.14	
	95% CI	-0.91	0.53	-1.54	0.06	-1.11	0.25	**0.03**	**1.87**	-1.66	0.41	-0.98	0.93	-0.96	0.64
	75% CI	-0.59	0.19	-1.23	-0.30	-0.82	-0.03	0.43	1.46	-1.27	-0.07	-0.55	0.54	-0.63	0.32
Pocillopora verrucosa	Median	-0.34		-0.40		-0.86		0.28		-0.73		-0.67		-0.14	
	95% CI	-1.05	0.31	-1.18	0.43	**-1.52**	**-0.21**	-0.67	1.19	-1.76	0.29	-1.59	0.25	-0.93	0.65
	75% CI	-0.75	0.03	-0.87	0.04	-1.26	-0.49	-0.27	0.82	-1.31	-0.11	-1.22	-0.15	-0.60	0.32
Porites cylindrica	Median	-0.33		-0.80		-0.40		-0.50		0.24		0.38		-0.64	
	95% CI	-1.01	0.38	**-1.61**	**-0.01**	-1.07	0.30	-1.45	0.38	-0.90	1.43	-0.64	1.34	-1.49	0.15
	75% CI	-0.72	0.09	-1.27	-0.31	-0.81	0.01	-1.02	0.03	-0.40	0.87	-0.17	0.91	-1.12	-0.17
Porites lutea	Median	-0.51		-1.38		-0.60		0.70		-0.30		-0.20		-0.05	
	95% CI	-1.27	0.33	**-2.35**	**-0.40**	-1.41	0.25	-0.44	1.81	-1.59	0.89	-1.39	0.92	-0.97	0.87
	75% CI	-0.97	-0.01	-1.91	-0.81	-1.04	-0.13	0.01	1.35	-1.05	0.38	-0.87	0.45	-0.61	0.48

References

Bates, D., Mächler, M., Bolker, B., and Walker, S. (2015). Fitting Linear Mixed-Effects Models Using lme4. *J. Stat. Softw.* 67, 1–48. doi:10.18637/jss.v067.i01.

Fox, J., and Weisberg, S. (2019). *An R Companion to Applied Regression*. Third. Thousand Oaks, CA: Sage Available at: https://socialsciences.mcmaster.ca/jfox/Books/Companion/.

R Core Team (2021). R: A Language and Environment for Statistical Computing. Available at: https://www.r-project.org/.

RStudio Team (2021). RStudio: Integrated Development Environment for R. Available at: http://www.rstudio.com/.

2 Flow Effects on Corals Under OA (Manuscript II)

Martins CPP, Simancas-Giraldo SM, Schubert P, Wall M, Wild C, Wilke T, Ziegler M (2024) Short periods of decreased water flow may modulate long-term ocean acidification in reef-building corals. Preprint (Version 1) at *bioRxiv*. DOI: 10.1101/2024.02.23.581783 *Submitted to the peer-reviewed journal Marine Biology*.

Short periods of decreased water flow may modulate long-term ocean acidification in reef-building corals

Catarina P.P. Martins*[1], Susana M. Simancas-Giraldo[2], Patrick Schubert[1], Marlene Wall[3], Christian Wild[2], Thomas Wilke[1], Maren Ziegler[1]

[1]Department of Animal Ecology & Systematics, Justus Liebig University Giessen, 35392 Giessen, Germany

[2]Marine Ecology Department, Faculty of Biology and Chemistry, University of Bremen, 28359 Bremen, Germany

[3]GEOMAR, Helmholtz Centre for Ocean Research, 24148 Kiel, Germany

*corresponding author: catarina.padilha-pires-martins@bio.uni-giessen.de

Running page head

Flow effects on corals under OA

ABSTRACT

Ocean acidification (OA) poses a major threat to reef-building corals. Although water flow variability is common in coral reefs and modulates coral physiology, the interactive effects of flow and OA on corals remain poorly understood. Therefore, we performed a three-month OA experiment investigating the effect of changes in flow on coral physiology. We exposed the reef-building corals *Acropora cytherea*, *Pocillopora verrucosa*, and *Porites cylindrica* to control (pH 8.0) and OA (pH 7.8) conditions at moderate flow (6 cm s^{-1}) and monitored OA effects on growth. Throughout the experiment, we intermittently exposed all corals to low flow (2 cm s^{-1}) for 1.5 h and measured their photosynthesis:photosynthesis (P:R) ratio under low and moderate flow. On average, corals under OA calcified 18 % less and grew 23 % less in surface area than those at ambient pH. We observed species-specific interactive effects of OA and flow on coral physiology. P:R ratios decreased after 12 weeks of OA in *A. cytherea* (22 %) and *P. cylindrica* (28 %) under moderate flow, but were unaffected by OA under low flow. P:R ratios were stable in *P. verrucosa*. These results suggest that short periods of decreased water flow may modulate OA effects on some coral species, indicating that flow variability is a factor to consider when assessing long-term effects of climate change.

KEYWORDS

ocean acidification, reef-building corals, water flow, coral physiology

1. INTRODUCTION

Ocean acidification (OA) constitutes a main future threat to reef-building corals (Doney et al. 2009), typically reducing their calcification rate (Kroeker et al. 2013). However, the effect of OA on respiration and photosynthesis of reef-building corals, i.e., key processes of coral physiology, may vary depending on environmental conditions and species. Although meta-analyses show that net photosynthesis generally remains stable under OA conditions (Kroeker et al. 2013; Godefroid et al. 2022), it has also been reported to decrease (e.g., Reynaud et al. 2003; Bedwell-Ivers et al. 2017) or increase (e.g., Comeau et al. 2018; Biscéré et al. 2019). Coral reefs are highly dynamic ecosystems where local environmental variability modulates coral physiology (McLachlan et al. 2021). For instance, natural diel oscillation of seawater pH in reefs (Hannan et al. 2020) may cause differences in the physiological response of coral species to OA and further complicate the assessment of its effects (Comeau et al. 2014a; Bedwell-Ivers et al. 2017; Enochs et al. 2018).

Additional physical factors such as water flow, which vary on short time scales, may underlie the complex responses of corals to OA. Water flow in coral reefs–typically high-energy ecosystems exposed to currents, waves, and tides (Sheppard et al. 2018)–can vary greatly within and among reefs (Lowe and Falter 2015). Flow velocities vary even within single reef locations (e.g., 0–30 cm s^{-1}; Roik et al. 2016), with temporal decreases during the diel cycle associated with tides (Green et al. 2018; Lindhart et al. 2021). Flow also differs between reef environments, with back-reef environments typically experiencing lower flow than reef-crest environments (Madin et al. 2006). Periods of low flow may be relatively common in some reefs (e.g., Hench et al. 2008), and flow immediately adjacent to coral colonies is further reduced due to the formation of recirculation zones in complex reef topographies (Hench and Rosman 2013).

In reef-building corals, water flow modulates respiration and photosynthesis (Dennison and Barnes 1988; Patterson et al. 1991) with species-specific effects (e.g., Rex et al. 1995; Schutter et al. 2010). Differences in physiological responses between species to water flow

may be associated with its effect on the coral boundary layer. This is the layer of seawater bordering the coral surface that controls mass transfer between the coral and bulk seawater (Atkinson and Bilger 1992; Shashar et al. 1993). Water flow variability also has implications for coral physiology. For instance, photochemical efficiency may be higher under alternating high-to-low flow conditions than under constant flow (Smith and Birkeland 2007). Thus, speed and short-term variability of water flow elicit complex patterns in coral physiology.

Although water flow is a prevailing characteristic of all coral reefs, knowledge of the interactive effects of different flow regimes and OA on reef-building corals remains limited (Noisette et al. 2022). While high-flow environments have been proposed as refuges from the effects of ocean warming (Fifer et al. 2021), low-flow environments are currently considered potential refuges from OA for calcifying organisms (Hurd 2015). Effects of flow and OA on coral physiology may be complex, potentially interactive, and differ by exposure time. For instance, during 1-h short-term OA exposure, net photosynthesis was similar between low (1 cm s^{-1}) and moderate water flow (4–13 cm s^{-1}; Osinga et al. 2017). Similarly, after two-day exposure to OA, coral communities briefly exposed to high (35 cm s^{-1}) and moderate flow (8 cm s^{-1}) also had similar net photosynthesis under OA (Anthony et al. 2013). Whereas, after two-month exposure to OA and different flow regimes (2.5 or 8 cm s^{-1}), net photosynthesis under low flow was decreased in *Acropora yongei* and increased in *Plesiastrea versipora* (Comeau et al. 2019a). Similarly, decreased calcification of reef-building corals under OA may be alleviated by temporary 24-h exposure to moderate water flow (5 and 10 cm s^{-1}) compared to low flow (2 cm s^{-1}; Comeau et al. 2014c). These results suggest that acclimatisation to OA and flow regimes may occur on different time scales. Thus, a systematic investigation of long-term OA effects on coral physiology combined with short-term fluctuations of water flow, as occur in coral reefs, is needed.

The overarching aim of this study was to assess the physiological response of three reef-building coral species, *Acropora cytherea* (Dana, 1846), *Pocillopora verrucosa* (Ellis & Solander, 1786), and *Porites cylindrica* Dana, 1846, to changes in water flow under control

and OA conditions. Specifically, we tested how OA conditions (pH 7.8) maintained for three months at constant moderate flow (6 cm s^{-1}) affected I) coral calcification and surface growth compared to control conditions (pH 8.0) and II) coral photosynthesis:respiration (P:R) ratios under short periods of low flow (2 cm s^{-1}) compared to responses under moderate flow. This study will help to disentangle the complex effects of OA on coral physiology and better understand the role of hydrodynamics in the response of reef-building corals to OA.

2. MATERIALS AND METHODS

2.1. Study species and experimental design

A three-month experiment was conducted to investigate the physiological response of three scleractinian coral species, *Acropora cytherea*, *Pocillopora verrucosa*, and *Porites cylindrica,* to OA together with the effect of changes in water flow conditions using respirometry assays. Coral colonies (Table S1) were maintained at the 'Ocean2100' long-term coral experimental facility (8,000 L closed recirculating system of artificial seawater, Table S2) at Justus Liebig University Giessen, Germany, for at least six months before the experiment. Conditions in the long-term culturing tanks (256 L) were 11:13 h light:dark photoperiod with a light intensity of 230 µmol m^{-2} s^{-1}, temperature of 26.0 ± 0.5 °C, and daily feeding of a mix of frozen *Artemia* sp., *Mysis* sp., and copepods. For the experiment, a total of four colonies per species were used and cut into eight fragments using a small angle grinder (Dremel Multitool 3000-15, The Netherlands). Fragments were attached to tiles with two-component glue (CoraFix SuperFast, Grotech, Germany) and transferred to the experimental setup. Corals were acclimated to the experimental setup for five weeks before the start of the experiment. During the first 10 days of the acclimation period, corals were administered the long-term culturing feed, after which the culturing feed was provided with lower frequency (2.7 mg L^{-1} of frozen copepods every two days) due to the lower density of coral fragments within experimental tanks. Corals also received constant dissolved nutrient conditions via the connected water system.

Experimental treatments consisted of two pH levels, with the control treatment mimicking present-day atmospheric pCO_2 concentration on some reefs (~500 µatm pCO_2; Ziegler et al. 2021), and the OA treatment with values projected in the long term (2081–2100) for surface ocean pH in coral reefs (UNEP-WCMC et al. 2021) under SSP2-4.5 (0.20 pH units lower relative to 1961–1990; Iturbide et al. 2022; IPCC 2023). The physiological response of the corals was monitored throughout both the acclimation and experimental period, which were conducted from 15 October 2019 to 28 February 2020. Buoyant weight was measured three weeks before the start of gradual pH decrease (t_{-3}) and after 13 weeks under OA (t_{13}), while surface area was documented four weeks before the start of gradual pH decrease (t_{-4}) and after 14 weeks under OA (t_{14}). The time points of these two parameters differed by one week due to the duration of measurements (buoyant weight measurement of all coral fragments took three days and surface area six days). P:R ratios were measured in low (2 cm s^{-1}) and moderate flow (6 cm s^{-1}) four times on all fragments (32 fragments per species per flow condition = 192 fragments per time point). Measurements of all fragments took six days to complete per time point and were performed once at the end of the acclimation period (t_{-1}, one week before the start of gradual pH decrease) and three times during the experimental period (t_3, after three weeks under OA; t_7, after seven weeks; t_{12}, after 12 weeks). A complete timeline of all physiological measurements can be found in Fig. 1A and details of the physiological assessments are outlined below.

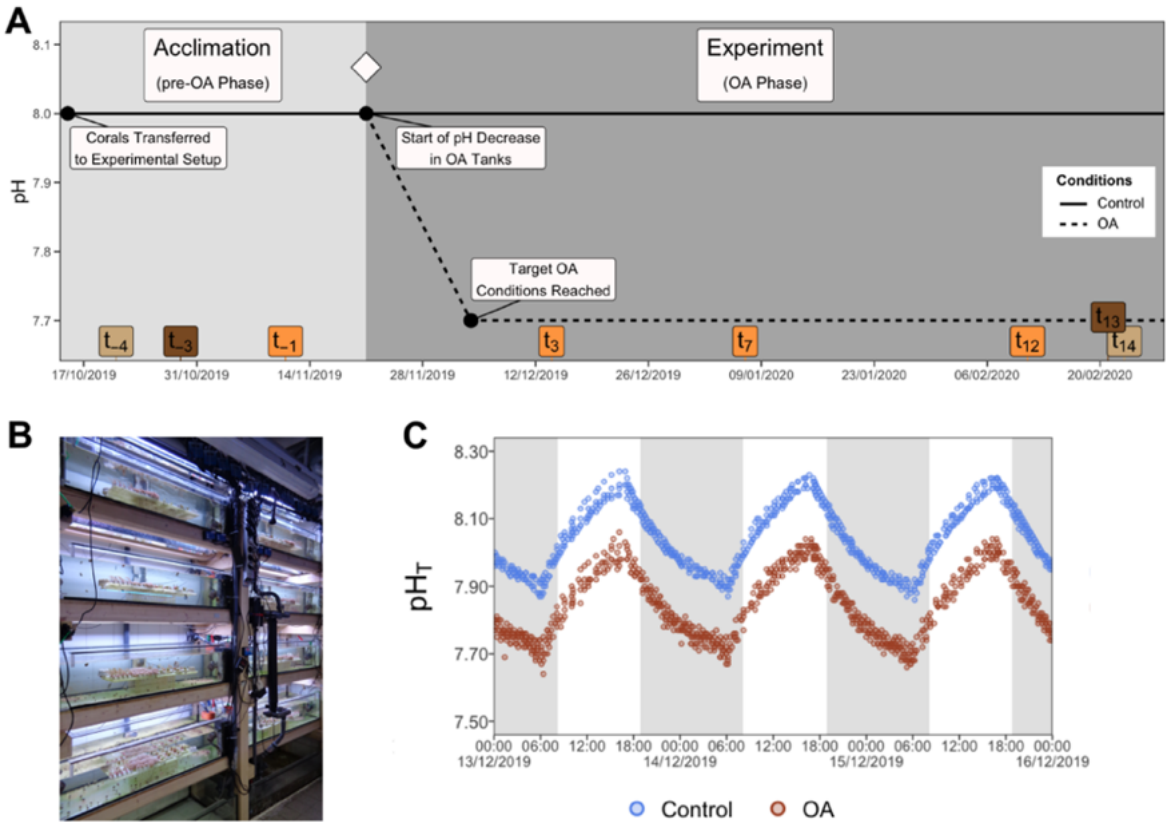

Fig. 1 Experimental design and setup. (A) Timeline of physiological measurements performed throughout the acclimation and experimental periods. Different colours indicate different types of physiological measurements (calcification, dark brown; surface growth, light brown; photosynthesis:respiration ratio, orange). The white diamond indicates the start of the experiment. Dates are provided as DD/MM/YYYY. (B) Overview of the experimental setup. See Fig. S1 for a detailed close-up of an individual experimental tank. (C) Snapshot of diel pH oscillation during the experiment. Shaded grey areas indicate nighttime. OA, ocean acidification; t_{-1}, one week before the start of gradual pH decrease; t_{-3}, three weeks before; t_{-4}, four weeks before; t_3, after three weeks under OA conditions, including two weeks of gradual pH decrease; t_7, after seven weeks; t_{12}, after 12 weeks; t_{13}, after 13 weeks; t_{14}, after 14 weeks; pH_T, pH on the total scale

2.2. Experimental setup and treatment conditions

The experimental setup consisted of eight 120 L tanks divided into two experimental pH treatments (four tanks per treatment, 16 fragments per species per treatment) (Fig. 1B). Each tank housed one fragment per colony (total of four fragments per species in each tank) with 15 cm spacing between them in the direction of flow. In addition, experimental tanks contained

other scleractinian and octocorals with the same number of individuals per tank (Fig. S1A). The experimental tanks were supplied with water from the 8,000 L closed recirculating system of artificial seawater (calcium concentration: 396 ± 6 mg L^{-1}, phosphate: < 0.02 mg L^{-1}, nitrate: < 0.02 mg L^{-1}, nitrite: < 0.01 mg L^{-1}) with an inflow rate of 20–40 L h^{-1} (corresponding to a 100 % tank volume turnover every 3–6 h). In addition, the large water system received weekly water changes of ~10 % of the water volume. Temperature was maintained at 26 °C through a feedback-controlled heater (300 W; 548, Schego, Germany). Water flow conditions, consisting of a flow velocity of 6 cm s^{-1} (measured at the position of coral fragments; OTT MF pro, OTT Hydromet GmbH, Germany) and a standing wave with an amplitude of 5 mm, were generated with two circulating pumps (ES-28, Aqualight, Germany) and one wave generator (6208, Tunze, Germany). Salinity in the tanks was monitored daily using a conductivity sensor (TetraCon 925, WTW, Germany) and maintained at 35. Light was provided by two T5 bulbs (54 W, Aqua-Science, Germany), producing a light intensity of 176 ± 31 µmol m^{-2} s^{-1} in an 11:13 h light:dark photoperiod. Light intensity in the experimental tanks differed slightly from conditions in the culturing tanks due to technical reasons.

Seawater pH was constantly monitored using a digital controller (Profilux 3, GHL, Germany) attached to pH electrodes in each tank (GHL, Germany), which were calibrated every two weeks using NBS buffers. Values of pH_{NBS} were converted to total scale (pH_T) using equations from Millero (2013) and Takahashi et al. (1982). pH values are expressed in total scale throughout the text. OA conditions in each treatment tank were generated individually via pH-controlled CO_2 dosing (bubbling) using solenoid valves, which controlled the release of CO_2. Pumping was done through one of the circulating pumps to aid CO_2 dissolution and dispersion in seawater. pH was gradually decreased in OA treatment tanks and lowered by 0.01–0.02 units every day over two weeks until target values were reached (Fig. S2A). Target OA conditions were maintained for 86 days, including diel oscillation of pH mimicking naturally occurring variability (Hannan et al. 2020; Ziegler et al. 2021). Total alkalinity (TA) was measured in each experimental tank by open-cell potentiometric titration using a titrator

(TitroLine 7000, SI Analytics, Germany) equipped with a glass pH-combination electrode (A 162 2M-DIN-ID, SI Analytics, Germany). Measurements were made following SOP3b (Dickson et al. 2007) on 50 g samples with 0.1N HCl (Titrisol, Merk, Germany) in 35 g L^{-1} NaCl and corrected using certified reference materials (Batch 183, A.G. Dickson Laboratory, Scripps Institution of Oceanography, UCSD, USA; Dickson et al. 2003). Measurements were performed every 2–4 days during the first two weeks of the experiment and then every 1–2 weeks. TA was calculated using a modified Gran approach (Millero 2013). Alkalinity was also monitored daily and maintained with two automatic in-house constructed calcium reactors (pH 6.2–6.4, coral rubble) and dosing of $NaHCO_3$ in a common reservoir tank. The calcium reactor was feedback controlled by an alkalinity controller (Alkatronic, Focustronic, Hong Kong) based on 3-hourly automatic titrations. Seawater carbonate chemistry was calculated from days with TA measurements using pH_{NBS} and temperature values for a whole day and the corresponding value of TA and salinity. TA and salinity values were assumed to be representative of the conditions of the entire day on which they were measured. Calculations were performed in the program CO2SYS (v25; Pelletier et al. 2007) with carbonic acid dissociation constants from Mehrbach et al. (1973) refit by Dickson and Millero (1987). This approach is suitable for biological OA experiments with treatments that have differences larger than 100 µatm pCO_2 (Watson et al. 2017) and allowed us to account for the diel oscillation of pH in the tanks.

2.3. Coral calcification and surface growth determination

Calcification was determined from measurements of buoyant weight (Jokiel et al. 1978) and calculated as the difference between final (t_{13}) and initial (t_{-3}) buoyant weight (accuracy 0.001 g; KB 360-3N, KERN & Sohn GmbH, Germany), converted to dry weight using an aragonite density of 2.93 g cm^{-3} (Spencer Davies 1989), and normalised by initial surface area (t_{-4}) and time. Surface growth was determined using 3D scanning (Artec Spider 3D with Artec Studio 9, Artec 3D, Luxembourg) by documenting coral surface area, following Reichert et al. (2016). Briefly, corals were placed on a rotating plate and scans were captured in air within 60–90 seconds. 3D models were calculated by performing fine serial registration, global

registration (minimal distance: 10, iterations: 2,000, based on texture and geometry), sharp fusion (resolution: 0.2, fill holes by radius, max. hole radius: 5), and outlier removal (*A. cytherea* and *P. cylindrica*, SD: 3; *P. verrucosa*, SD: 4). Artefact objects were removed (small objects filter). To determine coral surface areas, meshes were trimmed manually at the tissue border. All meshes were exported as Wavefront ".obj" files to MeshLab Visual Computing Lab-ISTI-CNR (v1.3.4, BETA, 2014; Cignoni et al. 2008), and surface area was calculated using the "compute geometric measures" tool. Surface growth rates were determined as the difference between final (t_{14}) and initial (t_{-4}) surface area and normalised by initial surface area and time.

2.4. Measurement of photosynthesis:respiration ratios

P:R ratios were derived from oxygen production and consumption rates at low and moderate flow conditions measured at the same time of day to avoid bias due to diurnal variation. Coral fragments were incubated individually in sealed 1 L glass chambers for 90 min at 191 ± 23 µmol m^{-2} s^{-1} to measure oxygen production, followed by 90 min in darkness to measure oxygen consumption. Chambers were filled with seawater from the corresponding treatment and maintained at 26 ºC. Low and moderate water flow conditions in the incubation chambers were generated with a magnetic stirring bar (Fig. S1B) (Rades et al. 2022) and measured by visual tracking of small, neutrally buoyant plastic beads. Dissolved oxygen concentration was measured in each chamber at the start and end of each incubation using an optical oxygen sensor (FDO 925, WTW, Germany). Four empty chambers were included in every incubation run to control for background biological activity. Rates of oxygen production and consumption were calculated as the change in dissolved oxygen per incubation volume (calculated as the difference between water volume and volume of the coral fragment with its tile) and normalised to incubation time. P:R ratios were calculated as the ratio of gross oxygen production (i.e., the sum of net oxygen production and consumption) to oxygen consumption with an 11:24 h metabolic cycle (i.e., the ratio of total oxygen produced during daylight hours to that consumed during a 24 h period) to estimate daily autotrophic capability (McCloskey et al. 1978). Rates

of respiration and photosynthesis were not analysed in this study due to the presence of inconclusive patterns between rates measured during the acclimation period (t_{-1}) and at the end of the experimental period (t_{12}), but are available for inspection in Fig. S3 and Table S3. Additional details are provided as Supplementary Text.

2.5. Statistical analysis

All statistical analyses were performed in R (v.4.1.0; R Core Team 2021) using RStudio (v1.4.1103; RStudio Team 2021). All plots were produced using the R package *ggplot2* (Wickham 2016). Changes in the physiological parameters of the three studied corals were investigated using linear mixed-effects models (LMMs). Differences between species in calcification and surface growth rates were assessed using LMMs with species (3 levels: *A. cytherea*, *P. verrucosa*, and *P. cylindrica*) as a fixed factor, and colony and treatment as random factors, while differences in P:R ratios were analysed using the same model structure but with the addition of coral fragment identity (ID) as a random effect. To test the effect of OA on calcification and surface growth, we used LMMs constructed for each species with treatment (2 levels: control and OA) as a fixed factor and colony as a random factor. The P:R ratio response to OA and flow over time was assessed using LMMs constructed for each species with treatment (2 levels: control and OA), flow (2 levels: low and moderate), and time (3 levels: t_3, t_7, and t_{12}) as fixed factors in a fully crossed design, and ID, colony, and tank as random factors. LMMs were performed using the R package *lme4* (Bates et al. 2015). Model validation was performed by graphically assessing homogeneity and normality assumptions, and models were inspected for any influential observations using the R package *performance* (Lüdecke et al. 2021). The numerical output of LMMs was extracted using the R package *sjPlot* (Lüdecke 2021) and is provided with model formulas in Tables S4 and S5. We then computed type-II ANOVA tables of the fixed effects of LMMs using the Kenward-Roger approximation for the degrees of freedom in the R package *car* (Fox & Weisberg 2019. Type II sums of squares was selected to compute ANOVAs, following previously recommended protocol for assessing main effects individually in the absence of interactions (Langsrud 2003;

Hector et al. 2010). Post hoc analyses were performed using the R package *emmeans* (Lenth 2021) with Bonferroni adjustment of p-values.

Differences in seawater chemistry between treatments were tested using daily mean values from days with TA measurements and the same approach as above (LMM-ANOVA) with treatment as a fixed factor (2 levels: control and OA) and tank and date as random factors.

All fragments of *A. cytherea* in one control tank bleached and subsequently died eight weeks into the experiment. The fragments of *P. verrucosa* from the same tank also showed signs of bleaching after 11 weeks into the experiment and were driving the response patterns in the data analyses (as revealed by correlation analysis, Fig. S4). Therefore, all fragments from this tank were excluded from the analyses. Based on the regular monitoring of water parameters, the underlying reason for the affected fragments could not be identified. The other fragments of these species appeared healthy. In addition, the coral fragments did not show visual signs of bleaching or necrosis in response to the OA treatment.

3. RESULTS

3.1. Ocean acidification conditions

During the three months of the experiment, pH of the control was significantly higher at 7.98 ± 0.13 (mean ± SD; daily range: 7.79–8.19) than in the OA treatment at 7.78 ± 0.13 (range: 7.60–8.01; LMM-ANOVA, $F = 298$, $p < 0.001$). The control and OA treatments had similar diel pH oscillations (Fig. 1C), with a diel range of 0.4 pH units in both treatments throughout the experiment (Fig. S2B; Table S6). pCO_2 values were significantly lower in the control at 480 ± 171 µatm (range: 244–769 µatm) than in the OA treatment at 813 ± 286 µatm (range: 416–1,262 µatm; LMM-ANOVA, $F = 273$, $p < 0.001$). Total alkalinity and temperature were similar between treatments (LMM-ANOVA, $F = 0.2/1.2$, $p > 0.05$; Table 1). Seawater chemistry per tank and a summary of the full recording of pH and temperature values are provided in the Supplementary Material (Fig. S2B,C; Tables S6,S7).

Table 1 Seawater chemistry during a three-month ocean acidification experiment. Values are expressed as mean ± SD with measurement replication (n). pH_T, pH on the total scale; TA, total alkalinity; pCO_2, partial pressure of CO_2; DIC, dissolved inorganic carbon; Ω_{ca}, calcite saturation; Ω_{ar}, aragonite saturation

	Control	Ocean Acidification
Salinity	34.6 ± 0.4 (10)	34.7 ± 0.4 (10)
Temperature (ºC)	25.9 ± 0.3 (1,736)	25.9 ± 0.2 (1,503)
pH_T	7.98 ± 0.13 (1,736)	7.78 ± 0.13 (1,503)
Daily Minimum pH_T	7.79 ± 0.12 (10)	7.60 ± 0.12 (10)
Daily Maximum pH_T	8.19 ± 0.04 (10)	8.01 ± 0.06 (10)
TA (µmol kg^{-1})	2,155 ± 52 (47)	2,155 ± 60 (44)
pCO_2 (µatm)	480 ± 171 (1,736)	813 ± 286 (1,503)
Daily Minimum pCO_2 (µatm)	244 ± 31 (10)	413 ± 67 (10)
Daily Maximum pCO_2 (µatm)	769 ± 195 (10)	1,262 ± 330 (10)
DIC (µmol kg^{-1})	1,906 ± 76 (1,736)	2,009 ± 74 (1,503)
CO_2 (µmol kg^{-1})	13 ± 5 (1,736)	23 ± 8 (1,503)
HCO_3^- (µmol kg^{-1})	1,709 ± 109 (1,736)	1,857 ± 94 (1,503)
CO_3^{2-} (µmol kg^{-1})	184 ± 43 (1,736)	129 ± 33 (1,503)
Ω_{ca}	4.45 ± 1.05 (1,736)	3.13 ± 0.81 (1,503)
Ω_{ar}	2.94 ± 0.69 (1,736)	2.07 ± 0.53 (1,503)

3.2. Ocean acidification decreased coral calcification and surface growth

During the experimental period, all coral fragments grew in weight and surface area, but increases differed between the three investigated species (LMM-ANOVA, F = 17.0/17.1, p < 0.01; Fig. 2). *Acropora cytherea* had a 16 % weight gain over the experiment (pooled over treatments) and a significantly lower overall calcification rate than *Pocillopora verrucosa* and *Porites cylindrica*, which presented a weight gain of 42 and 30 %, respectively (Tables S8,S9). Also, while the surface area of *A. cytherea* increased by 58 % during the experiment across treatments, it increased by 163 and 140 % in *P. verrucosa* and *P. cylindrica*, respectively, and was significantly higher than surface area growth in *A. cytherea* (Tables S8,S9).

The OA treatment decreased calcification and surface growth rates in all species (Fig. 2B,C). *Acropora cytherea* showed a 24 and 30 % reduction in calcification and surface growth, respectively (LMM-ANOVA, F = 14.1/11.1, p < 0.01) (Table S8). In *P. verrucosa,* calcification and surface growth decreased by 20 and 23 % (LMM-ANOVA, F = 6.8/13.8, p < 0.05/0.01),

and in *P. cylindrica* by 13 and 19 %, respectively (LMM-ANOVA, F = 7.3/5.8, p < 0.05) (Table S8).

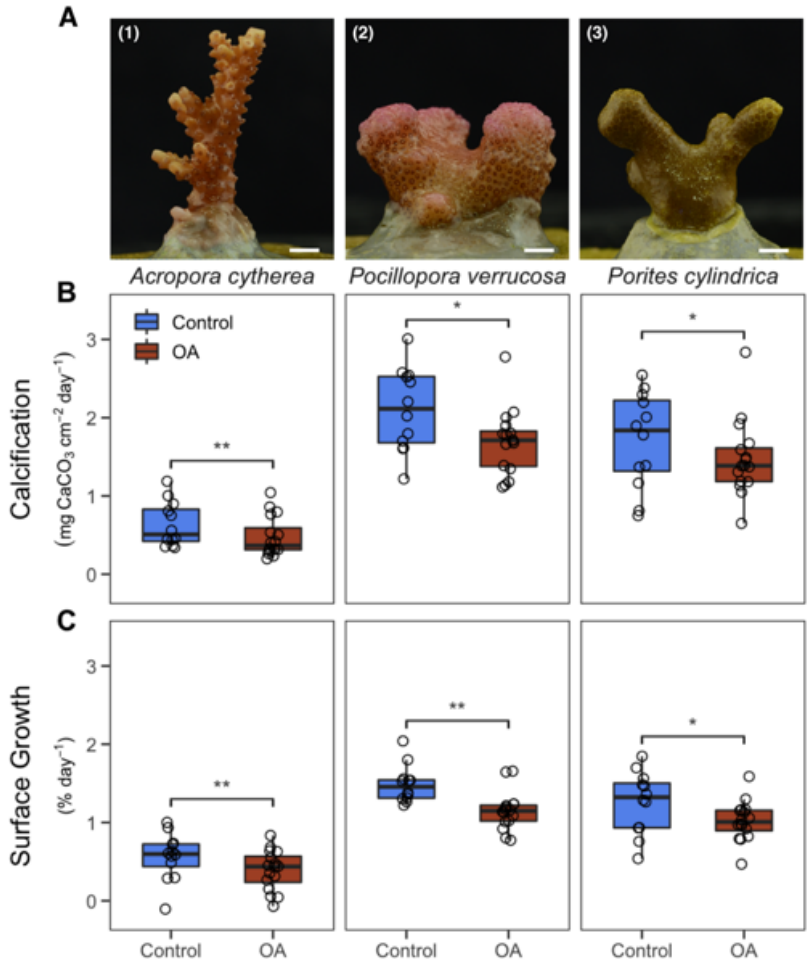

Fig. 2 Growth effects of ocean acidification (OA) on three reef-building coral species. (A) Photographs of the investigated reef-building coral species taken at the end of the acclimation period: (1) *Acropora cytherea*, (2) *Pocillopora verrucosa*, (3) *Porites cylindrica*. Scale bar = 5 mm. (B) Calcification and (C) surface growth of *A. cytherea*, *P. verrucosa*, and *P. cylindrica* during three months in a control and OA treatment. Boxes represent the first and third quartiles with lines as medians and whiskers as the minimum and maximum values or up to the 1.5 × interquartile range (IQR), whichever is reached first. Stars indicate significant differences between the control and OA treatment (p < 0.01**, p < 0.05*, from linear mixed-effects models with ANOVA).

3.3. Ocean acidification effects on photosynthesis:respiration ratios increased over time

The three investigated coral species displayed time-delayed physiological responses to OA treatments with complex interactions with water flow (Fig. 3). P:R ratios were overall similar between species during the experiment (pooled over treatments and time, LMM-ANOVA, $F = 3.9$, $p > 0.05$). They increased after the pre-OA phase (t_{-1}; Fig. 3; Table S10) and differed between time points during the OA-phase for all species (pooled over treatment, LMM-ANOVA, *A. cytherea*, $F = 11.1$, $p < 0.001$; *P. verrucosa*, $F = 11.3$, $p < 0.001$; *P. cylindrica*, $F = 63.0$, $p < 0.001$; Table S11). The P:R ratio was reduced in the OA treatment compared to the control with interactive effects with time (LMM-ANOVA, Treatment-Time interaction) in *A. cytherea* ($F = 13.9$, $p < 0.001$) and *P. cylindrica* ($F = 3.4$, $p < 0.05$) under moderate flow (Fig. 3; Table S10), but not in *P. verrucosa* ($F = 1.1$, $p > 0.05$). OA effects occurred from three weeks onward in *P. cylindrica* and after 12 weeks in *A. cytherea* (Table S11). P:R ratio was on average lower under low flow than moderate flow conditions (LMM-ANOVA, *A. cytherea*, $F = 6.0$, $p < 0.05$; *P. cylindrica*, $F = 20.9$, $p < 0.001$), except in *P. verrucosa*, for which this effect was reversed (LMM-ANOVA, $F = 150.9$, $p < 0.001$) (Fig. 3).

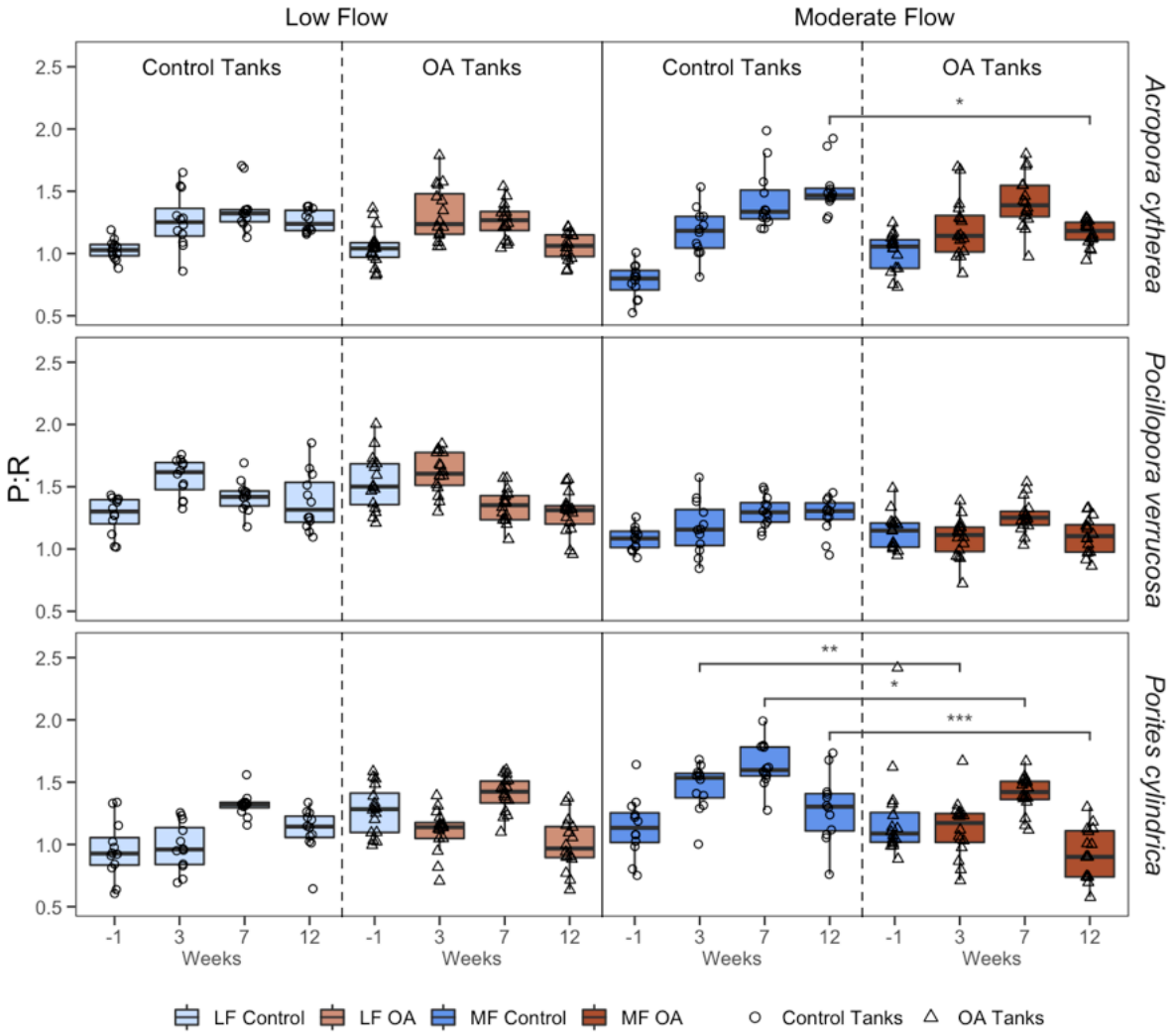

Fig. 3 Photosynthesis:Respiration (P:R) ratio of *Acropora cytherea*, *Pocillopora verrucosa*, and *Porites cylindrica* in a control and ocean acidification (OA) treatment and measured under low flow (LF, 2 cm s^{-1}) and moderate flow (MF, 6 cm s^{-1}) conditions during the acclimation period (measured one week before the start of gradual pH decrease) and experimental period (after three, seven, and 12 weeks under OA, including two weeks of gradual pH decrease). Data from the acclimation period are presented separated by the respective treatment applied during the OA phase. Boxes represent the first and third quartiles with lines as medians and whiskers as the minimum and maximum values or up to the 1.5 × interquartile range (IQR), whichever is reached first. Stars indicate significant differences between the control and OA treatment within each time point and flow condition ($p < 0.001$***, $p < 0.01$**, $p < 0.05$*, from linear mixed-effects models with ANOVA).

4. DISCUSSION

Our study shows that the physiological response of corals to future OA conditions varies with water flow conditions. In this study, all coral species showed reduced calcification and surface area growth rates under near-natural OA conditions with diel pH oscillation. In addition, short periods of low water flow modulated P:R ratios, which developed with OA-exposure time and differed among species with potential downstream effects on their calcification rates.

4.1. Decreased growth under ocean acidification with diel pH oscillation

In our study, calcification and surface growth decreased in all species under OA, which is consistent with previous findings (e.g., Sekizawa et al. 2017) and the generalised effect of OA on coral calcification (Kornder et al. 2018). Still, calcification in *Acropora cytherea* may be unaffected by OA at stable and even higher pCO_2 than tested here (1,000 µatm pCO_2; Godefroid et al. 2021). Likewise, *Pocillopora verrucosa* maintained stable calcification rates with moderately and highly elevated pCO_2 under stable pH conditions (700 and 1,000 µatm pCO_2; Comeau et al. 2019b). In coral reefs, pH oscillates naturally with diel ranges, which vary between and within reefs (Hannan et al. 2020; Cyronak et al. 2020) and are expected to increase under future OA conditions (Shaw et al. 2013). pH variability is thus an important element of biological OA manipulation experiments that is essential for extrapolating responses observed in the laboratory to coral reefs (Ziegler et al. 2021). In our study, pH was not stable but had a simulated diel oscillation of 0.4 pH units, which is representative of ranges present in some reefs (Cyronak et al. 2020). Since pH oscillation may exacerbate OA-induced calcification decreases (Comeau et al. 2014a), the calcification responses observed in our study are thus potentially associated with diel pH oscillation as observed in natural reef ecosystems.

4.2. Physiological response to ocean acidification dependent on exposure time and water flow

OA is a slowly developing press disturbance. Therefore, short-term acute assays will fail to capture the breadth of organismal responses to naturally-occurring acidification. Here, we assessed the progression of OA effects by monitoring P:R ratios over time. P:R ratios were in line with daily P:R ratios reported previously (~1.1; Jacquemont et al. 2022) and also when calculated as a direct P:R ratio (an estimate of autotrophic capability during daylight hours; ~2.3; Biscéré et al. 2019). Under OA, P:R ratios decreased at moderate flow, with time-delayed differential responses, except in *P. verrucosa*, where they remained stable. These results could suggest an increasing reliance on heterotrophically fixed energy under OA, consistent with the reported alleviation of OA effects on calcification with increased feeding (Towle et al. 2015). These data thus indicate different vulnerabilities among species with variable trophic dependence.

Specifically, the response of *A. cytherea*, which showed significant differences between treatments only after 12 weeks of exposure to OA, might indicate an initial compensation for adverse effects that the coral was then unable to sustain over time. Acroporids are highly autotrophic, which is a trophic mode associated with high susceptibility to environmental stress, such as high temperature (Conti-Jerpe et al. 2020). However, some *Acropora* spp. have the capacity to increase feeding rates under OA conditions and heterotrophically compensate for OA effects (Towle et al. 2015), which might explain the delayed response observed in *A. cytherea*. Therefore, our results support the classification of *A. cytherea* with other acroporids as OA-susceptible in the long term (Kornder et al. 2018), despite being able to potentially compensate for short-term OA challenges.

With changes in P:R ratios after just three weeks of exposure to OA, the response of *Porites cylindrica* to OA was the most immediate in our study. While massive *Porites* spp. are consistently observed to be OA-resilient (Fabricius et al. 2011; Comeau et al. 2019b), poritids with branching growth forms, such as *P. cylindrica,* appear more vulnerable (Comeau et al.

2014b). However, its overall milder response compared to *A. cytherea* may be due to the mixotrophic strategy of poritids, i.e., their more balanced contributions from autotrophy and heterotrophy (Conti-Jerpe et al. 2020). In contrast to *A. cytherea* and *P. cylindrica*, *P. verrucosa* maintained stable P:R ratios across treatments throughout the experiment and was thus more resilient to OA, supporting the current view that pocilloporids are highly resilient (Kornder et al. 2018). A higher contribution of heterotrophic feeding and physiological plasticity in *Pocillopora* than in *Acropora* or *Porites* spp. may underlie these differences (Hoogenboom et al. 2015; Radice et al. 2019).

Furthermore, our results from *A. cytherea* and *P. cylindrica* confirm the expectation of stronger effects under moderate flow than under low flow. Ecologically this means that some species threatened by OA on a global scale might benefit from local environmental variation and offset OA effects on local scales (e.g., in environments with large short-term OA fluctuations and/or low flow such as reef flats under calm weather; Lowe et al. 2009; Shaw et al. 2012). Accordingly, low-flow environments are considered refuge environments from OA for many calcifying organisms (Hurd 2015). Notably, the effects of heat stress, which is a pulse disturbance, may be stronger for *Acropora* spp. under low flow than high flow conditions (Nakamura and Van Woesik 2001; Page et al. 2021), and recovery from bleaching events may also be faster under high flow conditions (Fifer et al. 2021). Yet, field studies have found lower bleaching intensity at lagoon sites than high-flow environments (McClanahan et al. 2007; Hoogenboom et al. 2017), which may not be the case for all reef habitats (e.g., Ainsworth et al. 2021). Therefore, future coral reef conservation strategies to address climate change will likely benefit from a diverse portfolio of refugia to balance trade-offs associated with reef-specific characteristics and timescales of stressors.

The low-flow effects reported in this study might be underestimated when compared to laminar low-flow conditions. Given our respirometry setup, the flow regimes tested were likely relatively turbulent with lower intensity in the low flow condition due to its lower velocity. Under turbulent flow conditions, boundary layer behaviour may be limited (Reidenbach et al. 2006), reducing

418 the effect of flow changes on coral physiology (Lesser et al. 1994). Therefore, our results
419 support the notion of milder OA effects with reduced flow, even when flow is relatively
420 turbulent, as may occur on coral reefs. The flow conditions simulated in this study could be
421 representative of conditions in reef areas where oscillatory flow may limit the development of
422 boundary layers, such as reef flats (Davis et al. 2021). Still, *in situ* flow regimes are influenced
423 by various factors (Monismith 2007; Davis et al. 2021) and are thus generally more complex
424 than the flow conditions in our study. Also, coral colonies larger than the coral fragments in
425 our study may have a larger effect on the flow patterns around them (e.g., Hench and Rosman
426 2013; Hossain and Staples 2020). Therefore, future studies incorporating ecologically relevant
427 flow dynamics and a range of colony sizes and shapes will be important to disentangle OA
428 and flow effects.

429 **5. CONCLUSIONS**

430 Our study indicates that short periods of low flow modulate the physiological response of
431 corals to OA. We show that OA conditions of moderately elevated pCO_2 and naturally
432 oscillating pH I) reduce coral calcification and surface growth rates and that II) coral species
433 display differential time-delayed P:R ratio responses to OA, which may be mitigated by
434 temporarily reduced flow conditions. This differential progression of OA responses over time
435 may be related to differences in trophic strategy and explain the variable susceptibility to long-
436 term OA among coral species, which should be subject of follow-up work. Future research on
437 this topic could potentially inform the design and management of coral nurseries. Overall, our
438 results highlight that the combination of long-term OA exposure in the variable hydrodynamic
439 conditions of coral reefs may lead to complex biological outcomes that require consideration
440 of the spatial and temporal scales at which they occur. Finally, *in situ* flow regimes are
441 generally more complex than the low flow conditions in our study. Therefore, future studies
442 incorporating ecologically relevant flow regimes and dynamics will be important to disentangle
443 OA and flow effects and better understand the potential of low-flow environments as refugia.

DATA AVAILABILITY

The datasets and code for the analyses presented in this study can be found in the online Figshare repository and are accessible at https://doi.org/10.6084/m9.figshare.23538474.

ACKNOWLEDGEMENTS

We thank Giulia Puntin (JLU, Germany) for help during respirometry measurements. This study was conducted as part of the 'Ocean2100' global change simulation project of the Colombian-German Center of Excellence in Marine Sciences (CEMarin), funded by the German Academic Exchange Service (DAAD, project number 57480468).

REFERENCES

Ainsworth TD, Leggat W, Silliman BR, Lantz CA, Bergman JL, Fordyce AJ, Page CE, Renzi JJ, Morton J, Eakin CM, Heron SF (2021) Rebuilding relationships on coral reefs: Coral bleaching knowledge-sharing to aid adaptation planning for reef users. BioEssays. doi: 10.1002/bies.202100048

Anthony KRN, Diaz-Pulido G, Verlinden N, Tilbrook B, Andersson AJ (2013) Benthic buffers and boosters of ocean acidification on coral reefs. Biogeosciences 10:4897–4909. doi: 10.5194/bg-10-4897-2013

Atkinson MJ, Bilger RW (1992) Effects of water velocity on phosphate uptake in coral reef-flat communities. Limnol Oceanogr 37:273–279. doi: 10.4319/lo.1992.37.2.0273

Bates D, Mächler M, Bolker B, Walker S (2015) Fitting linear mixed-effects models using lme4. J Stat Softw 67:1–48. doi: 10.18637/jss.v067.i01

Bedwell-Ivers HE, Koch MS, Peach KE, Joles L, Dutra E, Manfrino C (2017) The role of *in hospite* zooxanthellae photophysiology and reef chemistry on elevated pCO_2 effects in two branching Caribbean corals: *Acropora cervicornis* and *Porites divaricata*. ICES J Mar Sci 74:1103–1112. doi: 10.1093/icesjms/fsw026

Biscéré T, Zampighi M, Lorrain A, Jurriaans S, Foggo A, Houlbrèque F, Rodolfo-Metalpa R (2019) High pCO_2 promotes coral primary production. Biol Lett 15:20180777. doi: 10.1098/rsbl.2018.0777

Cignoni P, Callieri M, Corsini M, Dellepiane M, Ganovelli F, Ranzuglia G (2008) MeshLab: An Open-Source Mesh Processing Tool. Sixth Eurographics Italian Chapter Conference 129–136. doi: 10.2312/LocalChapterEvents/ItalChap/ItalianChapConf2008/129-136

Comeau S, Edmunds PJ, Spindel NB, Carpenter RC (2014a) Diel pCO_2 oscillations modulate the response of the coral *Acropora hyacinthus* to ocean acidification. Mar Ecol Prog Ser 501:99–111. doi: 10.3354/meps10690

478 Comeau S, Edmunds PJ, Spindel NB, Carpenter RC (2014b) Fast coral reef calcifiers are
479 more sensitive to ocean acidification in short-term laboratory incubations. Limnol
480 Oceanogr 59:1081–1091. doi: 10.4319/lo.2014.59.3.1081
481 Comeau S, Edmunds PJ, Lantz CA, Carpenter RC (2014c) Water flow modulates the response
482 of coral reef communities to ocean acidification. Sci Rep 4:1–6. doi: 10.1038/srep06681
483 Comeau S, Cornwall CE, DeCarlo TM, Krieger E, McCulloch MT (2018) Similar controls on
484 calcification under ocean acidification across unrelated coral reef taxa. Glob Chang Biol
485 24:4857–4868. doi: 10.1111/gcb.14379
486 Comeau S, Cornwall CE, Pupier CA, DeCarlo TM, Alessi C, Trehern R, McCulloch MT (2019a)
487 Flow-driven micro-scale pH variability affects the physiology of corals and coralline
488 algae under ocean acidification. Sci Rep 9:12829. doi: 10.1038/s41598-019-49044-w
489 Comeau S, Cornwall CE, DeCarlo TM, Doo SS, Carpenter RC, McCulloch MT (2019b)
490 Resistance to ocean acidification in coral reef taxa is not gained by acclimatization. Nat
491 Clim Chang 9:477–483. doi: 10.1038/s41558-019-0486-9
492 Conti-Jerpe IE, Thompson PD, Wong CWM, Oliveira NL, Duprey NN, Moynihan MA, Baker
493 DM (2020) Trophic strategy and bleaching resistance in reef-building corals. Sci Adv.
494 doi: 10.1126/sciadv.aaz5443
495 Cyronak T, Takeshita Y, Courtney TA, DeCarlo EH, Eyre BD, Kline DI, Martz T, Page H, Price
496 NN, Smith J, Stoltenberg L, Tresguerres M, Andersson AJ (2020) Diel temperature and
497 pH variability scale with depth across diverse coral reef habitats. Limnol Oceanogr Lett
498 5:193–203. doi: 10.1002/lol2.10129
499 Davis KA, Pawlak G, Monismith SG (2021) Turbulence and coral reefs. Ann Rev Mar Sci
500 13:343–373. doi: 10.1146/annurev-marine-042120-071823
501 Dennison WC, Barnes DJ (1988) Effect of water motion on coral photosynthesis and
502 calcification. J Exp Mar Biol Ecol 115:67–77. doi: 10.1016/0022-0981(88)90190-6

503 Dickson AG, Millero FJ (1987) A comparison of the equilibrium constants for the dissociation
504 of carbonic acid in seawater media. Deep Sea Research Part A Oceanographic
505 Research Papers 34:1733–1743.
506 Dickson AG, Afghan JD, Anderson GC (2003) Reference materials for oceanic CO_2 analysis:
507 A method for the certification of total alkalinity. Mar Chem 80:185–197. doi:
508 10.1016/S0304-4203(02)00133-0
509 Dickson AG, Sabine CL, Christian JR (2007) Guide to best practices for ocean CO_2
510 measurements. PICES Special Publication 3, CA
511 Doney SC, Fabry VJ, Feely RA, Kleypas JA (2009) Ocean acidification: The other CO_2
512 problem. Ann Rev Mar Sci 1:169–192. doi: 10.1146/annurev.marine.010908.163834
513 Enochs IC, Manzello DP, Jones PJ, Aguilar C, Cohen K, Valentino L, Schopmeyer S, Kolodziej
514 G, Jankulak M, Lirman D (2018) The influence of diel carbonate chemistry fluctuations
515 on the calcification rate of *Acropora cervicornis* under present day and future
516 acidification conditions. J Exp Mar Biol Ecol 506:135–143. doi:
517 10.1016/j.jembe.2018.06.007
518 Fabricius KE, Langdon C, Uthicke S, Humphrey C, Noonan S, De'ath G, Okazaki R,
519 Muehllehner N, Glas MS, Lough JM (2011) Losers and winners in coral reefs
520 acclimatized to elevated carbon dioxide concentrations. Nat Clim Chang 1:165–169.
521 doi: 10.1038/nclimate1122
522 Fifer J, Bentlage B, Lemer S, Fujimura AG, Sweet M, Raymundo LJ (2021) Going with the
523 flow: How corals in high-flow environments can beat the heat. Mol Ecol 30:2009–2024.
524 doi: 10.1111/mec.15869
525 Fox J, Weisberg S (2019) An R companion to applied regression, Third. Sage, Thousand
526 Oaks, CA
527 Godefroid M, Arçuby R, Lacube Y, Espiau B, Dupont S, Gazeau F, Metian M, Hédouin L (2021)
528 More than local adaptation: High diversity of response to seawater acidification in

seven coral species from the same assemblage in French Polynesia. J Mar Biol Assoc United Kingdom 101:675–683. doi: 10.1017/S0025315421000618

Godefroid M, Dupont S, Metian M, Hédouin L (2022) Two decades of seawater acidification experiments on tropical scleractinian corals: Overview, meta-analysis and perspectives. Mar Pollut Bull 178:113552. doi: 10.1016/j.marpolbul.2022.113552

Green RH, Lowe RJ, Buckley ML (2018) Hydrodynamics of a tidally forced coral reef atoll. J Geophys Res Oceans 123:7084–7101. doi: 10.1029/2018JC013946

Hannan KD, Miller GM, Watson S-A, Rummer JL, Fabricius K, Munday PL (2020) Diel pCO_2 variation among coral reefs and microhabitats at Lizard Island, Great Barrier Reef. Coral Reefs 39:1391–1406. doi: 10.1007/s00338-020-01973-z

Hector A, von Felten S, Schmid B (2010) Analysis of variance with unbalanced data: An update for ecology & evolution. J Anim Ecol 79:308–316. doi: 10.1111/j.1365-2656.2009.01634.x

Hench JL, Rosman JH (2013) Observations of spatial flow patterns at the coral colony scale on a shallow reef flat. J Geophys Res Oceans 118:1142–1156. doi: 10.1002/jgrc.20105

Hench JL, Leichter JJ, Monismith SG (2008) Episodic circulation and exchange in a wave-driven coral reef and lagoon system. Limnol Oceanogr 53:2681–2694. doi: 10.4319/lo.2008.53.6.2681

Hoogenboom M, Rottier C, Sikorski S, Ferrier-Pagès C (2015) Among-species variation in the energy budgets of reef-building corals: Scaling from coral polyps to communities. J Exp Biol 218:3866–3877. doi: 10.1242/jeb.124396

Hoogenboom MO, Frank GE, Chase TJ, Jurriaans S, Álvarez-Noriega M, Peterson K, Critchell K, Berry KLE, Nicolet KJ, Ramsby B, Paley AS (2017) Environmental drivers of variation in bleaching severity of *Acropora* species during an extreme thermal anomaly. Front Mar Sci. doi: 10.3389/fmars.2017.00376

Hossain MM, Staples AE (2020) Effects of coral colony morphology on turbulent flow dynamics. PLoS One 15:1–25. doi: 10.1371/journal.pone.0225676

Hurd CL (2015) Slow-flow habitats as refugia for coastal calcifiers from ocean acidification. J Phycol 51:599–605. doi: 10.1111/jpy.12307

IPCC (2023) Atlas. In: Masson-Delmotte V, Zhai P, Pirani A, Connors SL, Péan C, Berger S, Caud N, Chen Y, Goldfarb L, Gomis MI, Huang M, Leitzell K, Lonnoy E, Matthews JBR, Maycock TK, Waterfield T, Yelekçi O, Yu R, Zhou B (eds) Climate Change 2021 – The Physical Science Basis: Working Group I Contribution to the Sixth Assessment Report of the Intergovernmental Panel on Climate Change. Cambridge University Press, Cambridge, UK and New York, NY, USA, pp 1927–2058

Iturbide M, Fernández J, Gutiérrez JM, Pirani A, Huard D, Al Khourdajie A, Baño-Medina J, Bedia J, Casanueva A, Cimadevilla E, Cofiño AS, De Felice M, Diez-Sierra J, García-Díez M, Goldie J, Herrera DA, Herrera S, Manzanas R, Milovac J, Radhakrishnan A, San-Martín D, Spinuso A, Thyng KM, Trenham C, Yelekçi Ö (2022) Implementation of FAIR principles in the IPCC: The WGI AR6 Atlas repository. Sci Data 9:629. doi: 10.1038/s41597-022-01739-y

Jacquemont J, Houlbrèque F, Tanvet C, Rodolfo-Metalpa R (2022) Long-term exposure to an extreme environment induces species-specific responses in corals' photosynthesis and respiration rates. Mar Biol 169:82. doi: 10.1007/s00227-022-04063-6

Jokiel PL, Maragos JE, Franzisket L (1978) Coral growth: Buoyant weight technique. In: Stoddart DR, Johannes RE (eds) Coral reefs: research methods. UNESCO, pp 529–542

Kornder NA, Riegl BM, Figueiredo J (2018) Thresholds and drivers of coral calcification responses to climate change. Glob Chang Biol 24:5084–5095. doi: 10.1111/gcb.14431

Kroeker KJ, Kordas RL, Crim R, Hendriks IE, Ramajo L, Singh GS, Duarte CM, Gattuso J (2013) Impacts of ocean acidification on marine organisms: Quantifying sensitivities and interaction with warming. Glob Chang Biol 19:1884–1896. doi: 10.1111/gcb.12179

Langsrud Ø (2003) ANOVA for unbalanced data: Use Type II instead of Type III sums of squares. Stat Comput 13:163–167. doi: 10.1023/A:1023260610025

583 Lenth R V. (2021) emmeans: Estimated Marginal Means, aka Least-Squares Means. R
584 package version 1.6.2-1. https://cran.r-project.org/package=emmeans.
585 Lesser MP, Weis VM, Patterson MR, Jokiel PL (1994) Effects of morphology and water motion
586 on carbon delivery and productivity in the reef coral, *Pocillopora damicornis* (Linnaeus):
587 Diffusion barriers, inorganic carbon limitation, and biochemical plasticity. J Exp Mar Biol
588 Ecol 178:153–179. doi: 10.1016/0022-0981(94)90034-5
589 Lindhart M, Rogers JS, Maticka SA, Woodson CB, Monismith SG (2021) Wave modulation of
590 flows on open and closed reefs. J Geophys Res Oceans 126:e2020JC016645. doi:
591 10.1029/2020JC016645
592 Lowe RJ, Falter JL (2015) Oceanic forcing of coral reefs. Ann Rev Mar Sci 7:43–66. doi:
593 10.1146/annurev-marine-010814-015834
594 Lowe RJ, Falter JL, Monismith SG, Atkinson MJ (2009) A numerical study of circulation in a
595 coastal reef-lagoon system. J Geophys Res 114:C06022. doi: 10.1029/2008JC005081
596 Lüdecke D (2021) sjPlot: Data visualization for statistics in social science. R package version
597 2.8.9. https://CRAN.R-project.org/package=sjPlot.
598 Lüdecke D, Ben-Shachar M, Patil I, Waggoner P, Makowski D (2021) performance: An R
599 package for assessment, comparison and testing of statistical models. J Open Source
600 Softw 6:3139. doi: 10.21105/joss.03139
601 Madin JS, Black KP, Connolly SR (2006) Scaling water motion on coral reefs: From regional
602 to organismal scales. Coral Reefs 25:635–644. doi: 10.1007/s00338-006-0137-2
603 McClanahan TR, Ateweberhan M, Muhando CA, Maina J, Mohammed MS (2007) Effects of
604 climate and seawater temperature variation on coral bleaching and mortality. Ecol
605 Monogr 77:503–525. doi: 10.1890/06-1182.1
606 McCloskey LR, Wethey DS, Porter JW (1978) Measurement and interpretation of
607 photosynthesis and respiration in reef corals. In: Stoddart DR, Johannes RE (eds)
608 Coral reefs: research methods. UNESCO, pp 379–396

609 McLachlan RH, Price JT, Muñoz-Garcia A, Weisleder NL, Jury CP, Toonen RJ, Grottoli AG
610 (2021) Environmental gradients drive physiological variation in Hawaiian corals. Coral
611 Reefs 40:1505–1523. doi: 10.1007/s00338-021-02140-8
612 Mehrbach C, Culberson CH, Hawley JE, Pytkowicx RM (1973) Measurement of the apparent
613 dissociation constants of carbonic acid in seawater at atmospheric pressure. Limnol
614 Oceanogr 18:897–907.
615 Millero FJ (2013) Chemical oceanography, 4th edn. CRC Press, Boca Raton, Florida
616 Monismith SG (2007) Hydrodynamics of coral reefs. Annu Rev Fluid Mech 39:37–55. doi:
617 10.1146/annurev.fluid.38.050304.092125
618 Nakamura T, Van Woesik R (2001) Water-flow rates and passive diffusion partially explain
619 differential survival of corals during the 1998 bleaching event. Mar Ecol Prog Ser
620 212:301–304. doi: 10.3354/meps212301
621 Noisette F, Pansch C, Wall M, Wahl M, Hurd CL (2022) Role of hydrodynamics in shaping
622 chemical habitats and modulating the responses of coastal benthic systems to ocean
623 global change. Glob Chang Biol 28:3812–3829. doi: 10.1111/gcb.16165
624 Osinga R, Derksen-Hooijberg M, Wijgerde T, Verreth JAJ (2017) Interactive effects of oxygen,
625 carbon dioxide and flow on photosynthesis and respiration in the scleractinian coral
626 *Galaxea fascicularis*. J Exp Biol 220:2236–2242. doi: 10.1242/jeb.140509
627 Page CE, Leggat W, Heron SF, Fordyce AJ, Ainsworth TD (2021) High flow conditions mediate
628 damaging impacts of sub-lethal thermal stress on corals' endosymbiotic algae. Conserv
629 Physiol 9:1–19. doi: 10.1093/conphys/coab046
630 Patterson MR, Sebens KP, Olson RR (1991) In situ measurements of flow effects on primary
631 production and dark respiration in reef corals. Limnol Oceanogr 36:936–948. doi:
632 10.4319/lo.1991.36.5.0936
633 Pelletier G, Lewis E, Wallace D (2007) CO2Sys. xls: A calculator for the CO_2 system in
634 seawater for Microsoft Excel/VBA. Washington State Department of
635 Ecology/Brookhaven National Laboratory, Olympia, WA/Upton, NY, USA

636 R Core Team (2021) R: A language and environment for statistical computing. R Foundation
637 for Statistical Computing, Vienna, Austria
638 Rades M, Schubert P, Ziegler M, Kröckel M, Reichert J (2022) Building plan for a temperature-
639 controlled multi-point stirring incubator. protocols.io. doi:
640 10.17504/protocols.io.dm6gpb34dlzp/v1
641 Radice VZ, Brett MT, Fry B, Fox MD, Hoegh-Guldberg O, Dove SG (2019) Evaluating coral
642 trophic strategies using fatty acid composition and indices. PLoS One 14:e0222327.
643 doi: 10.1371/journal.pone.0222327
644 Reichert J, Schellenberg J, Schubert P, Wilke T (2016) 3D scanning as a highly precise,
645 reproducible, and minimally invasive method for surface area and volume
646 measurements of scleractinian corals. Limnol Oceanogr Methods 14:518–526. doi:
647 10.1002/lom3.10109
648 Reidenbach MA, Koseff JR, Monismith SG, Steinbuckc J V., Genin A (2006) The effects of
649 waves and morphology on mass transfer within branched reef corals. Limnol Oceanogr
650 51:1134–1141. doi: 10.4319/lo.2006.51.2.1134
651 Rex A, Montebon F, Yap HT (1995) Metabolic responses of the scleractinian coral *Porites*
652 *cylindrica* Dana to water motion. I. Oxygen flux studies. J Exp Mar Biol Ecol 186:33–
653 52. doi: 10.1016/0022-0981(95)00150-P
654 Reynaud S, Leclercq N, Romaine-Lioud S, Ferrier-Pagés C, Jaubert J, Gattuso J (2003)
655 Interacting effects of CO_2 partial pressure and temperature on photosynthesis and
656 calcification in a scleractinian coral. Glob Chang Biol 9:1660–1668. doi:
657 10.1046/j.1529-8817.2003.00678.x
658 Roik A, Röthig T, Roder C, Ziegler M, Kremb SG, Voolstra CR (2016) Year-long monitoring of
659 physico-chemical and biological variables provide a comparative baseline of coral reef
660 functioning in the central Red Sea. PLoS One 11:e0163939. doi:
661 10.1371/journal.pone.0163939

662 RStudio Team (2021) RStudio: Integrated development environment for R. RStudio, PBC,
663 Boston, MA
664 Schutter M, Crocker J, Paijmans A, Janse M, Osinga R, Verreth AJ, Wijffels RH (2010) The
665 effect of different flow regimes on the growth and metabolic rates of the scleractinian
666 coral *Galaxea fascicularis*. Coral Reefs 29:737–748. doi: 10.1007/s00338-010-0617-2
667 Sekizawa A, Uechi H, Iguchi A, Nakamura T, Kumagai NH, Suzuki A, Sakai K, Nojiri Y (2017)
668 Intraspecific variations in responses to ocean acidification in two branching coral
669 species. Mar Pollut Bull 122:282–287. doi: 10.1016/j.marpolbul.2017.06.061
670 Shashar N, Cohen Y, Loya Y (1993) Extreme diel fluctuations of oxygen in diffusive boundary
671 layers surrounding stony corals. Biol Bull 185:455–461. doi: 10.2307/1542485
672 Shaw EC, McNeil BI, Tilbrook B (2012) Impacts of ocean acidification in naturally variable coral
673 reef flat ecosystems. J Geophys Res Oceans 117:C03038. doi:
674 10.1029/2011JC007655
675 Shaw EC, McNeil BI, Tilbrook B, Matear R, Bates ML (2013) Anthropogenic changes to
676 seawater buffer capacity combined with natural reef metabolism induce extreme future
677 coral reef CO_2 conditions. Glob Chang Biol 19:1632–1641. doi: 10.1111/gcb.12154
678 Sheppard CRC, Davy SK, Pilling GM, Graham NAJ (2018) The abiotic environment. In:
679 Sheppard C, Davy S, Pilling G, Graham N (eds) The Biology of Coral Reefs, 2nd edn.
680 Oxford University Press, Oxford, UK, pp 68–99
681 Smith LW, Birkeland C (2007) Effects of intermittent flow and irradiance level on back reef
682 *Porites* corals at elevated seawater temperatures. J Exp Mar Biol Ecol 341:282–294.
683 doi: 10.1016/j.jembe.2006.10.053
684 Spencer Davies P (1989) Short-term growth measurements of corals using an accurate
685 buoyant weighing technique. Mar Biol 101:389–395. doi: 10.1007/BF00428135
686 Takahashi T (1982) Carbonate chemistry. In: GEOSECS Pacific expedition, Volume 3,
687 Hydrographic Data 1973-1974. National Science Foundation, Washington, DC, pp 77–
688 83

689 Towle EK, Enochs IC, Langdon C (2015) Threatened Caribbean coral is able to mitigate the
690 adverse effects of ocean acidification on calcification by increasing feeding rate. PLoS
691 One 10:e0123394. doi: 10.1371/journal.pone.0123394
692 UNEP-WCMC, WorldFish Centre, WRI, TNC (2021) Global distribution of warm-water coral
693 reefs, compiled from multiple sources including the Millennium Coral Reef Mapping
694 Project. Version 4.1. Includes contributions from IMaRS-USF and IRD (2005), IMaRS-
695 USF (2005) and Spalding et al. (2001). In: UN Environment World Conservation
696 Monitoring Centre. Cambridge, UK. https://doi.org/10.34892/t2wk-5t34. Accessed 22
697 Jul 2023
698 Watson S-A, Fabricius KE, Munday PL (2017) Quantifying pCO_2 in biological ocean
699 acidification experiments: A comparison of four methods. PLoS One 12:e0185469. doi:
700 10.1371/journal.pone.0185469
701 Wickham H (2016) ggplot2: Elegant graphics for data analysis. Springer-Verlag, New York
702 Ziegler M, Anton A, Klein SG, Rädecker N, Geraldi NR, Schmidt-Roach S, Saderne V, Mumby
703 PJ, Cziesielski MJ, Martin C, Frölicher TL, Pandolfi JM, Suggett DJ, Aranda M, Duarte
704 CM, Voolstra CR (2021) Integrating environmental variability to broaden the research
705 on coral responses to future ocean conditions. Glob Chang Biol 27:5532–5546. doi:
706 10.1111/gcb.15840
707

SUPPLEMENTARY MATERIAL

Short periods of decreased water flow may modulate long-term ocean acidification in reef-building corals

Catarina P.P. Martins*[1], Susana M. Simancas-Giraldo[2], Patrick Schubert[1], Marlene Wall[3], Christian Wild[2], Thomas Wilke[1], Maren Ziegler[1]

[1]Department of Animal Ecology & Systematics, Justus Liebig University Giessen, 35392 Giessen, Germany

[2]Marine Ecology Department, Faculty of Biology and Chemistry, University of Bremen, 28359 Bremen, Germany

[3]GEOMAR, Helmholtz Centre for Ocean Research, 24148 Kiel, Germany

*corresponding author: catarina.padilha-pires-martins@bio.uni-giessen.de

Contents

Supplementary Text

Calculation of photosynthesis and respiration rates

Photosynthesis and respiration were calculated as the change in dissolved oxygen per incubation volume (calculated as the difference between water volume and volume of the coral fragment with its tile) and normalised to incubation time and surface area of the coral fragment. We used the surface area measured at t_{-4} and t_{14} to surface-normalise respiration and photosynthesis measured at t_{-1} and t_{12}, respectively. Respiration and photosynthesis rates were not calculated for t_3 and t_7 because no surface measurements were performed during these time points for surface normalisation. Gross photosynthesis was calculated as the sum of net photosynthesis and respiration values.

Supplementary Tables

Table S1 Details of coral species used in the experiment.

Species	Number of colonies	Origin	Collection year	CITES number
Acropora cytherea	4	Saudi Arabia (Red Sea)	2019	19-SA-000089-PD
Pocillopora verrucosa	2	Saudi Arabia (Red Sea)	2015	15-SA-000882-PD
	2	Indonesia (Indo-Pacific)	2007	14846/IV/SATS-LN/2007
Porites cylindrica	4	Indonesia (Indo-Pacific)	2017	17nl241924/11

Table S2 Brands of artificial-seawater salt used alternately during the acclimation and experimental period in the 'Ocean2100' experimental facility.

Salt	Brand
Deep Blue Sea-Salt	AquaPerfekt, Germany
Instant Ocean	Aquarium Systems, France
Reef Crystals	Aquarium Systems, France
Sea Salt	Aquaforest, Poland

Table S3 Respiration, net photosynthesis, and gross photosynthesis of *Acropora cytherea*, *Pocillopora verrucosa*, and *Porites cylindrica* in a control and ocean acidification (OA) treatment and measured in low and moderate flow (2 and 6 cm s^{-1}, respectively). Values are means ± SD (in µg O_2 cm^{-2} h^{-1}) of initial (t_{-1}, one week before the start of gradual pH decrease) and final rates (t_{12}, after 12 weeks under OA conditions, including two weeks of gradual pH decrease). Sample size (*n*) is provided and 'pre-OA' refers to the experimental OA group before the start of the OA treatment, with conditions equivalent to the control treatment.

Species	Time Point	Flow	Treatment	Respiration	Net Photosynthesis	Gross Photosynthesis	*n*
Acropora cytherea	t_{-1}	Low	Control	19.2 ± 3.8	23.8 ± 5.1	43.0 ± 8.3	12
Acropora cytherea	t_{-1}	Low	pre-OA	17.5 ± 3.4	22.3 ± 6.4	39.8 ± 8.5	16
Acropora cytherea	t_{-1}	Moderate	Control	23.3 ± 5.2	16.0 ± 6.9	39.3 ± 9.9	12
Acropora cytherea	t_{-1}	Moderate	pre-OA	18.4 ± 3.8	21.6 ± 5.7	40.0 ± 7.3	16
Acropora cytherea	t_{12}	Low	Control	14.9 ± 4.6	26.1 ± 8.9	41.0 ± 13.3	12
Acropora cytherea	t_{12}	Low	OA	12.1 ± 3.1	15.6 ± 4.3	27.7 ± 6.8	16
Acropora cytherea	t_{12}	Moderate	Control	9.8 ± 2.2	22.4 ± 6.7	32.2 ± 8.5	12
Acropora cytherea	t_{12}	Moderate	OA	9.1 ± 2.0	13.8 ± 3.1	22.9 ± 4.8	16
Pocillopora verrucosa	t_{-1}	Low	Control	20.2 ± 3.5	35.8 ± 8.0	56.0 ± 10.3	12
Pocillopora verrucosa	t_{-1}	Low	pre-OA	16.3 ± 3.1	37.4 ± 6.6	53.7 ± 8.4	16
Pocillopora verrucosa	t_{-1}	Moderate	Control	26.1 ± 5.1	35.4 ± 8.6	61.5 ± 12.8	12
Pocillopora verrucosa	t_{-1}	Moderate	pre-OA	21.0 ± 5.2	30.6 ± 7.3	51.6 ± 11.4	16
Pocillopora verrucosa	t_{12}	Low	Control	9.6 ± 1.3	19.0 ± 4.0	28.7 ± 4.2	12
Pocillopora verrucosa	t_{12}	Low	OA	9.4 ± 1.1	17.0 ± 3.9	26.4 ± 4.4	16
Pocillopora verrucosa	t_{12}	Moderate	Control	10.5 ± 1.1	18.5 ± 3.9	29.0 ± 4.6	12
Pocillopora verrucosa	t_{12}	Moderate	OA	10.1 ± 1.1	14.4 ± 3.8	24.5 ± 4.4	16
Porites cylindrica	t_{-1}	Low	Control	29.8 ± 7.6	32.0 ± 14.7	61.7 ± 18.7	12
Porites cylindrica	t_{-1}	Low	pre-OA	15.9 ± 4.5	27.9 ± 7.6	43.8 ± 10.9	16
Porites cylindrica	t_{-1}	Moderate	Control	25.8 ± 7.0	36.3 ± 10.5	62.1 ± 13.7	12
Porites cylindrica	t_{-1}	Moderate	pre-OA	17.5 ± 6.1	25.8 ± 7.8	43.3 ± 12.7	16
Porites cylindrica	t_{12}	Low	Control	8.4 ± 1.5	12.2 ± 4.1	20.6 ± 5.2	12
Porites cylindrica	t_{12}	Low	OA	8.6 ± 1.2	10.3 ± 4.2	18.9 ± 4.9	16
Porites cylindrica	t_{12}	Moderate	Control	9.0 ± 2.0	16.0 ± 5.4	25.1 ± 6.5	12
Porites cylindrica	t_{12}	Moderate	OA	9.2 ± 1.4	9.4 ± 4.4	18.5 ± 5.1	16

Table S4 Numerical output of linear mixed-effects models (LMMs) of calcification (C) and surface growth (Gs). Global models were constructed with species (3 levels: *Acropora cytherea* [Acy], *Pocillopora verrucosa* [Pve], and *Porites cylindrica* [Pcy]) as a fixed factor, and colony and treatment as random factors. Individual species' models were constructed with treatment (2 levels: control and ocean acidification [OA]) as a fixed factor and colony as a random factor. Model formulas are specified. σ^2, residual variance; τ_{00}, random intercept variance; ICC, intra-class correlation coefficient; N, number of levels of random effects groups; Marginal R^2, variance explained by the fixed effects; Conditional R^2, variance explained by the entire model

		Calcification		Surface Growth	
		C ~ Species + (1 | Treatment) + (1 | Colony)		Gs ~ Species + (1 | Treatment) + (1 | Colony)	
	Fixed Effects	Estimates	SE	Estimates	SE
All Species	(Intercept)	0.56	0.22	0.48	0.16
	species [Pve]	1.33	0.24	0.83	0.15
	species [Pcy]	0.99	0.24	0.66	0.15
	Random Effects				
	σ^2	0.09		0.05	
	$\tau_{00\ Treatment}$	0.04		0.03	
	$\tau_{00\ Colony}$	0.10		0.04	
	ICC	0.60		0.59	
	$N_{Treatment}$	2		2	
	N_{Colony}	12		12	
	Observations	83		83	
	Marginal R^2 / Conditional R^2	0.582 / 0.833		0.527 / 0.805	
		C ~ Treatment + (1 | Colony)		Gs ~ Treatment + (1 | Colony)	
	Fixed Effects	Estimates	SE	Estimates	SE
Acropora cytherea	(Intercept)	0.63	0.14	0.56	0.14
	treatment [OA]	-0.16	0.04	-0.17	0.05
	Random Effects				
	σ^2	0.01		0.02	
	$\tau_{00\ Colony}$	0.07		0.07	
	ICC	0.86		0.79	
	N_{Colony}	4		4	
	Observations	28		28	
	Marginal R^2 / Conditional R^2	0.069 / 0.868		0.078 / 0.810	
Pocillopora verrucosa	(Intercept)	2.10	0.17	1.49	0.07
	treatment [OA]	-0.41	0.16	-0.34	0.09
	Random Effects				
	σ^2	0.17		0.06	
	$\tau_{00\ Colony}$	0.06		< 0.01	
	ICC	0.24		0.02	
	N_{Colony}	4		4	
	Observations	28		28	
	Marginal R^2 / Conditional R^2	0.159 / 0.365		0.333 / 0.349	
Porites cylindrica	(Intercept)	1.71	0.22	1.26	0.13
	treatment [OA]	-0.32	0.12	-0.25	0.10
	Random Effects				
	σ^2	0.09		0.07	
	$\tau_{00\ Colony}$	0.17		0.04	
	ICC	0.65		0.37	
	N_{Colony}	4		4	

	Observations	27	27
	Marginal R^2 / Conditional R^2	0.090 / 0.678	0.123 / 0.450

Table S5 Numerical output of linear mixed-effects models (LMMs) of photosynthesis:respiration ratio (P:R). Global models were constructed with species (3 levels: *Acropora cytherea* [Acy], *Pocillopora verrucosa* [Pve], and *Porites cylindrica* [Pcy]) as fixed factor; and coral fragment identity (ID), colony, and treatment as random factors. Individual species' models were constructed with treatment (2 levels: control and OA), flow (2 levels: low and moderate), and time (3 levels: t_3, t_7, t_{12}) as fixed factors in a fully crossed design, and ID, colony, and tank as random factors. Model formulas are specified. σ^2, residual variance; τ_{00}, random intercept variance; ICC, intra-class correlation coefficient; N, number of levels of random effects groups; Marginal R^2, variance explained by the fixed effects; Conditional R^2, variance explained by the entire model; t_7, after seven weeks under OA, including two weeks of gradual pH decrease; t_{12}, after 12 weeks

		P:R ~ Species + (1 | Treatment) + (1 | Coral ID) + (1 | Colony) + (1 | Tank)	
	Fixed Effects	Estimates	SE
All Species	(Intercept)	1.28	0.05
	species [Pve]	0.04	0.03
	species [Pcy]	-0.06	0.03
	Random Effects		
	σ^2		0.05
	$\tau_{00\ Coral\ ID}$		< 0.01
	$\tau_{00\ Colony}$		< 0.01
	$\tau_{00\ Tank}$		0.01
	$\tau_{00\ Treatment}$		< 0.01
	$N_{Treatment}$		2
	$N_{Coral\ ID}$		84
	N_{Colony}		12
	N_{Tank}		7
	Observations		504
	Marginal R^2 / Conditional R^2		0.024 / 0.173
		P:R ~ Treatment * Flow * Time + (1 | Coral ID) + (1 | Colony) + (1 | Tank)	
	Fixed Effects	Estimates	SE
Acropora cytherea	(Intercept)	1.26	0.07
	treatment [OA]	0.05	0.09
	flow [moderate]	-0.09	0.07
	timepoint [t_7]	0.09	0.07
	timepoint [t_{12}]	-0.01	0.07
	treatment [OA] * flow [moderate]	-0.02	0.09
	treatment [OA] * timepoint [t_7]	-0.14	0.09
	treatment [OA] * timepoint [t_{12}]	-0.25	0.09
	flow [moderate] * timepoint [t_7]	0.17	0.09
	flow [moderate] * timepoint [t_{12}]	0.35	0.09
	(treatment [OA] * flow [moderate]) * timepoint [t_7]	0.10	0.12
	(treatment [OA] * flow [moderate]) * timepoint [t_{12}]	-0.13	0.12
	Random Effects		
	σ^2		0.03
	$\tau_{00\ Coral\ ID}$		< 0.01
	$\tau_{00\ Tank}$		0.01
	$\tau_{00\ Colony}$		< 0.01
	ICC		0.28
	$N_{Coral\ ID}$		28
	N_{Colony}		4
	N_{Tank}		7
	Observations		168
	Marginal R^2 / Conditional R^2		0.294 / 0.489
Pocillopora verrucosa	(Intercept)	1.58	0.07
	treatment [OA]	0.04	0.08
	flow [moderate]	-0.40	0.05

	timepoint [t_7]	-0.15	0.05
	timepoint [t_{12}]	-0.19	0.05
	treatment [OA] * flow [moderate]	-0.12	0.07
	treatment [OA] * timepoint [t_7]	-0.12	0.07
	treatment [OA] * timepoint [t_{12}]	-0.14	0.07
	flow [moderate] * timepoint [t_7]	0.28	0.07
	flow [moderate] * timepoint [t_{12}]	0.29	0.07
	(treatment [OA] * flow [moderate]) * timepoint [t_7]	0.17	0.10
	(treatment [OA] * flow [moderate]) * timepoint [t_{12}]	0.06	0.10
	Random Effects		
	σ^2		0.02
	$T_{00\ Coral\ ID}$		< 0.01
	$T_{00\ Tank}$		0.01
	$T_{00\ Colony}$		< 0.01
	ICC		0.42
	$N_{Coral\ ID}$		28
	N_{Colony}		4
	N_{Tank}		7
	Observations		168
	Marginal R^2 / Conditional R^2		0.481 / 0.700
Porites cylindrica	(Intercept)	0.98	0.06
	treatment [OA]	0.13	0.08
	flow [moderate]	0.48	0.07
	timepoint [t_7]	0.34	0.07
	timepoint [t_{12}]	0.13	0.07
	treatment [OA] * flow [moderate]	-0.46	0.10
	treatment [OA] * timepoint [t_7]	-0.04	0.10
	treatment [OA] * timepoint [t_{12}]	-0.24	0.10
	flow [moderate] * timepoint [t_7]	-0.16	0.10
	flow [moderate] * timepoint [t_{12}]	-0.30	0.10
	(treatment [OA] * flow [moderate]) * timepoint [t_7]	0.15	0.14
	(treatment [OA] * flow [moderate]) * timepoint [t_{12}]	0.21	0.14
	Random Effects		
	σ^2		0.03
	$T_{00\ Coral\ ID}$		< 0.01
	$T_{00\ Tank}$		< 0.01
	$T_{00\ Colony}$		< 0.01
	ICC		0.11
	$N_{Coral\ ID}$		28
	N_{Colony}		4
	N_{Tank}		7
	Observations		168
	Marginal R^2 / Conditional R^2		0.544 / 0.594

Table S6 Summary of the complete recording of temperature and pH during the experiment. Values are expressed as mean ± SD with measurement replication (*n*). OA, ocean acidification; pH_T, pH on the total scale

Tank	Treatment	Temperature (ºC)	pH_T	Daily Minimum pH_T	Daily Maximum pH_T	Daily Range pH_T
1	Control	25.9 ± 0.2 (3,988)	7.95 ± 0.12 (3,873)	7.77 ± 0.06 (84)	8.13 ± 0.06 (84)	0.36 ± 0.05 (84)
2	OA	25.9 ± 0.2 (3,606)	7.76 ± 0.13 (3,709)	7.58 ± 0.07 (84)	7.94 ± 0.07 (84)	0.36 ± 0.07 (84)
3	Control	25.9 ± 0.2 (3,963)	7.97 ± 0.12 (3,859)	7.78 ± 0.05 (84)	8.15 ± 0.05 (84)	0.36 ± 0.06 (84)
4	OA	25.9 ± 0.2 (3,771)	7.77 ± 0.13 (3,830)	7.59 ± 0.07 (84)	7.96 ± 0.06 (84)	0.37 ± 0.08 (84)
5	Control	26.0 ± 0.3 (3,413)	7.98 ± 0.13 (3,785)	7.80 ± 0.06 (84)	8.17 ± 0.07 (84)	0.36 ± 0.06 (84)
6	OA	26.0 ± 0.2 (3,408)	7.78 ± 0.13 (3,778)	7.61 ± 0.07 (84)	7.98 ± 0.07 (84)	0.37 ± 0.07 (84)
7	Control	25.7 ± 0.3 (3,736)	7.98 ± 0.13 (3,771)	7.80 ± 0.07 (84)	8.16 ± 0.06 (84)	0.36 ± 0.06 (84)
8	OA	26.0 ± 0.2 (3,452)	7.78 ± 0.13 (3,839)	7.61 ± 0.07 (84)	7.97 ± 0.07 (84)	0.37 ± 0.07 (84)

Table S7 Seawater chemistry in the eight experimental tanks. Values are expressed as mean ± SD with measurement replication (*n*). OA, ocean acidification; pH_T, pH on the total scale; TA, total alkalinity; pCO_2, partial pressure of CO_2; DIC, dissolved inorganic carbon; Ω_{ca}, calcite saturation; Ω_{ar}, aragonite saturation

Tank	Treatment	Salinity	Temperature (ºC)	pH_T	TA (μmol kg^{-1})	pCO_2 (μatm)	DIC (μmol kg^{-1})	CO_2 (μmol kg^{-1})	HCO_3^- (μmol kg^{-1})	CO_3^{2-} (μmol kg^{-1})	Ω_{ca}	Ω_{ar}
1	Control	34.6 ± 0.4 (10)	25.9 ± 0.2 (456)	7.96 ± 0.13 (456)	2,147 ± 52 (132)	497 ± 177 (456)	1,907 ± 75 (456)	14 ± 5 (456)	1,715 ± 107 (456)	179 ± 42 (456)	4.33 ± 1.01 (456)	2.86 ± 0.67 (456)
2	OA	34.6 ± 0.5 (10)	25.9 ± 0.2 (366)	7.77 ± 0.13 (366)	2,166 ± 54 (120)	838 ± 292 (366)	2,018 ± 70 (366)	23 ± 8 (366)	1,868 ± 89 (366)	127 ± 32 (366)	3.06 ± 0.78 (366)	2.02 ± 0.52 (366)
3	Control	34.6 ± 0.4 (10)	25.9 ± 0.2 (444)	7.98 ± 0.12 (444)	2,166 ± 42 (132)	472 ± 161 (444)	1,911 ± 73 (444)	13 ± 5 (444)	1,712 ± 105 (444)	186 ± 41 (444)	4.50 ± 1.00 (444)	2.97 ± 0.66 (444)
4	OA	34.7 ± 0.4 (10)	25.9 ± 0.2 (433)	7.78 ± 0.14 (433)	2,156 ± 60 (144)	829 ± 293 (433)	2,015 ± 75 (433)	23 ± 8 (433)	1,864 ± 96 (433)	128 ± 34 (433)	3.09 ± 0.82 (433)	2.04 ± 0.54 (433)
5	Control	34.6 ± 0.4 (10)	26.0 ± 0.3 (341)	7.99 ± 0.13 (341)	2,160 ± 54 (120)	464 ± 167 (341)	1,902 ± 77 (341)	13 ± 5 (341)	1,699 ± 112 (341)	190 ± 46 (341)	4.59 ± 1.11 (341)	3.04 ± 0.74 (341)
6	OA	34.7 ± 0.4 (10)	26.0 ± 0.2 (366)	7.80 ± 0.13 (366)	2,146 ± 62 (144)	779 ± 263 (366)	1,995 ± 75 (366)	22 ± 7 (366)	1,841 ± 95 (366)	133 ± 34 (366)	3.21 ± 0.81 (366)	2.12 ± 0.54 (366)
7	Control	34.6 ± 0.4 (10)	25.7 ± 0.3 (495)	7.97 ± 0.13 (495)	2,151 ± 55 (180)	482 ± 176 (495)	1,902 ± 80 (495)	13 ± 5 (495)	1,707 ± 111 (495)	182 ± 44 (495)	4.41 ± 1.06 (495)	2.91 ± 0.70 (495)
8	OA	34.7 ± 0.4 (10)	25.9 ± 0.2 (338)	7.79 ± 0.13 (338)	2,156 ± 60 (120)	802 ± 292 (338)	2,006 ± 75 (338)	22 ± 8 (338)	1,853 ± 94 (338)	131 ± 34 (338)	3.16 ± 0.81 (338)	2.09 ± 0.54 (338)

Table S8 Calcification and surface growth (mean ± SD) of *Acropora cytherea*, *Pocillopora verrucosa*, and *Porites cylindrica* in a control and ocean acidification (OA) treatment. *n*, sample size

Species	Treatment	Calcification (mg cm^{-2} day^{-1})	Total Calcification (mg cm^{-2})	Surface Growth (% day^{-1})	Total Surface Growth (%)	*n*
Acropora cytherea	Control	0.63 ± 0.29	72.93 ± 32.96	0.56 ± 0.30	70.03 ± 37.39	12
Acropora cytherea	OA	0.48 ± 0.25	54.40 ± 29.22	0.39 ± 0.25	49.10 ± 31.97	16
Pocillopora verrucosa	Control	2.10 ± 0.53	242.05 ± 60.79	1.49 ± 0.24	187.85 ± 30.26	12
Pocillopora verrucosa	OA	1.69 ± 0.42	193.79 ± 48.00	1.15 ± 0.24	144.45 ± 30.25	16
Porites cylindrica	Control	1.71 ± 0.61	197.80 ± 70.52	1.26 ± 0.40	157.50 ± 49.39	12
Porites cylindrica	OA	1.48 ± 0.49	169.40 ± 56.03	1.02 ± 0.25	127.27 ± 31.28	16

Table S9 Post hoc species comparison of linear mixed effects models (LMMs) for calcification and surface growth. Summarised output of LMMs and model information can be found in Table S4. p-values were adjusted with Bonferroni correction. Bold p-values indicate significant effects with α lower than 0.05. Acy, *Acropora cytherea*; Pve, *Pocillopora verrucosa*; Pcy, *Porites cylindrica*

	Calcification			Surface Growth		
Contrast (Species)	df	t	p	df	t	p
Acy vs. Pve	9.0	-5.6	**0.001**	9.0	-5.5	**0.001**
Acy vs. Pcy	9.0	-4.2	**0.007**	9.0	-4.4	**0.005**
Pve vs. Pcy	9.0	1.4	0.577	9.0	1.2	0.819

Table S10 Photosynthesis:Respiration (P:R) ratios of *Acropora cytherea*, *Pocillopora verrucosa*, and *Porites cylindrica* in a control and ocean acidification (OA) treatment measured in low and moderate flow (2 and 6 cm s^{-1}, respectively) during the acclimation period (t_{-1}, one week before the start of gradual pH decrease) and experimental period (t_3, after three weeks under OA conditions, including two weeks of gradual pH decrease; t_7, after seven weeks; t_{12}, after 12 weeks). Values are means ± SD, with sample size (*n*), and 'pre-OA' refers to the experimental OA group before the start of the OA treatment, with conditions equivalent to the control treatment.

Species	Time Point	Treatment	Flow	P:R	*n*
Acropora cytherea	t_{-1}	Control	Low	1.03 ± 0.08	12
Acropora cytherea	t_{-1}	pre-OA	Low	1.05 ± 0.15	16
Acropora cytherea	t_{-1}	Control	Moderate	0.78 ± 0.14	12
Acropora cytherea	t_{-1}	pre-OA	Moderate	1.01 ± 0.15	16
Acropora cytherea	t_3	Control	Low	1.26 ± 0.22	12
Acropora cytherea	t_3	OA	Low	1.32 ± 0.22	16
Acropora cytherea	t_3	Control	Moderate	1.17 ± 0.19	12
Acropora cytherea	t_3	OA	Moderate	1.20 ± 0.24	16
Acropora cytherea	t_7	Control	Low	1.35 ± 0.17	12
Acropora cytherea	t_7	OA	Low	1.26 ± 0.14	16
Acropora cytherea	t_7	Control	Moderate	1.43 ± 0.25	12
Acropora cytherea	t_7	OA	Moderate	1.41 ± 0.21	16
Acropora cytherea	t_{12}	Control	Low	1.26 ± 0.09	12
Acropora cytherea	t_{12}	OA	Low	1.06 ± 0.11	16
Acropora cytherea	t_{12}	Control	Moderate	1.51 ± 0.20	12
Acropora cytherea	t_{12}	OA	Moderate	1.16 ± 0.10	16
Pocillopora verrucosa	t_{-1}	Control	Low	1.27 ± 0.15	12
Pocillopora verrucosa	t_{-1}	pre-OA	Low	1.54 ± 0.22	16
Pocillopora verrucosa	t_{-1}	Control	Moderate	1.08 ± 0.09	12
Pocillopora verrucosa	t_{-1}	pre-OA	Moderate	1.14 ± 0.14	16
Pocillopora verrucosa	t_3	Control	Low	1.58 ± 0.15	12
Pocillopora verrucosa	t_3	OA	Low	1.61 ± 0.16	16
Pocillopora verrucosa	t_3	Control	Moderate	1.17 ± 0.21	12
Pocillopora verrucosa	t_3	OA	Moderate	1.09 ± 0.16	16
Pocillopora verrucosa	t_7	Control	Low	1.42 ± 0.13	12
Pocillopora verrucosa	t_7	OA	Low	1.34 ± 0.14	16
Pocillopora verrucosa	t_7	Control	Moderate	1.30 ± 0.12	12
Pocillopora verrucosa	t_7	OA	Moderate	1.26 ± 0.13	16
Pocillopora verrucosa	t_{12}	Control	Low	1.38 ± 0.23	12
Pocillopora verrucosa	t_{12}	OA	Low	1.29 ± 0.17	16
Pocillopora verrucosa	t_{12}	Control	Moderate	1.27 ± 0.15	12
Pocillopora verrucosa	t_{12}	OA	Moderate	1.11 ± 0.14	16
Porites cylindrica	t_{-1}	Control	Low	0.96 ± 0.23	12
Porites cylindrica	t_{-1}	pre-OA	Low	1.28 ± 0.19	16
Porites cylindrica	t_{-1}	Control	Moderate	1.14 ± 0.24	12
Porites cylindrica	t_{-1}	pre-OA	Moderate	1.21 ± 0.37	16
Porites cylindrica	t_3	Control	Low	0.98 ± 0.19	12
Porites cylindrica	t_3	OA	Low	1.11 ± 0.17	16
Porites cylindrica	t_3	Control	Moderate	1.46 ± 0.19	12

Porites cylindrica	t_3	OA	Moderate	1.13 ± 0.23	16
Porites cylindrica	t_7	Control	Low	1.32 ± 0.10	12
Porites cylindrica	t_7	OA	Low	1.40 ± 0.14	16
Porites cylindrica	t_7	Control	Moderate	1.63 ± 0.18	12
Porites cylindrica	t_7	OA	Moderate	1.41 ± 0.15	16
Porites cylindrica	t_{12}	Control	Low	1.12 ± 0.18	12
Porites cylindrica	t_{12}	OA	Low	1.00 ± 0.21	16
Porites cylindrica	t_{12}	Control	Moderate	1.29 ± 0.27	12
Porites cylindrica	t_{12}	OA	Moderate	0.92 ± 0.21	16

Table S11 Post hoc analyses of species' linear mixed effects models (LMMs) for photosynthesis:respiration (P:R) ratio. Summarised output of LMMs and model information can be found in Table S5. p-values were adjusted with Bonferroni correction. Bold p-values indicate significant effects with α lower than 0.05. t_3, after three weeks under ocean acidification (OA) conditions, including two weeks of gradual pH decrease; t_7, after seven weeks; t_{12}, after 12 weeks; LF, low flow; MF, moderate flow

	Acropora cytherea			*Pocillopora verrucosa*			*Porites cylindrica*		
	df	t	p	df	t	p	df	t	p
Contrast (Time)									
t_3 vs. t_7	130.0	-4.0	**< 0.001**	130.0	1.3	0.625	130.0	-7.8	< 0.001
t_3 vs. t_{12}	130.0	-0.3	1.000	130.0	4.3	**< 0.001**	130.0	2.5	**0.037**
t_7 vs. t_{12}	130.0	3.7	**0.001**	130.0	3.0	**0.010**	130.0	10.4	**< 0.001**
Contrast (Treatment:Flow)									
Control LF vs. OA LF	6.4	1.1	0.645	5.9	0.6	1.000	9.3	-0.6	1.000
Control MF vs. OA MF	6.4	1.5	0.373	5.9	1.4	0.449	9.3	5.6	**0.001**
Contrast (Treatment:Time)									
Control t_3 vs. OA t_3	8.0	-0.5	1.000	6.9	0.3	1.000	14.7	1.7	0.360
Control t_7 vs. OA t_7	8.0	0.6	1.000	6.9	0.8	1.000	14.7	1.2	0.787
Control t_{12} vs. OA t_{12}	8.0	3.5	**0.024**	6.9	1.8	0.357	14.7	3.9	**0.004**
Contrast (Flow:Time)									
LF t_3 vs. MF t_3	130.0	2.3	0.062	130.0	13.6	**< 0.001**	130.0	-5.1	**< 0.001**
LF t_7 vs. MF t_7	130.0	-2.6	**0.032**	130.0	2.9	**0.013**	130.0	-3.3	**0.004**
LF t_{12} vs. MF t_{12}	130.0	-4.1	**< 0.001**	130.0	4.3	**< 0.001**	130.0	-1.0	0.960
Contrast (Treatment:Flow:Time)									
Control LF t_3 vs. OA LF t_3	13.6	-0.6	1.000	10.2	-0.5	1.000	35.5	-1.6	0.680
Control MF t_3 vs. OA MF t_3	13.6	-0.4	1.000	10.2	1.1	1.000	35.5	4.2	**0.001**
Control LF t_7 vs. OA LF t_7	13.6	1.0	1.000	10.2	1.0	1.000	35.5	-1.1	1.000
Control MF t_7 vs. OA MF t_7	13.6	0.1	1.000	10.2	0.5	1.000	35.5	2.9	**0.039**
Control LF t_{12} vs. OA LF t_{12}	13.6	2.2	0.251	10.2	1.2	1.000	35.5	1.5	0.903
Control MF t_{12} vs. OA MF t_{12}	13.6	3.9	**0.010**	10.2	2.0	0.418	35.5	4.7	**< 0.001**

Supplementary Figures

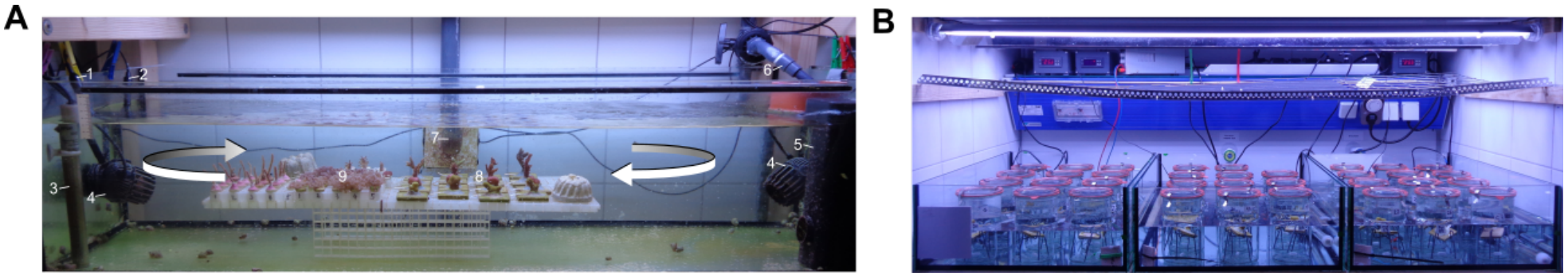

Fig. S1 Experimental setup. (A) Detail of an experimental tank with the main elements marked: (1) pH probe, (2) temperature probe, (3) heater, (4) pump, (5) wave generator, (6) inflow, (7) outflow, (8) scleractinian corals: (front to back) *Porites cylindrica, Pocillopora verrucosa, Acropora cytherea, Montipora digitata*, (9) octocorals: (front to back) *Xenia umbellata*, *Pinnigorgia flava*, *Sinularia* sp., *Plexaurella* sp. Arrows indicate the direction of water circulation. (B) Overview of the incubation setup of respirometry assays.

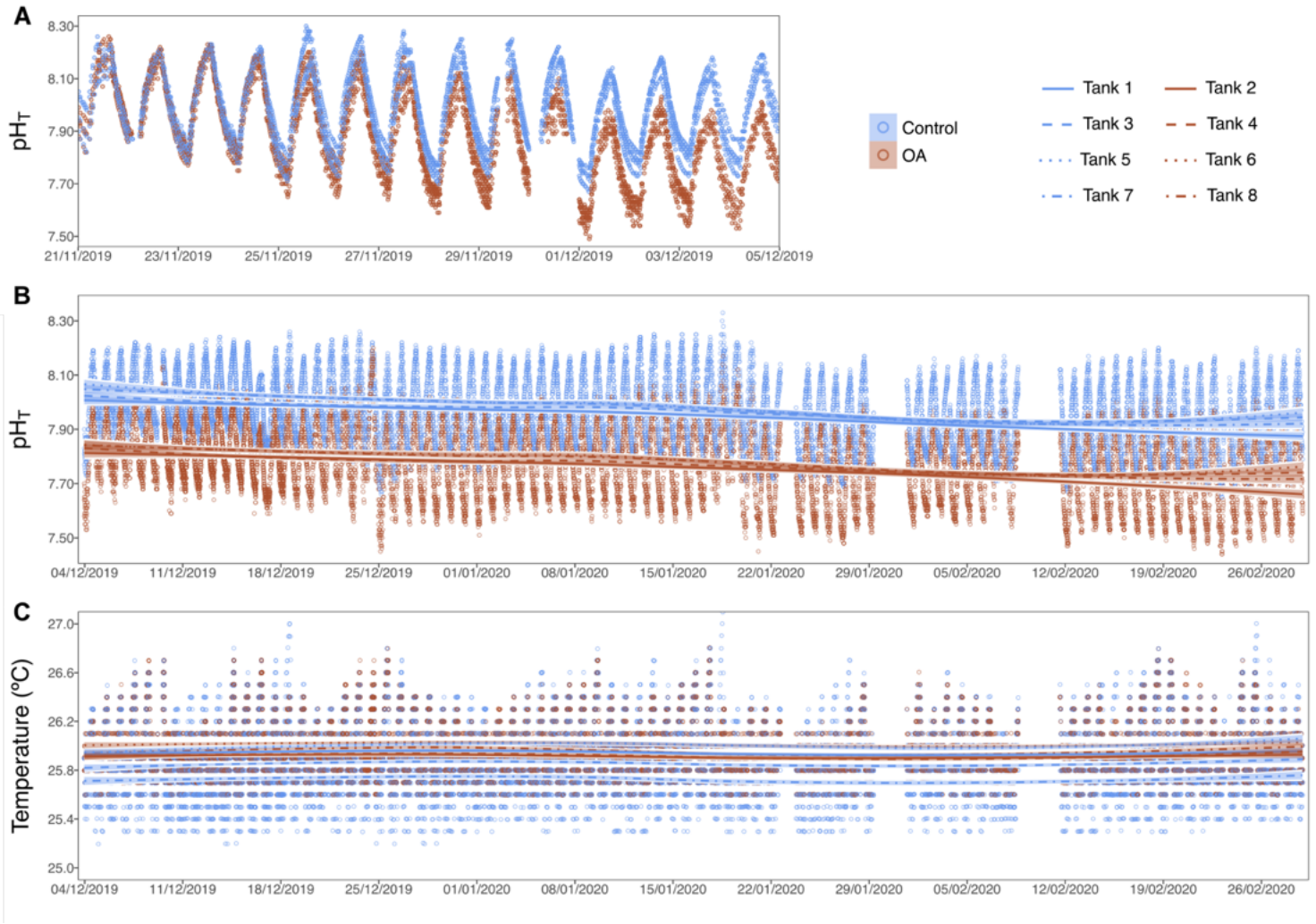

Fig. S2 Seawater conditions during the experiment. (A) pH during gradual establishment of ocean acidification (OA) treatment. (B) pH and (C) temperature during the experiment after reaching target OA conditions in OA treatment tanks. Lines are local polynomial regression fitting with 95% confidence intervals (shaded area). Dates are provided as DD/MM/YYYY. Data gaps reflect periods when values were not stored, which did not affect the measurement and manipulation of pH and temperature in the tanks, except on 09/12/2019 when the digital controller of the experimental system experienced a power failure. This stoppage lasted < 9 h, during which pH in the OA treatment tanks reverted to ambient levels and upon restarting the system, pH was gradually restored to target levels. pH_T, pH on the total scale

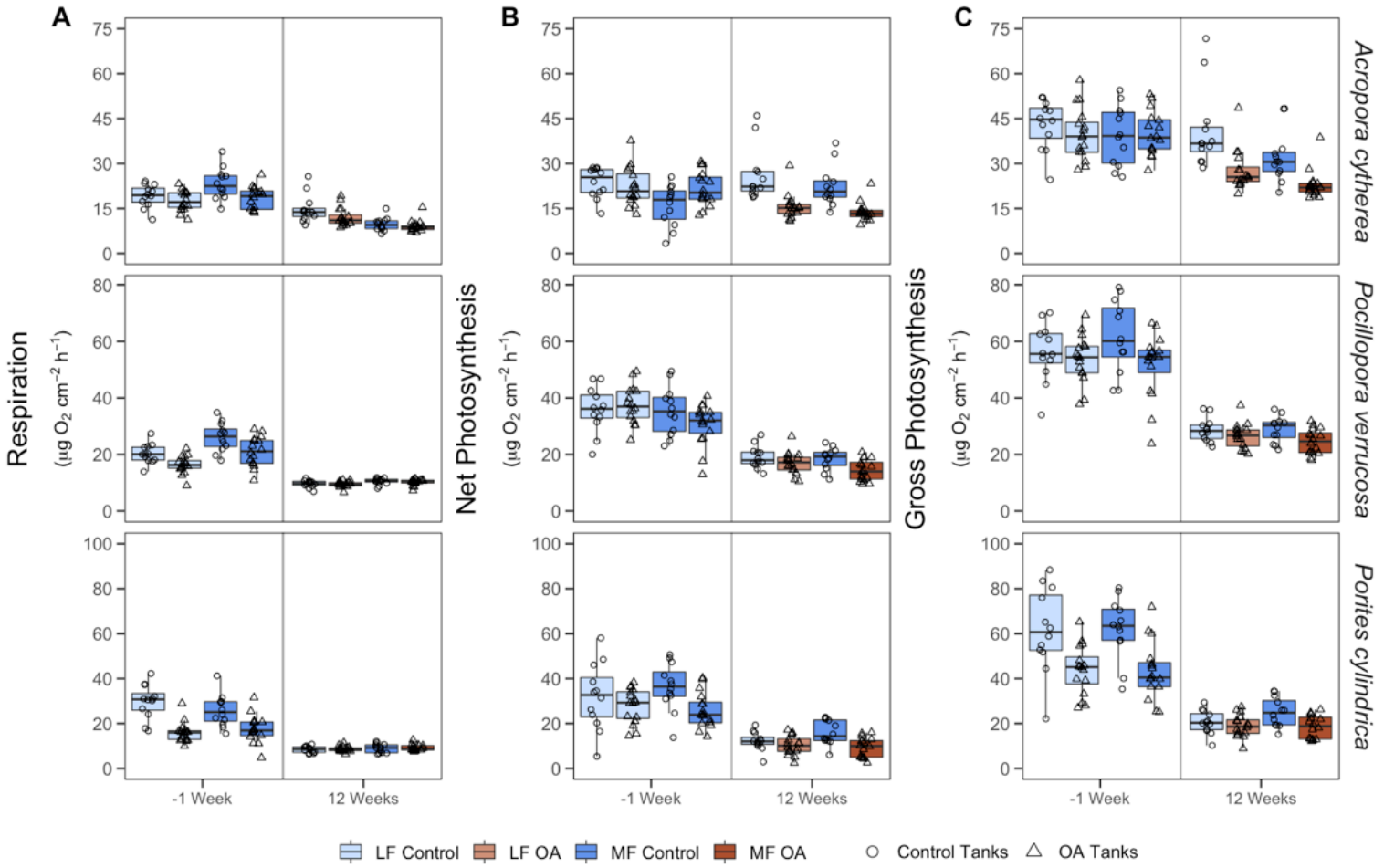

Fig. S3 Physiological responses in respiration and photosynthesis of three reef-building coral species. Rates of (A) respiration, (B) net photosynthesis, and (C) gross photosynthesis of *Acropora cytherea*, *Pocillopora verrucosa*, and *Porites cylindrica* in a control and ocean acidification (OA) treatment measured in low flow (LF, 2 cm s^{-1}) and moderate flow (MF, 6 cm s^{-1}) conditions during the acclimation period (measured one week before the start of the gradual pH decrease) and after 12 weeks under OA conditions, including two weeks of gradual pH decrease. Point shapes indicate treatment assignment. Data from the acclimation period are presented separated by the respective treatment applied during the OA phase. Boxes represent the first and third quartiles with lines as medians and whiskers as the minimum and maximum values or up to the 1.5 × interquartile range (IQR), whichever is reached first.

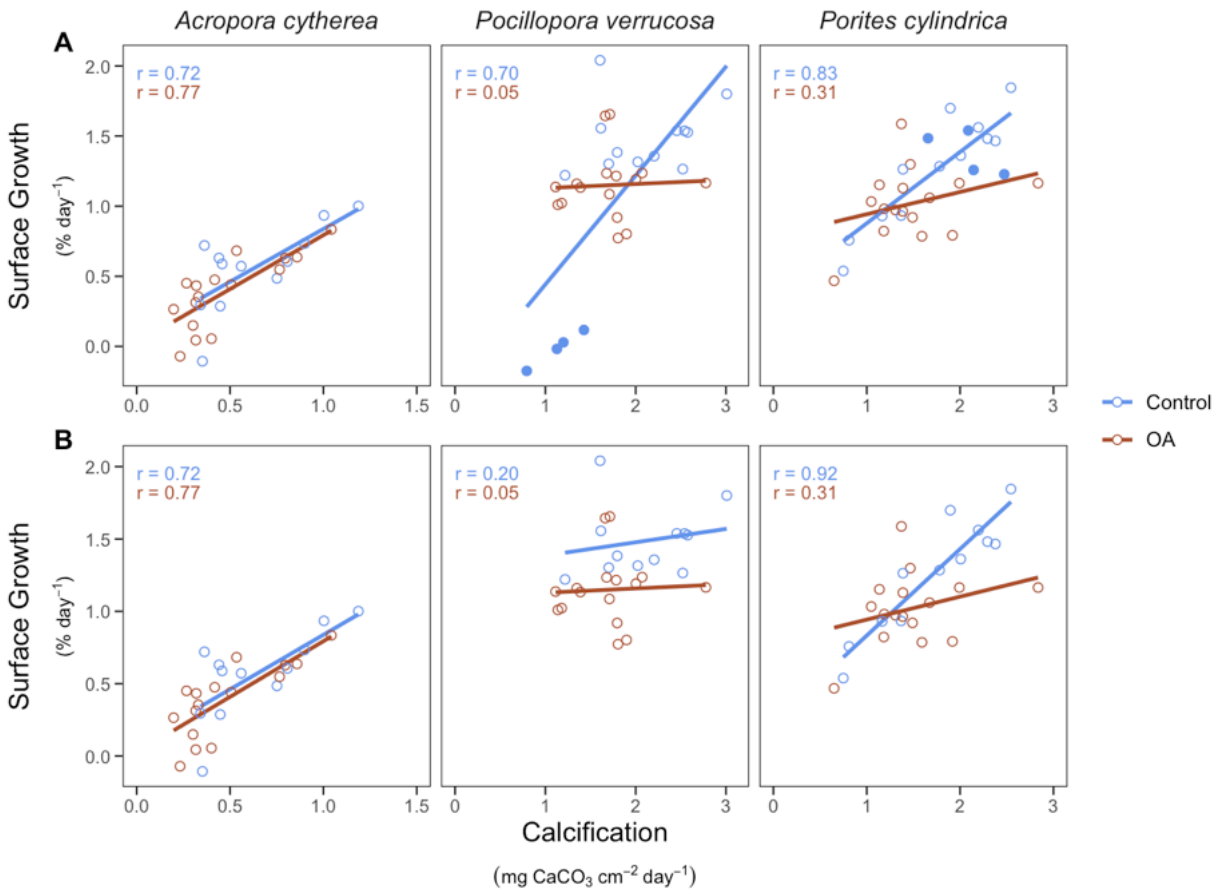

Fig. S4 Scatterplot of surface growth against calcification of *Acropora cytherea*, *Pocillopora verrucosa*, and *Porites cylindrica* after three months in a control and ocean acidification (OA) treatment. (A) Complete dataset. (B) Dataset with excluded fragments from the affected experimental tank (i.e., tank five) (see Materials and Methods). Coloured points indicate values from experimental tank five. Lines are linear regression fitting. r, Pearson correlation coefficient

3 Variability of Coral Concentration Boundary Layers (Manuscript III)

Martins CPP, Wall M, Schubert P, Wilke T, Ziegler M (2024) Variability of the surface boundary layer of reef-building coral species. *Coral Reefs* 43:1223–1233. DOI: 10.1007/s00338-024-02531-7

Coral Reefs (2024) 43:1223–1233
https://doi.org/10.1007/s00338-024-02531-7

REPORT

Variability of the surface boundary layer of reef-building coral species

Catarina P. P. Martins[1] · Marlene Wall[2] · Patrick Schubert[1] · Thomas Wilke[1] · Maren Ziegler[1]

Received: 22 November 2023 / Accepted: 30 June 2024 / Published online: 15 July 2024

Abstract The coral-seawater interface is an important, highly dynamic microenvironment for reef-building corals. Also known as the concentration boundary layer (CBL), it is a thin layer of seawater bordering the coral surface that dictates the biochemical exchange between the coral colony and bulk seawater. The CBL is thus a key feature that modulates coral metabolism. However, CBL variation among small-polyped coral species remains largely unknown. Therefore, we recorded over 100 profiles of dissolved O_2 concentration using microsensors to characterize CBL traits (thickness, surface O_2 concentration, and flux) of three small-polyped branching coral species, *Acropora cytherea*, *Pocillopora verrucosa*, and *Porites cylindrica*. Measurements were conducted during light and darkness combined with low or moderate water flow (2 and 6 cm s^{-1}). We found that CBL traits differed among species. CBL thickness was lowest in *A. cytherea*, while *P. verrucosa* showed the largest depletion of surface O_2 in dark and highest dark flux. In addition, we found that O_2 concentration gradients in the CBL occurred with three main profile shapes: diffusive, S-shaped, and complex. While diffusive profiles were the most common profile type, S-shaped and complex profiles were more frequent in *P. verrucosa* and *P. cylindrica*, respectively, and prevailed under low flow. Furthermore, profile types differed in CBL thickness and flux. Finally, low flow thickened CBLs, enhanced changes in surface O_2 concentration, and reduced flux, compared to moderate flow. Overall, our findings reveal CBL variability among small-polyped branching corals and help understand CBL dynamics in response to changes in light and water flow conditions.

Keywords Reef-building corals · Boundary layer · Water flow · Oxygen gradients

Introduction

Reef-building corals largely rely on gas exchange with the surrounding seawater to support key physiological processes such as photosynthesis and respiration. This biochemical exchange occurs in the coral boundary layer—a thin layer of seawater bordering the coral surface where concentration gradients of dissolved compounds (e.g., gases and nutrients) between the coral surface and the bulk seawater are formed (Lesser et al. 1994; Thomas and Atkinson 1997). The thickness and structure of the coral boundary layer, which dictate the coral biochemical exchange with seawater (Shashar et al. 1996), are dependent on flow conditions around the colony, coral surface microtopography, and polyp behavior (Shashar et al. 1993). Furthermore, metabolic activity also influences the CBL and may drive changes in CBL traits by altering the build-up of solutes at the coral surface (Hughes et al. 2020). While O_2 concentration gradients are often linear along a so-called diffusive boundary layer (DBL; Jørgensen and Revsbech 1985), they may also have a complex structure due to the presence of surface vortices created by epidermal cilia, particularly under no or slow water flow (Shapiro et al. 2014; Pacherres et al. 2020). Thus, this layer is also referred to as the concentration boundary layer (CBL; Nishihara and

Supplementary Information The online version contains supplementary material available at https://doi.org/10.1007/s00338-024-02531-7.

✉ Catarina P. P. Martins
catarina.padilha-pires-martins@bio.uni-giessen.de

[1] Department of Animal Ecology & Systematics, Justus Liebig University Giessen, 35392 Giessen, Germany

[2] GEOMAR Helmholtz Centre for Ocean Research Kiel, 24148 Kiel, Germany

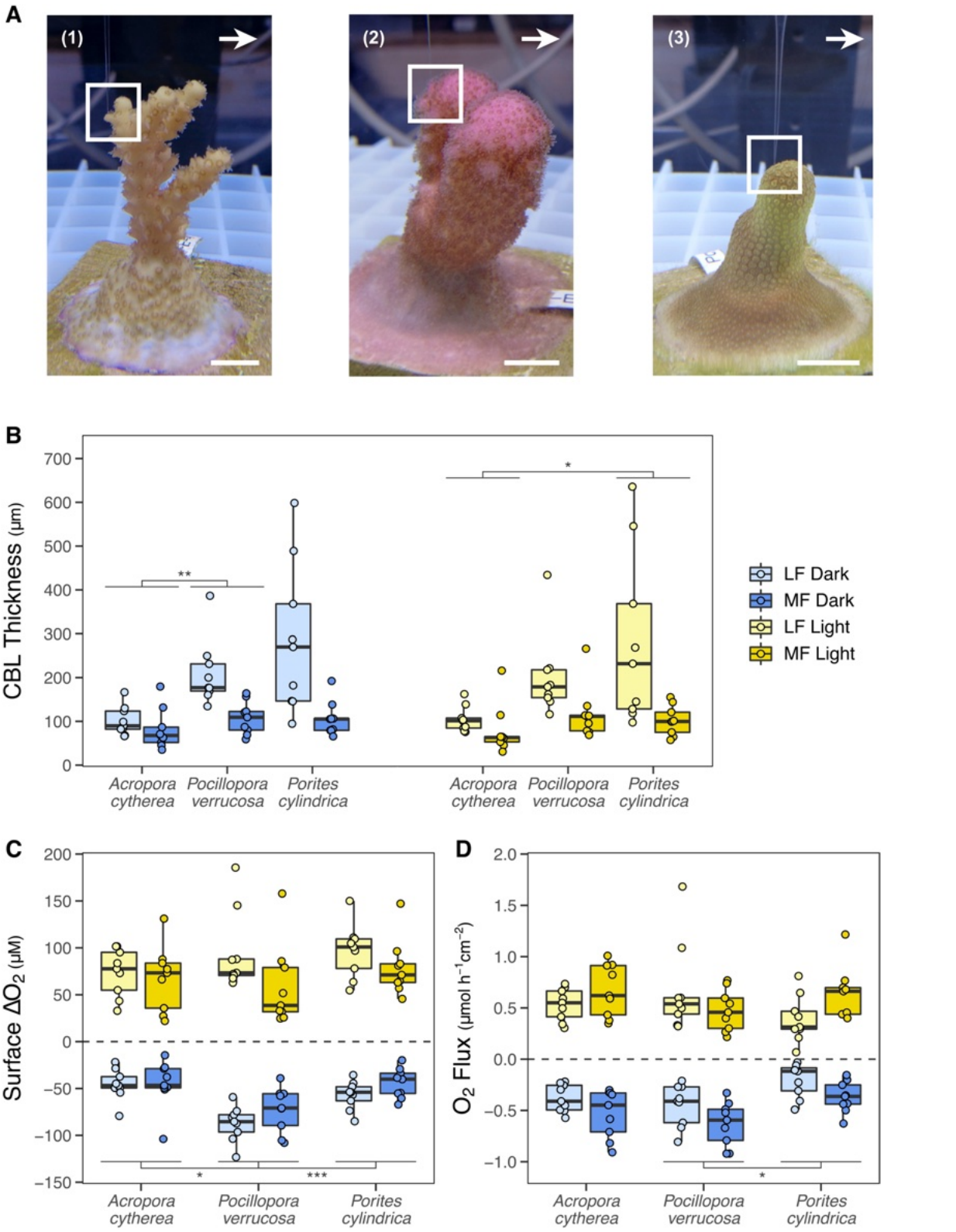

Ackerman 2007; Noisette et al. 2022), which is the term we use throughout the text.

Variation in CBL traits among coral species leads to differences in colony physiology (Patterson et al. 1991) and has been proposed to underlie differential susceptibility

◂**Fig. 1** Traits of the O_2 concentration boundary layer (CBL) of small-polyped reef-building corals. **A** Photographs of the investigated species during microsensor measurements: (1) *Acropora cytherea*, (2) *Pocillopora verrucosa*, and (3) *Porites cylindrica*. Rectangles mark representative locations of microsensor measurements across coral fragments, and arrows indicate the direction of water flow. Scale bar = 1 cm approx. **B** CBL thickness, **C** O_2 concentration change at the coral surface relative to bulk seawater (surface ΔO_2), and **D** O_2 flux, characterized under conditions of light, darkness, low flow (LF, 2 cm s^{-1}), and moderate flow (MF, 6 cm s^{-1}). Boxes represent the first and third quartiles with lines as medians and whiskers as the minimum and maximum values or up to the 1.5 × interquartile range (IQR), whichever is reached first; $n = 9$ per species, light, and flow. Stars indicate significant differences between species within light conditions ($p < 0.001$***, $p < 0.01$**, $p < 0.05$*, from post hoc of LMM-ANOVA)

to climate change effects (Putnam et al. 2017), including coral bleaching (Jimenez et al. 2008). Differences in CBL thickness between large- and small-polyped coral species are well-known, with thicker boundary layers in large-polyped massive species compared to small-polyped species due to the presence of topographical features such as protruding septae (Shashar et al. 1993; Jimenez et al. 2011). Small-polyped species have less differentiating surface features than large-polyped species and would thus be expected to be similar in CBL traits. However, recent studies have shown that coral species, including small-polyped corals, modulate their CBL by creating ciliary vortical flows at the coral surface (Shapiro et al. 2014; Pacherres et al. 2020). This ability to modify the CBL could differ among species, leading to interspecific variability in CBL traits, and thus explain the diversity of physiological rates and susceptibility to climate change effects among small-polyped species. However, variation in CBL traits among small-polyped species remains largely unknown. Furthermore, knowledge of the structure of O_2 concentration gradients within the coral boundary layer and their variability in structure also remains limited.

The aim of this study was to investigate the variability of the CBL of three major reef-building coral species, the small-polyped species *Acropora cytherea*, *Pocillopora verrucosa*, and *Porites cylindrica*. Specifically, we tested (i) whether CBL traits (thickness, surface O_2 concentration, and flux) differed between the three coral species. In addition, we characterized the structure of O_2 concentration gradients within the CBL and assessed (ii) profile structure among species and in response to low and moderate flow (2 and 6 cm s^{-1}) during light and darkness. Finally, we categorized the structure of profiles into three types and investigated (iii) differences in CBL traits among profile types and their response to light and flow. This study will therefore help understand boundary layer variability among reef-building corals and the dynamics of the coral-seawater interface.

Materials and methods

Experimental setup

The O_2 concentration gradient in the coral boundary layer was measured in the small-polyped branching corals *A. cytherea*, *P. verrucosa*, and *P. cylindrica*. Coral colonies (Table S1) were maintained at the 'Ocean2100' long-term coral experimental facility at Justus Liebig University Giessen, Germany. Long-term rearing conditions were 11:13 h light:dark photoperiod, with a light intensity of 230 µmol photons m^{-2} s^{-1}, and a temperature of 26.0 ± 0.5 °C for at least six months before the experiment (Martins et al. 2024b). Three colonies per species were cut into three fragments using a small angle grinder (Dremel Multitool 3000-15, The Netherlands) and attached to tiles with two-component glue (CoraFix SuperFast, Grotech, Germany). Measurements were performed six months after fragmentation on fully recovered and healthy fragments.

Profiles of dissolved O_2 concentration were measured using Clark-type O_2 microelectrodes (tip diameter 20–30 µm; OX-25, Unisense, Denmark) connected to a microsensor multimeter (Unisense, Denmark), whose signals were read on a PC using a 2-channel A/D converter (ADC-216, Unisense, Denmark). Oxygen microsensors were calibrated daily with air-saturated seawater and anoxic seawater prepared using yeast, following manufacturer's instructions. Profiles were measured on the top upstream face of coral fragments (Fig. 1A), above the coenosarc (connecting tissue between polyps), and on a spot where the tentacles of nearby polyps showed little to no movement. Profiles were performed by carefully placing the tip of the sensor on the coral surface and moving it up in steps of 5–60 µm within the gradient and of 50–200 µm in bulk seawater, using a motorized microprofiling system (Unisense, Denmark). The microsensor was programmed to automatically return to its starting position (i.e., the coral surface) after completing each profile measurement. All measurements were performed on coral fragments with open polyps and extended tentacles. The measuring spot was constantly monitored during all profiles using a stereo microscope (Stemi 508, Carl Zeiss AG, Germany) to verify tentacle extension and avoid artefacts due to tissue movement or polyp interaction. Sensor positioning and data acquisition were performed using the software SensorTrace Profiling (Unisense, Denmark). At each step, values were recorded for 30–60 s with a waiting period of 3 s after moving the sensor. Profiles were conducted in a flume (length 118 cm, width 18 cm, water depth 19 cm) with unidirectional recirculating flow, created by a circulating pump (ES-28, Aqualight, Germany). Flow straighteners were placed up- and downstream of the measurement section (upstream: PVC grid with length of 10.5 cm and 1.3 × 1.3 cm openings, attached to a layer of nylon net

with 500 µm pore size; downstream: PVC grid with length of 2.5 cm and 1.3 × 1.3 cm openings).

Microscale oxygen profiles

A total of 108 profiles were recorded. For each coral fragment, profiles were measured in a total of four conditions: light and darkness combined with low (2 cm s^{-1}) and moderate (6 cm s^{-1}) flow conditions ($n = 6$ profiles per genotype per species per light condition, $n = 6$ profiles per genotype per species per flow condition). To characterize flow conditions around the coral fragments under the two flow velocities, the dimensionless Reynolds number (Re) was calculated as $Re = uW/v$ from the flow velocity (u), the coral height (W) (Lesser et al. 1994), and the kinematic viscosity (v) of seawater at 26 °C and salinity 35 (Ramsing and Gundersen 2023). Coral height was estimated from photographs using ImageJ (v2.1.0/1.53c), and coral volume was estimated using 3D scanning (see Supplementary Text for methodological details). Flow conditions around coral fragments were overall similar (Table 1) and corresponded to Re values of 646 and 1,937 for the low and moderate flow velocities, respectively, indicating that the coral fragments experienced laminar flow (Patterson et al. 1991) under both velocities. Measurements were performed after coral fragments had been acclimated to light and flow conditions (light, 10 min; darkness, 5 min; flow, 10 min), and it was ensured that steady-state O_2 conditions had been reached before starting each profile. All flow and light conditions were measured, in succession, on the same spot for each coral fragment during daylight hours. Water temperature was maintained at 26 °C, salinity at 35, pH_T at 8.02, O_2 concentration at 240 ± 8 µM, and light intensity at 200 µmol photons m^{-2} s^{-1}.

Calculation of boundary layer traits

Oxygen concentration profiles were used to calculate total thickness of the CBL, diffusive flux through the CBL, and change of O_2 concentration at the coral surface relative to ambient seawater (surface ΔO_2). The CBL thickness was determined as the distance between the coral surface and the outer limit of the upper diffusive boundary layer (Pacherres et al. 2020), calculated by extrapolating the linear concentration gradient in the CBL to the ambient seawater concentration of the free-flow region (Jørgensen and Revsbech 1985). Oxygen flux was calculated using Fick's first law of diffusion (Jørgensen and Revsbech 1985; Nishihara and Ackerman 2007) with O_2 diffusion coefficient of 2.29×10^{-5} cm^2 s^{-1} at 26.0 °C and salinity of 35 (Ramsing and Gundersen 2023). Our data contained both linear and nonlinear profiles. To calculate CBL thickness and O_2 flux of nonlinear profiles using Fick's first law of diffusion, we followed the protocol developed by Pacherres et al. (2020) and used the upper linear gradient of the profiles—i.e., the linear gradient that preceded bulk seawater concentration. Flow in the upper linear gradient is laminar and calculations using this part of the profile provide a representative estimation of the flux across the coral CBL, without needing to resolve the mechanisms in the more complex, nonlinear parts of the profile (Pacherres et al. 2020). Additional details on our rationale for the chosen approach can be found in Martins et al. (2024b).

Statistical analysis

Oxygen concentration profiles were grouped by common characteristics, and the total number of profiles per profile type was recorded. Differences in CBL thickness, surface ΔO_2 concentration, and O_2 flux between profile types in light and darkness were assessed using linear mixed-effects models (LMMs). All models were constructed with profile type (3 levels: diffusive, S-shaped, and complex), species (3 levels: *A. cytherea*, *P. verrucosa*, and *P. cylindrica*) and flow (2 levels: low and moderate) as fixed factors, and coral fragment identity (ID) as random factor. Linear mixed-effects models were performed using the *R* package *lme4* (Bates et al. 2015). Model validation was done by graphically assessing homogeneity and normality assumptions. To meet model assumptions, we applied a log transformation to light and dark CBL thickness and light O_2 flux, followed by an inspection of the shape of trends. Models were selected based on AIC, BIC and R^2 values. Numerical output and model formulas of LMMs are given in Table S2. We then computed type-II ANOVA tables of the fixed effects of LMMs using Kenward–Roger approximation for the degrees of freedom in the *R* package *car* (Fox and Weisberg

Table 1 Dimensions (mean ± SD) of the investigated coral fragments of *Acropora cytherea*, *Pocillopora verrucosa*, and *Porites cylindrica* and the calculated dimensionless Reynolds number corresponding to low (Re_{LF}) and moderate (Re_{MF}) water flow velocities (2 and 6 cm s^{-1}, respectively)

Species	Height (cm)	Volume (cm^3)	Shape	Re_{LF}	Re_{MF}
Acropora cytherea	3.3 ± 0.4	3.7 ± 0.8	Branching	718 ± 93	2,153 ± 279
Pocillopora verrucosa	3.0 ± 0.6	7.5 ± 1.8	Branching	661 ± 120	1,983 ± 361
Porites cylindrica	2.6 ± 0.3	4.7 ± 1.2	Columnar	559 ± 62	1,676 ± 186

2019). Post hoc analyses were performed using the *R* package *emmeans* (Lenth 2021) with Tukey adjustment of *p* values. All plots were produced using the *R* package *ggplot2* (Wickham 2016). All statistical analyses were performed in *R* (v.4.1.0; R Core Team 2021) using RStudio (v1.4.1106; RStudio Team 2021).

Results

Traits of boundary layers differ between species

The three investigated coral species differed in the traits of their O_2 boundary layer, pooled over water flow conditions. CBL thickness differed between species in both light (LMM-ANOVA, $F = 4.2$, $p < 0.05$) and darkness (LMM-ANOVA, $F = 6.6$, $p < 0.01$) (Fig. 1B). *Acropora cytherea* generally had a thinner CBL (92 ± 45 µm) than *P. verrucosa* in darkness (159 ± 78 µm; post hoc, $t = -3.5$, $p < 0.01$) and *P. cylindrica* in light (192 ± 165 µm; post hoc, $t = -2.6$, $p < 0.05$), which were not significantly different from each other (light/dark, post hoc, $t = -0.2/0.9$, $p > 0.05$). In light, surface ΔO_2 concentration (range: 70.5–87.7 µM) and O_2 flux (range: 0.52–0.60 µmol cm^{-2} h^{-1}) were similar between species (Fig. 1C, D; flux/ΔO_2, LMM-ANOVA, $F = 0.5/1.0$, $p > 0.05$). In contrast, surface ΔO_2 concentration and O_2 flux in darkness differed between species (LMM-ANOVA, $F = 3.5/9.7$, $p < 0.05/0.001$). Dark surface ΔO_2 concentration was highest in *P. verrucosa* (-80.0 ± 22.1 µM), compared to *A. cytherea* (-45.6 ± 20.6 µM; post hoc, $t = 4.1$, $p < 0.001$) and *P. cylindrica* (-50.8 ± 16.3 µM; post hoc, $t = -3.3$, $p < 0.01$), which did not significantly differ from each other (post hoc, $t = 0.6$, $p > 0.05$) (Fig. 1C). *Pocillopora verrucosa* also had a significantly higher dark O_2 flux (-0.54 ± 0.22 µmol cm^{-2} h^{-1}) than *P. cylindrica* (-0.29 ± 0.17 µmol cm^{-2} h^{-1}; post hoc, $t = -2.6$, $p < 0.05$), but not *A. cytherea* (-0.46 ± 0.20 µmol cm^{-2} h^{-1}; post hoc, $t = 1.1$, $p > 0.05$), which were not significantly different from each other (post hoc, $t = -1.6$, $p > 0.05$) (Fig. 1D).

Flow conditions generally modulated CBL traits across species. CBL thickness was overall larger under low flow compared to moderate flow (light/dark, LMM-ANOVA, $F = 36.1/39.7$, $p < 0.001$), with the smallest increase in *A. cytherea* compared to *P. cylindrica*, which presented a wide range of thickness values (Fig. 1B). Surface ΔO_2 concentration was also larger under low flow compared to moderate flow (light/dark, LMM-ANOVA, $F = 12.3/7.7$, $p < 0.01/0.05$), but with similar changes across species (Fig. 1C). Flow conditions had a significant effect on O_2 flux in darkness only (LMM-ANOVA; light, $F = 1.9$, $p > 0.05$; dark, $F = 10.9$, $p < 0.01$), which was increased under moderate flow compared to low flow (Fig. 1D).

The shape of gradients within the coral boundary layer differs with species and water flow

We found that the O_2 concentration gradient in the CBL had different profile shapes, which we categorized into three main groups: diffusive, S-shaped, and complex. Diffusive profiles were characterized by a single linear concentration gradient, typical of a DBL (Fig. 2A); S-shaped profiles by a distanced linear gradient with a steeper slope at the coral surface (Fig. 2B); and complex profiles by multiple DBLs (Fig. 2C).

Overall, the three profile types were not equally frequent. Diffusive profiles were the most common type of profile (60%), while 32% of all measured profiles were S-shaped and only 8% were complex. The occurrence of the types of profiles differed between species (Fig. 2D). Diffusive profiles were more commonly observed in *A. cytherea* (75%) than in *P. verrucosa* (47%) or *P. cylindrica* (58%). S-shaped profiles were as frequent as diffusive profiles in *P. verrucosa* (50%), and more frequent compared to the other species (*A. cytherea*, 25%; *P. cylindrica*, 19%). In *A. cytherea* no complex profile and in *P. verrucosa* only one complex profile was observed, while they were as common as S-shaped profiles in *P. cylindrica* (22%).

The occurrence of profile types differed with light and flow conditions, depending on the species. In *A. cytherea*, diffusive profiles were the predominant profile type in all conditions (Fig. 2E). In this species, the less frequent S-shaped profiles occurred predominantly under moderate flow and in darkness (Fig. 2E). In *P. verrucosa*, although diffusive and S-shaped profiles were overall equally common, diffusive profiles were more common under low flow in darkness, while S-shaped profiles were more common under low flow in the light (Fig. 2F). Under moderate flow, this pattern was reversed. The two complex profiles observed in *P. verrucosa* occurred in light and under moderate flow. In *P. cylindrica*, diffusive profiles were predominant under all conditions, except in darkness and under low flow, where complex profiles were predominant (Fig. 2G). Similar to *A. cytherea*, S-shaped profiles occurred more frequently in darkness. Complex profiles occurred mostly under low flow, with only one profile observed under moderate flow, which occurred in darkness.

Quantitative traits of boundary layers of different shape

Boundary layers with different profile types were characterized by differences in their traits, which were largely determined by water flow (Table S3). Overall, profile types differed significantly in CBL thickness (light/dark, LMM-ANOVA, $F = 9.8/8.7$, $p < 0.001$), with complex profiles being three times as thick as diffusive (light/dark, post hoc,

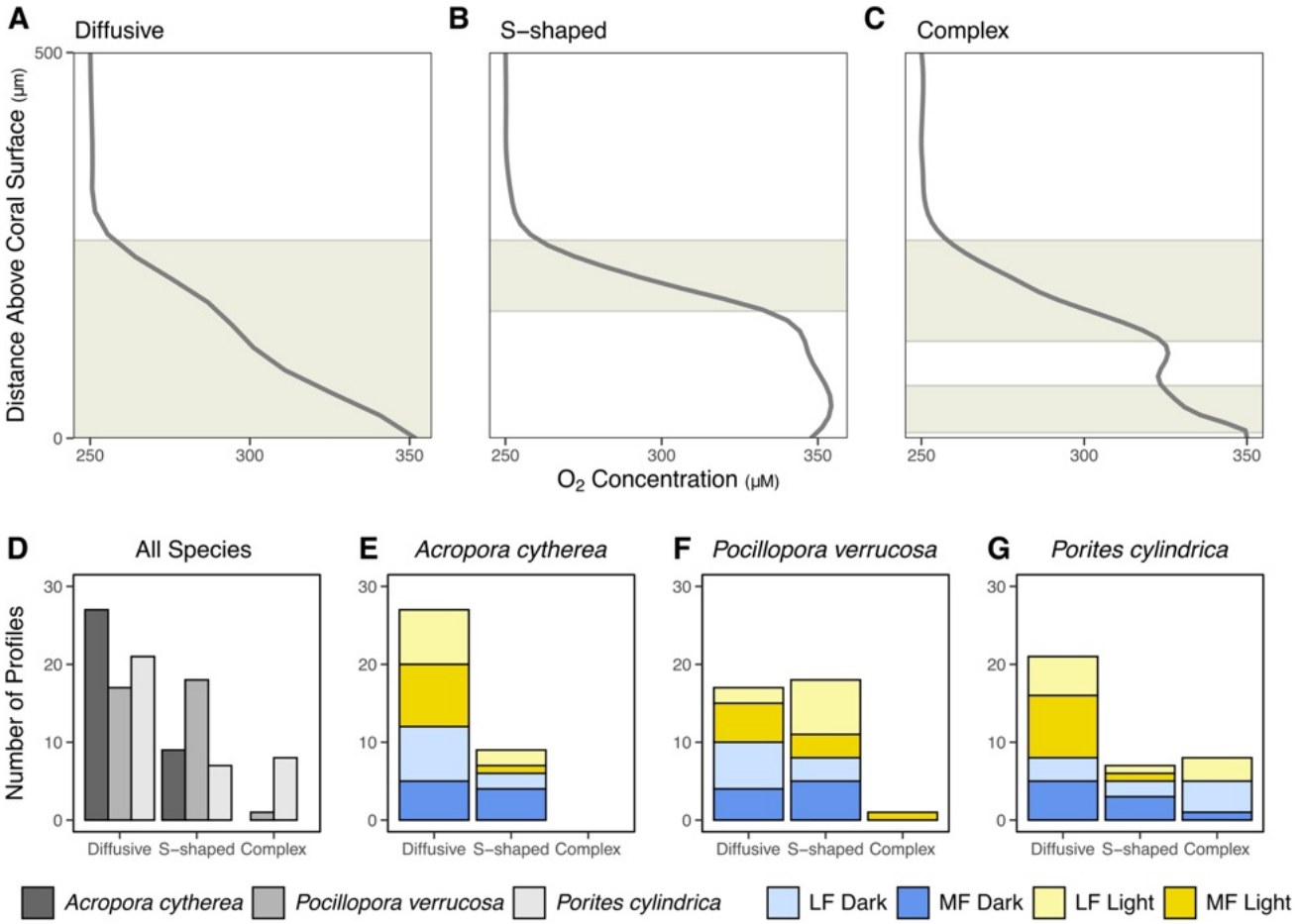

Fig. 2 Variability of O_2 gradients in the concentration boundary layer. Schematic diagrams representing O_2 concentration gradients in the boundary layer of three reef-building coral species with **A** diffusive, **B** S-shaped, and **C** complex structure. Diagrams represent profiles under light conditions, created to facilitate visualization of the three types of profile structure. Visual presentation of all measured profiles, including the individual profiles used to produce the schematic diagrams, is provided in Fig. S1. Shaded areas mark regions where mass transport is dominantly diffusive. **D** Number of profiles of O_2 concentration gradients in the coral boundary layer with diffusive, S-shaped, or complex structure across species and in **E** *Acropora cytherea*, **F** *Pocillopora verrucosa*, and **G** *Porites cylindrica*, in light and darkness, and low flow (LF, 2 cm s^{-1}) or moderate flow (MF, 6 cm s^{-1})

$t = -4.4/-4.2$, $p < 0.001$) and S-shaped profiles (light/dark, post hoc, $t = -2.9/-3.7$, $p < 0.05/0.01$), which were not significantly different from each other (light/dark, post hoc, $t = -1.2/-0.4$, $p > 0.05$) (Fig. 3A). Under low flow, complex profiles had an average CBL thickness of 437 ± 170 µm, while diffusive and S-shaped profiles had 147 ± 77 and 188 ± 95 µm, respectively. Under moderate flow, CBL thickness was more similar across profile types (diffusive, 93 ± 43; S-shaped, 104 ± 50; complex, 164 ± 40 µm).

Surface ΔO_2 concentration was overall similar between profile types (light/dark, LMM-ANOVA, $F = 2.7/0.7$, $p > 0.05$; Fig. 3B). In light, O_2 at the coral surface was overall 88.4 ± 33.2 and 68.2 ± 35.9 µM above seawater O_2 concentration under low and moderate flow, respectively. In darkness, it was 63.5 ± 24.1 and 54.1 ± 25.0 µM below seawater concentration under low and moderate flow, respectively.

Compared to thickness, flux displayed the inversed pattern of profile types (light/dark, LMM-ANOVA, $F = 4.0/10.9$, $p < 0.05/0.001$), with increased values under moderate flow compared to low flow in all profile types (Table S3). Light O_2 flux was overall highest in S-shaped profiles (0.64 ± 0.35 µmol cm^{-2} h^{-1}) and significantly higher than complex profiles (0.35 ± 0.28 µmol cm^{-2} h^{-1}; post hoc, $t = 2.8$, $p < 0.05$), but not diffusive profiles (0.56 ± 0.24 µmol cm^{-2} h^{-1}; post hoc, $t = -1.4$, $p > 0.05$), which were not significantly different from each other (post hoc, $t = 2.2$, $p > 0.05$) (Fig. 3C). In darkness, S-shaped profiles had a significantly higher O_2 flux than both diffusive (post hoc, $t = 3.6$, $p < 0.01$) and complex profiles (post hoc,

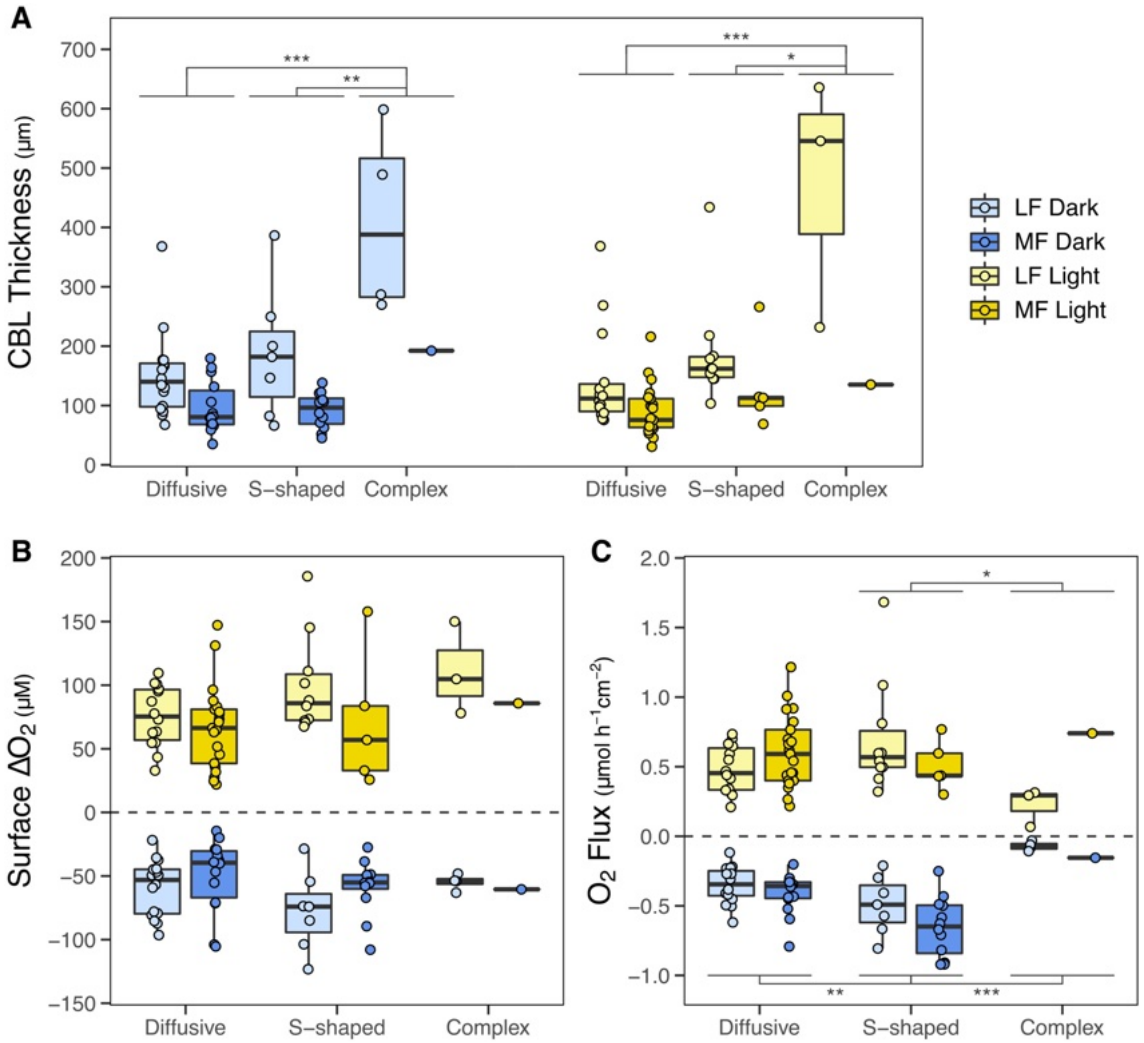

Fig. 3 Traits of profile types (diffusive, S-shaped, and complex) of the concentration boundary layer (CBL) under light and darkness and two levels of water flow. **A** CBL thickness, **B** O_2 concentration change at the coral surface relative to bulk seawater (surface ΔO_2), and **C** O_2 flux, measured in *Acropora cytherea*, *Pocillopora verrucosa*, and *Porites cylindrica,* under conditions of light, darkness, low flow (LF, 2 cm s^{-1}), and moderate flow (MF, 6 cm s^{-1}). Boxes represent the first and third quartiles with lines as medians and whiskers as the minimum and maximum values or up to the 1.5 × interquartile range (IQR), whichever is reached first; see Table S3 for *n*. Stars indicate significant differences between profile types pooled over flow conditions in light and darkness ($p < 0.001$***, $p < 0.01$**, $p < 0.05$*, from post hoc of LMM-ANOVA)

$t = -4.1$, $p < 0.001$), which were not significantly different from each other (post hoc, $t = -2.4$, $p > 0.05$) (Fig. 3C).

Discussion

This study shows that CBL traits differ between small-polyped coral species. In addition, we show that O_2 concentration gradients within the CBL may occur in different profile shapes, which differ in prevalence among species. The formation of these profile types was largely dependent on flow, with overall purely diffusive profiles dominating across flow conditions and more complex profiles prevailing under low flow. Some species may present structurally complex profiles even in moderate water flows. Finally, we show that boundary layers with different O_2 profile types also differed in CBL traits.

CBL traits differ between species

CBL traits differed among the small-polyped species studied, with differences strongest for CBL thickness. Such CBL variability among small-polyped corals could be associated with coral morphology (Chan et al. 2016), small-scale morphological complexity (e.g., surface roughness or fractal dimensions; Reichert et al. 2017), and species-specific

features and behavior, including the size, density, and activity of polyps (Shashar et al. 1993; Malul et al. 2020; Li et al. 2021) and surface cilia (Shapiro et al. 2014; Pacherres et al. 2020). While corallite size is similar among the investigated species (global range 0.5–1.5 mm; Pichon and Veron 1976), polyp density differs (*A. cytherea*, 12 polyps cm^{-2}; Irikawa et al. 2011; *P. verrucosa*, 129 polyps cm^{-2}; Sier and Olive 1994; *P. cylindrica*, 67 polyps cm^{-2}; Anthony 1999). Lower polyp density possibly results in lower hydrodynamic drag forces on the coral surface and, together with the weak feeding and cleaning ciliary currents reported for acroporids (Lewis and Price 1976; Stafford-Smith 1993), may explain the thinner CBL of *A. cytherea* compared to the other two species (Shapiro et al. 2014).

Differences in CBL thickness could also be attributed to spatial heterogeneity of surface topography in relation to the location of the microsensor measurement. Although the similarly thick CBL of *P. verrucosa* and *P. cylindrica* in our study was within ranges reported for other pocilloporids and poritids under similar flow conditions (Jimenez et al. 2011; Chan et al. 2016), up to ten times thicker CBLs have been reported for *Stylophora pistillata* (Shashar et al. 1993). In our study, CBL was measured above the coenosarc, where it is generally thinner but also more stable than in other areas of the coral because polyp behavior is less likely to disrupt it. In addition, we performed all measurements on the upstream side of coral fragments, which has a thinner CBL than the downstream side (Edmunds 2005; Murthy et al. 2023). Although our measurements were thus performed in a location assumed to be hydrodynamically similar for the tested species, differences in microscale flow conditions at the coral surface may still have occurred and could account for some of the CBL variability observed. These surface flow differences, however, would likely be generated by the coral itself or due to species differences in microtopography. Finally, CBL thickness displayed similar patterns in light and darkness across species, demonstrating the overall stability of this trait with variable light conditions.

Species differences in surface O_2 concentration and flux were only present in dark conditions in our study. *Pocillopora verrucosa* showed the largest depletion of surface O_2 concentration and highest dark flux, which may be related to its higher respiration rates compared to *A. cytherea* and *P. cylindrica* (Vetter et al. unpublished data). Furthermore, these patterns could also be due to differences in cilia activity. Although cilia activity has been shown to have no effect on O_2 flux across the CBL in light, it may enhance fluxes in the dark (Pacherres et al. 2020). This also suggests that cilia may have different roles during photosynthesis and dark respiration, with the latter depending on cilia activity to increase supply of O_2 during the night. Instead, during light, cilia appear to be important in reducing the risk of oxidative stress without modulating O_2 flux by redistributing O_2 in the CBL over the coral surface and maintaining low O_2 levels above areas with high chlorophyll concentration (Ahmerkamp et al. 2022; Pacherres et al. 2022).

As expected, water flow modulated CBL traits across species, with largely consistent effects. CBL thickness generally increased with reduced flow, as seen previously (e.g., Shashar et al. 1993; Kühl et al. 1995), while surface O_2 was more depleted under low flow than under moderate flow, suggesting a lower O_2 exchange with bulk seawater under the low flow. O_2 flux, however, was affected by flow conditions only during darkness in our study. Dark flux was reduced under low flow compared to moderate flow, which is in agreement with previous reports of decreased coral respiration with reduced flow (e.g., Patterson et al. 1991). During the night, coral internal and surface O_2 concentrations are undersaturated and may reach extreme depletion (Shashar et al. 1993; Kühl et al. 1995). This can limit coral respiration (Sebens et al. 2003), indicating that it may be limited by the diffusive supply of O_2 from bulk seawater (Kühl et al. 1995; Gardella and Edmunds 1999). Altogether, our results provide further evidence for the O_2 limitation that corals may experience at night, which may be exacerbated during periods of low flow.

CBL profile types across species and water flow conditions

The combination of surface topography, ciliary movement, metabolic rates, and environmental conditions leads to differences in the type and distribution of CBL profiles. Diffusive profiles were the predominant profile type in our study, which is in agreement with previous observations under moderate water flow (Shashar et al. 1993; Kühl et al. 1995). The formation of these profiles is due to viscous forces dominating near the coral surface and making flow laminar and molecular diffusion the dominant mechanism of mass transport (Jørgensen and Revsbech 1985; Nishihara and Ackerman 2007). Our S-shaped profiles corresponded to the profile shapes created by the activity of epidermal cilia, previously observed only under near-zero flows (Shapiro et al. 2014; Pacherres et al. 2020). Similarly to S-shaped profiles, the presence of complex profiles could also be due to ciliary activity since these could occur in profiles that go through the middle of ciliary vortices (Shapiro et al. 2014) or as a result of complex flow patterns caused by the coral microtopography. For instance, model simulations show that surface structures such as verrucae may modulate and slow down flow near the coral surface (Hossain and Staples 2020). Furthermore, scleractinian corals also generate horizontal surface currents (Bouderlique et al. 2022), which could influence profile structure.

Ciliary vortices have previously been observed in several species, including *Acropora* sp., *Montipora* sp., *Seriatopora*

hystrix, *S. pistillata*, and *Favia* sp. (Shapiro et al. 2014). Therefore, S-shaped and complex profiles are expected to occur in a range of species as observed herein. The influence of cilia activity on surface conditions has been observed to be greatest with flow velocities below 1 cm s^{-1} because faster flow tends to erase the vortices created by beating cilia and the resulting profile structure (Shapiro et al. 2014; Murthy et al. 2023). While this explains the prevalence of diffusive profiles in our study, S-shaped profiles were more abundant under both flow conditions here than expected based on previous conceptual models (Shapiro et al. 2014).

In this study, all profile types were observed in each species, except *A. cytherea*, which did not have complex profiles. However, the frequency of distinct O_2 CBL profiles differed between species. Profiles of *A. cytherea* were mostly diffusive, while *P. verrucosa* and *P. cylindrica* were characterized by a larger proportion of S-shaped and complex profiles. These differences in profile types may underlie differences in coral growth or photosynthesis. Both *A. cytherea* and *P. verrucosa* are fast-growing species and considered highly efficient at using environmental resources (Darling et al. 2012), which may be related to a prevalence of diffusive profiles with higher O_2 exchange across the coral surface. In contrast, branching *Porites* spp., such as *P. cylindrica*, have lower growth rates than *Acropora* spp. (Pratchett et al. 2015), which could be associated with a larger proportion of complex profiles, as observed herein.

Overall, the different frequency of profile types among the studied species may be indicative of their variable ability to alter the boundary layer, with potential downstream consequences on growth rates. Given the importance of mass transport to modulate coral colony physiology (Patterson et al. 1991), such differences may be key to understanding the response of coral species to changing environmental conditions (Schoepf et al. 2018).

Traits of CBL profile types

Boundary layers with different profile shapes differed in thickness and flux in our study, with complex profiles presenting the thickest CBL and lowest O_2 flux. Lower mass transfer associated with thick CBLs can limit photosynthesis, respiration, and calcification (Finelli et al. 2006; Colombo-Pallotta et al. 2010). Thick CBLs, however, also provide a better isolation from surrounding bulk seawater, which may be an advantage in the context of ocean acidification (Chan et al. 2016) and deoxygenation (Osinga et al. 2017; Hughes et al. 2020). Therefore, species with complex CBLs may be less vulnerable to ocean acidification and deoxygenation by reducing exposure to stressful conditions of bulk seawater (Noisette et al. 2022). In line with this, *P. cylindrica* has been shown to be less vulnerable to OA than *Acropora* spp. (Suggett et al. 2013; Martins et al. 2024a).

Our results of O_2 concentration at the coral surface among profile types, however, were unexpected. O_2 concentration varies along the coral surface (Pacherres et al. 2022), and particularly, within ciliary vortices. O_2 levels are generally reduced in the central and downward sections of vortices, which is associated with a mitigation strategy of high surface O_2 concentrations (Pacherres et al. 2020). In contrast, changes in surface O_2 concentration were similar between profile types in our study, which would rule out a direct link between surface O_2 levels and the formation of the different profile shapes. Alternatively, lower water flow conditions than those tested in our study may be necessary to observe differences in surface O_2 concentration among profile types.

Determining patterns and dynamics of the CBL is challenging due to spatial and temporal variability (Linsmayer et al. 2020; Pacherres et al. 2022). Spatial heterogeneity and coral circadian rhythms may present confounding factors when spot measurements are carried out throughout the day. Despite this, we detected significant patterns, which might be underestimated given the methodological approach. Further knowledge on CBL changes throughout a diel cycle will be essential for understanding the substantial CBL variability generally observed among species and environmental conditions across studies. Finally, future studies able of 3D mapping the CBL along the coral surface and better characterizing its spatial heterogeneity will help resolve the interspecific variability of coral CBL traits.

Conclusions

Our study indicates that small-polyped reef-building corals may have different O_2 boundary layers. Using profile measurements performed in the laboratory, we show that (i) CBL traits differ between small-polyped species, regardless of flow conditions, which could be related to differences in surface cilia activity. In addition, we found that (ii) O_2 concentration gradients in the coral CBL may have different profile shapes (diffusive, S-shaped, and complex), which occur with varying frequency among coral species, depending on surface topography, ciliary movement, and environmental conditions, particularly water flow. We show that some species can present structurally complex profiles even in moderate water flows. These findings may be indicative of variable ability of coral species to alter their boundary layer, with potential downstream consequences on growth rates. However, the feedback loops between coral physiological activity and CBL traits could further contribute to species differences at both the colony and CBL scales. Finally, we found that (iii) boundary layers with different O_2 profile shapes may differ in CBL traits, which are modulated by water flow conditions. Such CBL variability could underlie

the range of sensitivities to climate change of reef-building corals and be key to understanding coral responses.

Overall, our findings show that CBL variability exists even among small-polyped coral species and highlight the benefit of accurately identifying the profile structure and traits of O_2 concentration gradients within the CBL to better understand the coral-seawater interface. The coral surface displays pronounced spatial and temporal variability, which may present confounding factors for studies based on spot measurements of the coral surface. Therefore, future 3D mappings of the CBL along the coral surface will help resolve the interspecific variability of coral CBL traits.

Acknowledgements This study was conducted as part of the 'Ocean2100' global change simulation project of the Colombian-German Center of Excellence in Marine Sciences (CEMarin), funded by the German Academic Exchange Service (DAAD, project number 57480468).

Author contributions CM, MW, and MZ designed the study. CM and PS set up the experiment and maintained animals. CM collected and analyzed the data and prepared the figures and tables. MW provided the microsensor measuring system. TW secured funding. CM drafted the manuscript with assistance from MZ. All authors contributed to editing and reviewing of the manuscript.

Funding Open Access funding enabled and organized by Projekt DEAL.

Data availability The raw data are available as part of a larger dataset of microsensor measurements at https://doi.org/10.6084/m9.figshare.24534343.

Declarations

Conflict of interest On behalf of all authors, the corresponding author states that there is no conflict of interest.

References

Ahmerkamp S, Jalaluddin FM, Cui Y, Brumley DR, Pacherres CO, Berg JS, Stocker R, Kuypers MMM, Koren K, Behrendt L (2022) Simultaneous visualization of flow fields and oxygen concentrations to unravel transport and metabolic processes in biological systems. Cell Reports Methods 2:100216

Anthony KRN (1999) Coral suspension feeding on fine particulate matter. J Exp Mar Biol Ecol 232:85–106

Bates D, Mächler M, Bolker B, Walker S (2015) Fitting linear mixed-effects models using lme4. J Stat Softw 67:1–48

Bouderlique T, Petersen J, Faure L, Abed-Navandi D, Bouchnita A, Mueller B, Nazarov M, Englmaier L, Tesarova M, Frade PR, Zikmund T, Koehne T, Kaiser J, Fried K, Wild C, Pantos O, Hellander A, Bythell J, Adameyko I (2022) Surface flow for colonial integration in reef-building corals. Curr Biol 32:2596-2609.e7

Chan NCS, Wangpraseurt D, Kühl M, Connolly SR (2016) Flow and coral morphology control coral surface pH: implications for the effects of ocean acidification. Front Mar Sci 3:1–11

Colombo-Pallotta MF, Rodríguez-Román A, Iglesias-Prieto R (2010) Calcification in bleached and unbleached *Montastraea faveolata*: evaluating the role of oxygen and glycerol. Coral Reefs 29:899–907

Darling ES, Alvarez-Filip L, Oliver TA, McClanahan TR, Côté IM (2012) Evaluating life-history strategies of reef corals from species traits. Ecol Lett 15:1378–1386

Edmunds PJ (2005) Effect of elevated temperature on aerobic respiration of coral recruits. Mar Biol 146:655–663

Finelli CM, Helmuth BST, Pentcheff ND, Wethey DS (2006) Water flow influences oxygen transport and photosynthetic efficiency in corals. Coral Reefs 25:47–57

Fox J, Weisberg S (2019) An R companion to applied regression. Sage, Thousand Oaks, CA

Gardella DJ, Edmunds PJ (1999) The oxygen microenvironment adjacent to the tissue of the scleractinian *Dichocoenia stokesii* and its effects on symbiont metabolism. Mar Biol 135:289–295

Hossain MM, Staples AE (2020) Effects of coral colony morphology on turbulent flow dynamics. PLoS ONE 15:1–25

Hughes DJ, Alderdice R, Cooney C, Kühl M, Pernice M, Voolstra CR, Suggett DJ (2020) Coral reef survival under accelerating ocean deoxygenation. Nat Clim Chang 10:296–307

Irikawa A, Casareto BE, Suzuki Y, Agostini S, Hidaka M, van Woesik R (2011) Growth anomalies on *Acropora cytherea* corals. Mar Pollut Bull 62:1702–1707

Jimenez IM, Kühl M, Larkum AWD, Ralph PJ (2008) Heat budget and thermal microenvironment of shallow-water corals: Do massive corals get warmer than branching corals? Limnol Oceanogr 53:1548–1561

Jimenez IM, Kühl M, Larkum AWD, Ralph PJ (2011) Effects of flow and colony morphology on the thermal boundary layer of corals. J R Soc Interface 8:1785–1795

Jørgensen BB, Revsbech NP (1985) Diffusive boundary layers and the oxygen uptake of sediments and detritus. Limnol Oceanogr 30:111–122

Kühl M, Cohen Y, Dalsgaard T, Jørgensen B, Revsbech N (1995) Microenvironment and photosynthesis of zooxanthellae in scleractinian corals studied with microsensors for O_2, pH and light. Mar Ecol Prog Ser 117:159–172

Lenth RV (2021) Emmeans: estimated marginal means, aka least-squares means. R package version 1.6.2–1. https://cran.r-project.org/package=emmeans

Lesser MP, Weis VM, Patterson MR, Jokiel PL (1994) Effects of morphology and water motion on carbon delivery and productivity in the reef coral, *Pocillopora damicornis* (Linnaeus): diffusion barriers, inorganic carbon limitation, and biochemical plasticity. J Exp Mar Biol Ecol 178:153–179

Lewis JB, Price WS (1976) Patterns of ciliary currents in Atlantic reef corals and their functional significance. J Zool 178:77–89

Li S, Roger LM, Kumar L, Lewinski NA, Klein-Seetharaman J, Gagnon A, Putnam HM, Yang J (2021) Digital image processing to detect subtle motion in stony coral. Sci Rep 11:7722

Linsmayer LB, Deheyn DD, Tomanek L, Tresguerres M (2020) Dynamic regulation of coral energy metabolism throughout the diel cycle. Sci Rep 10:1–12

Malul D, Holzman R, Shavit U (2020) Coral tentacle elasticity promotes an *out-of-phase* motion that improves mass transfer. Proc R Soc B Biol Sci 287:20200180

Martins CPP, Simancas-Giraldo SM, Schubert P, Wall M, Wild C, Wilke T, Ziegler M (2024a) Short periods of decreased water flow may modulate long-term ocean acidification in reef-building corals. Preprint at bioRxiv

Martins CPP, Ziegler M, Schubert P, Wilke T, Wall M (2024b) Effects of water flow and ocean acidification on oxygen and pH gradients in coral boundary layer. Sci Rep 14:12757

Murthy S, Picioreanu C, Kühl M (2023) Modeling the radiative, thermal and chemical microenvironment of 3D scanned corals. Front Mar Sci 10:1–41

Nishihara GN, Ackerman JD (2007) On the determination of mass transfer in a concentration boundary layer. Limnol Oceanogr Methods 5:88–96

Noisette F, Pansch C, Wall M, Wahl M, Hurd CL (2022) Role of hydrodynamics in shaping chemical habitats and modulating the responses of coastal benthic systems to ocean global change. Glob Chang Biol 28:3812–3829

Osinga R, Derksen-Hooijberg M, Wijgerde T, Verreth JAJ (2017) Interactive effects of oxygen, carbon dioxide and flow on photosynthesis and respiration in the scleractinian coral *Galaxea fascicularis*. J Exp Biol 220:2236–2242

Pacherres CO, Ahmerkamp S, Schmidt-Grieb GM, Holtappels M, Richter C (2020) Ciliary vortex flows and oxygen dynamics in the coral boundary layer. Sci Rep 10:7541

Pacherres CO, Ahmerkamp S, Koren K, Richter C, Holtappels M (2022) Ciliary flows in corals ventilate target areas of high photosynthetic oxygen production. Curr Biol 32:4150-4158.e3

Patterson MR, Sebens KP, Olson RR (1991) In situ measurements of flow effects on primary production and dark respiration in reef corals. Limnol Oceanogr 36:936–948

Pichon M, Veron JEN (1976) Scleractinia of Eastern Australia. Australian Govt. Pub. Service, Canberra

Pratchett MS, Anderson KD, Hoogenboom MO, Widman E, Baird AH, Pandolfi JM, Edmunds PJ, Lough JM (2015) Spatial, temporal and taxonomic variation in coral growth—implications for the structure and function of coral reef ecosystems. Oceanogr Mar Biol Annu Rev 53:215–295

Putnam HM, Barott KL, Ainsworth TD, Gates RD (2017) The vulnerability and resilience of reef-building corals. Curr Biol 27:R528–R540

R Core Team (2021) R: a language and environment for statistical computing. R Foundation for Statistical Computing, Vienna, Austria

Ramsing N, Gundersen J (2023) Seawater and gases: tabulated physical parameters of interest to people working with microsensors in marine systems. Unisense. https://unisense.com/technical-information/#tables

Reichert J, Backes AR, Schubert P, Wilke T (2017) The power of 3D fractal dimensions for comparative shape and structural complexity analyses of irregularly shaped organisms. Methods Ecol Evol 8:1650–1658

RStudio Team (2021) RStudio: integrated development environment for R. RStudio, PBC, Boston, MA

Schoepf V, Cornwall CE, Pfeifer SM, Carrion SA, Alessi C, Comeau S, McCulloch MT (2018) Impacts of coral bleaching on pH and oxygen gradients across the coral concentration boundary layer: a microsensor study. Coral Reefs 37:1169–1180

Sebens KP, Helmuth B, Carrington E, Agius B (2003) Effects of water flow on growth and energetics of the scleractinian coral *Agaricia tenuifolia* in Belize. Coral Reefs 22:35–47

Shapiro OH, Fernandez VI, Garren M, Guasto JS, Debaillon-Vesque FP, Kramarsky-Winter E, Vardi A, Stocker R (2014) Vortical ciliary flows actively enhance mass transport in reef corals. Proc Natl Acad Sci 111:13391–13396

Shashar N, Cohen Y, Loya Y (1993) Extreme diel fluctuations of oxygen in diffusive boundary layers surrounding stony corals. Biol Bull 185:455–461

Shashar N, Kinane S, Jokiel PL, Patterson MR (1996) Hydromechanical boundary layers over a coral reef. J Exp Mar Biol Ecol 199:17–28

Sier CJS, Olive PJW (1994) Reproduction and reproductive variability in the coral *Pocillopora verrucosa* from the Republic of Maldives. Mar Biol 118:713–722

Stafford-Smith MG (1993) Sediment-rejection efficiency of 22 species of Australian scleractinian corals. Mar Biol 115:229–243

Suggett DJ, Dong LF, Lawson T, Lawrenz E, Torres L, Smith DJ (2013) Light availability determines susceptibility of reef building corals to ocean acidification. Coral Reefs 32:327–337

Thomas FIM, Atkinson MJ (1997) Ammonium uptake by coral reefs: effects of water velocity and surface roughness on mass transfer. Limnol Oceanogr 42:81–88

Wickham H (2016) ggplot2: elegant graphics for data analysis. Springer-Verlag, New York

Supplementary Material

Variability of the surface boundary layer of reef-building coral species

Catarina P. P. Martins*[1], Marlene Wall[2], Patrick Schubert[1], Thomas Wilke[1], Maren Ziegler[1]

[1]Department of Animal Ecology & Systematics, Justus Liebig University Giessen, 35392 Giessen, Germany

[2]GEOMAR Helmholtz Centre for Ocean Research Kiel, 24148 Kiel, Germany

*corresponding author: catarina.padilha-pires-martins@bio.uni-giessen.de

Supplementary Text

Volume of coral fragments was estimated using 3D scanning (Artec Spider 3D with Artec Studio 9, Artec 3D, Luxembourg), following Reichert et al. (2016). Briefly, corals were placed on a rotating plate and scans were captured in air within 60–90 seconds. 3D models were calculated by performing fine serial registration, global registration (minimal distance: 10, iterations: 2,000, based on texture and geometry), sharp fusion (resolution: 0.2, fill holes by radius, max. hole radius: 5), and outlier removal (*Acropora cytherea* and *Porites cylindrica*, SD: 3; *Pocillopora verrucosa*, SD: 4). Artefact objects were removed (small objects filter) and meshes were trimmed manually at the tissue border. All meshes were exported as Wavefront ".obj" files to MeshLab Visual Computing Lab-ISTI-CNR (v1.3.4, BETA, 2014; Cignoni et al. 2008) and coral volume values were calculated on watertight meshes using the "compute geometric measures" tool.

References

Cignoni P, Callieri M, Corsini M, Dellepiane M, Ganovelli F, Ranzuglia G (2008) MeshLab: An Open-Source Mesh Processing Tool. Sixth Eurographics Italian Chapter Conference 129–136

Reichert J, Schellenberg J, Schubert P, Wilke T (2016) 3D scanning as a highly precise, reproducible, and minimally invasive method for surface area and volume measurements of scleractinian corals. Limnol Oceanogr Methods 14:518–526

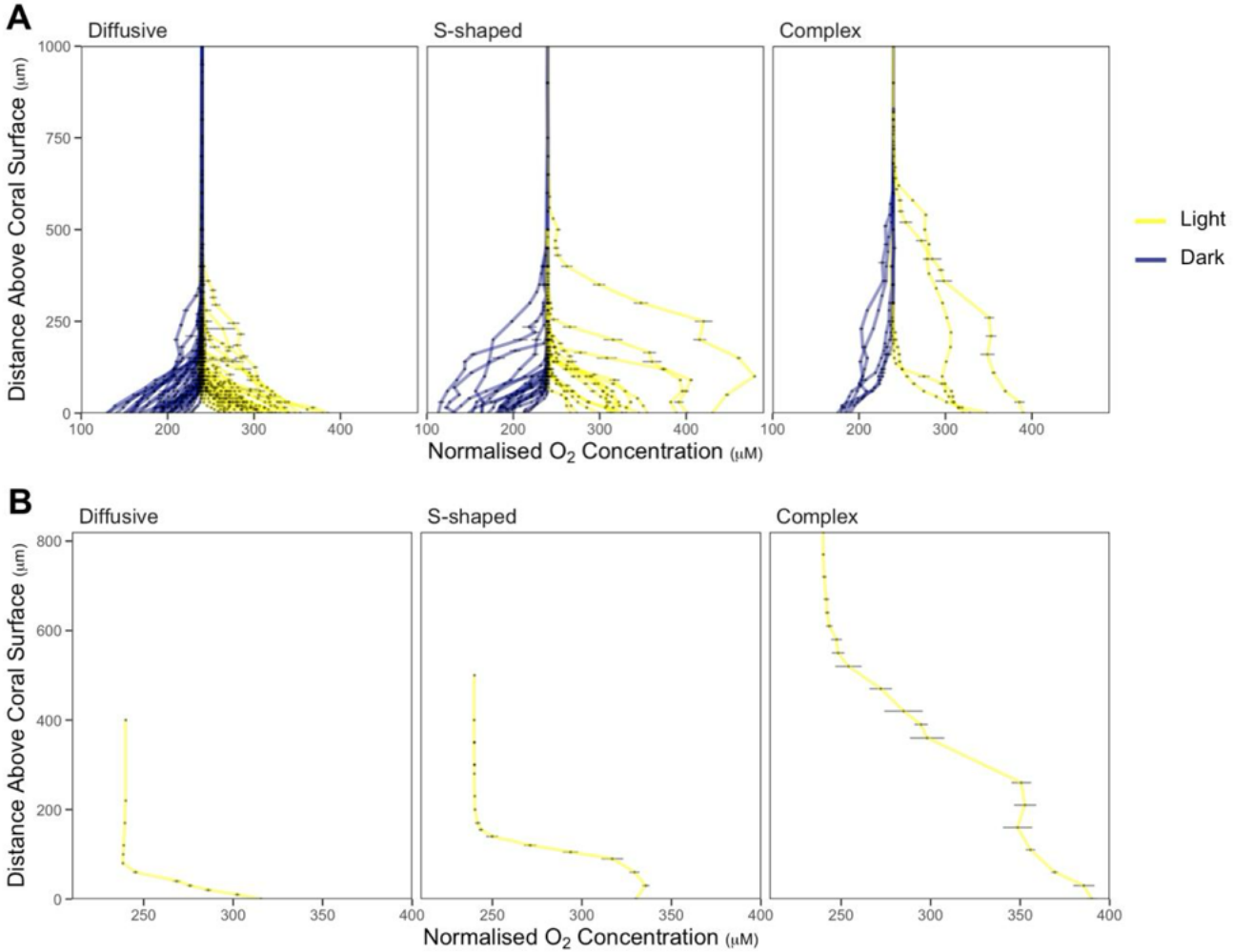

Fig. S1 Profiles of standardised O_2 concentration across the concentration boundary layer of *Acropora cytherea*, *Pocillopora verrucosa*, and *Porites cylindrica*, measured in light and darkness. (A) All measured profiles and (B) profiles used to produce the schematic diagrams of profile structure types in Fig. 2 are categorised into diffusive, S-shaped, or complex. Points are point measurements (recorded for 30–60s) and horizontal lines are SD for each measurement.

Table S1 Details on coral species used in the experiment.

Species	Origin	Collection Year	CITES Number
Acropora cytherea	Saudi Arabia (Red Sea)	2019	19-SA-000089-PD
Pocillopora verrucosa	Saudi Arabia (Red Sea) Indonesia (Indo-Pacific)	2015 2007	15-SA-000882-PD 14846/IV/SATS-LN/2007
Porites cylindrica	Indonesia (Indo-Pacific)	2017	17nl241924/11

Table S2 Numerical output of linear mixed-effects models (LMMs) of traits of the concentration boundary layer (CBL). Models were constructed with profile type (3 levels: diffusive, S-shaped [S], and complex [C]), species (3 levels: *Acropora cytherea*, *Pocillopora verrucosa* [Pve], and *Porites cylindrica* [Pcy]), and flow (2 levels: low and moderate) as fixed factors; and coral fragment identity (ID) as random factor. Model formulas are specified. Log-transformation was applied to light and dark CBL thickness and light O_2 flux to meet model assumptions. surface ΔO_2, change in O_2 concentration at the coral surface relative to bulk seawater; σ^2, residual variance; τ_{00}, random intercept variance; ICC, intra-class correlation coefficient; N, number of levels of random effects groups; Marginal R^2, variance explained by the fixed effects; Conditional R^2, variance explained by the entire model

		CBL Thickness		Surface ΔO_2		O_2 Flux	
		~ Profile Type + Species + Flow + (1 | ID)		~ Profile Type + Species + Flow + (1 | ID)		~ Profile Type + Species + Flow + (1 | ID)	
	Fixed Effects	Estimates	SE	Estimates	SE	Estimates	SE
Light	(Intercept)	4.64	0.13	74.69	11.36	-0.70	0.15
	profile type [S]	0.18	0.15	21.86	9.12	0.26	0.18
	profile type [C]	0.85	0.19	5.01	10.36	-0.60	0.26
	species [Pve]	0.43	0.18	-2.56	15.85	-0.18	0.19
	species [Pcy]	0.46	0.17	17.61	15.52	-0.13	0.18
	flow [moderate]	-0.51	0.08	-15.73	4.47	0.18	0.13
	Random Effects						
	σ^2	0.08		219.33		0.20	
	τ_{00}	0.09 $_{ID}$		961.16 $_{ID}$		0.05 $_{ID}$	
	ICC	0.53		0.81		0.19	
	N	27 $_{ID}$		27 $_{ID}$		27 $_{ID}$	
	Observations	54		54		54	
	Marginal R^2 / Conditional R^2	0.547 / 0.787		0.161 / 0.844		0.192 / 0.347	
Dark	(Intercept)	4.67	0.12	-48.63	6.18	-0.34	0.05
	profile type [S]	0.04	0.11	-6.60	5.28	-0.17	0.04
	profile type [C]	0.86	0.20	-0.66	9.45	0.20	0.08
	species [Pve]	0.53	0.15	-33.75	8.14	-0.07	0.06
	species [Pcy]	0.40	0.16	-5.38	8.52	0.11	0.06
	flow [moderate]	-0.53	0.08	10.55	3.79	-0.11	0.03
	Random Effects						
	σ^2	0.08		169.70		0.01	
	τ_{00}	0.06 $_{ID}$		211.49 $_{ID}$		0.01 $_{ID}$	
	ICC	0.42		0.55		0.42	
	N	27 $_{ID}$		27 $_{ID}$		27 $_{ID}$	
	Observations	54		54		54	
	Marginal R^2 / Conditional R^2	0.606 / 0.771		0.412 / 0.738		0.545 / 0.738	

Table S3 Quantitative traits (mean ± SD) of profile types of the concentration boundary layer (CBL) measured in *Acropora cytherea*, *Pocillopora verrucosa*, and *Porites cylindrica*, in light or darkness combined with low flow (2 cm s^{-1}) or moderate flow (6 cm s^{-1}). Surface $\Delta O2$ concentration = difference in O_2 concentration between coral surface and bulk seawater, n = sample size.

Profile Type	Condition	Flow	CBL Thickness (µm)	Surface ΔO_2 Concentration (µM)	O_2 Flux (µmol cm^{-2} h^{-1})	*n*
Diffusive	Light	Low	142 ± 85	75.3 ± 24.0	0.48 ± 0.17	14
		Moderate	90 ± 43	66.6 ± 33.0	0.61 ± 0.26	21
	Dark	Low	151 ± 72	-59.5 ± 22.0	-0.35 ± 0.13	16
		Moderate	97 ± 44	-49.8 ± 28.5	-0.41 ± 0.15	14
S-shaped	Light	Low	189 ± 91	99.9 ± 38.5	0.70 ± 0.41	10
		Moderate	132 ± 77	71.4 ± 53.4	0.51 ± 0.18	5
	Dark	Low	188 ± 109	-77.5 ± 31.1	-0.49 ± 0.21	7
		Moderate	92 ± 30	-58.6 ± 21.5	-0.65 ± 0.21	12
Complex	Light	Low	471 ± 212	111.0 ± 36.4	0.23 ± 0.14	3
		Moderate	135	85.8	0.74	1
	Dark	Low	411 ± 160	-54.7 ± 6.2	-0.07 ± 0.03	4
		Moderate	192	-60.5	-0.15	1

4 Coral Boundary Layers Under OA (Manuscript IV)

Martins CPP, Ziegler M, Schubert P, Wilke T, Wall M (2024) Effects of water flow and ocean acidification on oxygen and pH gradients in coral boundary layer. *Scientific Reports* 14:12757. DOI: 10.1038/s41598-024-63210-9

scientific reports

Check for updates

OPEN

Effects of water flow and ocean acidification on oxygen and pH gradients in coral boundary layer

Catarina P. P. Martins[1]✉, Maren Ziegler[1], Patrick Schubert[1], Thomas Wilke[1] & Marlene Wall[2]

Reef-building corals live in highly hydrodynamic environments, where water flow largely controls the complex chemical microenvironments surrounding them—the concentration boundary layer (CBL). The CBL may be key to alleviate ocean acidification (OA) effects on coral colonies by partially isolating them. However, OA effects on coral CBL remain poorly understood, particularly under different flow velocities. Here, we investigated these effects on the reef-building corals *Acropora cytherea*, *Pocillopora verrucosa*, and *Porites cylindrica*. We preconditioned corals to a control (pH 8.0) and OA (pH 7.8) treatment for four months and tested how low flow (2 cm s^{-1}) and moderate flow (6 cm s^{-1}) affected O_2 and H^+ CBL traits (thickness, surface concentrations, and flux) inside a unidirectional-flow chamber. We found that CBL traits differed between species and flow velocities. Under OA, traits remained generally stable across flows, except surface pH. In all species, the H^+ CBL was thin and led to lower surface pH. Still, low flow thickened H^+ CBLs and increased light elevation of surface pH. In general, our findings reveal a weak to null OA modulation of the CBL. Moreover, the OA-buffering capacity by the H^+ CBL may be limited in coral species, though low flow could enhance CBL sheltering.

Coral reefs are highly hydrodynamic habitats, with spatially variable hydrodynamic regimes depending on reef zones and structures (e.g., uniform calm flow in lagoons vs high-energy wave-driven flow on reef crests)[1]. Importantly, water flow also varies temporally in reefs, where flow velocities may range from 0 to 30 cm s^{-1} within single locations[2] and some sites may present low flow lasting only a few hours[3].

For reef-building corals, water flow is a key environmental factor due to its influence on the coral concentration boundary layer (CBL)[4]. It represents a thin layer of seawater bordering the coral surface where concentration gradients of dissolved compounds (e.g., gases[5] and nutrients[6]) are formed between the coral and bulk seawater[7]. These gradients shape key physiological processes, such as photosynthesis, and their properties are largely determined by water flow conditions[8]. For instance, under reduced water flow, the O_2 CBL becomes thicker and O_2 flux is decreased[9,10]. Besides flow conditions, the characteristics of the CBL are also dependent on coral surface topography, polyp behaviour and traits, and cilia activity[11–13], with the steepness of gradients being further modulated by the metabolic activity of the organism itself[7]. The CBL is thus a very dynamic chemical microenvironment at the coral surface that acts as a partial chemical barrier between the coral and its environment.

Under ocean acidification (OA)—a process characterised by decreased pH and altered carbonate chemistry, with negative effects on coral metabolism[14]—the CBL may be key in partially isolating coral colonies from surrounding acidified seawater. For instance, massive coral species have shown similar surface pH under control and OA after 30-min and 5-day exposure to OA conditions[15,16]. This ability to maintain stable surface pH, despite the lower pH of the surrounding seawater, occurred while maintaining stable O_2 CBL flux. Therefore, pH in the CBL under OA may be linked to O_2 CBL traits. However, whether this ability to increase the elevation of surface pH under OA is also present in branching coral species remains unclear[17]. Furthermore, CBL traits could potentially be affected by OA due to changes in coral microtopography and surface cilia activity. For instance, OA has been shown to affect cilia in marine organisms[18,19], and OA effects on coral skeletons[20] could alter the topography of the tissue surface, modifying the flow patterns at the coral-seawater interface.

The effects of OA on CBL traits may also differ with exposure time and display complex interactions with water flow. During 30-min exposure to OA, O_2 CBL thickness of *Favites* sp. was stable under low flow (below 2 cm s^{-1}) but increased under moderate flow (5 cm s^{-1}), while elevation of surface pH was larger under low flow[16]. Moreover, after over four months under OA, surface pH in light was similar to seawater pH in *Acropora*

[1]Department of Animal Ecology & Systematics, Justus Liebig University Giessen, 35392 Giessen, Germany. [2]GEOMAR Helmholtz Centre for Ocean Research Kiel, 24148 Kiel, Germany. ✉email: catarina.padilha-pires-martins@bio.uni-giessen.de

yongei, but in *Plesiastrea versipora* it was elevated above seawater level, with a greater magnitude under low than moderate flow (2.5 and 8 cm s^{-1}, respectively)[17].

Although long-term OA effects on the coral CBL remain poorly understood, differences in CBL traits may help explain the range of sensitivities to OA among reef-building corals[21]. In addition, the magnitude of daily pH fluctuation at the coral surface may further determine responses to OA. However, while coral colonies with higher surface pH in light generally also have lower surface pH in darkness[22], CBL traits under OA are rarely documented in darkness. Finally, despite recent studies, knowledge of how water flow may modulate coral responses to OA at the scale of the CBL remains limited. Under future OA scenarios, seawater pH will decrease, and together with amplified fluctuation[23] shift the natural variability of pH to lower values. Reef hydrodynamics will also be affected by climate change[24], as well as sea level rise and increased storm activity[25]. Although high resolution projections of reef flow patterns are still limited[24], individual locations may continue to experience flow ranging from high to near-zero velocities[26]. Thus, a comprehensive assessment of the interactive effects of water flow and long-term OA on O_2 and pH gradients in the CBL of reef-building coral species is needed to better understand their responses to future climate change.

The general aim of this study was therefore to characterise the effects of water flow and OA on the CBL of three major reef-building coral species, *Acropora cytherea* (Dana, 1846), *Pocillopora verrucosa* (Ellis & Solander, 1786), and *Porites cylindrica* Dana, 1846, during light and dark conditions. Specifically, we preconditioned corals to either OA (pH 7.8) or control (pH 8.0) treatments for four months and tested how low flow (2 cm s^{-1}) and moderate flow (6 cm s^{-1}) affected I) thickness of O_2 and pH gradients in the coral CBL, II) O_2 and pH values at the coral surface, and III) O_2 flux across the CBL, inside a unidirectional-flow chamber. Responses to OA in H^+ CBL traits were assessed in *A. cytherea* only. Taken together, this will help disentangle the complex interacting effects of water flow and OA on coral physiology and better understand the role of the coral CBL in coral susceptibility to OA.

Materials and methods

Experimental design

Three scleractinian coral species, *A. cytherea*, *P. verrucosa*, and *P. cylindrica*, were preconditioned to ambient pH and OA conditions for four months, and the OA effects on the coral CBL were studied under low flow and moderate flow. Coral colonies (see Supplementary Table S1 for origin and CITES numbers) were maintained at the 'Ocean2100' long-term coral experimental facility (7000 L closed recirculating system of artificial seawater, Supplementary Table S2) at Justus Liebig University Giessen, Germany, for at least six months before the experiment. Conditions in the long-term culturing tanks (256 L) were 11:13 h light:dark photoperiod, with a light intensity of 230 µmol photons m^{-2} s^{-1}, temperature of 26.0 ± 0.5 °C (mean ± 1 SD), flow velocity of 5–10 cm s^{-1}, and daily feeding of a mix of frozen *Artemia* sp., *Mysis* sp., and copepods. For the experiment, three colonies per species were cut into six fragments (using a small angle grinder, Dremel Multitool 3000-15, The Netherlands). Fragments were attached to tiles with two-component glue (CoraFix SuperFast, Grotech, Germany) and transferred to the experimental setup. Corals were acclimated to the experimental setup for five weeks before the start of the experiment. Experimental pH treatments consisted of two levels, with the control treatment (ambient pH) mimicking present-day atmospheric pCO_2 concentration in some reefs (~ 500 µatm pCO_2)[27], and the OA treatment with values projected in the long term (2081–2100) for surface ocean pH in coral reefs[28] under SSP2-4.5 (0.20 pH units lower relative to 1961–1990)[29,30]. The experiment was conducted from 15 October 2019 to 26 March 2020. The coral response in O_2 and H^+ CBL traits was measured after 15–18 weeks (107–126 days) in the experimental pH treatments, taking almost three weeks to complete all microsensor measurements, during which whole-colony health was visually unchanged (i.e., no bleaching, discolourations, necrosis). Microsensor profiles were measured in light and darkness, and under bulk mean flow velocities of 2 cm s^{-1} (low flow) and 6 cm s^{-1} (moderate flow) (n = 9 profiles per species per profile condition per treatment), mimicking natural reef velocities (e.g.[2]). Details of the microsensor measurements are outlined below.

Experimental setup and treatment conditions

The preconditioning to the two experimental pH treatments was conducted in six 120 L tanks (three tanks per treatment, nine fragments per species per treatment). Each experimental tank housed one fragment per colony (total of three fragments per species in each tank) with 15 cm spacing between them in the direction of flow. In addition, experimental tanks contained other scleractinian and octocorals with the same number of individuals per tank. The experimental tanks were supplied with water from the 7000 L closed recirculating system (calcium: 400 ± 6 mg L^{-1}; phosphate: < 0.02 mg L^{-1}; nitrate: < 0.02 mg L^{-1}; nitrite: < 0.01 mg L^{-1}) with a water inflow rate of 20–40 L h^{-1} (corresponding to a 100% tank volume turnover every 3–6 h). In addition, the large water system received weekly water changes of ~ 10% of the water volume. Temperature was maintained at 26 °C through a feedback-controlled heater (300 W, 548, Schego, Germany). Water flow was generated with two circulating pumps (ES-28, Aqualight, Germany) and one wave generator (6208, Tunze, Germany), and consisted of a standing wave with an amplitude of 5 mm and a flow velocity of 6 cm s^{-1} (OTT MF pro, OTT Hydromet GmbH, Germany), which is a common velocity across reef zones throughout the year (e.g.[2]). Flow velocity was measured in all experimental tanks at the position of the coral fragments before starting the preconditioning phase and at the end of the experiment (i.e., after all microsensor measurements were completed). Salinity in the tanks was monitored daily using a conductivity sensor (TetraCon 925, WTW, Germany) and maintained at 35. Light was provided by two T5 bulbs (54 W, Aqua-Science, Germany) producing a light intensity of 176 ± 31 µmol photons m^{-2} s^{-1} in a 11:13 h light:dark photoperiod. Corals received 2.7 mg L^{-1} of frozen copepods every two days and dissolved nutrients via the connected water system.

Seawater pH was constantly monitored using a digital controller (Profilux 3, GHL, Germany) attached to pH electrodes in each tank (GHL, Germany), which were calibrated using NBS buffers. Values of pH_{NBS} were converted to the total scale (pH_T) and are expressed on this scale throughout the text. OA treatment conditions were generated individually via pH-controlled CO_2 dosing (bubbling) using solenoid valves, which controlled the release of CO_2 into each treatment tank, and pumping was done through one of the circulating pumps to aid CO_2 dissolution and dispersion in seawater. pH was gradually decreased in OA treatment tanks and was lowered 0.01–0.02 units every day over two weeks until target values were reached. Target OA conditions were maintained for a total of 16 weeks (113 days), including diel oscillation of pH mimicking naturally occurring variability[27,31]. Total alkalinity (TA) was measured in each experimental tank by open-cell potentiometric titration using a titrator (TitroLine 7000, SI Analytics, Germany) equipped with a glass pH-combination electrode (A 162 2M-DIN-ID, SI Analytics, Germany). Measurements were made following SOP3b[32] on 50 g samples with 0.1N HCl (Titrisol, Merk, Germany) in 35 g L^{-1} NaCl and corrected using certified reference materials (Batch 183, 194; A.G. Dickson laboratory, Scripps Institution of Oceanography, UCSD, USA)[33]. Measurements were performed every 2–4 days during the first two weeks of the experiment and then every 1–2 weeks. TA was calculated using a modified Gran approach. Alkalinity was also monitored daily and maintained with two automatic in-house constructed calcium reactors (pH 6.2–6.4, coral rubble) and dosing of $NaHCO_3$ in a common reservoir tank. The calcium reactor was feedback controlled by an alkalinity controller (Alkatronic, Focustronic, Hong Kong) based on three-hourly automatic titrations.

Seawater carbonate chemistry was calculated from days with TA measurements using pH and temperature values of a whole day and the value of TA and salinity measured on that day. TA and salinity values were assumed to be representative of the conditions of the whole day they were measured on. The calculation was performed using the program CO2SYS v25[34] and the R package *seacarb* v3.2.16[35], following Nisumaa et al.[36]. Briefly, values of TA, salinity, pH_{NBS}, and temperature were used to first calculate total dissolved inorganic carbon (DIC) in CO2SYS, with carbonic acid dissociation constants from Mehrbach et al.[37] refit by Dickson et al.[38], which was subsequently used in *seacarb* to calculate carbonate chemistry parameters, with carbonic acid dissociation constants from Lueker et al.[39]. Our approach is suitable for biological OA experiments with treatments that have differences larger than 100 µatm pCO_2[40] and allowed us to account for the diel oscillation of pH in the experimental tanks.

Microsensor measurements

Microsensor measurements were conducted in a flume (length 118 cm, width 18 cm, water depth 19 cm) with unidirectional recirculating flow, created by a circulating pump (ES-28, Aqualight, Germany). Flow straighteners were placed up- and downstream of the measurement section (upstream: PVC grid with length of 10.5 cm and 1.3 × 1.3 cm openings, attached to a layer of nylon net with 500 µm pore size; downstream: PVC grid with length of 2.5 cm and 1.3 × 1.3 cm openings). Coral fragments were measured 9.5 cm above the flume bottom, placed on a PVC grid and at an approximate distance of 30 cm from the upstream flow straightener, and were thus assumed to be within the mean bulk flow of the flume. Flow velocity in the flume was measured at the position of the coral fragment for the microsensor measurements using an electromagnetic water flow meter (OTT MF pro, OTT Hydromet GmbH, Germany), and bulk flow velocities of 2 and 6 cm s^{-1} were accomplished by defining different settings for the circulating pump. To estimate the characteristics of the flow entering the flume for the two flow velocities, the dimensionless Reynolds number (Re) was calculated as Re = uW/v from the flow velocity (u), the hydraulic diameter of the flume (W), and the kinematic viscosity (v) of seawater at 26 °C and salinity 35[41]. To characterise the flow around the coral fragments within the flume under the two flow velocities, Re was calculated (where W is the coral height[5]) based on the average height of coral fragments (3 cm) at the time of microsensor measurements. In the flume, the velocities of 2 and 6 cm s^{-1} corresponded to Re_{flume} of 4006 and 12,019, respectively, indicating that flume bulk flow was transitionally turbulent at the low velocity and fully turbulent at the moderate velocity[42]. Around the coral fragments, however, Re_{coral} was 650 and 1950 for the low and moderate flow velocities, respectively, indicating that the flow experienced by the coral fragments was laminar[42] for both flows. Light in the flume was provided by two T5 bulbs (80 W, Aqua-Science, Germany) producing a light intensity of 203 ± 9 µmol photons m^{-2} s^{-1} (n = 17), measured before and after the 19-day measurement session of microsensor profiles. Water temperature and pH in the flume were monitored and maintained in the same way as in the experimental tanks (see above). Seawater carbonate chemistry in the flume was calculated using TA values measured during the period of microsensor measurements and daily recording of pH, temperature, and salinity.

O_2 and pH profiles were measured separately using a Unisense microprofiling system (Unisense, Denmark). Profiles of dissolved O_2 concentration were measured using Clark-type O_2 microelectrodes (tip diameter 20–30 µm, spatial resolution 25 µm, 90% response time < 4 s; OX-25, Unisense, Denmark) calibrated daily with air-saturated seawater and anoxic seawater prepared using yeast, following manufacturer's instructions. pH profiles were measured using a pH microelectrode (tip diameter 40–60 µm, spatial resolution 75 µm, 90% response time < 10 s; pH-50, Unisense, Denmark) and an external reference electrode (Radiometer Analytical), calibrated daily with NBS buffers. Values of pH_{NBS} were converted to pH_T using equations from Millero[43] and Takahashi[44].

Microelectrodes were connected to a microsensor multimeter (Unisense, Denmark), whose signals were read on a PC using a two-channel A/D converter (ADC-216, Unisense, Denmark). Profiles were performed using a motorised microprofiling system (Unisense, Denmark), by carefully placing the tip of the sensor on the coral surface and moving it up in a series of steps within the gradient (expected range: 200–300 µm) and in bulk seawater, following a protocol developed during prior test runs to ensure that the profile structure was captured for the three species and keep measurement time similar across species. To better resolve the profiles, we used step sizes that were below the spatial resolution at times and thus, integrate values from below steps. Profiles of O_2 were done in steps of 10–20 µm. At the height of 100 µm above the coral surface, if the electrochemical signal

was still close to the value measured at the coral surface, the step size was increased to 30–40 µm until the signal was within 70–80% of the signal corresponding to bulk seawater level, after which the profile was continued with steps of 10–20 µm until the bulk seawater level was reached. In fragments with an estimated larger CBL (thickness > 300 µm), the step size at the height of 100 µm was increased to 40–60 µm until the signal was within 70–80% of the level of bulk seawater. Five coral fragments (four fragments of *A. cytherea* and one of *P. cylindrica*) presented a particularly small O_2 CBL (thickness < 70 µm) and thus, the first step of their O_2 profile was done within 5 µm of the coral surface. Profiles of pH were performed in steps of 30–60 µm, except in fragments with a small H^+ CBL (thickness < 100 µm), for which profiles were done in steps of 20–40 µm. Upon reaching the bulk seawater level, the profiles of O_2 and pH continued in steps of 50 µm for the first three measurements in bulk seawater, after which profiles continued in steps of 100–200 µm up to 500 µm above the coral surface or up to 1,000 µm above the coral surface for fragments with a larger CBL (thickness > 300 µm). Sensor positioning and data acquisition were performed using the software SensorTrace Profiling (v3.1, Unisense, Denmark, https://unisense.com). At each step, values were recorded for 30–60 s with a waiting period of 3 s after moving the sensor. A total of 356 profiles were recorded. O_2 profiles were measured in all species under control and OA treatment (n = 72 profiles per species). pH profiles were measured in *A. cytherea* from the control and OA treatment (n = 68), but in *P. verrucosa* and *P. cylindrica* only from the OA treatment (n = 36 per species) due to logistical constraints. Measurements were performed on the top upstream side of coral fragments (Supplementary Fig. S1) after they had been acclimated to flume light and flow conditions (light, 10 min; darkness, 5 min; flow, 10 min), and it was ensured that steady-state conditions (i.e., stable electrochemical signal of O_2 or pH) had been reached before starting each profile. The chosen acclimation times did not yield visibly different results to longer acclimation (dark, 25 min; flow, 45 min) in prior test runs and fulfilled the need to minimise differences in OA-exposure by allowing the measurement of the large number of profiles within a relatively short period of time. Profiles were measured sequentially under both flow velocities in light and darkness, on the same spot for each coral fragment. The measuring spot was constantly monitored during all profiles using a stereo microscope (Stemi 508, Carl Zeiss AG, Germany) to avoid artefacts due to tissue movement or polyp interaction.

Calculation of boundary layer traits

O_2 concentration profiles were used to calculate total thickness of the O_2 CBL, diffusive flux through the CBL, and O_2 concentration change at the coral surface relative to bulk seawater (surface ΔO_2). Thickness of pH gradients across the CBL and pH change at the coral surface relative to bulk seawater (surface ΔpH) were calculated using pH profiles, with pH converted to H^+ concentration. The CBL thickness was calculated by extrapolating the linear concentration gradient in the CBL to the bulk seawater concentration of the free-flow region[7], and defined the distance between the coral surface and the outer limit of the CBL. O_2 flux was calculated using Fick's first law of diffusion[7,45] with O_2 diffusion coefficient of 2.29×10^{-5} cm^2 s^{-1} at 26.0 °C and a salinity of 35[41]. Ciliary vortices at the coral surface may modify the O_2 transport in the lower part of the CBL, creating S-shaped profiles with shape variability dependent on their position within the vortex[13,46], which were present in our data. In addition, some profiles in our study presented multiple linear concentration gradients within the CBL, giving them a more complex structure than S-shaped profiles. Within these complex profiles, O_2 concentration monotonically approached bulk seawater O_2 values, and this type of profiles is characterised in detail in Martins et al.[47]. Complex profiles constituted 7% of all measured profiles and were present in all species (Supplementary Table S3). CBL thickness and O_2 flux of these profiles were calculated using the upper linear gradient of the profiles (i.e., the linear gradient preceding the reaching of bulk seawater concentration), following Pacherres et al.[46]. Additional details on the rationale for this approach are provided in Supplementary Text. Thickness values were pooled over light conditions and profile shapes, and effects associated with complex profiles are visualised in the supplementary material (Supplementary Fig. S2). Surface ΔO_2 and ΔpH were calculated from the discrete values at the coral surface and bulk seawater. Variation between light and darkness in surface O_2 concentration and pH was estimated by calculating the difference between light and dark of surface ΔO_2 and ΔpH in absolute values. The flow ratio for O_2 CBL traits was calculated as the ratio of values under low flow to moderate flow, pooled over treatments and light conditions.

Statistical analysis

All statistical analyses were performed in R v.4.1.0[48] using RStudio v1.4.1106[49]. All plots were produced using the R package *ggplot2*[50]. Changes in the CBL traits of the three studied coral species were investigated using linear mixed-effects models (LMMs). To test differences between species in O_2 CBL traits we used LMMs with species (3 levels: *A. cytherea*, *P. verrucosa*, and *P. cylindrica*) as a fixed factor. Differences between species in H^+ CBL traits were assessed considering coral fragments from the OA treatment because pH profiles were measured only under OA for some species (see above). The effects and interaction of flow and OA on O_2 CBL traits (within each species) and on H^+ CBL traits of *A. cytherea* were examined using LMMs constructed for each species with flow (2 levels: low and moderate) and treatment (2 levels: control and OA) as fixed factors in a fully crossed design. The effects of flow on H^+ CBL traits of *P. verrucosa* and *P. cylindrica* were investigated using LMMs constructed for each species with the same structure as above, but without the factor of treatment. All models were constructed with coral fragment identity (ID), coral colony, day of measurement, and tank as random factors, except when the factor had near-zero variance, and treatment was additionally incorporated into global models as a random factor following the same guideline. Models were selected considering AIC, BIC and R^2 values. LMMs were performed using the R package *lme4*[51]. Model validation was performed by graphically assessing homogeneity and normality assumptions. To meet model assumptions, we applied a log-transformation to O_2 CBL thickness (global model with all species included) and a square-root transformation to surface ΔpH values of *P. cylindrica* in darkness. The numerical output of LMMs was extracted using the R package *sjPlot*[52] and is provided with

model formulas in Supplementary Tables S4, S5. We then computed type-II ANOVA tables of the fixed effects of LMMs using Kenward-Roger approximation for the degrees of freedom in the R package *car*[53]. Type II sums of squares was selected to compute ANOVAs, following recommended protocol for assessing main effects individually in the absence of interactions[54,55]. Post hoc analyses were performed using estimated marginal means with Bonferroni adjustment of p-values, using the R package *emmeans*[56]. In addition, the effect size of flow effects was evaluated for O_2 CBL thickness, H^+ CBL thickness, surface ΔO_2, and surface ΔpH using the R package *dabestr*[57]. The relationship between O_2 CBL flux and surface ΔpH was investigated for each species in the OA treatment, pooled over flow conditions, using Pearson correlations.

Differences in seawater chemistry between experimental pH treatments were tested using daily mean values (n = 72) from days with TA measurements, and the same approach as above (LMM-ANOVA) with treatment as a fixed factor (2 levels: control and OA) and tank and date as random factors.

Results

Seawater conditions

During the four months of preconditioning, pH was significantly higher in the control treatment at 7.97 ± 0.13 (mean ± 1 SD; daily range: 7.77–8.19) than in the OA treatment at 7.77 ± 0.14 (range: 7.58–7.99) (LMM-ANOVA, $F = 231$, $p < 0.001$) and was similar across replicate tanks (Supplementary Table S6). Both treatments showed a diel oscillation of 0.4 pH units (Table 1). pCO_2 in the control at 497 ± 190 µatm (range: 249–810 µatm) was significantly different from values in the OA treatment at 844 ± 333 µatm (range: 435–1,329 µatm) (LMM-ANOVA, $F = 217$, $p < 0.001$), as were other seawater carbonate parameters (Supplementary Table S7). Total alkalinity and temperature were similar between treatments (LMM-ANOVA, $F < 0.1/F = 3.6$, $p > 0.05$; Table 1). During the microsensor measurements, pH in the flume was on average 8.02 ± 0.02 and 7.77 ± 0.03 for control and OA treatment, respectively, and seawater parameters resembled the experimental treatments (Supplementary Table S8). In addition, seawater O_2 was similar during measurements (Supplementary Table S8), with an average of 240 ± 8 µM across treatments and a variation of ± 2 µM within an individual day, indicating that the sequential measurement of profiles did not modify bulk seawater O_2 concentration.

Effects of water flow and ocean acidification on boundary layer thickness

The thickness of the CBL in light and darkness showed the same patterns across species and in response to flow velocities and treatments (Table 2). Thickness of the O_2 CBL differed between species (pooled over light, flow, and treatment; LMM-ANOVA, $F = 4.5$, $p < 0.05$), with an overall thinner CBL in *A. cytherea* compared to the rather similar thick CBL in *P. verrucosa* and *P. cylindrica* (Table 2, Supplementary Table S9). The O_2 CBL was generally thicker under low flow compared to moderate flow but the effect size differed between species (Supplementary Fig. S3A). Thickness increased, respectively, by 61 and 55% in *A. cytherea* and *P. verrucosa* (LMM-ANOVA, $F = 53.9/F = 62.2$, $p < 0.001$), whereas in *P. cylindrica* it was 159% thicker (LMM-ANOVA, $F = 65.3$, $p < 0.001$) (Supplementary Table S10). Alternatively, *A. cytherea* and *P. verrucosa* presented a low-to-moderate flow ratio of 1.61 and 1.55, respectively, for O_2 CBL thickness, while the O_2 CBL of *P. cylindrica* under low flow was 2.58 times as thick as under moderate flow.

Parameter	Control	Ocean Acidification
Salinity	34.6 ± 0.4 (36)	34.6 ± 0.4 (36)
Temperature (°C)	25.8 ± 0.3 (1,406)	26.0 ± 0.2 (1,224)
pH_T	7.97 ± 0.13 (1,406)	7.77 ± 0.14 (1,224)
Daily Minimum pH_T	7.77 ± 0.12 (12)	7.58 ± 0.12 (12)
Daily Maximum pH_T	8.19 ± 0.04 (12)	7.99 ± 0.06 (12)
TA (µmol kg^{-1})	2,155 ± 53 (43)	2,156 ± 58 (39)
pCO_2 (µatm)	497 ± 190 (1,406)	844 ± 333 (1,224)
Daily Minimum pCO_2 (µatm)	249 ± 32 (12)	435 ± 90 (12)
Daily Maximum pCO_2 (µatm)	810 ± 215 (12)	1,329 ± 370 (12)
fCO_2 (µatm)	496 ± 189 (1,406)	841 ± 332 (1,224)
DIC (µmol kg^{-1})	1,911 ± 80 (1,406)	2,008 ± 79 (1,224)
CO_2 (µmol kg^{-1})	14 ± 5 (1,406)	23 ± 9 (1,224)
HCO_3^-(µmol kg^{-1})	1,717 ± 112 (1,406)	1,858 ± 98 (1,224)
CO_3^{2-}(µmol kg^{-1})	180 ± 44 (1,406)	127 ± 35 (1,224)
Ω_{ar}	2.88 ± 0.71 (1,406)	2.02 ± 0.56 (1,224)
Ω_{ca}	4.36 ± 1.07 (1,406)	3.06 ± 0.84 (1,224)

Table 1. Seawater chemistry during four-month preconditioning to a control (ambient pH) and ocean acidification treatment. Partial pressure of CO_2 (pCO_2), fugacity of CO_2 (fCO_2), dissolved inorganic carbon (DIC), CO_2, HCO_3^-, CO_3^{2-}, aragonite saturation (Ω_{ar}), and calcite saturation (Ω_{ca}) were calculated using pH and temperature values of a whole day and the value of total alkalinity (TA) and salinity measured on that day. Values are expressed as mean ± 1 SD with sample size (n) of measured parameters (salinity, temperature, pH, TA) and calculated parameters (pCO_2, fCO_2, DIC, CO_2, HCO_3^-, CO_3^{2-}, Ω_{ar}, Ω_{ca}). pH_T, pH on the total scale.

Species	Flow	Treatment	Light	O_2 CBL Thickness (µm)	H^+ CBL Thickness (µm)	O_2 CBL Thickness (µm)	H^+ CBL Thickness (µm)	Surface ΔO_2 (µM)	Surface ΔpH	O_2 Flux (µmol cm^{-2} h^{-1})
Acropora cytherea	Low	Control	Light	124 ± 75 (72)	94 ± 53 (32)	104 ± 29 (9)	119 ± 38 (8)	73.8 ± 25.2 (9)	0.05 ± 0.02 (8)	0.53 ± 0.16 (9)
	Low	Control	Dark			101 ± 33 (9)	102 ± 80 (8)	−45.7 ± 16.5 (9)	−0.02 ± 0.01 (8)	−0.38 ± 0.13 (9)
	Moderate	Control	Light			79 ± 56 (9)	88 ± 46 (8)	67.2 ± 34.6 (9)	0.03 ± 0.02 (8)	0.67 ± 0.25 (9)
	Moderate	Control	Dark			81 ± 46 (9)	65 ± 28 (8)	−45.4 ± 25.2 (9)	−0.02 ± 0.01 (8)	−0.53 ± 0.23 (9)
	Low	OA	Light		107 ± 54 (36)	202 ± 101 (9)	137 ± 45 (9)	73.4 ± 25.9 (9)	0.05 ± 0.03 (9)	0.32 ± 0.16 (9)
	Low	OA	Dark			203 ± 92 (9)	120 ± 54 (9)	−46.1 ± 14.3 (9)	−0.03 ± 0.01 (9)	−0.23 ± 0.12 (9)
	Moderate	OA	Light			108 ± 45 (9)	70 ± 25 (9)	57.0 ± 29.4 (9)	0.02 ± 0.01 (9)	0.41 ± 0.28 (9)
	Moderate	OA	Dark			111 ± 44 (9)	100 ± 68 (9)	−40.5 ± 17.4 (9)	−0.01 ± 0.00 (9)	−0.35 ± 0.13 (9)
Pocillopora verrucosa	Low	Control	Light	162 ± 75 (72)	n/a	201 ± 93 (9)	n/a	94.7 ± 42.2 (9)	n/a	0.68 ± 0.44 (9)
	Low	Control	Dark			209 ± 75 (9)	n/a	−87.5 ± 18.5 (9)	n/a	−0.45 ± 0.20 (9)
	Moderate	Control	Light			118 ± 60 (9)	n/a	58.7 ± 43.4 (9)	n/a	0.48 ± 0.20 (9)
	Moderate	Control	Dark			108 ± 37 (9)	n/a	−72.5 ± 23.8 (9)	n/a	−0.63 ± 0.21 (9)
	Low	OA	Light		106 ± 72 (36)	211 ± 82 (9)	148 ± 99 (9)	101.9 ± 40.6 (9)	0.02 ± 0.04 (9)	0.51 ± 0.29 (9)
	Low	OA	Dark			166 ± 29 (9)	144 ± 55 (9)	−86.2 ± 25.1 (9)	−0.09 ± 0.05 (9)	−0.45 ± 0.13 (9)
	Moderate	OA	Light			155 ± 64 (9)	57 ± 37 (9)	52.6 ± 22.3 (9)	0.01 ± 0.01 (9)	0.37 ± 0.21 (9)
	Moderate	OA	Dark			129 ± 74 (9)	76 ± 31 (9)	−67.1 ± 16.4 (9)	−0.05 ± 0.04 (9)	−0.51 ± 0.15 (9)
Porites cylindrica	Low	Control	Light	192 ± 147 (72)	n/a	282 ± 196 (9)	n/a	96.6 ± 28.5 (9)	n/a	0.39 ± 0.23 (9)
	Low	Control	Dark			287 ± 170 (9)	n/a	−57.2 ± 15.0 (9)	n/a	−0.20 ± 0.16 (9)
	Moderate	Control	Light			102 ± 34 (9)	n/a	78.8 ± 29.8 (9)	n/a	0.65 ± 0.28 (9)
	Moderate	Control	Dark			106 ± 39 (9)	n/a	−44.3 ± 15.8 (9)	n/a	−0.37 ± 0.15 (9)
	Low	OA	Light		103 ± 51 (36)	252 ± 140 (9)	119 ± 44 (9)	100.1 ± 53.5 (9)	0.04 ± 0.02 (9)	0.43 ± 0.45 (9)
	Low	OA	Dark			287 ± 166 (9)	128 ± 62 (9)	−44.0 ± 12.7 (9)	−0.05 ± 0.03 (9)	−0.17 ± 0.13 (9)
	Moderate	OA	Light			117 ± 81 (9)	81 ± 50 (9)	83.1 ± 37.3 (9)	0.02 ± 0.01 (9)	0.78 ± 0.60 (9)
	Moderate	OA	Dark			104 ± 58 (9)	86 ± 36 (9)	−37.9 ± 11.3 (9)	−0.02 ± 0.01 (9)	−0.34 ± 0.08 (9)

Table 2. Quantitative traits of the concentration boundary layer (CBL) measured in *Acropora cytherea*, *Pocillopora verrucosa*, and *Porites cylindrica*, in light or darkness combined with low flow (2 cm s^{-1}) or moderate flow (6 cm s^{-1}), under control or ocean acidification (OA) treatments. Values are expressed as mean ± 1 SD, with measurement replication (n).

The effect of OA differed between species (Fig. 1A). In *A. cytherea*, the O_2 CBL thickness increased under OA (LMM-ANOVA, flow–OA interaction, $F = 20.3$, $p < 0.001$) and doubled in the OA treatment compared to the control under low flow, but under moderate flow it remained stable between treatments (Table 2, Supplementary Table S9). In *P. verrucosa* and *P. cylindrica*, O_2 CBL thickness was similar between treatments (LMM-ANOVA, $F < 0.1$, $p > 0.05$; Supplementary Table S11). CBL thickness was generally higher in complex profiles (Supplementary Fig. S2), but OA effects were not dependent on the presence of this profile type (Supplementary Table S12).

The H^+ CBL was generally thinner than the O_2 CBL and we did not see differences between the three species (comparing OA treatment pooled over flow and light; LMM-ANOVA, $F < 0.1$, $p > 0.05$; Table 2). Again, the H^+ CBL was thicker under low flow than moderate flow (Fig. 1B) in all species (LMM-ANOVA, *A. cytherea*: $F = 14.2$, $p < 0.001$, *P. verrucosa*: $F = 36.0$, $p < 0.001$, *P. cylindrica*: $F = 21.2$, $p < 0.001$; Supplementary Table S10). In contrast to OA effects on the O_2 CBL thickness, the H^+ CBL of *A. cytherea* had similar thickness in the control and OA treatments (pooled over flow and light; LMM-ANOVA, $F = 0.2$, $p > 0.05$; Fig. 1B, Table 2).

O_2 and pH changes at the coral surface

O_2 concentration at the coral surface in light was super-saturated with respect to bulk seawater with similar magnitude across species (LMM-ANOVA, $F = 0.9$, $p > 0.05$), which was on average 78.2 ± 37.6 µM above seawater concentration (pooled over flow and treatment). In darkness, however, surface ΔO_2 differed between species (LMM-ANOVA, $F = 10.6$, $p < 0.05$), with larger under-saturation in *P. verrucosa* than the similar reduction in surface O_2 in *A. cytherea* and *P. cylindrica* (Supplementary Tables S9, S13). *Pocillopora verrucosa* thus presented a larger variation in surface O_2 concentration between light and darkness (pooled over flow and treatment, 155.31 ± 52.83 µM) than *A. cytherea* (112.26 ± 44.06 µM) and *P. cylindrica* (135.51 ± 45.17 µM). Response to flow and OA in surface ΔO_2 showed similar patterns in light and dark conditions (Fig. 2A, Table 2). Although average differences between flows were relatively small (Supplementary Table S10), ΔO_2 was larger under low flow (light/dark, LMM-ANOVA, *A. cytherea*: $F = 9.9$, $p < 0.01$; *P. verrucosa*: $F = 38.6/F = 17.8$, $p < 0.001/0.01$; *P. cylindrica*: $F = 11.2/F = 4.9$, $p < 0.01/0.05$), except in *A. cytherea* in dark (LMM-ANOVA, $F = 1.8$, $p > 0.05$), with notable uncertainty in effect sizes for *A. cytherea* and *P. verrucosa* in light (Supplementary Fig. S3C). Overall, these differences resulted in a higher ratio of low to moderate flow in *P. verrucosa* (1.48) than *A. cytherea* (1.14) and *P. cylindrica* (1.22).

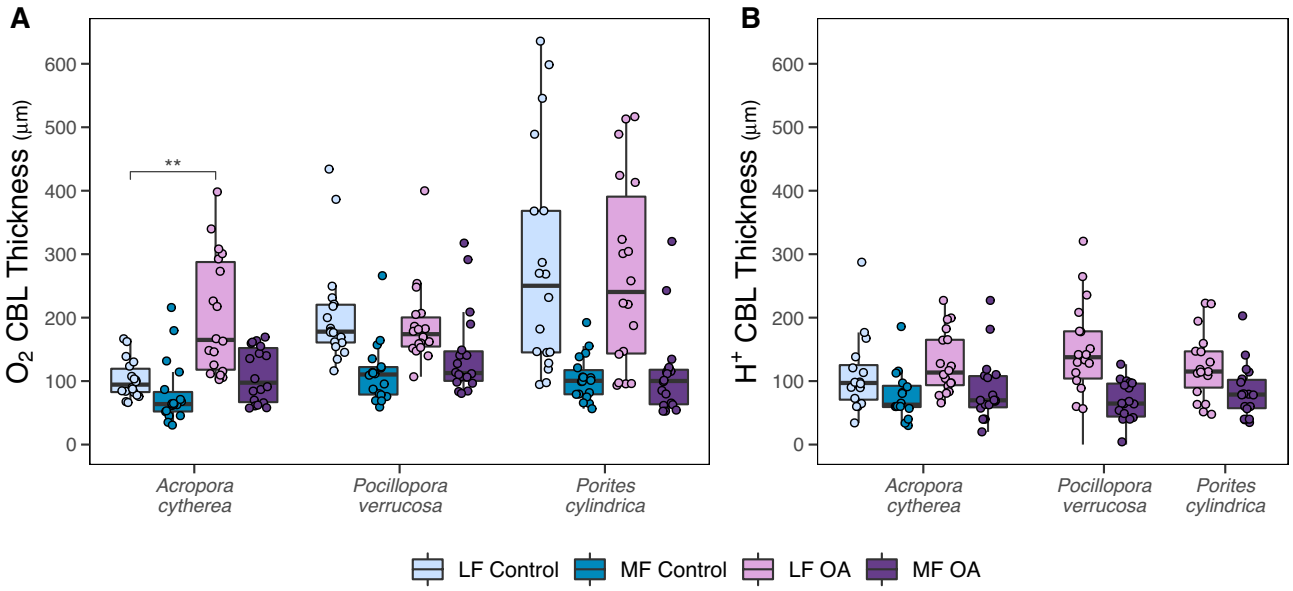

Figure 1. Effects of water flow and ocean acidification (OA) on the thickness of the concentration boundary layer (CBL) of *Acropora cytherea*, *Pocillopora verrucosa*, and *Porites cylindrica*. (**A**) O_2 and (**B**) H^+ CBL thickness after four months in a control and OA treatment and measured in light or darkness combined with low flow (LF, 2 cm s^{-1}) and moderate flow (MF, 6 cm s^{-1}). Values are presented pooled over light and dark conditions. Boxes represent the first and third quartiles with lines as medians and whiskers as the minimum and maximum values or up to the 1.5 * interquartile range (IQR), whichever is reached first. Stars indicate significant differences between the control and OA treatment within each flow condition ($p < 0.01$**, from linear mixed-effects models with ANOVA).

In contrast, OA did not significantly modulate surface ΔO_2 across species (light/dark, LMM-ANOVA, *A. cytherea*: $F = 0.9/F = 0.3$, $p > 0.05$; *P. verrucosa*: $F < 0.1/F = 0.1$, $p > 0.05$; *P. cylindrica*: $F < 0.1/F = 2.7$, $p > 0.05$; Supplementary Table S11).

Generally, pH was elevated at the coral surface in light conditions and reduced in darkness compared to bulk seawater (Fig. 2B). However, the magnitude differed between species in light and dark conditions (comparing OA treatment pooled over flow; LMM-ANOVA, $F = 4.5/F = 88.5$, $p < 0.05/0.001$). *Pocillopora verrucosa* showed the lowest pH elevation in light but the strongest decrease in darkness compared to similar pH elevation in light and decrease in darkness in *A. cytherea* and *P. cylindrica* (Supplementary Table S11). Flow significantly affected the pH change in both *A. cytherea* and *P. cylindrica* with larger pH elevation in the light (LMM-ANOVA, $F = 35.6/F = 24.4$, $p < 0.001/0.01$) and larger decrease in darkness (LMM-ANOVA, $F = 11.9/F = 9.9$, $p < 0.01/0.05$) under low flow compared to moderate flow (Supplementary Table S10). In *P. verrucosa* the effect was less clear, with similar values between flows under light conditions (LMM-ANOVA, $F = 1.1$, $p > 0.05$) and a weak pH reduction in darkness under low flow compared to moderate flow (LMM-ANOVA, $F = 9.9$, $p < 0.05$; Supplementary Fig. S3D) (Supplementary Table S10). Overall, surface pH of *P. verrucosa* under OA varied between light and darkness by 0.11 ± 0.05 and 0.06 ± 0.05 pH units in low and moderate flow, respectively, which was similar to the light–dark variation observed in *A. cytherea* (low flow: 0.08 ± 0.04; moderate flow: 0.03 ± 0.01 pH units) and *P. cylindrica* (low flow: 0.09 ± 0.05; moderate flow: 0.04 ± 0.02 pH units). As observed for surface ΔO_2, the relative change in surface pH of *A. cytherea* was also similar between the control and OA treatments (light/dark, LMM-ANOVA, $F = 0.3/F < 0.1$, $p > 0.05$; Supplementary Table S11) and presented a light–dark variation of 0.06 ± 0.03 pH units in both treatments (pooled over flow velocities).

O_2 flux across the coral boundary layer

O_2 flux rates across the CBL were overall similar among species in light (LMM-ANOVA, $F < 0.1$, $p > 0.05$) but not in dark (LMM-ANOVA, $F = 13.9$, $p < 0.001$) (pooled over flow and treatment), where mean flux values were higher in *P. verrucosa* compared to the similar flux in *A. cytherea* and *P. cylindrica* (Supplementary Tables S9, S13). Like CBL thickness and surface ΔO_2, responses to flow and OA in O_2 flux generally showed similar patterns under light and dark conditions. O_2 flux was generally lower under low flow compared to moderate flow (light/dark, LMM-ANOVA, *A. cytherea*: $F = 6.6/F = 14.6$, $p < 0.05/0.01$; *P. verrucosa*: $F = 16.7$, $p < 0.01$; *P. cylindrica*: $F = 9.3/F = 13.1$, $p < 0.01$), except in *P. verrucosa* in light (LMM-ANOVA, $F = 3.4$, $p > 0.05$) (Fig. 2C). Differences between flows were largest in *P. cylindrica* (Supplementary Table S10), which presented the lowest low-to-moderate flow ratio (0.56) compared to *A. cytherea* (0.75) and *P. verrucosa* (1.06), showcasing thus the same pattern as O_2 CBL thickness but with the opposite direction. The response to OA in O_2 flux also displayed the same species-specific patterns as O_2 CBL thickness. While in *A. cytherea* O_2 flux was reduced in the OA treatment compared to the control (light/dark, LMM-ANOVA, $F = 7.3/F = 6.1$, $p < 0.05$), it remained similar between treatments in *P. verrucosa* and *P. cylindrica* (light/dark, LMM-ANOVA, *P. verrucosa*: $F = 1.7/F = 0.6$, $p > 0.05$; *P. cylindrica*: $F = 0.1/F$

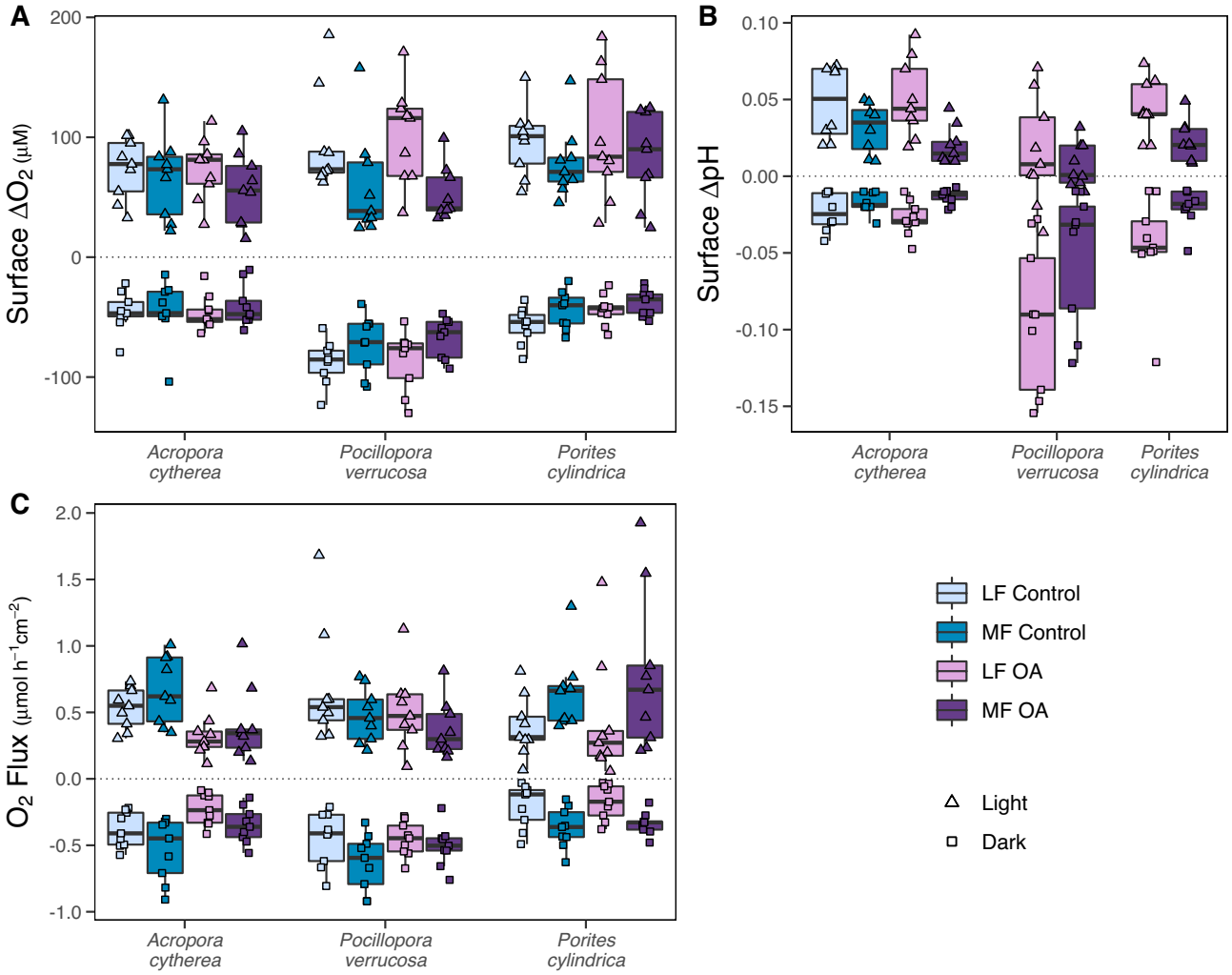

Figure 2. Effects of water flow and ocean acidification (OA) on traits of the concentration boundary layer (CBL) of *Acropora cytherea*, *Pocillopora verrucosa*, and *Porites cylindrica*. (**A**) O_2 concentration change at the coral surface relative to bulk seawater (surface ΔO_2), (**B**) pH change at the coral surface relative to bulk seawater (surface ΔpH), and (**C**) O_2 flux, after four months in a control and OA treatment and measured in light or darkness combined with low flow (LF, 2 cm s^{-1}) and moderate flow (MF, 6 cm s^{-1}). Boxes represent the first and third quartiles with lines as medians and whiskers as the minimum and maximum values or up to the 1.5 * interquartile range (IQR), whichever is reached first. No significant interactive effects of flow and OA were observed.

= 0.5, $p > 0.05$) (Supplementary Table S11). Similarly, to the assessments in O_2 CBL thickness, the flux of complex profiles fell within the lower range of the observed fluxes but did not drive OA responses (Supplementary Fig. S4).

Coral O_2 flux in light was not correlated with change in surface pH in any species, while in darkness it was negatively correlated in *A. cytherea*, but not in *P. verrucosa* or *P. cylindrica* (Supplementary Fig. S5).

Discussion

Our study shows that the coral CBL is strongly influenced by changes in water flow, while OA may have weak or null effects (Fig. 3), even after prolonged exposure. In this study, CBL traits were distinct between species but low flow thickened boundary layers across species and enhanced the relative change of surface O_2 and pH, compared to moderate flow. In contrast, CBL traits remained largely stable under OA, except the absolute values of surface pH, which were considerably lower under OA. Finally, O_2 flux across the CBL was strongly influenced by changes in its thickness.

CBL traits differed between the three species investigated in this study. Thickness of the O_2 CBL, in particular, was the most species-differentiating trait and was thinnest in *A. cytherea*. Although variation in CBL traits has been documented previously, branching species are underrepresented in microsensor studies and comparative studies have generally focused on the differences between large- and small-polyped species[12]. Our dataset builds upon this knowledge and shows that CBL variation exists even among small-polyped species. In addition, a

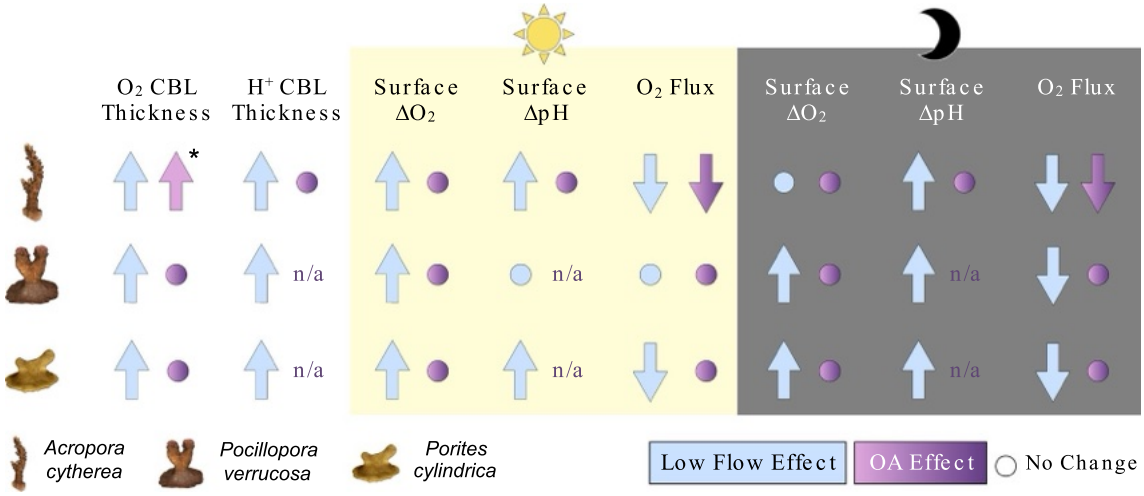

Figure 3. Summary diagram of the effects of water flow and ocean acidification (OA) on traits of the concentration boundary layer (CBL) of *Acropora cytherea*, *Pocillopora verrucosa*, and *Porites cylindrica*. Effects on CBL thickness are presented pooled over light conditions, while change in surface O_2 concentration (surface ΔO_2) and pH (surface ΔpH) relative to bulk seawater, and O_2 flux are presented in light and darkness. Asterisk indicates OA effects present exclusively under low flow. n/a, not available.

previous report of similar O_2 CBL thickness between *Stylophora pistillata* and *Porites lobata*[10] supports our finding of similar CBL thickness between pocilloporids and poritids.

While our data is in line with the notion that morphologically complex corals have thinner CBLs[58] due to the potential of complex geometries to isolate ciliary flows from bulk water flow[13], other factors could also underlie this variation. CBL thickness may decrease when cilia activity is arrested[13], suggesting that the thinner CBL of *A. cytherea* in this study could also be due to a lower abundance and/or beating frequency of cilia. Acroporids are reported to have weak feeding and cleaning ciliary currents[59,60], which could indicate that ciliary surface ventilation is also weaker in *Acropora* spp. than other taxa. Differences in cilia traits and activity among reef-building corals, however, are poorly characterised to date.

The effects of water flow on CBL traits in this study were consistent across species and molecules. Boundary layers of both O_2 and pH gradients were thicker under low flow compared with moderate flow in all tested species, which is in agreement with the known effects of reduced flow on the CBL (e.g.[9,12]). However, the magnitude of this increase differed between species in our study, which indicates that the coral response to flow in CBL thickness is influenced by additional species-specific factors. Here, the largest flow ratio was observed in *P. cylindrica*. Polyp size is known to be similar across the three species tested[61], and *P. verrucosa* and *P. cylindrica* have similar polyp densities[62,63], with no differences in cilia activity reported to date between these two species. Therefore, the different flow response of *P. cylindrica* could be associated with other small-scale differences in the topography of the coral tissue surface and with different polyp behaviour. For instance, *Porites* spp. have been described to have greater powers of polyp expansion than most small-polyped species[64,65] and water flow can affect polyp expansion[66,67]. During our measurements, polyp expansion appeared to be more prevalent and to occur to a greater extent in *P. cylindrica* under low flow than in the other species (quantitative characterisation not available). Furthermore, mathematical models predict thicker CBLs and lower flux for expanded polyps[68], which is in line with the patterns observed in this study. Nonetheless, future studies using computational fluid dynamics may be able to further disentangle the relationship between flow velocity and CBL thickness across small-polyped coral species.

In contrast to flow effects, we found that CBL thickness remained stable under OA, except in *A. cytherea*, which experienced a thickening of the O_2 CBL under OA with low flow. Changes in coral microtopography and surface cilia activity could potentially underlie the thickening of the O_2 CBL of *A. cytherea* under OA[12,13]. OA has been shown to alter the internal structure of coral skeletons[20,69], reduce skeletal density[70] and septal rugosity[71], and alter corallite size[72]. However, it remains untested whether long-term OA can alter the roughness of the coral tissue surface enough to affect CBL thickness. OA has also been shown to reduce cilia beat frequency[18] and gene expression involved in cilia formation in bivalves[73] as well as decrease formation and stability of flagella in phytoplankton[19]. Thus, changes in surface cilia activity of *A. cytherea* may have occurred under OA, thereby resulting in the thickening of its O_2 boundary layer. Given that cilia effects on the coral boundary layer are more visible under low flow than under moderate flow[46], this hypothesis would also explain the presence of an OA effect exclusively under low flow. The presence of the five complex O_2 concentration profiles in *A. cytherea* under OA with low flow could further point to cilia changes. However, although *P. cylindrica* also presented complex profiles under low flow, these were equally frequent in both treatments. Therefore, the significance of the occurrence of these profiles here remains unclear.

The only other investigation of OA effects on coral CBL thickness to date has been on *Favites* sp. and also found interactive flow and OA effects but with the opposite pattern (i.e., thicker O_2 CBL under OA with moderate

flow than low flow)[16]. Responses to OA at the scale of the CBL may thus be species-specific, with susceptibility potentially associated with differences in surface cilia, and differentially modulated by water flow.

While our results indicate that low flow could modulate the CBL to better isolate the coral colony from acidified bulk seawater, low flow conditions could become less frequent in future reefs. Most surface ocean currents are projected to accelerate with climate change[74] and sea level rise is predicted to overall increase wave energy in coral reefs[75]. While this effect is likely exacerbated in degraded reefs[76], the effects of sea level rise also differ among reef types[3] and vary spatially within single reefs[77]. For instance, reefs with an estimated general increase in wave energy will also present zones where flow velocities decrease[26]. In addition, several major surface ocean currents are also predicted to weaken, including tropical currents that affect coral reefs such as the Indonesian Throughflow[78,79]. Altogether, future changes to reef hydrodynamics make the inclusion of low-flow refuge areas all the more important in coral reef conservation strategies that address OA challenges on coral species.

Although the H^+ CBL partially isolates the coral from bulk seawater pH and could determine coral susceptibility to OA[80], it has never been characterised in scleractinian corals under OA. Thus, our study constitutes the first report of the thickness of the coral H^+ CBL under OA. We found that the H^+ CBL was similarly thin across species. Given that the three species investigated here are known to differ in their susceptibility to OA, with acroporids generally regarded as more OA-susceptible than pocilloporids[81] and poritids[82], our findings suggest that susceptibility may not be associated with the thickness of the H^+ CBL.

In addition, we found that the thickness of the H^+ CBL of *A. cytherea* was not modulated by the OA treatment, suggesting that the markedly thin H^+ CBL could be intrinsic to the tested species. For instance, *Acropora yongei* has been shown to have no H^+ CBL under ambient pH[17] (possibly too thin to measure with microsensors). However, other *Acropora* spp. featured a H^+ CBL thicker than 300 µm[9,58]. The high variability reported for pH boundary layers could be due to spatial heterogeneity of the coral surface, but also due to experimental differences.

In this study, the H^+ CBL was generally thinner than O_2 gradients under OA, which contrasts with previous reports of O_2 and H^+ CBL with similar thickness under ambient reef conditions[9,58]. The observed dissociation of O_2 and pH gradients in our study could be due to spatial heterogeneity of the coral surface since O_2 and pH profiles were measured on separate occasions and thus on different locations of the coral fragment; though, care was taken to perform all measurements in a similar area of the fragment (top area of the upstream side). O_2 concentration, for instance, has been shown to vary greatly along the coral surface[83,84]. This hypothesis would also explain the absence of a correlation between surface ΔpH and O_2 flux in this study, despite surface pH being closely linked to photosynthesis and respiration via coral CO_2 uptake and release[9,85]. However, such a result could also indicate that the CO_2 used during photosynthesis in the tested corals was not coming from seawater but had metabolic origins[86]. Future studies that simultaneously characterise both O_2 and pH gradients across the CBL will be crucial to unravel the relationship between these two CBLs under OA, the potential uncoupling of the associated physiological processes (e.g., photosynthesis, respiration, and calcification), and better understand carbon fluxes in scleractinian corals.

The surface microenvironment of reef-building corals is shaped by the dynamic build-up and depletion of metabolic molecules at the coral surface and thus fluctuates drastically between day and night, with O_2 and pH levels above seawater values during the day and below during the night[9,85]. This behaviour was successfully replicated in our study in light and dark conditions but changes in surface pH relative to bulk seawater were overall small in the tested corals (< 0.1 ΔpH). Although the literature is still limited, such low elevation of surface pH may be typical of some coral taxa under ambient pH, particularly of branching species[16,58]. For instance, under ambient pH and flow velocities similar to our study, *Acropora aspera* has been shown to have a pH elevation of similar magnitude to that recorded here for *A. cytherea*[58], while no elevation was found in *A. yongei*[17]. As observed here and in previous studies[9,16], the coral surface microenvironment is further modulated by water flow, with reduced flow velocities inducing larger elevation and depletion of O_2 and pH levels. Like CBL thickness, the response to flow in surface values also differed in magnitude among species as suggested by the flow ratios observed in this study. However, in surface dynamics, the highest flow ratio was observed in *P. verrucosa*, which could indicate a more responsive physiology to flow changes in this species.

The pH microenvironment at the coral surface is considered a defining factor of coral susceptibility to OA[21] because elevating surface pH may provide a crucial buffer during daylight that shelters the coral from the acidified bulk seawater[15,87]. In line with this, environmental pH variability can influence coral responses to OA[88,89], though higher pH during daytime may not be the sole determinant of reduced OA effects on whole-colony physiology[90]. In this study, while the amplitude of light–dark variation of surface pH was similar among species, pH behaviour was not symmetric in light and darkness and differed between species. The smallest pH elevation was observed in *P. verrucosa* under OA, which also had the largest pH reduction in darkness. However, this did not underlie a larger reduction in growth under OA (investigated in a study that assessed the OA-induced metabolic changes in the same coral fragments as studied here[91]), which was overall similar between *P. verrucosa* and *P. cylindrica*, and larger in *A. cytherea*. These results suggest that coral OA susceptibility is not determined by the magnitude of pH fluctuation at the coral surface, consistent with previous findings that greater seawater pH variability does not systematically enhance OA resistance[92]. Still, pH variability effects may depend on physiological response curves[90] and differ among species[93,94]. Low pH at the coral surface likely alters H^+ gradients across tissue layers[95,96]. This leads to decreased pH within coral cells[89,97,98], in the mesoglea above the calcifying cell layer[99], and of the calcifying fluid[100], which has been observed in *P. verrucosa* even when calcification remains stable under OA[101]. Therefore, our findings suggest that *P. verrucosa* may undergo large internal pH changes under OA with limited effects on growth, indicating an enhanced capacity for internal pH regulation. However, countering this strong pH reduction in coral tissues may be energetically costly, as shown by trends of decreased lipid content in *P. verrucosa*[102]. Moreover, pH regulation could be additionally aided by increasing tissue thickness under OA, which would further separate the calcifying cell layer and the coral surface, and expand the space

where pH is actively regulated. Although not observed in *P. verrucosa*, other pocilloporids have shown tissue thickening under OA[102,103].

Similarly to *P. verrucosa*, the lack of substantial elevation of surface pH observed here in *P. cylindrica* is remarkable, considering its mild metabolic response to OA[91]. However, given that *P. cylindrica* may maintain a constant pH of the calcifying fluid under OA[104], acid–base regulation could potentially differ between these two species[97]. Knowledge of these mechanisms and of the pH gradients between tissue layers and extracellular compartments, however, remains limited in scleractinian corals[99]. Furthermore, although *P. cylindrica* does not increase tissue thickness under OA[102], it has characteristically thicker tissues than *P. verrucosa*[105], which could underlie a greater ability to counter internal pH changes.

Bulk seawater pH did not affect the relative change in surface pH of *A. cytherea*, meaning that the absolute values of surface pH were considerably lower in the OA treatment than the control. These findings contrast with the higher surface pH elevation under OA (compared to ambient pH) observed previously in large-polyped massive species (*Favites* sp. and *Galaxea fascicularis*), with Δ values up to 0.8 pH units[15,16]. These differences could be due to morphological variation, which has been previously proposed as an underlying factor of differential pH elevation among coral species[58]. However, although our study shows that under OA surface ΔpH was overall similar between branching species (*A. cytherea* and *P. verrucosa*) and encrusting species with long uprights (*P. cylindrica*)[106], we are unable to address here the link between morphological complexity and responses to OA due to the lack of H^+ CBL data for *P. verrucosa* and *P. cylindrica* under ambient pH. Still, given the small relative change in pH in *P. cylindrica* under OA, an OA-enhanced elevation of surface pH seems unlikely. Future studies able to accurately characterise a range of coral morphologies and CBL responses to OA will be key to elucidate the role of morphological complexity and establish whether the response of *A. cytherea* in H^+ CBL traits is common to small-polyped species.

Overall, our findings demonstrate the absence of a buffer from OA conditions at the coral surface and highlight the importance of pH regulation mechanisms under OA, which, however, may become impaired under heat stress[107]. The pH microenvironment of *P. verrucosa* and *P. cylindrica* recorded here could be specific to OA conditions. Therefore, future studies that characterise the pH microenvironment of these species under both ambient pH and OA will help establish the response of their surface pH to OA. Nonetheless, *Pocillopora damicornis* has also shown surface ΔpH below 0.1 pH units under ambient pH[16], further supporting our finding that the resilience of pocilloporids to OA does not rely on being sheltered by their boundary layer.

Characterising diffusive fluxes across the CBL provides a comprehensive understanding of coral responses at the CBL scale. The values of O_2 flux in this study are based on diffusive transport, derived most commonly through the entire CBL and only in a few cases from the upper linear gradient. The fluxes recorded here are in line with previous reports (< 1 μmol cm^{-2} h^{-1}; e.g.[9,46]). The assessment of fluxes in corals can become more complicated when cilia activity modulates the flow within the CBL, creating vortices that result in O_2 concentration profiles with a complex shape[13,46]. Although in our study we did not aim to resolve the microscale flow patterns and conditions within the CBL, the frequency of complex profiles observed here was low (7% of all profiles). This low occurrence is likely due to the moderately high bulk flow velocities used in our study, which are expected to compress surface vortices[13]. Further detailed evaluation of our profiles indicated that there were only small deviations in the fluxes derived from the upper linear gradient of complex profiles. This supports the assumption that these derived fluxes are representative of the total flux across the CBL[46], but further assessments, including microscale visualisation of the flow patterns within the CBL, are desirable. Such in-depth studies that capture all the mechanisms that modulate CBL dynamics, including molecular diffusion, turbulence, and other unknown mechanisms[13,46,84,108], will help to build a more robust mechanistic understanding of mass transfer within the coral CBL.

O_2 flux decreases with decreasing water flow due to the thickening of the CBL[9]. In this study, the O_2 flux response to short-term exposure to low flow (< 1 h) reflected this same pattern, in both light and darkness. This result is in line with the decreasing effect of reduced flow on whole-colony net photosynthesis and respiration[109,110]. Thus, our findings support the notion that flow may modulate coral photosynthesis and respiration through changes on the boundary layer that affect the mass transfer of O_2 between the coral and seawater[111].

OA effects on coral O_2 flux have been previously investigated in only one other study, which found no changes in light O_2 flux of *Favites* sp. after 30-min exposure to OA[16]. In our study, we demonstrate that some species may maintain stable O_2 flux even after prolonged exposure to OA (as observed in *P. verrucosa* and *P. cylindrica*), while others experience a reduction (as seen in *A. cytherea*). In addition, *A. cytherea* was also the only species with OA effects on the thickness of the O_2 CBL, highlighting the strong relationship between O_2 flux and CBL thickness. Small-scale changes could, therefore, be one of the underlying factors of the OA-induced decrease in net photosynthesis of the studied coral fragments of *A. cytherea*[91] and of other acroporids (e.g.[112,113]). If so, photosynthesis of *Acropora* spp. may be mass transfer limited by the thicker CBL under OA, specifically the lower efflux of O_2. Accumulating O_2 within the coral during light may increase photorespiration, thereby decreasing photosynthetic activity[110]. In addition, reduced O_2 flux may have physiological effects other than reduced photosynthesis, such as increased oxidative stress[114]. Overall, our results indicate that in some species reduced photosynthesis under OA could be linked to CBL changes, with potential downstream effects in overall growth due to the reduction in energy supply from the microalgae to the coral host.

Although individual CBL traits could potentially influence whole-colony responses to OA in different ways, the overall limited effects of OA on the CBL in our study, except in surface absolute values, suggest that OA-induced changes in surface values may have the largest influence on whole-colony physiology by altering coral internal gradients. However, since responses at the CBL scale may be species-specific, the pathways and mechanisms underlying whole-colony responses to OA could differ among species.

Conclusions

Our study reinforces that the coral boundary layer is strongly modulated by changes in water flow and suggests an overall weak to null modulation by OA, even after prolonged exposure. We show that I) while CBL thickness increases under reduced flow, it may remain largely stable under OA. Nonetheless, the coral H^+ CBL was markedly thin under OA, providing limited buffering against OA conditions. We also demonstrate that II) the relative change of O_2 and pH at the coral surface may be enhanced by reduced flow but not OA, which, in turn, lowered the absolute value of surface pH. These OA effects contrast with previous findings of OA-induced elevation of surface pH in large-polyped reef-building corals and could thus be specific to small-polyped species. Therefore, our results reveal for the first time that reef-building coral species may lack a significantly differentiated pH microenvironment separating the coral from bulk seawater under OA, indicating that the physiological resilience to OA of some coral taxa may not rely on being sheltered by their boundary layer. Still, other environmental factors, such as reduced water flow, may modulate the CBL to offer some shelter. Finally, we confirm that III) responses in O_2 flux to flow and OA may reflect the same species-specific patterns as responses in CBL thickness and show that some coral species may maintain O_2 flux stable under long-term OA.

In this study, however, the assessment of the OA response in H^+ CBL traits was possible for *A. cytherea* only. Future investigation in more species will help establish whether the H^+ CBL response observed in *A. cytherea* is common among small-polyped corals. Furthermore, we observed no clear relationship between O_2 and pH gradients, which may have been due to spatial heterogeneity across the coral surface. Future studies able to simultaneously characterise both O_2 and pH gradients across the CBL under OA will be crucial to unravel the relationship between these two gradients and the potential uncoupling of the associated physiological processes. Finally, although our data suggest that cilia influence on the CBL was limited in our study, we did not characterise the microscale flow conditions during the measurement of profiles and thus, are unable to resolve their microscale flow context. Future in-depth microsensor studies capable of integrating across the various mechanisms that may modulate CBL dynamics will improve our mechanistic understanding of the processes that govern mass transfer within the coral CBL, particularly the enhancement by vortical ciliary flow. Understanding how small-scale elements and whole-colony physiological responses integrate will be key to explain the diversity of coral responses to OA.

Data availability

The datasets generated and analysed in the current study are available in the Figshare repository, https://doi.org/10.6084/m9.figshare.24534343.

Received: 10 November 2023; Accepted: 27 May 2024
Published online: 04 June 2024

References

1. Davis, K. A., Pawlak, G. & Monismith, S. G. Turbulence and coral reefs. *Ann. Rev. Mar. Sci.* **13**, 343–373 (2021).
2. Roik, A. *et al.* Year-long monitoring of physico-chemical and biological variables provide a comparative baseline of coral reef functioning in the central Red Sea. *PLoS One* **11**, e0163939 (2016).
3. Green, R. H., Lowe, R. J. & Buckley, M. L. Hydrodynamics of a tidally forced coral reef atoll. *J. Geophys. Res. Oceans* **123**, 7084–7101 (2018).
4. Noisette, F., Pansch, C., Wall, M., Wahl, M. & Hurd, C. L. Role of hydrodynamics in shaping chemical habitats and modulating the responses of coastal benthic systems to ocean global change. *Glob. Chang. Biol.* **28**, 3812–3829 (2022).
5. Lesser, M. P., Weis, V. M., Patterson, M. R. & Jokiel, P. L. Effects of morphology and water motion on carbon delivery and productivity in the reef coral, *Pocillopora damicornis* (Linnaeus): Diffusion barriers, inorganic carbon limitation, and biochemical plasticity. *J. Exp. Mar. Biol. Ecol.* **178**, 153–179 (1994).
6. Thomas, F. I. M. & Atkinson, M. J. Ammonium uptake by coral reefs: Effects of water velocity and surface roughness on mass transfer. *Limnol. Oceanogr.* **42**, 81–88 (1997).
7. Jørgensen, B. B. & Revsbech, N. P. Diffusive boundary layers and the oxygen uptake of sediments and detritus. *Limnol. Oceanogr.* **30**, 111–122 (1985).
8. Shashar, N., Kinane, S., Jokiel, P. L. & Patterson, M. R. Hydromechanical boundary layers over a coral reef. *J. Exp. Mar. Biol. Ecol.* **199**, 17–28 (1996).
9. Kühl, M., Cohen, Y., Dalsgaard, T., Jørgensen, B. & Revsbech, N. Microenvironment and photosynthesis of zooxanthellae in scleractinian corals studied with microsensors for O_2, pH and light. *Mar. Ecol. Prog. Ser.* **117**, 159–172 (1995).
10. Jimenez, I. M., Kühl, M., Larkum, A. W. D. & Ralph, P. J. Effects of flow and colony morphology on the thermal boundary layer of corals. *J. R. Soc. Interface* **8**, 1785–1795 (2011).
11. de Beer, D., Kühl, M., Stambler, N. & Vaki, L. A microsensor study of light enhanced Ca^{2+} uptake and photosynthesis in the reef-building hermatypic coral *Favia* sp.. *Mar. Ecol. Prog. Ser.* **194**, 75–85 (2000).
12. Shashar, N., Cohen, Y. & Loya, Y. Extreme diel fluctuations of oxygen in diffusive boundary layers surrounding stony corals. *Biol. Bull.* **185**, 455–461 (1993).
13. Shapiro, O. H. *et al.* Vortical ciliary flows actively enhance mass transport in reef corals. *Proc. Natl. Acad. Sci.* **111**, 13391–13396 (2014).
14. Godefroid, M., Dupont, S., Metian, M. & Hédouin, L. Two decades of seawater acidification experiments on tropical scleractinian corals: Overview, meta-analysis and perspectives. *Mar. Pollut. Bull.* **178**, 113552 (2022).
15. Agostini, S. *et al.* The effects of thermal and high-CO_2 stresses on the metabolism and surrounding microenvironment of the coral *Galaxea fascicularis*. *C. R. Biol.* **336**, 384–391 (2013).
16. Chan, N. C. S., Wangpraseurt, D., Kühl, M. & Connolly, S. R. Flow and coral morphology control coral surface pH: Implications for the effects of ocean acidification. *Front. Mar. Sci.* **3**, 1–11 (2016).
17. Comeau, S. *et al.* Flow-driven micro-scale pH variability affects the physiology of corals and coralline algae under ocean acidification. *Sci. Rep.* **9**, 12829 (2019).
18. Meseck, S. L., Sennefelder, G., Krisak, M. & Wikfors, G. H. Physiological feeding rates and cilia suppression in blue mussels (*Mytilus edulis*) with increased levels of dissolved carbon dioxide. *Ecol. Indic.* **117**, 106675 (2020).
19. Wang, Y. *et al.* Decreased motility of flagellated microalgae long-term acclimated to CO_2-induced acidified waters. *Nat. Clim. Chang* **10**, 561–567 (2020).

20. Tambutté, E. *et al.* Morphological plasticity of the coral skeleton under CO_2-driven seawater acidification. *Nat. Commun.* **6**, 7368 (2015).
21. Putnam, H. M., Barott, K. L., Ainsworth, T. D. & Gates, R. D. The vulnerability and resilience of reef-building corals. *Curr. Biol.* **27**, R528–R540 (2017).
22. Al-Horani, F. A. Effects of changing seawater temperature on photosynthesis and calcification in the scleractinian coral *Galaxea fascicularis*, measured with O_2, Ca^{2+} and pH microsensors. *Sci. Mar.* **69**, 347–354 (2005).
23. Shaw, E. C., McNeil, B. I., Tilbrook, B., Matear, R. & Bates, M. L. Anthropogenic changes to seawater buffer capacity combined with natural reef metabolism induce extreme future coral reef CO_2 conditions. *Glob. Chang. Biol.* **19**, 1632–1641 (2013).
24. Wilson, L. J. *et al.* Climate-driven changes to ocean circulation and their inferred impacts on marine dispersal patterns. *Glob. Ecol. Biogeogr.* **25**, 923–939 (2016).
25. Woodruff, J. D., Irish, J. L. & Camargo, S. J. Coastal flooding by tropical cyclones and sea-level rise. *Nature* **504**, 44–52 (2013).
26. East, H. K., Perry, C. T., Beetham, E. P., Kench, P. S. & Liang, Y. Modelling reef hydrodynamics and sediment mobility under sea level rise in atoll reef island systems. *Glob. Planet Change* **192**, 103196 (2020).
27. Ziegler, M. *et al.* Integrating environmental variability to broaden the research on coral responses to future ocean conditions. *Glob. Chang. Biol.* **27**, 5532–5546 (2021).
28. UNEP-WCMC, WorldFish Centre, WRI & TNC. Global distribution of warm-water coral reefs, compiled from multiple sources including the Millennium Coral Reef Mapping Project. Version 4.1. Includes contributions from IMaRS-USF and IRD (2005), IMaRS-USF (2005) and Spalding et al. (2001). *UN Environment World Conservation Monitoring Centre. Cambridge, UK* https://doi.org/10.34892/t2wk-5t34 (2021).
29. IPCC. Atlas. in *Climate Change 2021–The Physical Science Basis: Working Group I Contribution to the Sixth Assessment Report of the Intergovernmental Panel on Climate Change* (eds. Masson-Delmotte, V. et al.) 1927–2058 (Cambridge University Press, Cambridge, UK and New York, NY, USA, 2023). https://doi.org/10.1017/9781009157896.021.
30. Iturbide, M. *et al.* Implementation of FAIR principles in the IPCC: The WGI AR6 Atlas repository. *Sci. Data* **9**, 629 (2022).
31. Hannan, K. D. *et al.* Diel pCO_2 variation among coral reefs and microhabitats at Lizard Island, Great Barrier Reef. *Coral Reefs* **39**, 1391–1406 (2020).
32. Dickson, A. G., Sabine, C. L. & Christian, J. R. *Guide to Best Practices for Ocean CO_2 Measurements*. *PICES Special Publication 3* (PICES Special Publication 3, CA, 2007).
33. Dickson, A. G., Afghan, J. D. & Anderson, G. C. Reference materials for oceanic CO_2 analysis: A method for the certification of total alkalinity. *Mar. Chem.* **80**, 185–197 (2003).
34. Pelletier, G., Lewis, E. & Wallace, D. CO2Sys. xls: A calculator for the CO_2 system in seawater for Microsoft Excel/VBA. *Washington State Department of Ecology/Brookhaven National Laboratory, Olympia, WA/Upton, NY, USA* (2007).
35. Gattuso, J.-P., Epitalon, J.-M., Lavigne, H. & Orr, J. seacarb: Seawater carbonate chemistry. R package version 3.2.16. https://cran.r-project.org/package=seacarb (2021).
36. Nisumaa, A.-M. *et al.* EPOCA/EUR-OCEANS data compilation on the biological and biogeochemical responses to ocean acidification. *Earth Syst. Sci. Data* **2**, 167–175 (2010).
37. Mehrbach, C., Culberson, C. H., Hawley, J. E. & Pytkowicx, R. M. Measurement of the apparent dissociation constants of carbonic acid in seawater at atmospheric pressure. *Limnol. Oceanogr.* **18**, 897–907 (1973).
38. Dickson, A. G. & Millero, F. J. A comparison of the equilibrium constants for the dissociation of carbonic acid in seawater media. *Deep Sea Res. Part A Oceanogr. Res. Pap.* **34**, 1733–1743 (1987).
39. Lueker, T. J., Dickson, A. G. & Keeling, C. D. Ocean pCO_2 calculated from dissolved inorganic carbon, alkalinity, and equations for K_1 and K_2: Validation based on laboratory measurements of CO_2 in gas and seawater at equilibrium. *Mar. Chem.* **70**, 105–119 (2000).
40. Watson, S.-A., Fabricius, K. E. & Munday, P. L. Quantifying pCO_2 in biological ocean acidification experiments: A comparison of four methods. *PLoS One* **12**, e0185469 (2017).
41. Ramsing, N. & Gundersen, J. Seawater and gases: Tabulated physical parameters of interest to people working with microsensors in marine systems. Unisense. *Unisense* https://unisense.com/technical-information/#tables (2023).
42. Patterson, M. R., Sebens, K. P. & Olson, R. R. In situ measurements of flow effects on primary production and dark respiration in reef corals. *Limnol. Oceanogr.* **36**, 936–948 (1991).
43. Millero, F. J. *Chemical Oceanography* (CRC Press, 2013).
44. Takahashi, T. Carbonate chemistry. in *GEOSECS Pacific expedition, Volume 3, Hydrographic Data 1973–1974* 77–83 (National Science Foundation, Washington, DC, 1982).
45. Nishihara, G. N. & Ackerman, J. D. On the determination of mass transfer in a concentration boundary layer. *Limnol. Oceanogr. Methods* **5**, 88–96 (2007).
46. Pacherres, C. O., Ahmerkamp, S., Schmidt-Grieb, G. M., Holtappels, M. & Richter, C. Ciliary vortex flows and oxygen dynamics in the coral boundary layer. *Sci. Rep.* **10**, 7541 (2020).
47. Martins, C. P. P., Wall, M., Schubert, P., Wilke, T. & Ziegler, M. Variability of the surface boundary layer of reef-building coral species. Preprint (Version 1) at *Research Square* (2024) https://doi.org/10.21203/rs.3.rs-3860900/v1.
48. R Core Team. *R: A Language and Environment for Statistical Computing*. (R Foundation for Statistical Computing, Vienna, Austria, 2021).
49. RStudio Team. *RStudio: Integrated Development Environment for R*. (RStudio, PBC, 2021).
50. Wickham, H. *ggplot2: Elegant Graphics for Data Analysis* (Springer-Verlag, 2016).
51. Bates, D., Mächler, M., Bolker, B. & Walker, S. Fitting linear mixed-effects models using lme4. *J. Stat. Softw.* **67**, 1–48 (2015).
52. Lüdecke, D. sjPlot: Data visualization for statistics in social science. R package version 2.8.9. https://CRAN.R-project.org/package=sjPlot (2021).
53. Fox, J. & Weisberg, S. *An R Companion to Applied Regression* (Sage, 2019).
54. Langsrud, Ø. ANOVA for unbalanced data: Use Type II instead of Type III sums of squares. *Stat. Comput.* **13**, 163–167 (2003).
55. Hector, A., von Felten, S. & Schmid, B. Analysis of variance with unbalanced data: An update for ecology & evolution. *J. Anim. Ecol.* **79**, 308–316 (2010).
56. Lenth, R. V. emmeans: Estimated Marginal Means, aka Least-Squares Means. R package version 1.6.2–1. https://cran.r-project.org/package=emmeans (2021).
57. Ho, J., Tumkaya, T., Aryal, S., Choi, H. & Claridge-Chang, A. Moving beyond *P* values: Data analysis with estimation graphics. *Nat. Methods* **16**, 565–566 (2019).
58. Schoepf, V. *et al.* Impacts of coral bleaching on pH and oxygen gradients across the coral concentration boundary layer: A microsensor study. *Coral Reefs* **37**, 1169–1180 (2018).
59. Stafford-Smith, M. G. Sediment-rejection efficiency of 22 species of Australian scleractinian corals. *Mar. Biol.* **115**, 229–243 (1993).
60. Lewis, J. B. & Price, W. S. Patterns of ciliary currents in Atlantic reef corals and their functional significance. *J. Zool.* **178**, 77–89 (1976).
61. Pichon, M. & Veron, J. E. N. *Scleractinia of Eastern Australia*. https://doi.org/10.5962/bhl.title.60617 (Australian Govt. Pub. Service, 1976).

62. Sier, C. J. S. & Olive, P. J. W. Reproduction and reproductive variability in the coral *Pocillopora verrucosa* from the Republic of Maldives. *Mar. Biol.* **118**, 713–722 (1994).
63. Anthony, K. R. N. Coral suspension feeding on fine particulate matter. *J. Exp. Mar. Biol. Ecol.* **232**, 85–106 (1999).
64. Yonge, C. M. Studies on the physiology of corals: I. Feeding mechanisms and food. *Sci. Rep. Great Barrier Reef Exp.* **1**, 13–57 (1930).
65. Lewis, J. B. & Price, W. S. Feeding mechanisms and feeding strategies of Atlantic reef corals. *J. Zool.* **176**, 527–544 (1975).
66. Sebens, K. P., Witting, J. & Helmuth, B. Effects of water flow and branch spacing on particle capture by the reef coral *Madracis mirabills* (Duchassaing and Michelotti). *J. Exp. Mar. Biol. Ecol.* **211**, 1–28 (1997).
67. Levy, O., Mizrahi, L., Chadwick-Furman, N. E. & Achituv, Y. Factors controlling the expansion behavior of *Favia favus* (Cnidaria: Scleractinia): Effects of light, flow, and planktonic prey. *Biol. Bull.* **200**, 118–126 (2001).
68. Patterson, M. R. A chemical engineering view of cnidarian symbioses. *Am. Zool.* **32**, 566–582 (1992).
69. Liew, Y. J. *et al.* Epigenome-associated phenotypic acclimatization to ocean acidification in a reef-building coral. *Sci. Adv.* **4**, 1–10 (2018).
70. Mollica, N. R. *et al.* Ocean acidification affects coral growth by reducing skeletal density. *Proc. Natl. Acad. Sci.* **115**, 1754–1759 (2018).
71. Horvath, K. M. *et al.* Next-century ocean acidification and warming both reduce calcification rate, but only acidification alters skeletal morphology of reef-building coral *Siderastrea siderea*. *Sci. Rep.* **6**, 29613 (2016).
72. Cohen, A. L., McCorkle, D. C., de Putron, S., Gaetani, G. A. & Rose, K. A. Morphological and compositional changes in the skeletons of new coral recruits reared in acidified seawater: Insights into the biomineralization response to ocean acidification. *Geochem. Geophys. Geosyst.* **10**, 52 (2009).
73. Ertl, N. G., O'Connor, W. A., Wiegand, A. N. & Elizur, A. Molecular analysis of the Sydney rock oyster (*Saccostrea glomerata*) CO_2 stress response. *Clim. Chang. Responses* **3**, 1–19 (2016).
74. Peng, Q. *et al.* Surface warming–induced global acceleration of upper ocean currents. *Sci. Adv.* **8**, eabj8394 (2022).
75. Storlazzi, C. D. *et al.* Most atolls will be uninhabitable by the mid-21st century because of sea-level rise exacerbating wave-driven flooding. *Sci. Adv.* **4**, eaap9741 (2018).
76. Harris, D. L. *et al.* Coral reef structural complexity provides important coastal protection from waves under rising sea levels. *Sci. Adv.* **4**, eaao4350 (2018).
77. Taebi, S. & Pattiaratchi, C. Hydrodynamic response of a fringing coral reef to a rise in mean sea level. *Ocean Dyn.* **64**, 975–987 (2014).
78. Sun, C. *et al.* Marine downscaling of a future climate scenario for Australian boundary currents. *J. Clim.* **25**, 2947–2962 (2012).
79. Sen Gupta, A. *et al.* Future changes to the upper ocean Western Boundary Currents across two generations of climate models. *Sci. Rep.* **11**, 9538 (2021).
80. Jokiel, P. L. Coral reef calcification: Carbonate, bicarbonate and proton flux under conditions of increasing ocean acidification. *Proc. R. Soc. B Biol. Sci.* **280**, 52 (2013).
81. Kornder, N. A., Riegl, B. M. & Figueiredo, J. Thresholds and drivers of coral calcification responses to climate change. *Glob. Chang Biol.* **24**, 5084–5095 (2018).
82. Fabricius, K. E. *et al.* Losers and winners in coral reefs acclimatized to elevated carbon dioxide concentrations. *Nat. Clim. Chang* **1**, 165–169 (2011).
83. Ahmerkamp, S. *et al.* Simultaneous visualization of flow fields and oxygen concentrations to unravel transport and metabolic processes in biological systems. *Cell Rep. Methods* **2**, 100216 (2022).
84. Pacherres, C. O., Ahmerkamp, S., Koren, K., Richter, C. & Holtappels, M. Ciliary flows in corals ventilate target areas of high photosynthetic oxygen production. *Curr. Biol.* **32**, 1–9 (2022).
85. Al-Horani, F. A., Al-Moghrabi, S. M. & De Beer, D. The mechanism of calcification and its relation to photosynthesis and respiration in the scleractinian coral *Galaxea fascicularis*. *Mar. Biol.* **142**, 419–426 (2003).
86. Cai, W.-J. *et al.* Microelectrode characterization of coral daytime interior pH and carbonate chemistry. *Nat. Commun.* **7**, 11144 (2016).
87. Hurd, C. L. *et al.* Metabolically induced pH fluctuations by some coastal calcifiers exceed projected 22nd century ocean acidification: A mechanism for differential susceptibility?. *Glob. Chang. Biol.* **17**, 3254–3262 (2011).
88. Comeau, S. *et al.* pH variability at volcanic CO_2 seeps regulates coral calcifying fluid chemistry. *Glob. Chang Biol.* **28**, 2751–2763 (2022).
89. Brown, K. T. *et al.* Environmental memory gained from exposure to extreme pCO_2 variability promotes coral cellular acid–base homeostasis. *Proc. R. Soc. B Biol. Sci.* **289**, 52 (2022).
90. Enochs, I. C. *et al.* The influence of diel carbonate chemistry fluctuations on the calcification rate of *Acropora cervicornis* under present day and future acidification conditions. *J. Exp. Mar. Biol. Ecol.* **506**, 135–143 (2018).
91. Martins, C. P. P. *et al.* Short periods of decreased water flow may modulate long-term ocean acidification in reef-building corals. Preprint (Version 1) at *bioRxiv* (2024) https://doi.org/10.1101/2024.02.23.581783.
92. Cornwall, C. E. *et al.* Resistance of corals and coralline algae to ocean acidification: Physiological control of calcification under natural pH variability. *Proc. R. Soc. B Biol. Sci.* **285**, 20181168 (2018).
93. Comeau, S., Edmunds, P. J., Spindel, N. B. & Carpenter, R. C. Diel pCO_2 oscillations modulate the response of the coral *Acropora hyacinthus* to ocean acidification. *Mar. Ecol. Prog. Ser.* **501**, 99–111 (2014).
94. Chan, W. Y. & Eggins, S. M. Calcification responses to diurnal variation in seawater carbonate chemistry by the coral *Acropora formosa*. *Coral Reefs* **36**, 763–772 (2017).
95. Jokiel, P. L. Ocean acidification and control of reef coral calcification by boundary layer limitation of proton flux. *Bull. Mar. Sci.* **87**, 639–657 (2011).
96. Jokiel, P. L. The reef coral two compartment proton flux model: A new approach relating tissue-level physiological processes to gross corallum morphology. *J. Exp. Mar. Biol. Ecol.* **409**, 1–12 (2011).
97. Venn, A. A. *et al.* Effects of light and darkness on pH regulation in three coral species exposed to seawater acidification. *Sci. Rep.* **9**, 2201 (2019).
98. Gibbin, E. M., Putnam, H. M., Davy, S. K. & Gates, R. D. Intracellular pH and its response to CO_2-driven seawater acidification in symbiotic *versus* non-symbiotic coral cells. *J. Exp. Biol.* **217**, 1963–1969 (2014).
99. Venn, A. A., Tambutté, E., Comeau, S. & Tambutté, S. Proton gradients across the coral calcifying cell layer: Effects of light, ocean acidification and carbonate chemistry. *Front. Mar. Sci.* **9**, 1–15 (2022).
100. Venn, A. A. *et al.* Impact of seawater acidification on pH at the tissue–skeleton interface and calcification in reef corals. *Proc. Natl. Acad. Sci.* **110**, 1634–1639 (2013).
101. Comeau, S. *et al.* Resistance to ocean acidification in coral reef taxa is not gained by acclimatization. *Nat. Clim. Chang* **9**, 477–483 (2019).
102. Martins, C. P. P. *et al.* Growth response of reef-building corals to ocean acidification is mediated by interplay of taxon-specific physiological parameters. *Front. Mar. Sci.* **9**, 1–11 (2022).
103. Krief, S. *et al.* Physiological and isotopic responses of scleractinian corals to ocean acidification. *Geochim. Cosmochim. Acta* **74**, 4988–5001 (2010).

104. Georgiou, L. *et al.* pH homeostasis during coral calcification in a free ocean CO_2 enrichment (FOCE) experiment, Heron Island reef flat, Great Barrier Reef. *Proc. Natl. Acad. Sci.* **112**, 13219–13224 (2015).
105. Loya, Y. *et al.* Coral bleaching: The winners and the losers. *Ecol. Lett.* **4**, 122–131 (2001).
106. Madin, J. S. *et al.* The Coral Trait Database, a curated database of trait information for coral species from the global oceans. *Sci. Data* **3**, 160017 (2016).
107. Innis, T. *et al.* Marine heatwaves depress metabolic activity and impair cellular acid–base homeostasis in reef-building corals regardless of bleaching susceptibility. *Glob. Chang Biol.* **27**, 2728–2743 (2021).
108. Stocking, J. B., Laforsch, C., Sigl, R. & Reidenbach, M. A. The role of turbulent hydrodynamics and surface morphology on heat and mass transfer in corals. *J. R. Soc. Interface* **15**, 20180448 (2018).
109. Sebens, K. P., Helmuth, B., Carrington, E. & Agius, B. Effects of water flow on growth and energetics of the scleractinian coral *Agaricia tenuifolia* in Belize. *Coral Reefs* **22**, 35–47 (2003).
110. Hoogenboom, M. O. & Connolly, S. R. Defining fundamental niche dimensions of corals: Synergistic effects of colony size, light, and flow. *Ecology* **90**, 767–780 (2009).
111. Mass, T., Genin, A., Shavit, U., Grinstein, M. & Tchernov, D. Flow enhances photosynthesis in marine benthic autotrophs by increasing the efflux of oxygen from the organism to the water. *Proc. Natl. Acad. Sci.* **107**, 2527–2531 (2010).
112. Anthony, K. R. N., Kline, D. I., Diaz-Pulido, G., Dove, S. & Hoegh-Guldberg, O. Ocean acidification causes bleaching and productivity loss in coral reef builders. *Proc. Natl. Acad. Sci.* **105**, 17442–17446 (2008).
113. Kaniewska, P. *et al.* Major cellular and physiological impacts of ocean acidification on a reef building coral. *PLoS One* **7**, e34659 (2012).
114. Finelli, C. M., Helmuth, B. S. T., Pentcheff, N. D. & Wethey, D. S. Water flow influences oxygen transport and photosynthetic efficiency in corals. *Coral Reefs* **25**, 47–57 (2006).

Acknowledgements

This study was conducted as part of the 'Ocean2100' global change simulation project of the Colombian-German Center of Excellence in Marine Sciences (CEMarin), funded by the German Academic Exchange Service (DAAD, project number 57480468).

Author contributions

C.M., M.Z., and M.W. designed the study. C.M. performed the experiment with assistance from P.S. C.M. collected and analysed the data and prepared the figures and tables. M.W. provided the microsensor measuring system. T.W. secured funding. C.M. drafted the manuscript with assistance from M.W. All authors contributed to writing, reviewing, and editing of the final manuscript.

Funding

Open Access funding enabled and organized by Projekt DEAL.

Competing interests

The authors declare no competing interests.

Additional information

Supplementary Information The online version contains supplementary material available at https://doi.org/10.1038/s41598-024-63210-9.

Correspondence and requests for materials should be addressed to C.P.P.M.

Reprints and permissions information is available at www.nature.com/reprints.

Publisher's note Springer Nature remains neutral with regard to jurisdictional claims in published maps and institutional affiliations.

Supplementary material

Effects of water flow and ocean acidification on oxygen and pH gradients in coral boundary layer

Catarina P.P. Martins*[1], Maren Ziegler[1], Patrick Schubert[1], Thomas Wilke[1], Marlene Wall[2]

[1]Department of Animal Ecology & Systematics, Justus Liebig University Giessen, 35392 Giessen, Germany

[2]GEOMAR Helmholtz Centre for Ocean Research Kiel, 24148 Kiel, Germany

*corresponding author: catarina.padilha-pires-martins@bio.uni-giessen.de

Supplementary Text

In our study, we followed the approach of Pacherres et al.[1] and calculated O_2 flux using the upper linear gradient of the profile. Briefly, we chose this approach because all the calculations of flux of Pacherres et al.[1] are performed using Fick's first law of diffusion (i.e., based on molecular diffusion) and the diffusion coefficient based on temperature and salinity. Additionally, we followed this procedure because in their study Pacherres et al.[1] provided a first proof that the flux in the upper linear gradient of complex profiles (upper flux) is representative of the actual flux across the concentration boundary layer (CBL) of the coral. Specifically, they compared fluxes under the arrested cilia state (calculated using almost the entire profile) and under the active cilia state (calculated using the upper gradient of the profile), which revealed the same flux under both cilia states. This indicates that the flux is independent of the overall underlying transport mechanisms (diffusion vs. a combination of diffusion and enhanced transport by vortical movement) across the CBL. In our study, however, we did not characterise the microscale flow conditions surrounding the measuring spot at the coral surface during profile measurement or perform additional measurements under arrested cilia activity. Thus, we are unable to ascertain how much the approach used to derive the O_2 flux of complex profiles deviates from the actual flux. However, in our data, complex profiles were few (Supplementary Table S3) and the CBL was generally thin (see the Results section), which suggests that the effect of ciliary vortices is negligible in our data. Thus, by following Pacherres et al.[1] and using only the linear section and diffusive parts to calculate fluxes we grasp the major transport process that govern the flux in our profiles.

Alternative approaches for the treatment of these complex profiles would be to exclude them from the study or to calculate O_2 flux without considering their profile structure and using only the total CBL thickness and maximum O_2 concentration at the coral surface (i.e., treating them as if all profiles had the same structure). However, we believe that it is important to include these profiles in our study to fully capture the variability of the CBL of the three tested species and their biological responses. Additionally, we categorised all profiles into three main shapes (diffusive, S-shaped, and complex), as outlined in Martins et al.[2], and did not detect extreme deviation associated with the complex profiles (Figure i). Furthermore, while the alternative calculation approach might be a valid option for studies with thick CBLs and strong cilia influence, this was not the case for our study. The limited influence of cilia activity in our data is mostly likely due to the moderately high bulk flow velocities used here, which are expected to compress surface vortices and strongly reduce the effects of cilia movement on the CBL[3]. In line with this, the O_2 flux of the complex profiles derived following both approaches—based on the upper liner gradient of profiles vs. based on total CBL thickness and maximum surface O_2 concentration—on average differ by only 0.04 µmol h^{-1} cm^{-2} (n = 23) (Table i). Altogether, this suggests that calculating the O_2 flux of the complex profiles in our study following the approach outlined by Pacherres et al.[1] provides a representative estimation of coral activity and flux.

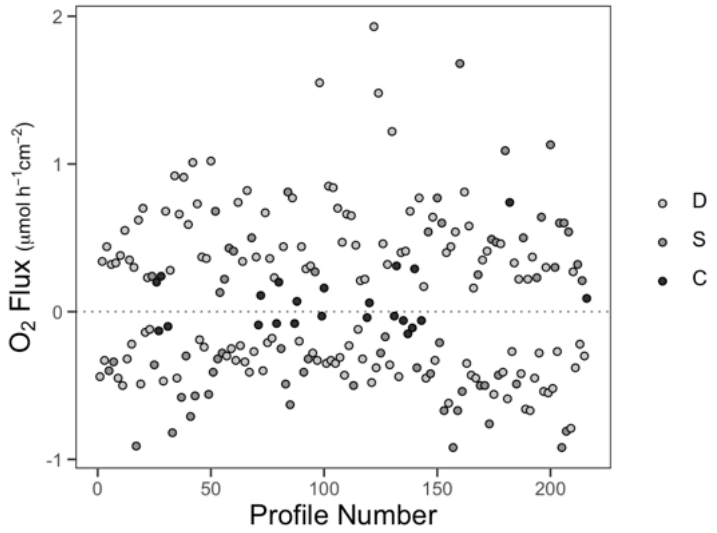

Figure i. Derived O_2 flux values for all measured O_2 concentration profiles, categorised into three main profile shapes (D, diffusive; S, S-shaped; C, complex).

Table i. Slope and respective fluxes of complex profiles calculated based on (1) the upper linear gradient of profiles, and (2) the total CBL height and the maximum O_2 concentration at the coral surface. Values of slopes and fluxes are presented in µmol cm^{-2} h^{-1}. Acy, *Acropora cytherea*; Pve, *Pocillopora verrucosa*; Pcy, *Porites cylindrica*; OA, ocean acidification.

Species	Colony	Fragment	Flow	Light	Treatment	Slope[1]	Flux[1]	Slope[2]	Flux[2]
Acy	B	1	moderate	light	OA	-2,43	0,2	-5,26	0,43
Acy	B	1	low	light	OA	-2,91	0,24	-2,94	0,24
Acy	B	1	low	dark	OA	1,6	-0,13	1,41	-0,12
Acy	B	2	low	dark	OA	1,26	-0,1	1,34	-0,11
Acy	C	7	low	light	OA	-1,39	0,11	-2,12	0,17
Acy	C	7	low	dark	OA	1,04	-0,09	1,89	-0,16
Pve	B	5	moderate	light	control	-8,97	0,74	-6,16	0,51
Pve	C	7	low	light	OA	-1,14	0,09	-3,17	0,26
Pcy	A	2	low	light	OA	-2,42	0,2	-1,35	0,11
Pcy	A	2	low	dark	OA	0,99	-0,08	0,94	-0,08
Pcy	A	5	low	light	control	-0,82	0,07	-4,69	0,39
Pcy	A	5	low	dark	control	1,02	-0,08	2,08	-0,17
Pcy	B	1	low	light	OA	-1,92	0,16	-5,33	0,44
Pcy	B	1	low	dark	OA	0,37	-0,03	1,4	-0,12
Pcy	B	7	low	light	OA	-0,7	0,06	-1,51	0,12
Pcy	B	7	low	dark	OA	0,44	-0,04	0,57	-0,05
Pcy	C	4	low	light	control	-3,8	0,31	-1,16	0,1
Pcy	C	4	low	dark	control	0,38	-0,03	0,83	-0,07
Pcy	C	5	low	dark	control	0,74	-0,06	2,01	-0,17
Pcy	C	6	low	light	control	-3,56	0,29	-2,61	0,22
Pcy	C	6	moderate	dark	control	1,87	-0,15	3,15	-0,26
Pcy	C	6	low	dark	control	1,3	-0,11	0,98	-0,08
Pcy	C	7	low	dark	OA	0,69	-0,06	0,78	-0,06

References

1. Pacherres, C. O., Ahmerkamp, S., Schmidt-Grieb, G. M., Holtappels, M. & Richter, C. Ciliary vortex flows and oxygen dynamics in the coral boundary layer. *Sci Rep* **10**, 7541 (2020).

2. Martins, C. P. P., Wall, M., Schubert, P., Wilke, T. & Ziegler, M. Variability of the surface boundary layer of reef-building coral species. *Preprint (Version 1) at Research Square* (2024) doi:10.21203/rs.3.rs-3860900/v1.

3. Shapiro, O. H. *et al.* Vortical ciliary flows actively enhance mass transport in reef corals. *Proceedings of the National Academy of Sciences* **111**, 13391–13396 (2014).

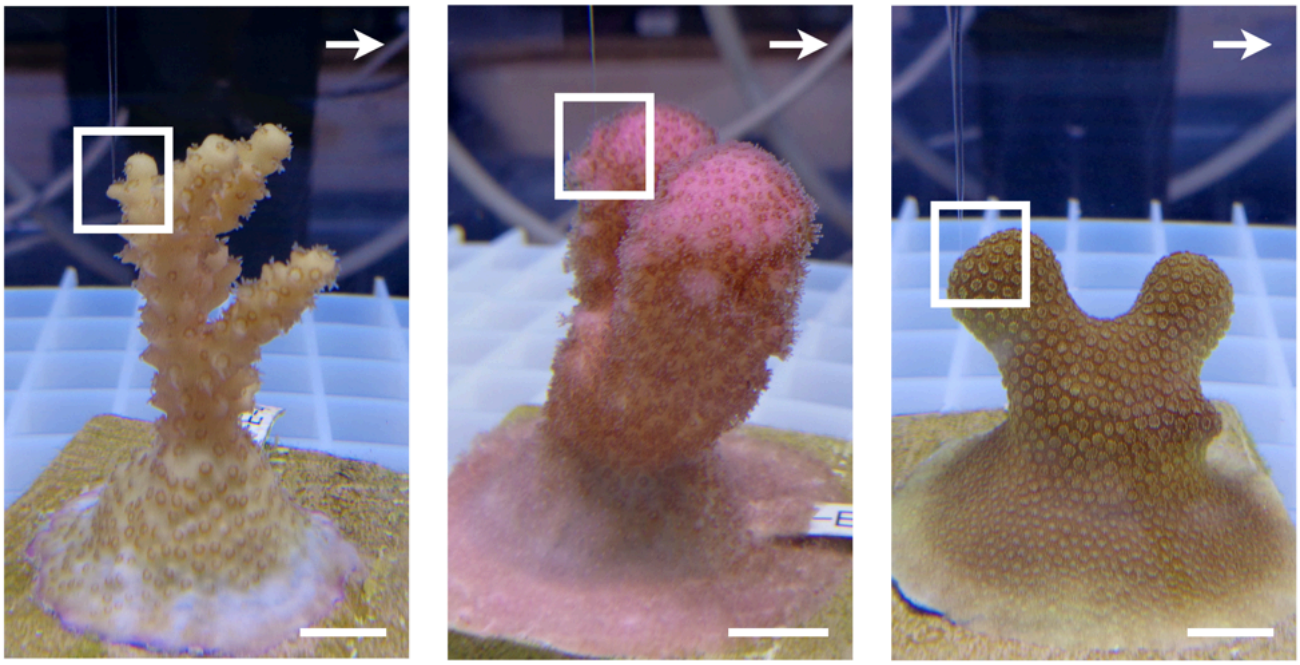

Supplementary Fig. S1. Photographs of *Acropora cytherea*, *Pocillopora verrucosa*, and *Porites cylindrica* (from left to right) during microsensor measurements. Rectangles mark representative locations of microsensor measurements across coral fragments and arrows indicate the direction of water flow. Scale bar = 1 cm approx.

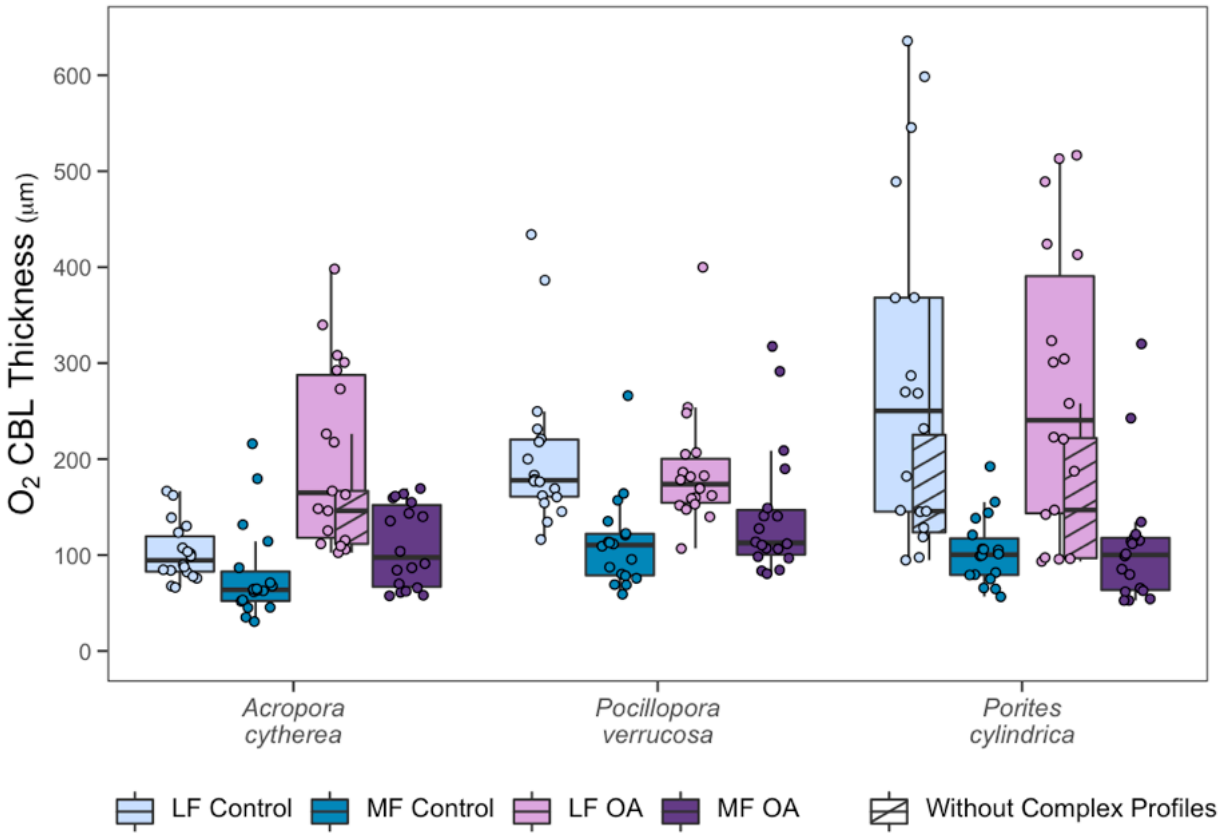

Supplementary Fig. S2. Visualisation of the effects of water flow and ocean acidification (OA) on the thickness of the concentration boundary layer (CBL) of *Acropora cytherea*, *Pocillopora verrucosa*, and *Porites cylindrica*, with and without including complex profiles (i.e., microsensor profiles with multiple linear gradients within the CBL). Profiles were measured in light and dark combined low flow (LF, 2 cm s^{-1}) and moderate flow (MF, 6 cm s^{-1}) and values are presented pooled over light conditions. No complex profiles were observed for the H^+ CBL. Boxes represent the first and third quartiles with lines as medians and whiskers as the minimum and maximum values or up to the 1.5 * interquartile range (IQR), whichever is reached first.

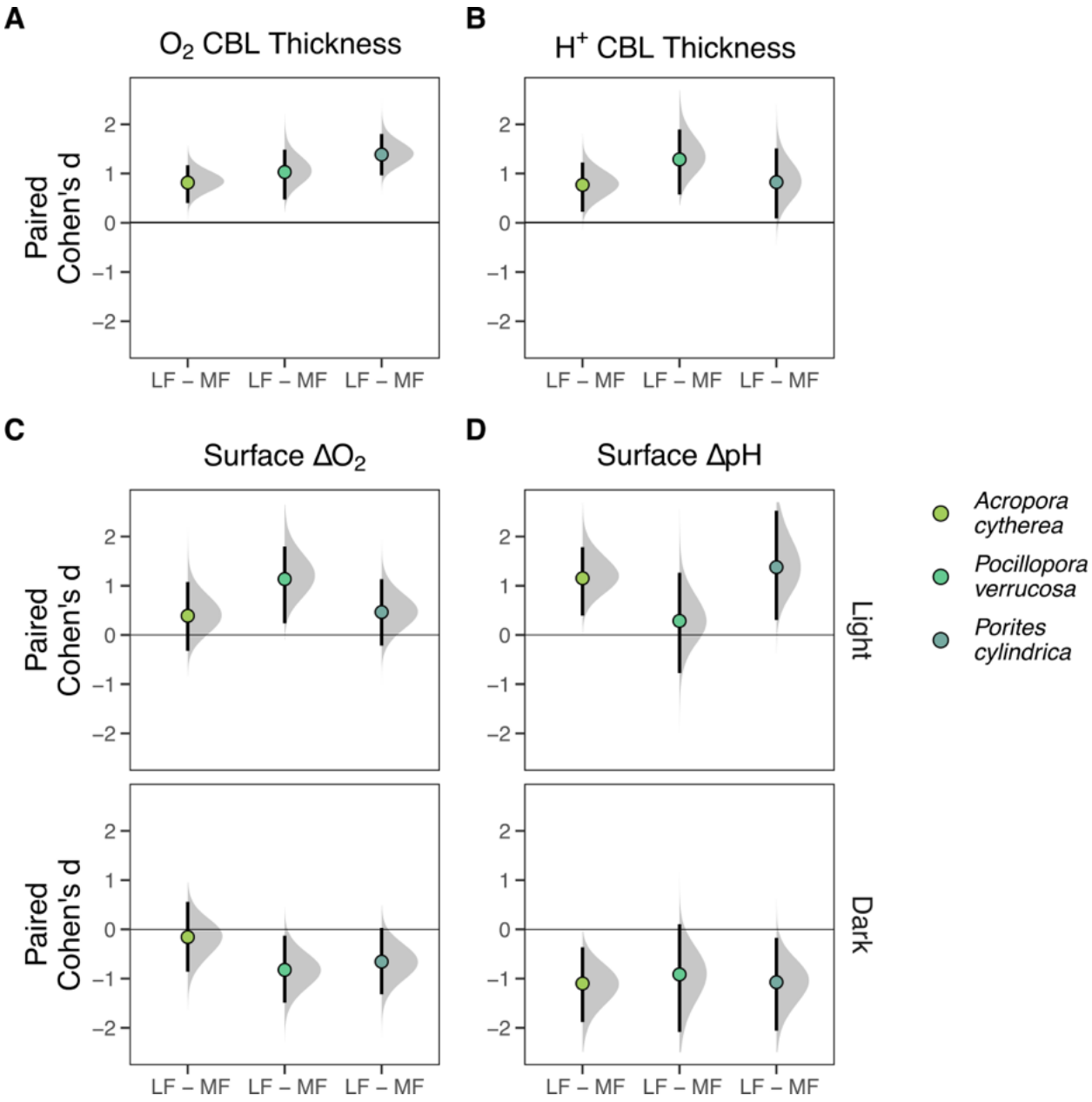

Supplementary Fig. S3. Visualisation of the effect size of flow effects on the concentration boundary layer (CBL) of *Acropora cytherea*, *Pocillopora verrucosa*, and *Porites cylindrica*. Cohen's d effect size between low flow (LF, 2 cm s^{-1}) and moderate flow (MF, 6 cm s^{-1}) for (A) O_2 CBL thickness, (B) H^+ CBL thickness, (C) change in O_2 at the coral surface relative to bulk seawater concentration (surface ΔO_2), and (D) change in pH at the coral surface relative to bulk seawater level (surface ΔpH), measured in light and dark. Values of CBL thickness are pooled over light conditions. Black vertical lines are 95% confidence intervals from nonparametric bootstrap resampling and grey-shaded areas illustrate the resampled distribution of the effect size.

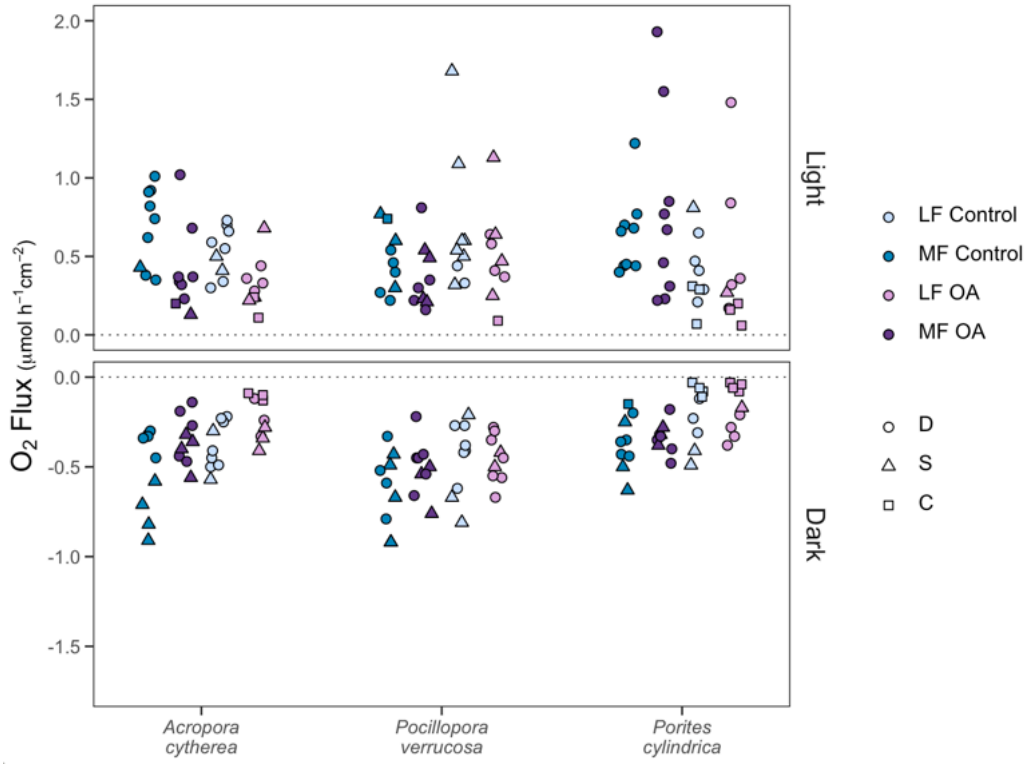

Supplementary Fig. S4. Visualisation of the effects of water flow and ocean acidification (OA) on the O_2 flux of *Acropora cytherea*, *Pocillopora verrucosa*, and *Porites cylindrica*, derived from O_2 concentration profiles categorised into three main profile shapes (D, diffusive; S, S-shaped; C, complex). Profiles were measured in light and dark combined with low flow (LF, 2 cm s^{-1}) and moderate flow (MF, 6 cm s^{-1})

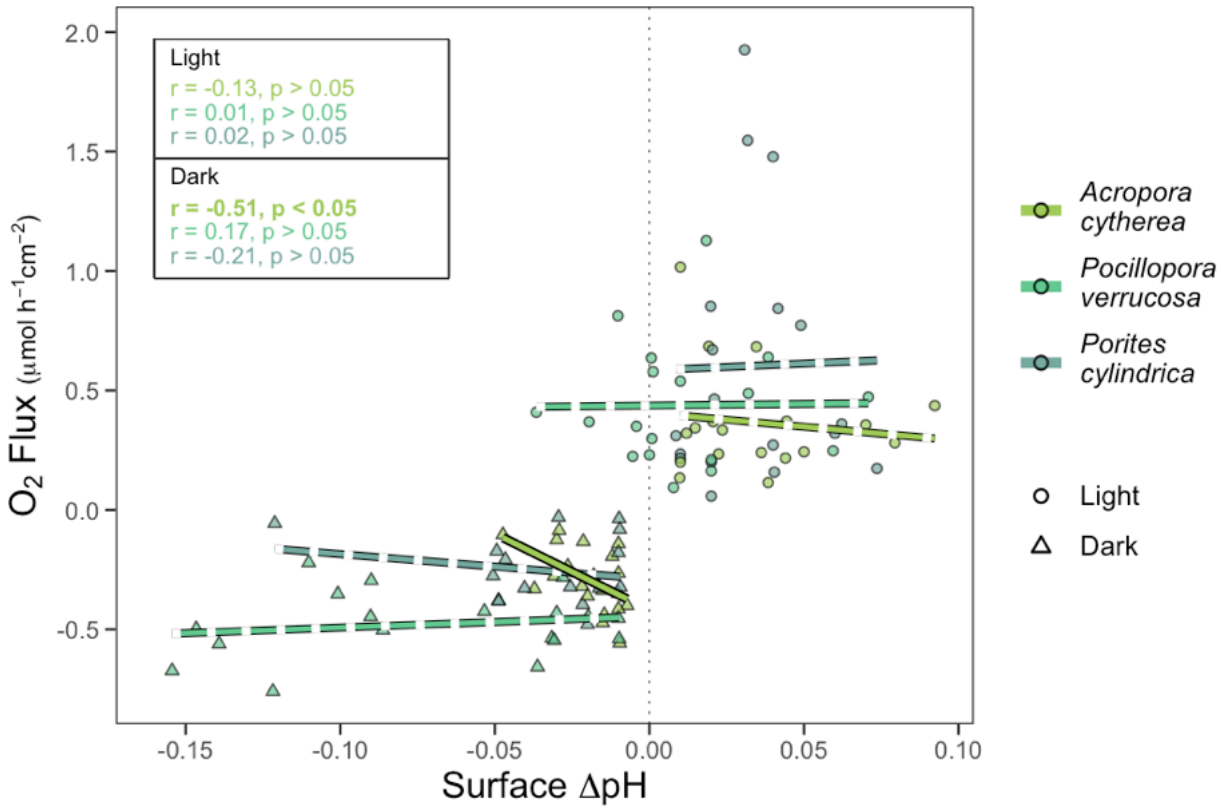

Supplementary Fig. S5. Relationship between pH changes at the coral surface relative to bulk seawater pH (surface ΔpH) and O_2 flux across the concentration boundary layer of *Acropora cytherea*, *Pocillopora verrucosa*, and *Porites cylindrica* in the ocean acidification treatment, measured in light and dark. Measurements under low and moderate flow are pooled together. Significant Pearson correlation coefficients (r) at the level of $\alpha < 0.05$ are marked in bold. Lines are linear regression fitting for significant (solid) and non-significant (dashed) correlations.

Supplementary Table S1. Details on coral species used in the experiment.

Species	Number of colonies	Origin	Collection year	CITES number
Acropora cytherea	3	Saudi Arabia (Red Sea)	2019	19-SA-000089-PD
Pocillopora verrucosa	2 1	Saudi Arabia (Red Sea) Indonesia (Indo-Pacific)	2015 2007	15-SA-000882-PD 14846/IV/SATS-LN/2007
Porites cylindrica	3	Indonesia (Indo-Pacific)	2017	17nl241924/11

Supplementary Table S2. Brands of artificial-seawater salt used alternately during the acclimation and experimental period in the 'Ocean2100' experimental facility.

Salt	Brand
Deep Blue Sea-Salt	AquaPerfekt, Germany
Instant Ocean	Aquarium Systems, France
Reef Crystals	Aquarium Systems, France
Sea Salt	Aquaforest, Poland

Supplementary Table S3. Number of complex profiles measured in *Acropora cytherea*, *Pocillopora verrucosa*, and *Porites cylindrica* in the control and ocean acidification (OA) treatments and under low flow (2 cm s^{-1}) and moderate flow (6 cm s^{-1}).

Species	Flow	Treatment	*n*
Acropora cytherea	Low	Control	2
Acropora cytherea	Low	OA	5
Acropora cytherea	Moderate	Control	1
Acropora cytherea	Moderate	OA	1
Pocillopora verrucosa	Low	OA	1
Pocillopora verrucosa	Moderate	Control	1
Porites cylindrica	Low	Control	7
Porites cylindrica	Low	OA	8
Porites cylindrica	Moderate	Control	1
Porites cylindrica	Moderate	OA	1

Supplementary Table S4. Numerical output of linear mixed-effects models (LMMs) of concentration boundary layer (CBL) thickness of O_2 and H^+ gradients (pooled over light conditions). Global models were constructed with species (3 levels: *Acropora cytherea* [Acy], *Pocillopora verrucosa* [Pve], and *Porites cylindrica* [Pcy]) as a fixed factor. The global model of H^+ CBL thickness was computed using corals only from the ocean acidification (OA) treatment (see Materials and Methods). Individual species' models of O_2 CBL thickness and of H^+ CBL thickness of *A. cytherea* were constructed with flow (2 levels: low and moderate) and treatment (2 levels: control and OA) as fixed factors in a fully crossed design. Models of H^+ CBL thickness of *P. verrucosa* and *P. cylindrica* were constructed with the same structure, but without the treatment factor. All models were constructed with coral fragment identity (ID), colony, day of measurement (Day), and tank as random factors, except when the factor had near-zero variance, and treatment was additionally incorporated into global models as a random factor following the same guideline. Model formulas are specified. Log-transformation was applied to O_2 CBL thickness (global model) to meet model assumptions. σ^2, residual variance; τ_{00}, random intercept variance; ICC, intra-class correlation coefficient; N, number of levels of random effects groups; Marginal R^2, variance explained by the fixed effects; Conditional R^2, variance explained by the entire model

		O_2 CBL Thickness		H^+ CBL Thickness	
All Species		~ Species + (1 | ID) + (1 | Tank) + (1 | Treatment)		~ Species + (1 | ID) + (1 | Colony)	
	Fixed Effects	Estimates	SE	Estimates	SE
	(Intercept)	2.027	0.051	106.76	18.51
	species [Pve]	0.143	0.057	-0.38	26.17
	species [Pcy]	0.151	0.057	-3.47	26.17
	Random Effects				
	σ^2	0.038		2238.17	
	τ_{00}	0.020 $_{ID}$		1446.18 $_{ID}$	
		0.001 $_{Tank}$		478.62 $_{Colony}$	
		0.002 $_{Treatment}$			
	ICC	0.37		0.41	
	N	54 $_{ID}$		27 $_{ID}$	
		6 $_{Tank}$		9 $_{Colony}$	
		2 $_{Treatment}$			
	Observations	216		108	
	Marginal R^2 / Conditional R^2	0.074 / 0.416		0.001 / 0.412	
Acropora cytherea		~ Treatment + Flow + Treatment:Flow + (1 | ID) + (1| Day)		~ Treatment + Flow + Treatment:Flow + (1 | ID) + (1| Colony) + (1| Tank)	
	Fixed Effects	Estimates	SE	Estimates	SE
	(Intercept)	104.68	26.78	110.40	15.60
	treatment [OA]	96.14	24.37	18.08	20.70
	flow [moderate]	-22.41	11.16	-33.53	15.02
	treatment [OA] * flow [moderate]	-71.05	15.78	-9.92	20.65
	Random Effects				
	σ^2	1120.07		1806.00	
	τ_{00}	2090.31 $_{ID}$		709.08 $_{ID}$	
		843.07 $_{Day}$		51.92 $_{Colony}$	
				70.18 $_{Tank}$	
	ICC	0.72		0.32	
	N	18 $_{ID}$		17 $_{ID}$	
		2 $_{Day}$		3 $_{Colony}$	
				6 $_{Tank}$	
	Observations	72		68	
	Marginal R^2 / Conditional R^2	0.342 / 0.818		0.141 / 0.411	

Pocillopora verrucosa		~ Treatment + Flow + Treatment:Flow + (1 | ID)		~ Flow + (1 | ID) + (1| Colony) + (1| Tank)	
	Fixed Effects	Estimates	SE	Estimates	SE
	(Intercept)	205.45	21.01	146.17	27.54
	treatment [OA]	-17.02	29.71		
	flow [moderate]	-92.82	12.48	-79.59	13.27
	treatment [OA] * flow [moderate]	46.51	17.64		
	Random Effects				
	σ^2	1400.66		1584.29	
	τ_{00}	3271.42 $_{ID}$		843.70 $_{ID}$	
				1258.89 $_{Colony}$	
				471.38 $_{Tank}$	
	ICC	0.70		0.62	
	N	18 $_{ID}$		9 $_{ID}$	
				3 $_{Colony}$	
				3 $_{Tank}$	
	Observations	72		36	
	Marginal R^2 / Conditional R^2	0.227 / 0.768		0.281 / 0.726	
Porites cylindrica		~ Treatment + Flow + Treatment:Flow + (1 | ID)) + (1| Day)		~ Flow + (1 | ID) + (1| Colony)	
	Fixed Effects	Estimates	SE	Estimates	SE
	(Intercept)	286.84	37.82	123.06	18.71
	treatment [OA]	-22.30	50.80		
	flow [moderate]	-180.57	29.67	-39.54	8.59
	treatment [OA] * flow [moderate]	22.13	41.96		
	Random Effects				
	σ^2	7921.87		664.66	
	τ_{00}	7237.68 $_{ID}$		1357.44 $_{ID}$	
		526.87 $_{Day}$		486.79 $_{Colony}$	
	ICC	0.49		0.74	
	N	18 $_{ID}$		9 $_{ID}$	
		3 $_{Day}$		3 $_{Colony}$	
	Observations	72		36	
	Marginal R^2 / Conditional R^2	0.319 / 0.656		0.138 / 0.772	

Supplementary Table S5. Numerical output of linear mixed-effects models (LMMs) of change in O_2 (surface ΔO_2) and pH (surface ΔpH) at the coral surface relative to bulk seawater, and of O_2 flux across the concentration boundary layer, measured in light and dark. Global models were constructed with species (3 levels: *Acropora cytherea* [Acy], *Pocillopora verrucosa* [Pve], and *Porites cylindrica* [Pcy]) as a fixed factor. Global models of surface ΔpH were computed using corals only from the ocean acidification (OA) treatment (see Materials and Methods). Individual species' models of surface ΔO_2, surface ΔpH of *A. cytherea*, and O_2 flux were constructed with flow (2 levels: low and moderate) and treatment (2 levels: control and OA) as fixed factors in a fully crossed design. Models of surface ΔpH of *P. verrucosa* and *P. cylindrica* were constructed with the same structure, but without the treatment factor. All models were constructed with coral fragment identity (ID), colony, day of measurement (Day), and tank as random factors, except when the factor had near-zero variance, and treatment was additionally incorporated into global models as a random factor following the same guideline. Model formulas are specified. Square-root transformation was applied to dark surface ΔpH of *P. cylindrica* to meet model assumptions. σ^2, residual variance; τ_{00}, random intercept variance; ICC, intra-class correlation coefficient; N, number of levels of random effects groups; Marginal R^2, variance explained by the fixed effects; Conditional R^2, variance explained by the entire model

		Surface ΔO_2		Surface ΔpH		O_2 Flux	
All Species		~ species + (1 | ID) + (1 | Day) + (1 | Tank)		~ species + (1 | ID)		~ species + (1 | ID) + (1 | Tank) + (1 | Treatment)	
	Fixed Effects	Estimates	SE	Estimates	SE	Estimates	SE
Light	(Intercept)	67.85	12.18	0.035	0.006	-0.375	0.081
	species [Pve]	6.50	16.87	-0.023	0.009	0.011	0.079
	species [Pcy]	20.77	16.29	-0.002	0.009	0.005	0.079
	Random Effects						
	σ^2	620.84		< 0.001		0.055	
	τ_{00}	635.52 $_{ID}$		< 0.001 $_{ID}$		0.015 $_{ID}$	
		191.51 $_{Day}$				0.007 $_{Tank}$	
		0.51 $_{Tank}$				0.006 $_{Treatment}$	
	ICC	0.57		0.24		0.34	
	N	54 $_{ID}$		27 $_{ID}$		54 $_{ID}$	
		8 $_{Day}$				6 $_{Tank}$	
		6 $_{Tank}$				2 $_{Treatment}$	
	Observations	108		54		108	
	Marginal R^2 / Conditional R^2	0.050 / 0.593		0.173 / 0.374		0.000 / 0.339	
Dark		~ species + (1 | ID) + (1 | Day)		~ species + (1 | ID)		~ species + (1 | ID) + (1 | Tank) + (1 | Treatment)	
	(Intercept)	-44.41	5.75	-0.020	0.009	-0.372	0.050
	species [Pve]	-33.84	8.00	-0.051	0.013	-0.138	0.046
	species [Pcy]	-1.54	7.73	-0.012	0.013	0.101	0.046
	Random Effects						
	σ^2	174.53		0.001		0.022	

	τ_{00}	156.00 $_{ID}$		< 0.001 $_{ID}$		0.007 $_{ID}$	
		39.03 $_{Day}$				< 0.001 $_{Tank}$	
						0.003 $_{Treatment}$	
	ICC	0.53		0.33		0.29	
	N	54 $_{ID}$		27 $_{ID}$		54 $_{ID}$	
		8 $_{Day}$				6 $_{Tank}$	
						2 $_{Treatment}$	
	Observations	108		54		108	
	Marginal R^2 / Conditional R^2	0.385 / 0.709		0.301 / 0.532		0.226 / 0.475	
Acropora cytherea		~ Treatment + Flow + Treatment:Flow + (1 | ID) + (1 | Day)		~ Treatment + Flow + Treatment:Flow + (1 | ID)		~ Treatment + Flow + Treatment:Flow + (1 | ID)	
	Fixed Effects	Estimates	SE	Estimates	SE	Estimates	SE
Light	(Intercept)	75.68	19.33	0.048	0.007	0.533	0.073
	treatment [OA]	-4.16	19.45	0.002	0.010	-0.210	0.103
	flow [moderate]	-6.58	5.17	-0.017	0.006	0.138	0.063
	treatment [OA] * flow [moderate]	-9.85	7.32	-0.014	0.008	-0.053	0.089
	Random Effects						
	σ^2	120.45		< 0.001		0.018	
	τ_{00}	366.03 $_{ID}$		< 0.001 $_{ID}$		0.030 $_{ID}$	
		638.69 $_{Day}$					
	ICC	0.89		0.66		0.63	
	N	18 $_{ID}$		17 $_{ID}$		18 $_{ID}$	
		2 $_{Day}$					
	Observations	36		34		36	
	Marginal R^2 / Conditional R^2	0.052 / 0.898		0.291 / 0.758		0.271 / 0.729	
Dark		~ Treatment + Flow + Treatment:Flow + (1 | ID) + (1 | Day)		~ Treatment + Flow + Treatment:Flow + (1 | ID)		~ Treatment + Flow + Treatment:Flow + (1 | ID)	
	(Intercept)	-46.63	10.23	-0.024	0.003	-0.382	0.054
	treatment [OA]	0.39	3.18	-0.004	0.005	0.155	0.076
	flow [moderate]	0.39	3.18	0.006	0.004	-0.148	0.050
	treatment [OA] * flow [moderate]	5.18	4.50	0.008	0.006	0.024	0.071
	Random Effects						
	σ^2	45.51		< 0.001		0.011	
	τ_{00}	225.05 $_{ID}$		< 0.001 $_{ID}$		0.015 $_{ID}$	
		148.84 $_{Day}$					
	ICC	0.89		0.12		0.57	
	N	18 $_{ID}$		17 $_{ID}$		18 $_{ID}$	

		2 $_{Day}$					
	Observations	36		34		36	
	Marginal R^2 / Conditional R^2	0.019 / 0.894		0.266 / 0.355		0.313 / 0.703	
Pocillopora verrucosa		~ Treatment + Flow + Treatment:Flow + (1 | ID) + (1 | Colony)		~ Flow + (1 | ID)		~ Treatment + Flow + Treatment:Flow + (1 | ID)	
	Fixed Effects	Estimates	SE	Estimates	SE	Estimates	SE
Light	(Intercept)	94.71	13.89	0.016	0.0090	0.677	0.101
	treatment [OA]	7.18	17.37			-0.169	0.142
	flow [moderate]	-36.03	9.71	-0.009	0.0084	-0.201	0.132
	treatment [OA] * flow [moderate]	-13.26	13.73			0.061	0.186
	Random Effects						
	σ^2	424.46		< 0.001		0.078	
	τ_{00}	933.95 $_{ID}$		< 0.001 $_{ID}$		0.013 $_{ID}$	
		125.61 $_{Colony}$					
	ICC	0.71		0.57		0.15	
	N	18 $_{ID}$		9 $_{ID}$		18 $_{ID}$	
		3 $_{Colony}$					
	Observations	36		18		36	
	Marginal R^2 / Conditional R^2	0.244 / 0.784		0.026 / 0.577		0.122 / 0.249	
Dark		~ Treatment + Flow + Treatment:Flow + (1 | ID) + (1 | Colony) + (1 | Tank)		~ Flow + (1 | ID)		~ Treatment + Flow + Treatment:Flow + (1 | ID)	
	(Intercept)	-87.54	9.29	-0.093	0.015	-0.450	0.060
	treatment [OA]	1.32	12.61			-0.003	0.084
	flow [moderate]	15.01	5.73	0.042	0.013	-0.180	0.040
	treatment [OA] * flow [moderate]	4.13	8.10			0.127	0.057
	Random Effects						
	σ^2	147.73		< 0.001		0.007	
	τ_{00}	196.33 $_{ID}$		0.001 $_{ID}$		0.024 $_{ID}$	
		20.32 $_{Colony}$					
		123.91 $_{Tank}$					
	ICC	0.70		0.62		0.77	
	N	18 $_{ID}$		9 $_{ID}$		18 $_{ID}$	
		3 $_{Colony}$					
		6 $_{Tank}$					
	Observations	36		18		36	
	Marginal R^2 / Conditional R^2	0.139 / 0.740		0.181 / 0.689		0.147 / 0.804	

Porites cylindrica		~ Treatment + Flow + Treatment:Flow + (1 | ID) + (1 | Day) + (1 | Tank)		~ Flow + (1 | ID)		~ Treatment + Flow + Treatment:Flow + (1 | ID) + (1 | Tank)	
	Fixed Effects	Estimates	SE	Estimates	SE	Estimates	SE
Light	(Intercept)	97.41	17.65	0.044	0.005	0.391	0.178
	treatment [OA]	1.10	24.19			0.038	0.252
	flow [moderate]	-17.83	7.36	-0.022	0.004	0.257	0.140
	treatment [OA] * flow [moderate]	0.87	10.41			0.091	0.198
	Random Effects						
	σ^2	243.76		< 0.001		0.088	
	τ_{00}	829.42 $_{ID}$		< 0.001 $_{ID}$		0.047 $_{ID}$	
		71.16 $_{Day}$				0.050 $_{Tank}$	
		501.47 $_{Tank}$					
	ICC	0.85		0.65		0.52	
	N	18 $_{ID}$		9 $_{ID}$		18 $_{ID}$	
		3 $_{Day}$				6 $_{Tank}$	
		6 $_{Tank}$					
	Observations	36		18		36	
	Marginal R^2 / Conditional R^2	0.046 / 0.859		0.333 / 0.768		0.122 / 0.581	
Dark		~ Treatment + Flow + Treatment:Flow + (1 | ID) + (1 | Colony) + (1 | Tank)		~ Flow + (1 | ID)		~ Treatment + Flow + Treatment:Flow + (1 | ID)	
	(Intercept)	-57.16	5.46	0.200	0.020	-0.204	0.045
	treatment [OA]	13.13	7.30			0.030	0.064
	flow [moderate]	12.81	6.04	-0.064	0.014	-0.165	0.064
	treatment [OA] * flow [moderate]	-6.69	8.54			0.002	0.091
	Random Effects						
	σ^2	163.93		< 0.001		0.019	
	τ_{00}	0.79 $_{ID}$		0.003 $_{ID}$		< 0.001 $_{ID}$	
		9.46 $_{Colony}$					
		24.92 $_{Tank}$					
	ICC	0.14		0.74		< 0.01	
	N	18 $_{ID}$		9 $_{ID}$		18 $_{ID}$	
		3 $_{Colony}$					
		6 $_{Tank}$					
	Observations	36		18		36	
	Marginal R^2 / Conditional R^2	0.203 / 0.343		0.231 / 0.801		0.279 / 0.279	

Supplementary Table S6. Summary of the complete recording of temperature and pH during the experiment. Values are expressed as mean ± 1 SD with measurement replication (*n*). pH_T, pH on the total scale

Tank	Treatment Name	Temperature (ºC)	pH_T	Daily Minimum pH_T	Daily Maximum pH_T
1	Control	25.9 ± 0.2 (5,054)	7.94 ± 0.13 (4,927)	7.75 ± 0.06 (110)	8.11 ± 0.08 (110)
2	Ocean Acidification	25.9 ± 0.2 (4,573)	7.74 ± 0.14 (4,727)	7.56 ± 0.08 (110)	7.92 ± 0.09 (110)
3	Control	25.9 ± 0.2 (5,010)	7.96 ± 0.13 (4,915)	7.77 ± 0.06 (110)	8.14 ± 0.07 (110)
4	Ocean Acidification	26.0 ± 0.2 (4,364)	7.76 ± 0.14 (4,853)	7.58 ± 0.09 (110)	7.95 ± 0.10 (110)
5	Control	25.7 ± 0.3 (4,717)	7.96 ± 0.14 (4,831)	7.77 ± 0.09 (110)	8.14 ± 0.09 (110)
6	Ocean Acidification	26.0 ± 0.2 (4,323)	7.77 ± 0.14 (4,785)	7.59 ± 0.08 (110)	7.96 ± 0.10 (110)

Supplementary Table S7. Results of ANOVAs testing differences between treatments in seawater carbonate parameters, from linear mixed effects (LMMs). Significant effects at the level of $\alpha < 0.05$ are marked in bold. fCO_2, fugacity of CO_2; DIC, dissolved inorganic carbon; Ω_{ar}, aragonite saturation; Ω_{ca}, calcite saturation

Variable	Effect	df	F	p
fCO_2	Treatment	1	217.1	**< 0.001**
DIC	Treatment	1	108.8	**< 0.001**
CO_2	Treatment	1	205.1	**< 0.001**
HCO_3^-	Treatment	1	165.7	**< 0.001**
CO_3^{2-}	Treatment	1	201.1	**< 0.001**
Ω_{ar}	Treatment	1	203.7	**< 0.001**
Ω_{ca}	Treatment	1	205.2	**< 0.001**

Supplementary Table S8. Summary of seawater conditions in the flume during microsensor measurements. Partial pressure of CO_2 (pCO_2), fugacity of CO_2 (fCO_2), dissolved inorganic carbon (DIC), CO_2, HCO_3^-, CO_3^{2-}, aragonite saturation (Ω_{ar}), and calcite saturation (Ω_{ca}) were calculated using values of total alkalinity (TA) measured during the period of microsensor measurements and daily recording of pH, temperature, and salinity. Values are expressed as mean ± 1 SD, with sample size (n) of measured parameters (salinity, temperature, pH, TA) and calculated parameters (pCO_2, fCO_2, DIC, CO_2, HCO_3^-, CO_3^{2-}, Ω_{ar}, Ω_{ca}). pH_T, pH on the total scale

Parameter	Control	Ocean Acidification
Salinity	34.6 ± 0.3 (8)	34.6 ± 0.2 (11)
Temperature (ºC)	26.0 ± 0.1 (14)	26.0 ± 0.0 (20)
pH_T	8.02 ± 0.02 (14)	7.77 ± 0.03 (20)
TA (µmol kg^{-1})	2,184 ± 8 (2)	2,239 (1)
pCO_2 (µatm)	407 ± 30 (14)	820 ± 63 (20)
fCO_2 (µatm)	406 ± 30 (14)	817 ± 63 (20)
DIC (µmol kg^{-1})	1,904 ± 22 (14)	2,077 ± 13 (20)
CO_2 (µmol kg^{-1})	11 ± 1 (14)	23 ± 2 (20)
HCO_3^- (µmol kg^{-1})	1,695 ± 29 (14)	1,928 ± 19 (20)
CO_3^{2-} (µmol kg^{-1})	197 ± 9 (14)	127 ± 8 (20)
Ω_{ar}	3.16 ± 0.14 (14)	2.03 ± 0.12 (20)
Ω_{ca}	4.77 ± 0.20 (14)	3.07 ± 0.18 (20)
O_2 (µM)	238 ± 9 (108)	241 ± 6 (108)

Supplementary Table S9. Post hoc analysis of global linear mixed effects models (LMMs) with significant species differences in LMM-ANOVAs and of individual species' LMMs with significant interaction terms in LMM-ANOVAs. Species contrasts of surface ΔpH are from global models computed using coral fragments only from the ocean acidification treatment (see Materials and Methods). Summarised output of LMMs and model information can be found in Supplementary Tables S3, S4. p-values were adjusted with Bonferroni correction and significant effects with α lower than 0.05 are marked in bold. Acy, *Acropora cytherea*; Pve, *Pocillopora verrucosa*; Pcy, *Porites cylindrica*; CBL, concentration boundary layer; surface ΔO_2, change in surface O_2 concentration relative to bulk seawater concentration; surface ΔpH, change in surface pH relative to bulk seawater pH; LF, low flow; MF, moderate flow

	Model Term	Light	Parameter	Contrast	df	t	p
Global Models	Species	Pooled	O_2 CBL Thickness	Acy vs. Pve	46.0	-2.52	**0.046**
	Species	Pooled	O_2 CBL Thickness	Acy vs. Pcy	46.0	-2.66	**0.032**
	Species	Pooled	O_2 CBL Thickness	Pve vs. Pcy	46.0	0.14	1.000
	Species	Dark	Surface ΔO_2	Acy vs. Pve	3.7	4.03	0.055
	Species	Dark	Surface ΔO_2	Acy vs. Pcy	3.9	0.20	1.000
	Species	Dark	Surface ΔO_2	Pve vs. Pcy	4.5	4.03	**0.037**
	Species	Light	Surface ΔpH	Acy vs. Pve	24.0	2.69	**0.039**
	Species	Light	Surface ΔpH	Acy vs. Pcy	24.0	0.20	1.000
	Species	Light	Surface ΔpH	Pve vs. Pcy	24.0	-2.48	0.061
	Species	Dark	Surface ΔpH	Acy vs. Pve	24.0	2.69	**0.038**
	Species	Dark	Surface ΔpH	Acy vs. Pcy	24.0	-9.94	**< 0.001**
	Species	Dark	Surface ΔpH	Pve vs. Pcy	24.0	-12.63	**< 0.001**
	Species	Dark	O_2 Flux	Acy vs. Pve	46.0	3.03	**0.012**
	Species	Dark	O_2 Flux	Acy vs. Pcy	46.0	-2.22	0.094
	Species	Dark	O_2 Flux	Pve vs. Pcy	46.0	5.25	**< 0.001**
Acropora cytherea	Treatment:Flow	Pooled	O_2 CBL Thickness	Control LF vs. OA LF	18.8	-3.92	**0.002**
	Treatment:Flow	Pooled	O_2 CBL Thickness	Control MF vs. OA MF	18.8	-1.02	0.638

Supplementary Table S10. Summary of quantitative traits of the concentration boundary layer (CBL) of *Acropora cytherea*, *Pocillopora verrucosa*, and *Porites cylindrica* measured in light and darkness, calculated for low flow (2 cm s^{-1}) and moderate flow (6 cm s^{-1}) conditions. Values are mean ± 1 SD with sample size (*n*) and are pooled over the control and ocean acidification (OA) treatments. CBL thickness values are additionally pooled over light conditions. Values of H^+ CBL thickness and surface ΔpH of *P. verrucosa* and *P. cylindrica* are from the OA treatment only (see Materials and Methods). surface ΔO_2, change in surface O_2 concentration relative to bulk seawater concentration; surface ΔpH, change in surface pH relative to bulk seawater pH

Species	Flow	Light	O_2 CBL Thickness (µm)	H^+ CBL Thickness (µm)	Surface ΔO_2 (µM)	Surface ΔpH	O_2 Flux (µmol cm^{-2} h^{-1})
Acropora cytherea	Low	Light	153 ± 86 (36)	120 ± 55 (34)	73.6 ± 24.8 (18)	0.05 ± 0.02 (17)	0.43 ± 0.19 (18)
	Low	Dark			-45.9 ± 15.0 (18)	-0.03 ± 0.01 (17)	-0.30 ± 0.15 (18)
	Moderate	Light	95 ± 48 (36)	81 ± 45 (34)	62.1 ± 31.6 (18)	0.03 ± 0.01 (17)	0.54 ± 0.29 (18)
	Moderate	Dark			-42.9 ± 21.2 (18)	-0.02 ± 0.01 (17)	-0.44 ± 0.21 (18)
Pocillopora verrucosa	Low	Light	197 ± 73 (36)	146 ± 78 (18)	98.3 ± 40.3 (18)	0.02 ± 0.04 (9)	0.59 ± 0.37 (18)
	Low	Dark			-86.9 ± 21.4 (18)	-0.09 ± 0.05 (9)	-0.45 ± 0.17 (18)
	Moderate	Light	127 ± 60 (36)	67 ± 34 (18)	55.6 ± 33.6 (18)	0.01 ± 0.01 (9)	0.42 ± 0.21 (18)
	Moderate	Dark			-69.8 ± 20.0 (18)	-0.05 ± 0.04 (9)	-0.57 ± 0.19 (18)
Porites cylindrica	Low	Light	277 ± 162 (36)	123 ± 53 (18)	98.3 ± 41.6 (18)	0.04 ± 0.02 (9)	0.41 ± 0.35 (18)
	Low	Dark			-50.6 ± 15.1 (18)	-0.05 ± 0.03 (9)	-0.19 ± 0.15 (18)
	Moderate	Light	107 ± 54 (36)	84 ± 42 (18)	81.0 ± 32.8 (18)	0.02 ± 0.01 (9)	0.71 ± 0.46 (18)
	Moderate	Dark			-41.1 ± 13.7 (18)	-0.02 ± 0.01 (9)	-0.35 ± 0.12 (18)

Supplementary Table S11. Summary of quantitative traits of the concentration boundary layer (CBL) of *Acropora cytherea*, *Pocillopora verrucosa*, and *Porites cylindrica* measured in light and darkness, calculated for the control and ocean acidification (OA) treatment. Values are mean ± 1 SD with sample size (*n*) and are pooled over water flow conditions. CBL thickness values are additionally pooled over light conditions. Surface ΔO_2, change in surface O_2 concentration relative to bulk seawater concentration; surface ΔpH, change in surface pH relative to bulk seawater pH

Species	Treatment	Light	O_2 CBL Thickness (µm)	H^+ CBL Thickness (µm)	Surface ΔO_2 (µM)	Surface ΔpH	O_2 Flux (µmol cm^{-2} h^{-1})
Acropora cytherea	Control	Light	91 ± 42 (36)	94 ± 53 (32)	70.5 ± 29.5 (18)	0.04 ± 0.02 (16)	0.60 ± 0.22 (18)
	Control	Dark			-45.6 ± 20.6 (18)	-0.02 ± 0.01 (16)	-0.46 ± 0.20 (18)
	OA	Light	156 ± 86 (36)	107 ± 54 (36)	65.2 ± 28.2 (18)	0.04 ± 0.02 (18)	0.37 ± 0.22 (18)
	OA	Dark			-43.3 ± 15.7 (18)	-0.02 ± 0.01 (18)	-0.29 ± 0.14 (18)
Pocillopora verrucosa	Control	Light	159 ± 82 (36)	n/a	76.7 ± 45.5 (18)	n/a	0.58 ± 0.35 (18)
	Control	Dark			-80.0 ± 22.1 (18)	n/a	-0.54 ± 0.22 (18)
	OA	Light	165 ± 69 (36)	106 ± 72 (36)	77.2 ± 40.7 (18)	0.01 ± 0.03 (18)	0.44 ± 0.26 (18)
	OA	Dark			-76.6 ± 22.8 (18)	-0.07 ± 0.05 (18)	-0.48 ± 0.14 (18)
Porites cylindrica	Control	Light	194 ± 156 (36)	n/a	87.7 ± 29.7 (18)	n/a	0.52 ± 0.28 (18)
	Control	Dark			-50.8 ± 16.3 (18)	n/a	-0.29 ± 0.17 (18)
	OA	Light	190 ± 140 (36)	103 ± 51 (36)	91.6 ± 45.6 (18)	0.03 ± 0.02 (18)	0.60 ± 0.54 (18)
	OA	Dark			-41.0 ± 12.0 (18)	-0.03 ± 0.03 (18)	-0.26 ± 0.14 (18)

Supplementary Table S12. Cohen's d effect size for ocean acidification (OA) effects on the O_2 CBL thickness of *Acropora cytherea* under low flow (LF) and moderate flow (MF), calculated for the dataset with and without the inclusion of complex profiles.

Dataset	Group 1	Group 2	Cohen's d	95 % Confidence Interval	
				Lower	Upper
With complex profiles	Control LF	OA LF	1.432	0.877	2.046
With complex profiles	Control MF	OA MF	0.624	-0.155	1.426
Without complex profiles	Control LF	OA LF	1.131	0.380	1.765
Without complex profiles	Control MF	OA MF	0.500	-0.262	1.328

Supplementary Table S13. Summary of change in O_2 (surface ΔO_2) and pH (surface ΔpH) at the coral surface relative to bulk seawater levels, and O_2 flux across the concentration boundary layer of *Acropora cytherea*, *Pocillopora verrucosa*, and *Porites cylindrica* in light and darkness. Values are mean ± 1 SD with sample size (*n*) and are pooled over flow conditions and treatments, except for surface ΔpH.

Species	Treatment	Light	Surface ΔO_2 (µM)	Surface ΔpH	O_2 Flux (µmol cm^{-2} h^{-1})
Acropora cytherea	Control	Light	67.8 ± 28.6 (36)	0.04 ± 0.02 (16)	0.48 ± 0.25 (36)
	OA	Light		0.04 ± 0.02 (18)	
	Control	Dark	-44.4 ± 18.1 (36)	-0.02 ± 0.01 (16)	-0.37 ± 0.19 (36)
	OA	Dark		-0.02 ± 0.01 (18)	
Pocillopora verrucosa	Control	Light	77.0 ± 42.5 (36)	n/a	0.51 ± 0.31 (36)
	OA	Light		0.01 ± 0.03 (18)	
	Control	Dark	-78.3 ± 22.2 (36)	n/a	-0.51 ± 0.19 (36)
	OA	Dark		-0.07 ± 0.05 (18)	
Porites cylindrica	Control	Light	89.7 ± 38.0 (36)	n/a	0.56 ± 0.43 (36)
	OA	Light		0.03 ± 0.02 (18)	
	Control	Dark	-45.9 ± 15.0 (36)	n/a	-0.27 ± 0.16 (36)
	OA	Dark		-0.03 ± 0.03 (18)	

APPENDIX

1 Acknowledgements

Heading this chorus of gratitude, I thank my doctoral supervisor Prof. Dr. Thomas Wilke for giving me this opportunity and for his valued support. His guidance and constructive suggestions throughout my thesis, as well as the freedom and trust to carve my own research project, helped me grow into a better scientist and writer. Further, I am deeply grateful to Prof. Dr. Maren Ziegler for her scientific insight and steady guidance throughout this thesis. I thank Dr. Marlene Wall for introducing me to the microsensing world, and for her generous support and thoughtful discussions. I am grateful to Dr. Jessica Reichert for sharing her expertise, thoughtful advice, and continued support. I carry forward everything they taught me about corals and about science. I also expressly thank Dr. Patrick Schubert for all I learned from him about coral aquarium systems and for tirelessly supporting all my experimental work. His involvement was essential to the success of this research.

I gratefully acknowledge the Center of Excellence in Marine Sciences (CEMarin) for providing financial support for this thesis.

Thank you to my colleagues and friends at Justus Liebig University Giessen during my doctoral thesis—especially Dr. Arthur Sands, Dr. Catalina Ramírez, Dr. Elena Quintanilla, Kathrin Metzger, Dr. Marvin Rades, Olivia Metz, Silvia Nachtigall, and Dr. Thorsten Hauffe—for their support of my work, scientific discussions, and insightful advice. Special thanks also to Dr. Susana Simancas, who worked with me as a fellow doctoral student during the OA experiment in Manuscript II and III and was both a partner and a friend. As with many doctoral journeys, mine was considerably bumpy and I am especially thankful to Giulia Puntin, Dr. Kim Kirchhoff, and Dr. Laura Espinosa for their continued support, kind encouragement, engaging discussions, and much-cherished friendship.

Finally, and most importantly, I want to heartily thank my parents for their unending support, love, and understanding.

2 Curriculum Vitae